AD-A060 430 SPERRY SYSTEMS MANAGEMENT RESTON VA F/G 9/5

A STATISTICAL DESIGN MANUAL FOR HIGH SPEED ANALOG-DIGITAL-ANALO--ETC(U)

1974 J F HOLLAND N00039-77-C-0124

UNCLASSIFIED NL

1 OF 3

AD
A060430

SIFIED

1 OF 3

AD
AO 60430

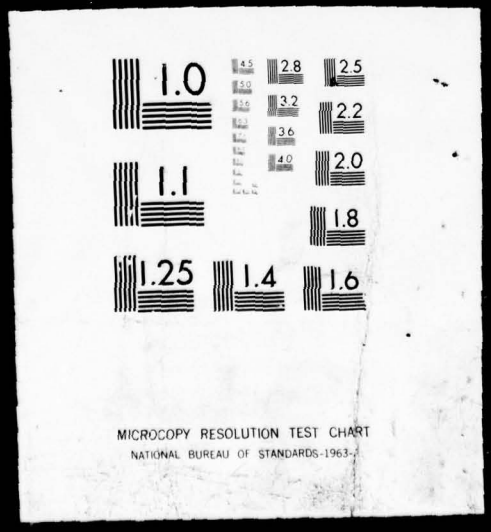

AD A060430

DDC FILE COPY

LEVEL II

DISTRIBUTION STATEMENT A
Approved for public release;
Distribution Unlimited

SPERRY
SYSTEMS MANAGEMENT

RESTON ENGINEERING CENTER

DDC
RECEIVED
OCT 27 1978
A

78 9 25 031

AD A060430

DDC FILE COPY

(1)

(6) A STATISTICAL DESIGN MANUAL FOR

HIGH SPEED

ANALOG-DIGITAL-ANALOG SYSTEMS,

(10) John F. Holland

(11) 1974 (12) 248p.

(15) N00039-77-C-0124

DISTRIBUTION STATEMENT A
Approved for public release;
Distribution Unlimited

PREPARED FOR

Department of the Navy

NAVAL ELECTRONIC SYSTEMS COMMAND

NAVELEX 350

Arlington, Va.

DDC
RECEIVED
OCT 22 1978
A

SPERRY
SYSTEMS MANAGEMENT,
Reston, VA

RESTON ENGINEERING CENTER
11517 SUNSET HILLS ROAD
RESTON, VIRGINIA 22090

SPERRY IS A DIVISION OF SPERRY RAND CORPORATION

78 9 22 037

410909

CONTENTS

		Page
I.	INTRODUCTION	1-1
	1.1 Introduction	1-1
	1.2 Requirement for A-D-A System Design Curves	1-3
	1.3 The Concept of A-D-A System Analysis and Optimization	1-5
	1.4 Preview of Results	1-12
II.	ANALYSIS OF A-D-A SYSTEMS	2-1
	2.1 Introduction	2-1
	2.2 Statistical Analysis of A-D-A Systems	2-2
	2.3 Choice of Performance Criterion	2-13
	2.4 A-D-A System Measurements	2-18
	2.5 Specification of Test Input Processes	2-25
	2.6 Use of Design Curves	2-26
III.	UNIFORM QUANTIZATION DESIGN CURVES	3-1
	3.1 Introduction	3-1
	3.2 Uniform Amplitude Statistics	3-4
	3.3 Gaussian Amplitude Statistics	3-5
	3.4 Design Curves for Gaussian Statistics	3-11
IV.	LOGARITHMIC QUANTIZATION DESIGN CURVES	4-1
	4.1 Introduction	4-1
	4.2 Logarithmic Companding	4-1
	4.3 Design Curves For Gaussian Statistics	4-7
	4.4 Design Curves For Laplacian Statistics	4-19
V.	ALIASING ERROR DESIGN CURVES	5-1
	5.1 Introduction	5-1
	5.2 Design Curves	5-5
VI.	EFFECT OF DITHER SIGNALS IN A-D-A SYSTEMS	6-1
	6.1 Introduction	6-1
	6.2 Effect of Dither Signals	6-1
	6.3 Performance With Dither Signals	6-14
	6.4 Optimization With Dither Signals	6-18
APPENDIX A	- DERIVATION OF QUANTIZATION NOISE FORMULAS	A-1
	A1 Introduction	A-1
	A2 Derivation Of General Noise Formulas	A-1
	A3 Formulas For Gaussian Amplitude Statistics	A-7
	A4 Formulas For Laplace Amplitude Statistics	A-8
	A5 A/D Converter Transition And Output Values	A-9

CONTENTS (Cont'd)

APPENDIX B - EFFECT OF DITHER SIGNALS IN A-D-A SYSTEMS B-1

B1 Introduction B-1
B2 Problem Formulation B-2
B3 Independent Dither Signal Case B-5
B4 Identical Dither Signal Case B-9
B5 Formulas For The Independent Dither Case B-14
B6 Formulas For The Identical Dither Case B-17

ACCESSION for
NTIS White Section ☑
DDC Buff Section ☐
UNANNOUNCED ☐
JUSTIFICATION Letter on file
BY
DISTRIBUTION/AVAILABILITY CODES
Dist. AVAIL. and/or SPECIAL
A

ILLUSTRATIONS

Figure	Title	Page
1-1	Example A-D-A System	1-5
1-2	SNR Vs. Butterworth Spectrum Order for Gaussian Input and Sampling at Twice the 3 dB Frequency. Noise is Due to Aliasing Error Only	1-6
1-3	SNSR Vs. Frequency in Data Band. 5th Order Butterworth Input Signal Spectrum With Gaussian Amplitude Statistics. Number of Quantization Levels = 32 (5 Bits)	1-8
1-4	Normalized $SNSR_{MIN}$ = 20 dB Bandwidth Vs. Sampling Rate for a Butterworth Input Signal Spectrum With Gaussian Amplitude Statistics. Number of Quantization Levels = 32	1-9
1-5	SNSR Vs. Frequency in Data Band. Sampling at Twice the Highest Baseband Frequency. Number of Quantization Levels = 32	1-10
1-6	SNSR Vs. Frequency in Data Band. Sampling at 2.8 Times the Highest Baseband Frequency. Number of Quantization Levels = 32	1-11
1-7	SNSR Vs. Frequency in Data Band. 5th Order Butterworth Input Signal Spectrum With Gaussian Amplitude Statistics. Number of Quantization Levels = 4 (2 Bits)	1-13
1-8	SNSR Vs. Frequency in Data Band. 5th Order Butterworth Input Signal Spectrum With Gaussian Amplitude Statistics. Number of Quantization Levels = 1024 (10 bits)	1-14
2-1	Example A-D-A System	2-3
2-2	A General A-D-A System	2-6
2-3	Simplified A-D-A System Model	2-8
2-4	Final A-D-A System Model	2-9
2-5	Performance Measurement Diagram	2-13
2-6	Block Diagram for NPR Measurement	2-15
2-7	Block Diagram of Combined A/D and A/D/A Level Error Measurement	2-19
2-8	Plot of A/D/A Level Errors for a Uniform 9 Bit Quantizer, $E = 3.21 * 10^{-3}$ and $\sigma_{ad} = 0.632$	2-20
2-9	Block Digram of D/A Level Error Measurement	2-22
2-10	NPR Measurement Test Setup for a Sampler	2-23
2-11	NPR Measurement Test Setup for an A-D-A System	2-24
2-12	Total System NPR Versus Frequency	2-27

ILLUSTRATIONS (Cont'd)

Figure	Title	Page
3-1	Definition of Signal Bandwidth	3-2
3-2	Relation Between SNSR And SNR Versus Normalized Sampling Rate	3-3
3-3	SNR Versus Number of Bits For Uniform Amplitude Statistics	3-6
3-4	Quantization SNR Versus Crest Factor For 10 Bits and Gaussian Amplitude Statistics	3-8
3-5	Optimum Crest Factor Versus Number of Bits for Gaussian Amplitude Statistics	3-9
3-6	Quantization SNR Versus Number of Bits for Gaussian Amplitude Statistics	3-10
4-1	Logarithmically Companded A-D-A System	4-2
4-2	Logarithmic Compressor Characteristic	4-3
4-3	SNR Versus Crest Factor For 5 Bits And Gaussian Amplitude Statistics	4-4
4-4	SNR Versus Crest Factor For 5 Bits And Laplacian Amplitude Statistics	4-5
5-1	SNSR Versus Normalized Frequency for a 6 Pole 1.0 dB Ripple Factor Chebyshev Signal Spectrum	5-2
5-2	Definition of Signal Bandwidth	5-3
5-3	Illustration of a Bandpass Signal Power Spectrum Before and After Sampling	5-4
6-1	A-D-A System With Dither Signals	6-2
6-2	Quantization Error Versus Input Signal Amplitude For A 2 Bit A-D-A System With $\mu = 0$ And Crest Factor Of 2	6-4
6-3	A Blow-up Of The Quantization Error Shown In Figure 6-2	6-5
6-4	Quantization Error Versus Input Signal Amplitude For A 2 Bit A-D-A System With $\mu = 0$ And Crest Factor Of 4	6-6
6-5	Same Case As Figure 6-4 Except The Values Of B Are 6.0 dB Less	6-7
6-6	Quantization Error Versus Input Signal Amplitude For A 5 Bit A-D-A System With $\mu = 0$ And Crest Factor Of 3	6-8
6-7	A Blow-up Of The Quantization Error Shown In Figure 6-6 Plus Additional Cases	6-9

ILLUSTRATIONS (Cont'd)

Figure	Title	Page
6-8	Quantization Error Versus Input Signal Amplitude For A 5 Bit A-D-A System With $\mu = 0$ And Crest Factor Of 3	6-10
6-9	Quantization Error Versus Input Signal Amplitude For A 5 Bit A-D-A System With $\mu = 100$ And A Crest Factor Of 4	6-11
6-10	A Blow-up Of The Quantization Error Shown In Figure 6-9	6-12
6-11	A Blow-up Of The Quantization Error Shown In Figure 6-10	6-13
6-12	Quantization Error Versus Input Signal Amplitude For A 5 Bit A-D-A System With $\mu = 0$ And Crest Factor Of 4	6-15
6-13	Same Case As Figure 6-12 Except The Values Of B Are 2.5 dB Less	6-16
6-14	Quantization Error Versus Input Signal Amplitude For A 5 Bit A-D-A System With $\mu = 0$ And Crest Factor Of 15	6-17
6-15	Quantization Error For 2 Bits	6-20
6-16	Quantization Error For 3 Bits	6-21
6-17	Quantization Error For 4 Bits	6-22
6-18	Quantization Error For 5 Bits	6-23
6-19	Quantization Error For 6 Bits	6-24
6-20	Quantization Error For 7 Bits	6-25
6-21	Quantization Error For 8 Bits	6-26
6-22	Quantization Error For 9 Bits	6-27
6-23	Quantization Error For 10 Bits	6-28

TABLES

Table	Title	Page
2-1	Degradation By Second Error Source	2-17
3-1	Equivalent Number of Lost Bits	3-5
6-1	Value For B With 5 Bits	6-18
6-2	Approximate Optimum Values Of B	6-19

DESIGN CURVES

Type	Pages
Uniform Quantization SNR Versus Crest Factor For 2 Through 30 Bits, Gaussian Amplitude Statistics, And 0, 10, ...80, 90 Percent Normalized Level Errors	3-12 to 3-40
Logarithmic Quantization SNR Versus Crest Factor For 2 Through 12 Bits And Gaussian Amplitude Statistics	4-8 to 4-18
Logarithmic Quantization SNR Versus Crest Factor For 2 Through 12 Bits And Laplacian Amplitude Statistics	4-20 to 4-30
Aliasing Error SNSR Versus Normalized Frequency For Normalized Sampling Rates Of 2.0, 2.1, ...3.9, 4.0, And 2 Through 10 Pole Butterworth And Chebyshev Filters With A Number Of Ripple Factors	5-6 to 5-75

SECTION I

INTRODUCTION

1. Introduction*

Various facets of analog-digital-analog (A-D-A) systems have been studied by researchers over the past four decades. These research efforts have generally followed two distinct lines of interest. The first is the theoretical approach where the mathematicians have demonstrated the analytical feasibility of various A-D-A system data processing techniques. While they have derived a variety of computational formulas, optimization techniques, and bounds on performance, there has generally been much discrepancy between their results and the performance actually obtained from hardware systems. This is probably due to the mathematicians lack of interest in the hardware realization problem and hence their unawareness of many of the actual hardware constraints and performance limiting errors in A-D-A systems.

The other line of interest is the hardware realization problem where design engineers have studied the actual errors in A-D-A systems. However, their lack of interest in mathematics has often impaired their ability to formulate good statistical models for these errors. As a result, design engineers have often been limited to following heuristic trial-by-error approaches which often result in over-designed systems that are wasteful of both bandwidth and money.

In his research, Holland has attempted to close the gap between the mathematical theories for A-D-A systems and the hardware realization problem. He has tried to generalize and unify all of the existing analytical theories for

*Portions of this material are reprinted here with permission from: J.F. Holland, Statistical Analysis of Analog-Digital-Analog Systems, Ph.D. dissertation, Stanford University, March 1974.

these systems while avoiding assumptions which are inconsistent with the hardware realization problem. A method is given by which the actual errors in sophisticated A-D-A systems can be jointly modeled, studied, and design tradeoffs made in order to minimize the power spectrum of the error. The method has been shown to agree within tenths of a dB with measurements taken on many actual high speed A-D-A systems.

In his work a variety of new first and second order multidimensional sampling theorems are given for nonstationary processes. Both bandlimited and non-bandlimited processes are considered as well as the impact of aliasing error. These theorems are then generalized to include the effects of read-in, read-out and locked timing jitter. New modeling results for track and hold amplifiers are also presented with a simplified Fokker-Planck method of evaluating the joint probability density function for nonlinear systems with memory and driven by Gaussian colored noise.

New results are given in his dissertation for the second order statistics of the output and error processes arising from arbitrary quantizers with multidimensionally sampled nonstationary input processes having arbitrary amplitude statistics. All previous results are shown to be special cases of his results. The effect of A/D and D/A level errors is included in the analysis. These results are then generalized to include the effect of symbol errors arising from arbitrary channels.

The equations are formulated so that the input signal dependent error noise spectrum at the A-D-A system output can be studied. The approach allows the system designer to determine which errors are significantly limiting performance. The generality of this analysis is consistent with recent psychophysical testing results for picture images. Extensions to data compression techniques such as differential PCM are also considered.

2. Requirement for A-D-A System Design Curves*

Speech, image, and other signals obtained from sensors and transducers are generally in analog form. Likewise, most of the signals that control electromechanical devices are also in analog form. However, the processing of analog signals has many limitations such as poor resolution due to the presence of noise, problems with analog multipliers, and difficulties with synchronization. Also, the accuracy of analog processed signals becomes degraded after every operation. Consequently, with the decreasing cost of digital hardware, there is a growing interest in digital processing.

Digital techniques offer the advantages of increased accuracy, effective noise minimization, and better processing, transmission, and storage of data. Unlike analog processing, accuracy is not degraded after every operation, but rather remains a constant. In addition, digital processing makes feasible the application of adaptive noncausal precision operations such as the filtering of data. Finally, digital processing is almost fundamental to the concept of data compression and the efficient communication of information.

The unique advantages of digital control, computation, and communication have found application in practically every field: process control, simulation, navigation, telemetry, traffic control, measuring and recording instrumentation, displays, commerical and military aerospace systems, ground and satellite communication systems -- the list seems endless. However, the success of any application depends on how well the digital processor is interfaced with the analog world. It is the practical limitations and statistical characteristics of this interface that are the focuses of this research.

---

*Portions of this material are reprinted here with permission from: J.F. Holland, Statistical Analysis of Analog-Digital-Analog Systems, Ph.D. dissertation, Stanford University, March 1974.

While the literature contains hundreds of analyses and optimization schemes for analog-digital-analog (A-D-A) systems, all have ignored one or more of the fundamental error sources in such systems. The most common omission is aliasing (spectral folding) error arising from sampling, which can result in a 20 dB discrepancy between rate distortion theory bounds and actual measured performance. Another common omission is the effect of level errors which in high speed systems may result in a 12 dB loss in dynamic range (2 bits) from theoretical. In addition, many of the available papers contain other unfounded assumptions which give rise to performance predictions which are in total disagreement with experiment.

Holland's approach, though very mathematical, deals with the combined effect of the actual errors in A-D-A systems and their impact on system performance. The equations are formulated so that the input analog signal dependent A-D-A interface and transmission errors can be studied and design trade-offs made between the various error sources. This report is a companion volume to the Statistical Analysis of Analog-Digital-Analog Systems. It provides dozens of design curves which allow the design engineer to analyze, specify, and predict the performance of A-D-A systems without a strong mathematical background.

3. The Concept of A-D-A System Analysis and Optimization*

In order to motivate the problem further, consider the example A-D-A system in Figure 1-1. It consists of an analog-to-digital (A/D) converter and a digital-to-analog (D/A) converter. Suppose the hardware is over-designed so that quantization error and aliasing (spectral folding) error are the only significant sources of error in the system. Define the input analog signal to be Gaussian white noise passed through an Nth order Butterworth filter. Let us examine how well the input signal is reproduced at the output as a function of the sampling rate, the number of quantization levels, and the order of the Butterworth filter.

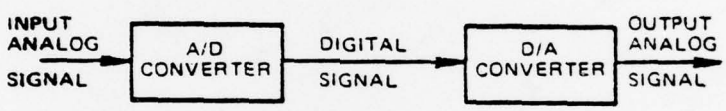

Figure 1-1. Example A-D-A System

Our first result is shown in Figure 1-2 where we have computed signal-to-noise ratio (SNR), the noise being due to aliasing error only. This curve shows that when a 60 pole Butterworth-filtered white noise process is Nyquist sampled at twice the 3 dB nominal bandwidth, the SNR after sampling is only 25 dB. Hence, bandlimiting filters are not easily approximated and over-sampling is the only reasonable way to drop the aliasing error to a tolerable level. Some manufacturers make it a practice to over-sample as much as five times the nominal 3 dB bandwidth Nyquist rate, then struggle to stay within channel bandwidth.

---

*Portions of this material are reprinted here with permission from: J.F. Holland, Statistical Analysis of Analog-Digital-Analog Systems, Ph.D. dissertation, Stanford University, March 1974.

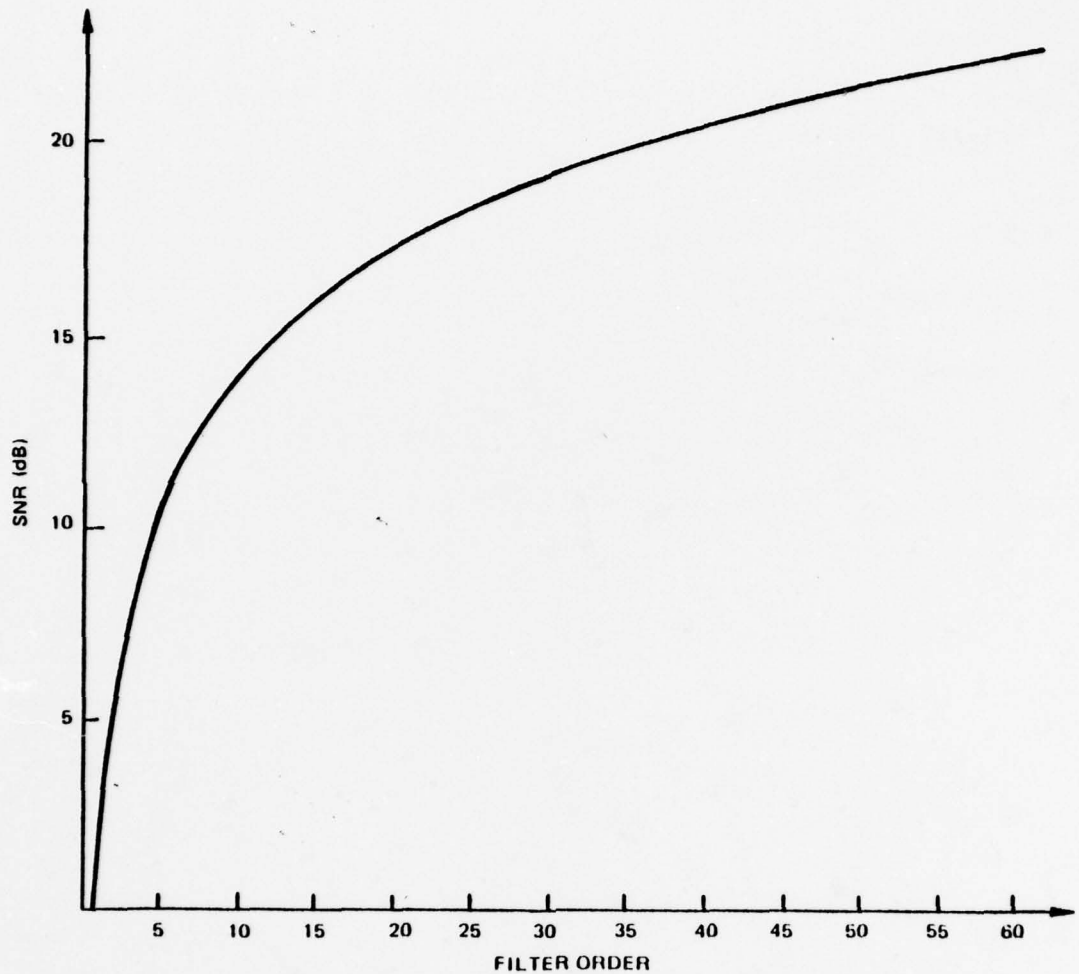

Figure 1-2. SNR Vs. Butterworth Spectrum Order for Gaussian Input and Sampling at Twice the 3 dB Frequency. Noise is Due to Aliasing Error Only.

Figure 1-2 does not show that the ratio of signal power to noise power in a narrow frequency slot of the data band is good at low frequencies and poor at high frequencies. This phenomenon is shown in the typical set of curves in Figure 1-3 where the signal-to-noise power spectrum ratio (SNSR) is plotted versus frequency normalized to the data band for 32 quantization levels. Observe that for sampling at the Nyquist rate of 2.0 times the input 3 dB frequency, the SNSR varies by 22 dB over the data band. For an input signal consisting of many frequency multiplexed channels, this variation obviously cannot be tolerated. However, there is considerable improvement for sampling at 2.8 times the signal bandwidth since the SNSR varies by only 6 dB.

Suppose we require a minimum of 20 dB SNSR over the data band. At what frequency should we sample? We expect that the required sampling rate will decrease as the order of the Butterworth spectrum increases, but increasing the filter order also increases the phase distortion. Figure 1-4 gives a set of curves for determining the optimum sampling frequency. The intersection of these curves and the dashed line is the optimum sampling rate. For a fourth order filter, 3.0 is best since any lower sampling rate will not yield a 20 dB SNSR over the entire data band and any higher sampling rate will waste channel bandwidth. Similarly, 2.4 is best for a ten pole filter and 3.7 for a three pole filter.

In Figures 1-5 and 1-6 the same phenomenon is shown as a function of the order of the Butterworth spectrum with the sampling frequency fixed at 2.0 and 2.8 times the highest baseband frequency. While the SNSR at low frequencies is mostly determined by the number of quantization levels, that at higher frequencies is again dominated by aliasing error. In terms of effective 3 dB bandwidths, the bandwidths of the recovered signals are 37 and 88 percent of the bandwidth of the input signal as shown by the dashed lines. Hence, by increasing the sampling rate by a factor of 1.4 the effective bandwidth of the recovered signal is increased by a factor of 88/37 = 2.4.

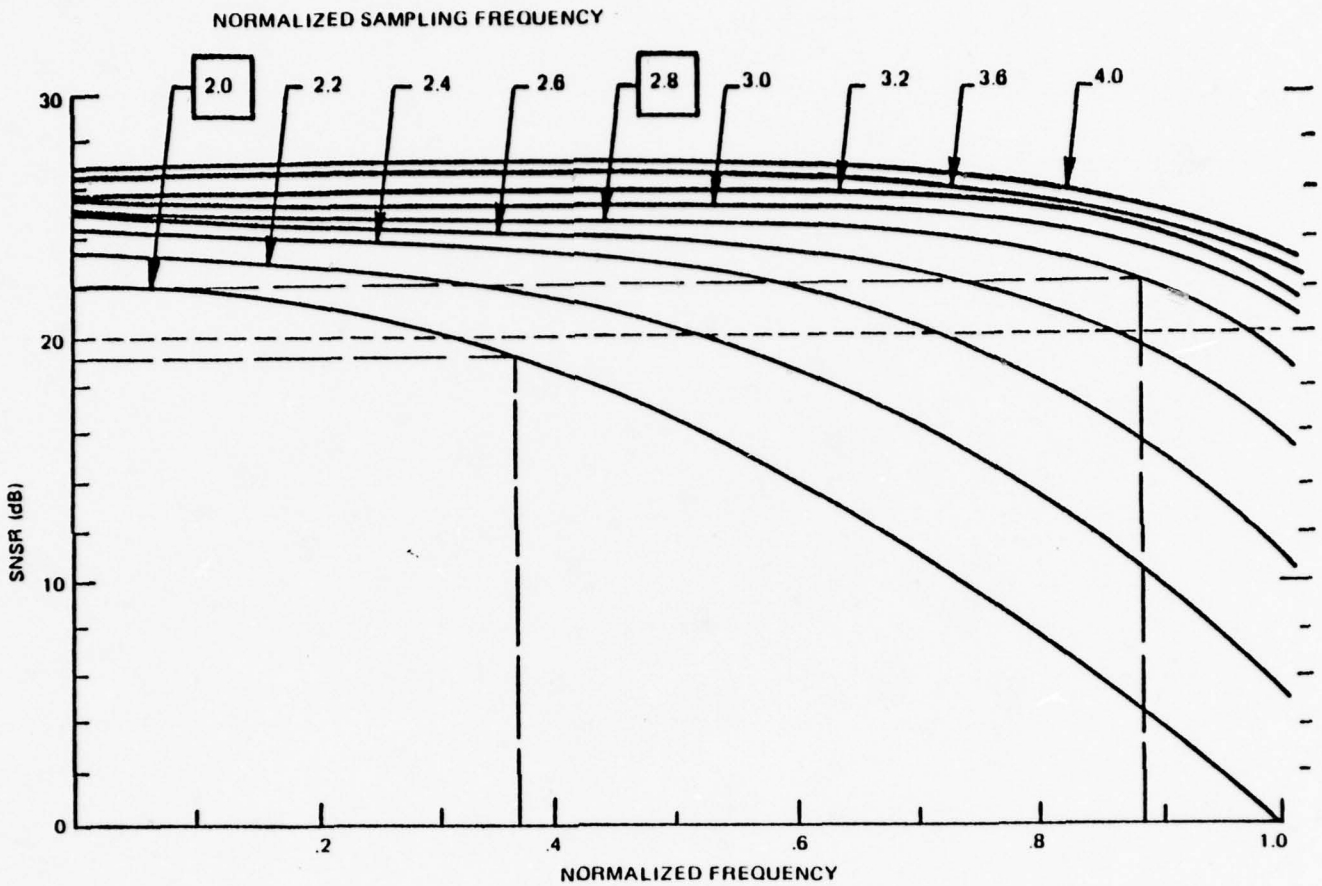

Figure 1-3. SNSR Vs. Frequency in Data Band. 5th Order Butterworth Input Signal Spectrum With Gaussian Amplitude Statistics. Number of Quantization Levels = 32 (5 Bits).

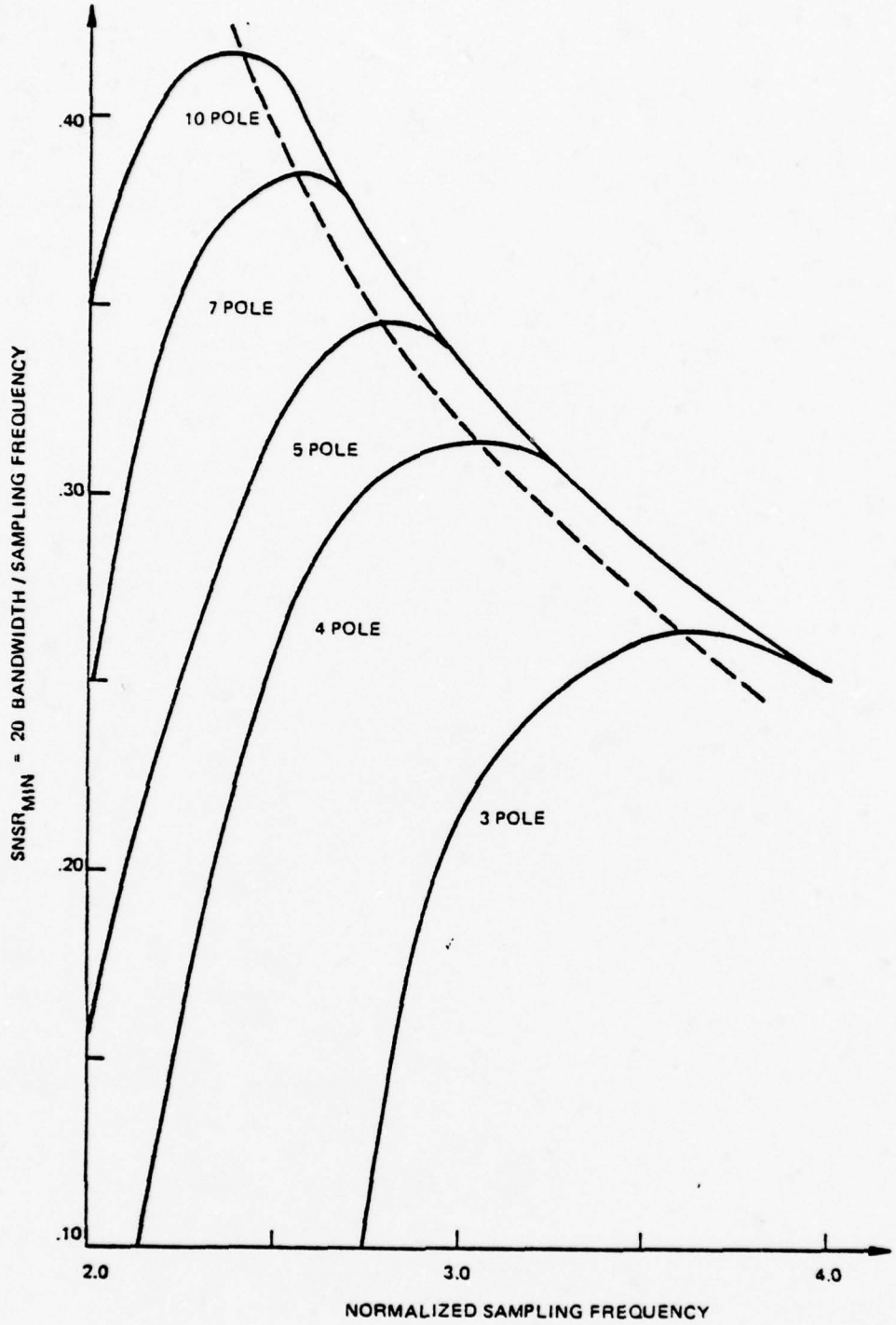

Figure 1-4. Normalized $SNSR_{MIN}$ = 20 dB Bandwidth Vs. Sampling Rate for a Butterworth Input Signal Spectrum With Gaussian Amplitude Statistics. Number of Quantization Levels = 32.

Figure 1-5. SNSR Vs. Frequency in Data Band. Sampling at Twice the Highest Baseband Frequency. Number of Quantization Levels = 32.

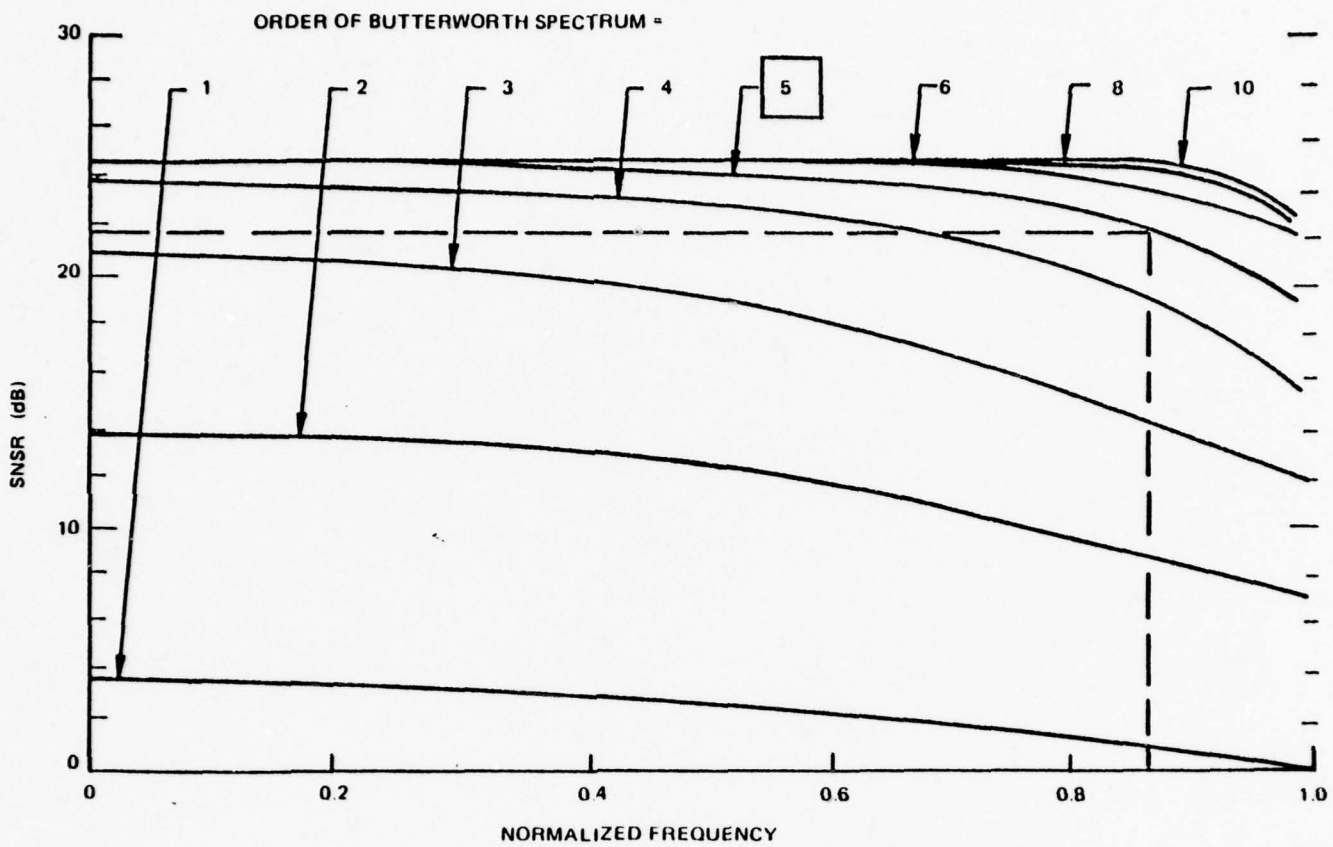

Figure 1-6. SNSR Vs. Frequency in Data Band. Sampling at 2.8 Times the Highest Baseband Frequency. Number of Quantization Levels = 32.

We also expect SNSR to vary greatly with the number of quantization levels. This variation is shown in Figures 1-7 and 1-8 where SNSR is plotted for 2 and 10 bits, respectively.

From this simple example, we conclude there are many design trade-offs to be made in A-D-A systems. While here we have only considered two error sources, there are many more in practical systems. Since each of these error sources produce noise in the output analog signal which is dependent not only on the A-D-A system parameters, but also on the input analog signal, the analysis and optimization of such systems is difficult.

4. Preview of Results

The purpose of this design manual is to present curves which allow the design engineer to evaluate the performance of an A-D-A system. The manual Section 2 gives an overview of A-D-A system analysis and experimental methods for measuring performance. Quantization design curves are then given in Sections 3 and 4 for linearly and logarithmically companded quantizers. Aliasing error design curves are given in Section 5 for Butterworth and Chebyshev spectrums, and The effect of dither signals is examined in Section 6.

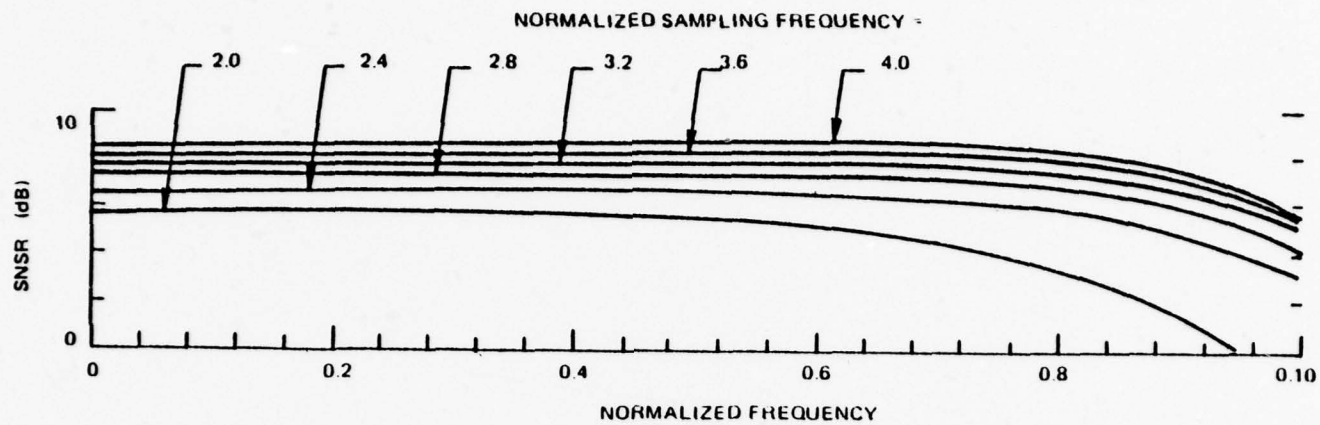

Figure 1-7. SNSR Vs. Frequency in Data Band. 5th Order Butterworth Input Signal Spectrum With Gaussian Amplitude Statistics. Number of Quantization Levels = 4 (2 bits).

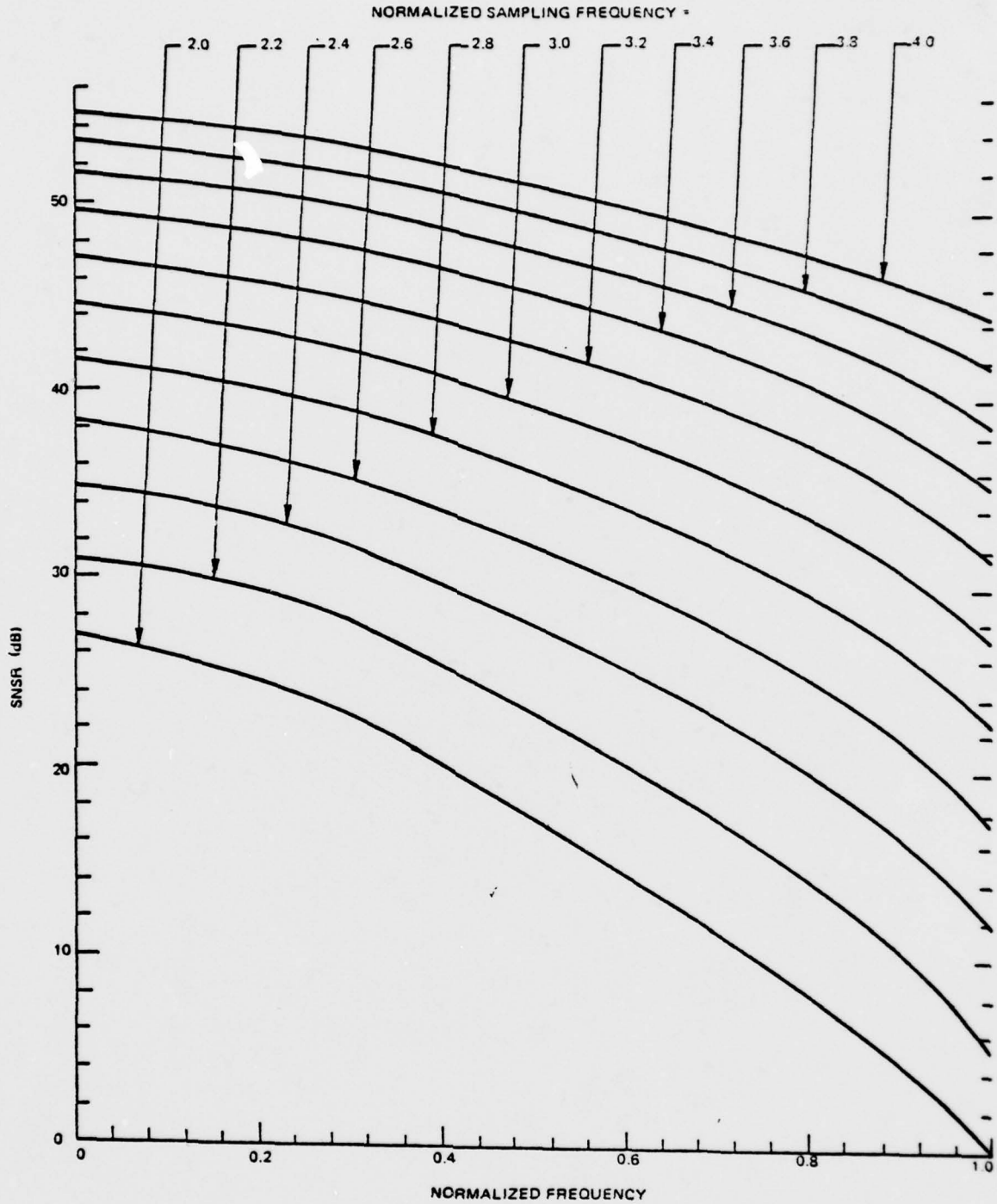

Figure 1-8. SNSR Vs. Frequency in Data Band. 5th Order Butterworth Input Signal Spectrum With Gaussian Amplitude Statistics. Number of Quantization Levels = 1024 (10 bits).

SECTION II

ANALYSIS OF A-D-A SYSTEMS

1. Introduction

The various components which comprise an A-D-A system have been rigorously analyzed in the Statistical Analysis of Analog-Digital-analog Systems. Included in these analyses are detailed discussions of the various error sources associated with each component:

- Sampler
  1) Aliasing error
  2) Slew rate error
  3) Aperture error
  4) Read-in sampling jitter
- PCM or DPCM encoder
  1) Quantizing error
  2) A/D level error
- Modulator-channel-demodulator
  1) Transmission (symbol) error
- D/A converter
  1) D/A level error
  2) Read-out sampling jitter
  3) Reconstruction filter error
- Thermal noise from each component in high performance low power systems.

This section gives an overview of modeling these errors and experimentally measuring the performance of A-D-A systems. More detail and experimental verification of the modeling approach are given in the Statistical Analysis of Analog-Digital-Analog Systems.

2. Statistical Analysis of A-D-A Systems *

Consider the example telecommunications system shown in Figure 2-1. It consists of a track and hold amplifier, a quantizer, a channel, and D/A subsystem. The track and hold amplifier is a bistable device controlled by timing logic. In the track mode the storage capacitor voltage follows the input voltage within the limitations of the available charging current. This limitation on charging current gives rise to a slew rate error. During the hold mode the capacitor is isolated from the input and its voltage remains essentially constant. However, depending on the design of the sampling switch, an input signal dependent discharge of the capacitor may occur during switching from the track to hold states which gives rise to an aperture error. Finally, phase instabilities in the clock may result in irregularities in the track and hold periods resulting in read-in timing jitter.

The quantizer encodes the analog output of the track and hold amplifier into a digital word during the hold period. This encoding is implemented by a successive approximation algorithm. At each step of the approximation a binary decision is made and then fed back to the comparator through a D/A converter to prepare for the next step of the approximation. The collection of these binary decisions forms the output digital word. The successive approximation algorithm can be extended to the encoding of three bits at each step, but requires seven comparators.

This encoding of the anlog output of the track and hold amplifier results in quantization error. In addition, imperfections in the equipment give rise to level errors which cause errors in the encoding. These level errors occur in two ways:

---

*Portions of this material are reprinted here with permission from: J.F. Holland, Statistical Analysis of Analog-Digital-Analog Systems, Ph.D. dissertation, Stanford University, March 1974.

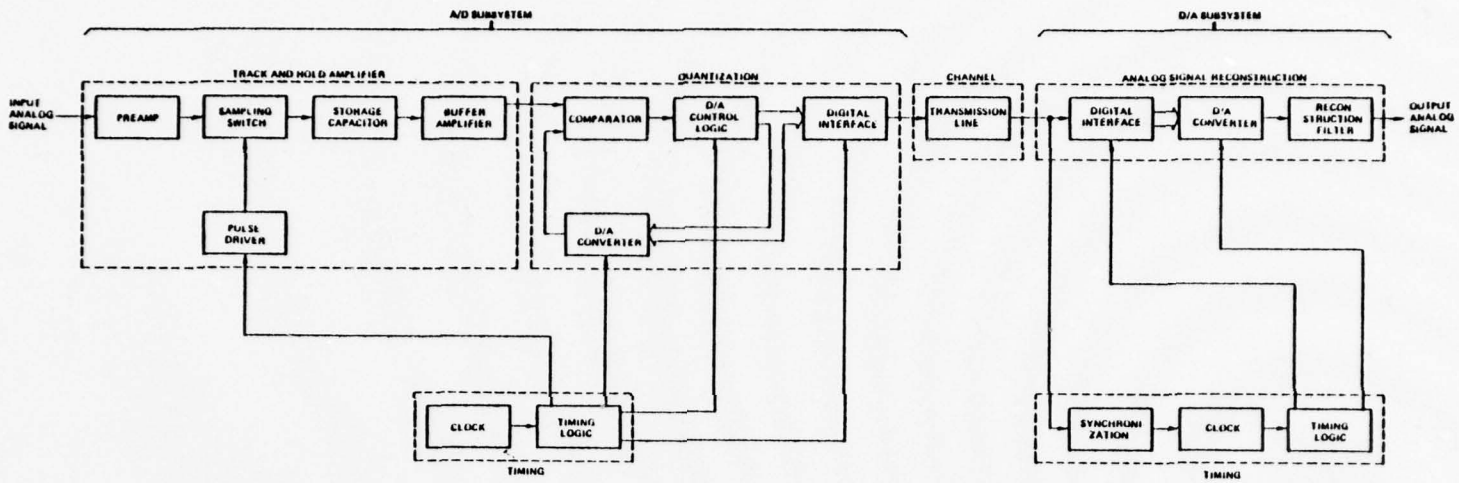

Figure 2-1. Example A-D-A System

- A/D level errors
- A/D/A level errors

The first is associated with the comparator decision threshold level and results in an A/D level error. Through careful analysis it can be shown that this kind of level error results in a noise which is highly correlated with the signal being encoded, which distinguishes it from A/D/A level errors. This second kind of level error results from inaccuracies in the D/A converter due to resistor tolerances and settling times. It can be shown that D/A, thus A/D/A level errors, are uncorrelated with the signal and therefore may be represented as an additive noise. While one might conjecture the equivalence of these two level errors on the basis that they both produce level offsets, this heuristic equivalence argument breaks down in the rigorous analysis of these errors. Observe that the effect of an A/D level error in an A/D converter with only one comparator is to add a constant voltage to the signal before encoding. When more than one comparator is used, the effect is more complex.

The channel produces transmission errors in the digital signal received by the D/A subsystem. From the received digital signal the D/A converter reconstructs the analog signal. Irregularities in synchronization result in read-out timing jitter. Also, there will be inaccuracies in the D/A converter used for reconstructing at the output. Observe that the time domain transients of the quantizer D/A converter were gated out by the D/A control logic. Hence, they only resulted in A/D/A level errors. In order to prevent these transients from corrupting the reconstructed analog signal, the output D/A converter is often followed by another track and hold amplifier (deglitcher). This amplifier gates out the transients so that their only effect is to produce additional level errors known as D/A level errors. We specify deglitching and do not model the output D/A converter transients.

From the preceding discussion it is clear that our example A-D-A system contains many error sources. In its present form this system is far too complex to rigorously analyze. The track and hold amplifier alone constitutes a challenging analysis for any of the available network analysis programs. However, the A-D-A system modeling approach developed in this section will allow us to examine trade-offs between the many system errors and locate the dominant ones.

Consider the general A-D-A system shown in Figure 2-2 of which the system in Figure 2-1 is a special case. It has been broken down into an A/D, a channel, and a D/A subsystem. Each subsystem introduces errors into the output analog signal. In some cases the names of the blocks have deliberately been chosen unconventionally, in an effort to be more definitive as to the function of the blocks and the nature of their errors. In order to identify these error sources and ascertain the degree to which they degrade performance, we now derive an equivalent A-D-A system which contains mathematically analyzable hardware, but retains the salient error sources of the original system.

The first step is to replace the actual channel subsystem by one which is mathematically tractable. The fact that this is possible follows from several observations. The first is that the digital signals entering and leaving possibly for some kind of timing jitter. This synchronization is generally performed by clocks and digital logic. The second observation is that a digital signal may only take on discrete values. Hence, regardless of what modulator, channel, and demodulator comprises the channel subsystem, the only external effect of this subsystem is to introduce errors in the digital signal at the output. Thus, we may replace the channel subsystem by a discrete noisy channel which in general is neither memoryless nor time invariant.

Our third observation is that telecommunications systems operating over fading channels, burst error channels, or noisy channels with strong interference are generally designed to compensate for the deficiencies of the channel.

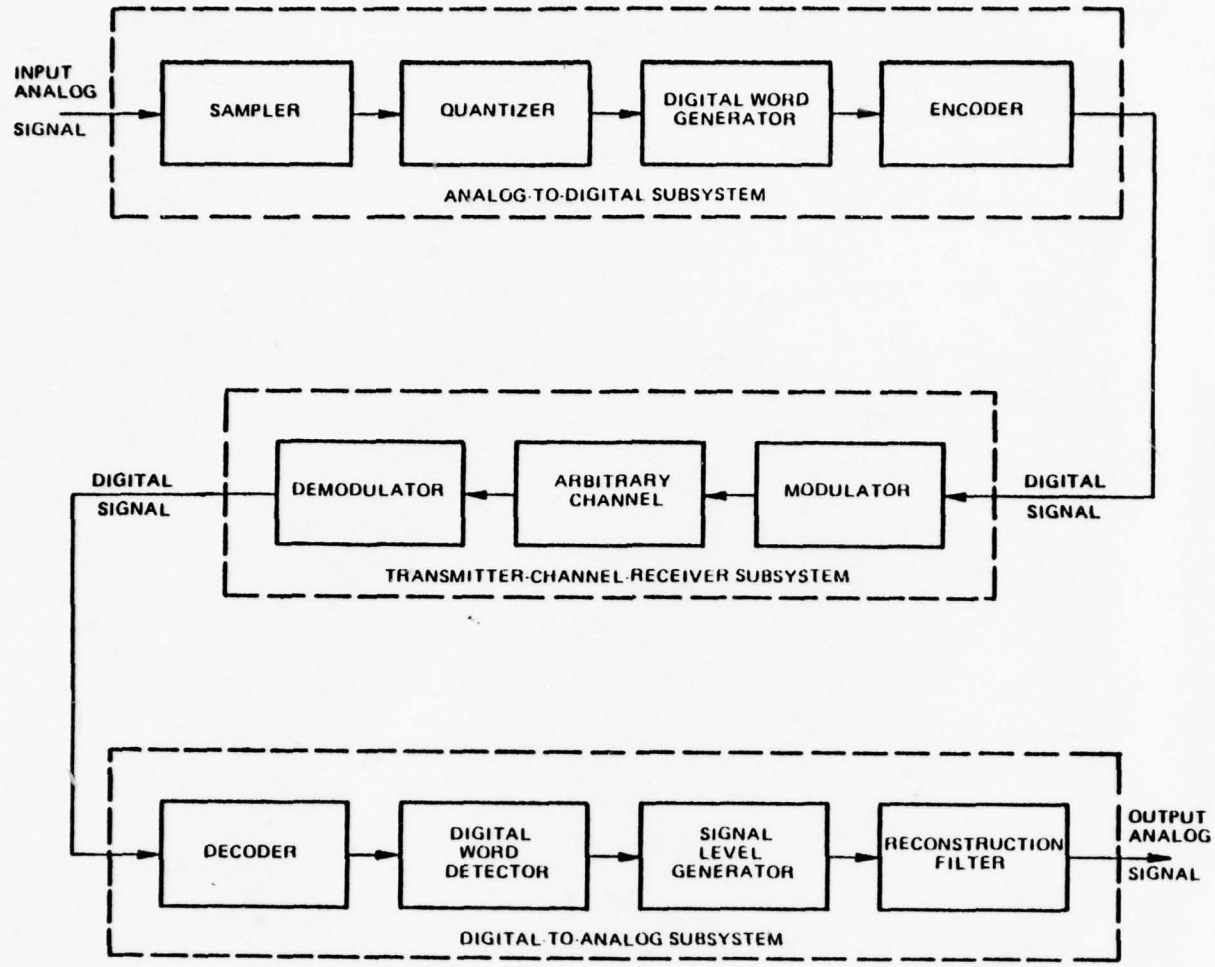

Figure 2-2. A General A-D-A System

Temporal diversity, frequency diversity, spacial diversity, channel coding, and choice of modulation format are some of the standard techniques. Consequently, in many, if not most applications, an adequate model for the channel subsystem is a discrete memoryless time invariant noisy channel where the transition probabilities are derived from the channel subsystem taking into account the effect of encoding. The result is the simplified A-D-A system model shown in Figure 2-3.

Our new A-D-A system model can be simplified even further. Observe that the sampler provides the quantizer with a constant voltage over each hold period. At the end of this hold period it is assumed that the quantizer circuitry has reached steady state and the quantizer output is then gated through logic circuitry (sampled) into the digital word generator. The output of the digital word generator is then gated through the channel and into the digital word detector by means of various synchronization clocks. The digital word detector in turn controls the signal level generator which synchronously pulses the reconstruction filter. The final output analog signal is then obtained at the output of the reconstruction filter. Hence, sampling and resampling occurs throughout the entire A-D-A system to compensate for the physical time constants of the hardware.

For analysis purposes, it suffices to replace much of the A-D-A system hardware of our model with memoryless hardware which makes the same errors. Remembering that memoryless devices commute with impulse sampling, we can then collapse our system model into one which is tractable for analysis but still contains the salient error sources of the original system. In the resulting system model the continuous time quantizer and channel are memoryless, and the effect of sampling is modeled by three devices distributed over the A-D-A system, as shown in Figure 2-4.

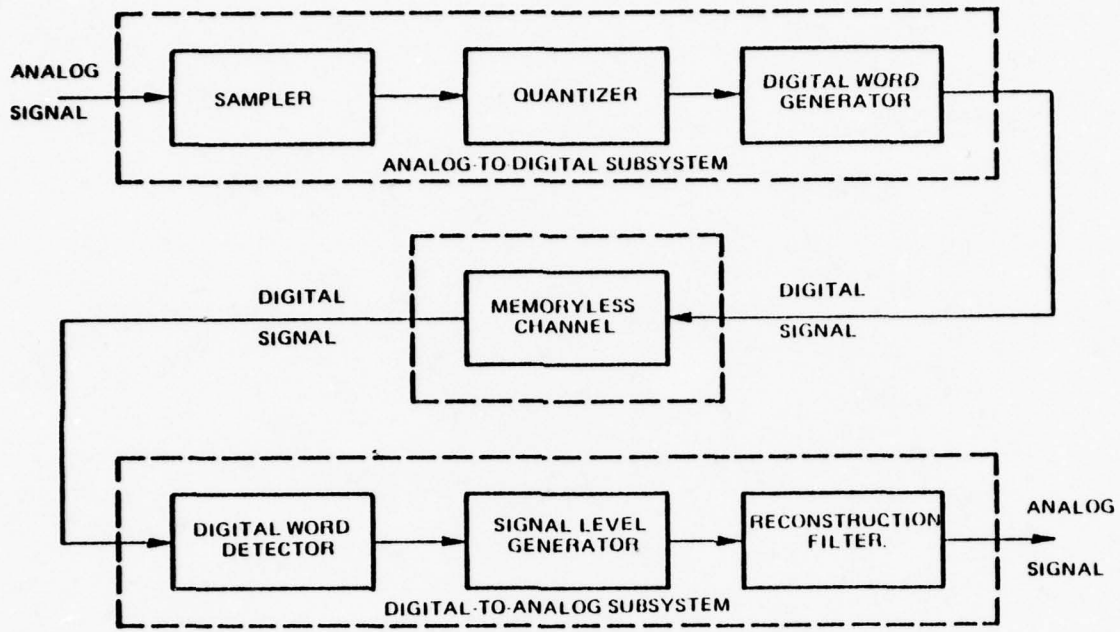

Figure 2-3. Simplified A-D-A System Model

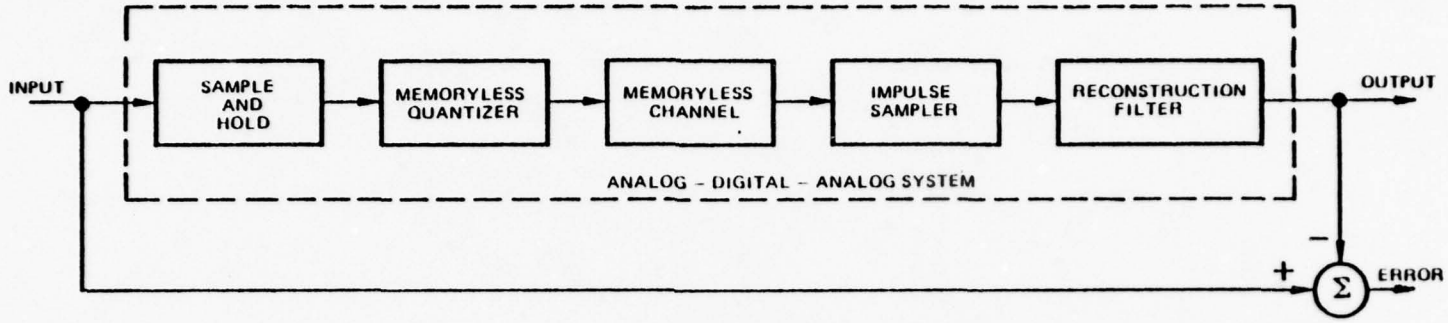

Figure 2-4. Final A-D-A System Model

The sample and hold block models the non-memoryless nonlinear distortion occuring in samplers. For example, this is where we model the deleterious effects of slew rate and aperture error associated with high speed track and hold amplifiers. Since non-memoryless nonlinear devices do not commute with any other portion of our A-D-A system model, the sample and hold block must be placed ahead of the memoryless quantizer. The memoryless quantizer block models the effect of quantizing a signal. In addition, it models the A/D and A/D/A level errors associated with quantization and the D/A level errors associated with the analog signal level generator.

In A-D-A systems using a large number of levels, the A/D/A level error noise power is much less than that of the signal. Consequently, this noise will have negligible effect on the quantization noise and that of the A/D and D/A level errors. Thus, the A/D/A level error noise measured at the reconstruction filter will appear to be additional D/A level error noise. Since these D/A and A/D/A level error noises have the same form of covariance function and are uncorrelated, they may be added together. This aggregate noise is then modeled by the memoryless quantizer block.

The impulse sampler, which commutes with both the memoryless channel and the memoryless quantizer, models performance degradation due to aliasing. Observe that every error process in an A-D-A system is sampled prior to the reconstruction filter. Hence, not only does the signal arriving at the reconstruction filter contain noise plus aliasing error due to the input signal, but it also contains additional noise due to the aliasing of the noise processes and all of the crosscorrelation spectra between the signal and the various noises.

The impulse sampler also models several types of jitter. The first is read-in jitter, the departure from intended sampling times in sampling the analog

input process. The second in read-out jitter, the departure from the intended pulsing times of the analog signal level generator which drives the reconstruction filter. When these two operations (sampling and pulsing) are performed by different pieces of hardware, the jitters may usually be assumed statistically independent. In this case the read-out jitter may be due to poor synchronization. However, when the same clock is used to time both operations, the jitters will usually be identically equal. In these applications the two jitters are called lock jitter.

The last block in our A-D-A system model is the reconstruction filter, which is generally not the same reconstruction filter as in the original system. Two standard types of signal level generators are ones whose output simulates that of an impulse sampler and ones whose output approximates that of an impulse sampler cascaded with a zero order hold filter. When the second type of signal level generator is used, the reconstruction filter it pulses in the actual system may be regarded as the cascade of two filters. The first is an equalization filter which is designed to have an approximate inverse zero order hold frequency response. The output of this equalization filter will then be approximately the same as the output signal of the first type of signal level generator. The filter following the equalization filter is then the same filter as the reconstruction filter that would be used in conjunction with the first type of signal level generator.

In the first case where the signal level generator approximates an impulse sampler, at best we can choose the reconstruction filter to pass what is in the data band and to block what is not in the data band. Since realizable filters never completely block the noise outside the data band, a reconstruction error occurs. This may be included in our A-D-A system model by using the actual reconstruction filter (the filter following the equalization filter for the second case) in our model.

Hence, the A-D-A system model given in Figure 2-4 contains all of the dominant error sources of the original A-D-A system in Figure 2-2, and thus, those in Figure 2-1. By dynamically measuring the level errors associated with the quantizer and the signal level generator, even settling times will be incorporated in the model. Should thermal noise in some portion of the original system become a significant factor, it is easily modeled by introducing an independent additive noise source at the appropriate place of the model in Figure 2-4.

3. Choice of Performance Criterion.*

There are a variety of performance measures used to evaluate A-D-A systems. Probably the most commonly used measure is mean square error. Its choice generally stems more from mathematical tractability than its relationship to an observers concept of quality. In fact, it is fairly easy to juggle the spectrum of a signal in speech and picture processing such as to obtain two reproductions of the original signal, the best sounding (looking) one having the largest mean square error. This result follows from one very simple observation. Consider the system shown in Figure 2-5. The power spectrum of the error is given by

$$S_{\xi\xi}(\omega) = S_{yy}(\omega) - S_{xx}(\omega) + S_{x\xi}(\omega) + S_{\xi x}(\omega) \qquad (2\text{-}1)$$

while $S_{\xi\xi}(\omega)$, $S_{yy}(\omega)$, and $S_{xx}(\omega)$ must be non-negative for all ω, $S_{x\xi}(\omega)$ and $S_{\xi x}(\omega)$ are not non-negative. Now the mean square error is the area under the $S_{\xi\xi}(\omega)$ curve. Thus, we can choose the system to produce a fairly small mean square error while keeping $S_{\xi\xi}(\omega)$ quite large for some frequencies. Consequently, mean square error is often a very poor performance measure when the noise is signal dependent and arises from nonlinearities and aliasing.

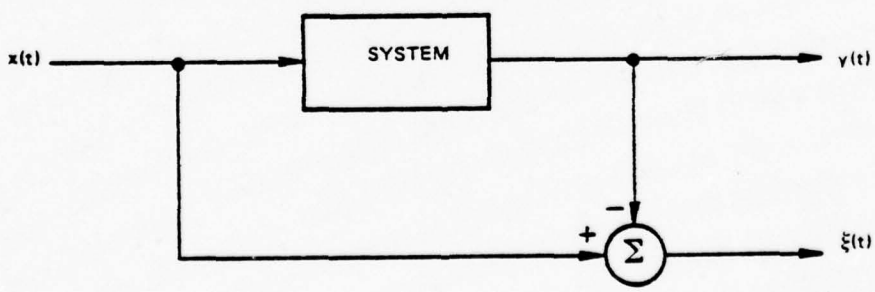

Figure 2-5. Performance Measurement Diagram

*Portions of this material are reprinted here with permission from: J.F. Holland, Statistical Analysis of Analog-Digital-Analog Systems, Ph.D. dissertation, Stanford University, March 1974.

From our discussion in the previous section, we may conclude that the performance of an A-D-A system is essentially determined ahead of the reconstruction filter. This follows from the fact that once the signal and A-D-A system noises have been sampled, thus aliased, there is no way of unscrambling the spectrum. Furthermore, depending on the choice of system parameters, the resulting noise power in the data band may vary with frequency by as much as 60 dB. Hence, a good performance measure must provide information on the frequency distribution of the noise relative to the signal over the data band. Finally, the effect of the crosscorrelation spectra must not be ignored.

Our performance criterion,

$$\text{SNSR}\ (\omega) = \frac{S_{xx}(\omega)}{S_{\xi\xi}(\omega)} \qquad (2\text{-}2)$$

the ratio of the signal and noise power spectrums over the data band, has all of these advantages. In addition, it is essentially independent of the choice of reconstruction filter, consistent with our view that A-D-A system performance is essentially determined ahead of the reconstruction filter. It furthermore, is a performance measure that may easily be used in the lab to obtain performance data, due to its similarity to the standard noise power ratio (NPR) measurement.

Since the dominant errors in A-D-A systems are signal dependent, system noise cannot be measured in the absence of an input signal. Consequently, NPR must be computed from the two measurements shown in Figure 2-6. The first measurement gives the total signal plus noise power at a specified frequency. In the second measurement the signal is notched out at that specified frequency so that only noise is measured. The ratio of these two measurements gives the NPR.

$$\text{NPR}\ (\omega) = \frac{S_{yy}(\omega)}{S_{\xi\xi}(\omega)} = \text{SNSR}\ (\omega) + 1 \qquad (2\text{-}3)$$

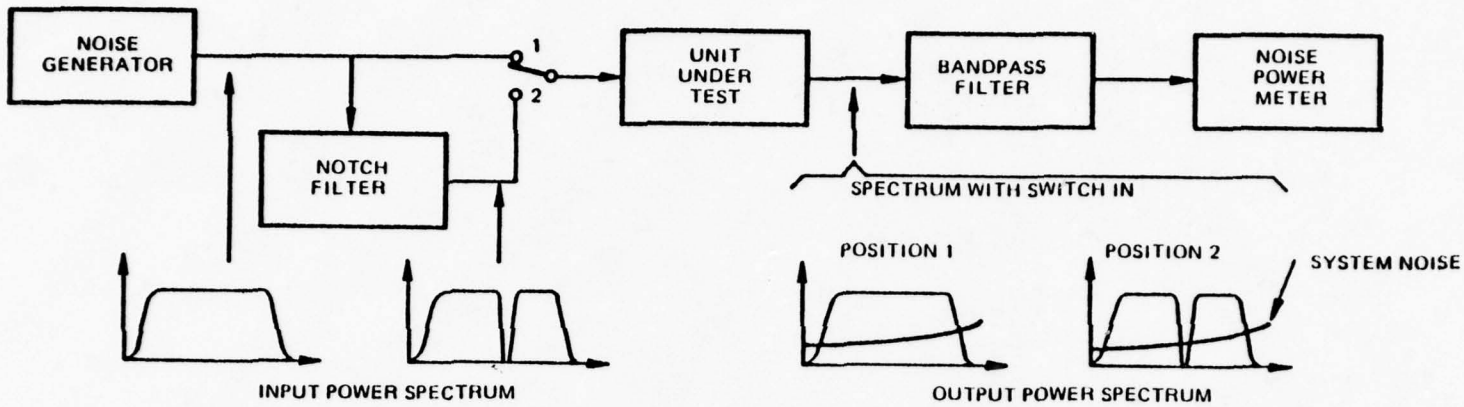

Figure 2-6. Block Diagram for NPR Measurement

From (2-3) we have that

$$NPR\ (\omega) \sim SNSR\ (\omega) \qquad S_{xx}(\omega) >> S_{\xi\xi}(\omega) \tag{2-4}$$

The individual SNSRs due to the various error sources in an A-D-A system add like resistors in parrallel. Let $SNSR_n\ (\omega)$ be the SNSR resulting from the nth error source. Then the total system SNSR is given by

$$SNSR\ (\omega) = \left[\sum_{n=1}^{N} \frac{1}{SNSR_n(\omega)} \right]^{-1} \tag{2-5}$$

For example, suppose only two error sources are of interest and the SNRs due to each are $SNSR_1$ and $SNSR_2$ where $SNSR_1 \geq SNSR_2$. Then the second error source dominates the the total SNSR is

$$\frac{SNSR_1\ SNSR_2}{SNSR_1 + SNSR_2} = \frac{SNSR_2}{1 + \left(\frac{SNSR_1}{SNSR_2}\right)^{-1}} \tag{2-6}$$

Table 2-1 shows how much the total SNSR is degraded from $SNSR_2$ as a function of $(SNSR_1/SNSR_2)$.

TABLE 2-1. DEGRADATION BY SECOND ERROR SOURCE

$\frac{SNSR_1}{SNSR_2}$ in dB	$1 + \left(\frac{SNSR_1}{SNSR_2}\right)^{-1}$ in dB
0	3.01
2	2.12
4	1.46
6	0.97
8	0.64
10	0.41
12	0.27
14	0.17
16	0.11
18	0.07
20	0.04

4. A-D-A System Measurements.*

One of the important applications of our A-D-A system modeling and analysis is in the determination of which elements of the system impair performance most. Since it makes no sense to compare analog signals with digital ones, there are only two places where system performance can be measured. The first is between the sampler and quantizer, and the second is at the output of the A-D-A system. Consequently, given only measurements from these two locations, it is very difficult to ascertain the source of the dominant errors and thus determine how to compensate for them.

However, our system modeling approach coupled with a few hardware measurements allows us to examine trade-offs between the many A-D-A system errors and locate the dominant error sources. This is accomplished by experimentally determining the A/D, A/D/A, and D/A level error variances, the read-in and read-out timing jitter probability densities, and the channel transmission error characteristics. This information plus various A-D-A system specifications are then combined with our A-D-A system equations on a computer to evaluate total system performance. The result of this approach is a set of curves giving SNSR (NPR) as a function of frequency by error source in addition to a plot of SNSR (NPR) for all error sources. The dominant error sources may immediately be identified from these curves.

Figure 2-7 shows a standard test setup for measuring the joint effect of A/D and A/D/A level errors. A typical set of measurements is given in Figure 2-8 for a 9 bit uniform quantizer like the one shown in Figure 2-1. Because there is only one comparator, all of the error shown is due to A/D/A level errors.

---

*Portions of this material are reprinted here with permission from: J.F. Holland, Statistical Analysis of Analog-Digital-Analog Systems, Ph.D. dissertation, Stanford University, March 1974.

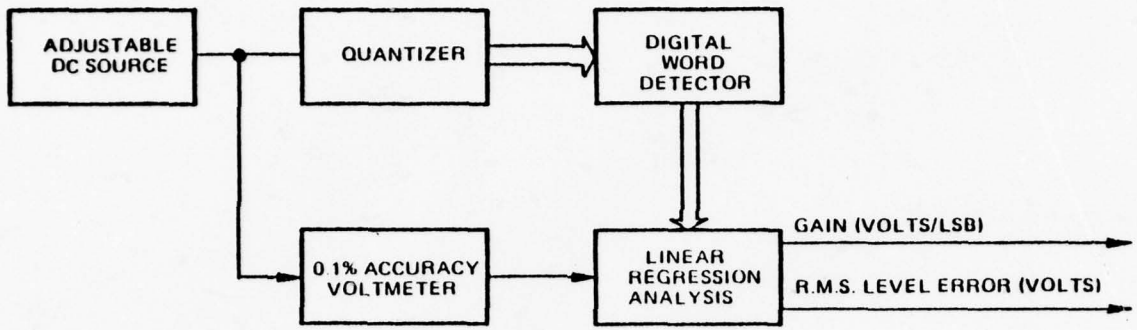

Figure 2-7. Block Diagram of Combined A/D and A/D/A Level Error Measurement

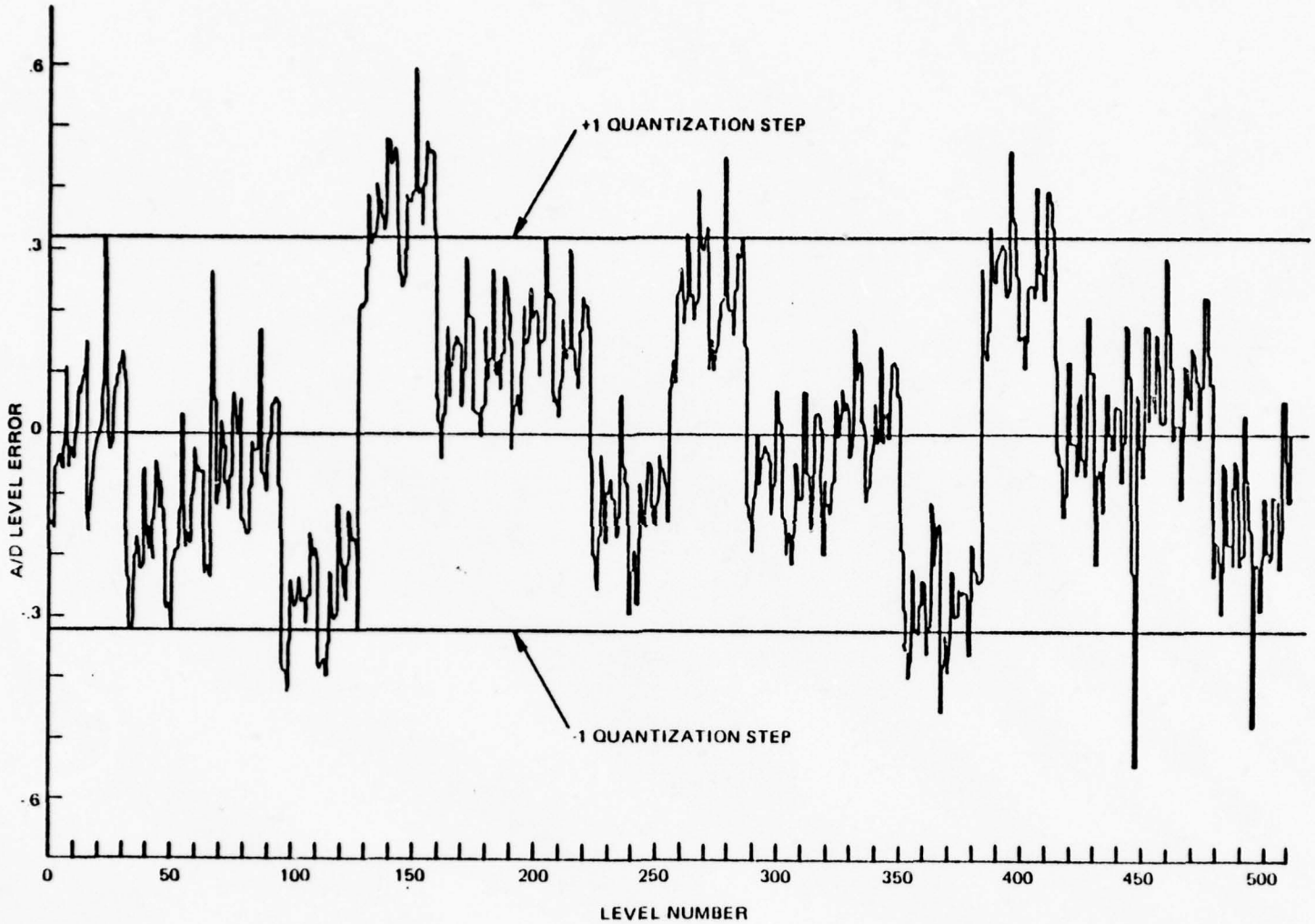

Figure 2-8. Plot of A/D/A Level Errors for a Uniform 9 Bit Quantizer, $E = 3.21 * 10^{-3}$ and $\sigma_{ad} = 0.632$

These measurements are entered into a computer program which performs a least squares curve fit of a line to the data and then evaluates the mean square error. The resulting slope of the line is then taken as the intended step size E and the resulting mean square error is then used as an estimate of the true A/D/A level error variance $E^2\sigma^2_{ad}$. D/A level errors are measured similarly as shown in Figure 2-9.

A variety of standard techniques for measuring timing jitter and channel bit error rates are discussed in the literature. Since such measurements are not central to our purpose, we do not elaborate on them. Figures 2-10 and 2-11 show test setups for measuring the NPR at the output of a sampler and of an A-D-A system.

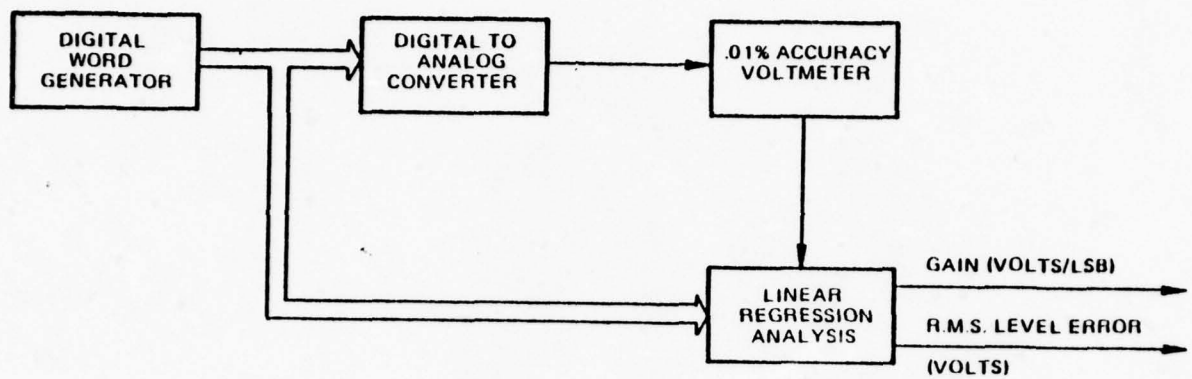

Figure 2-9. Block Diagram of D/A Level Error Measurement

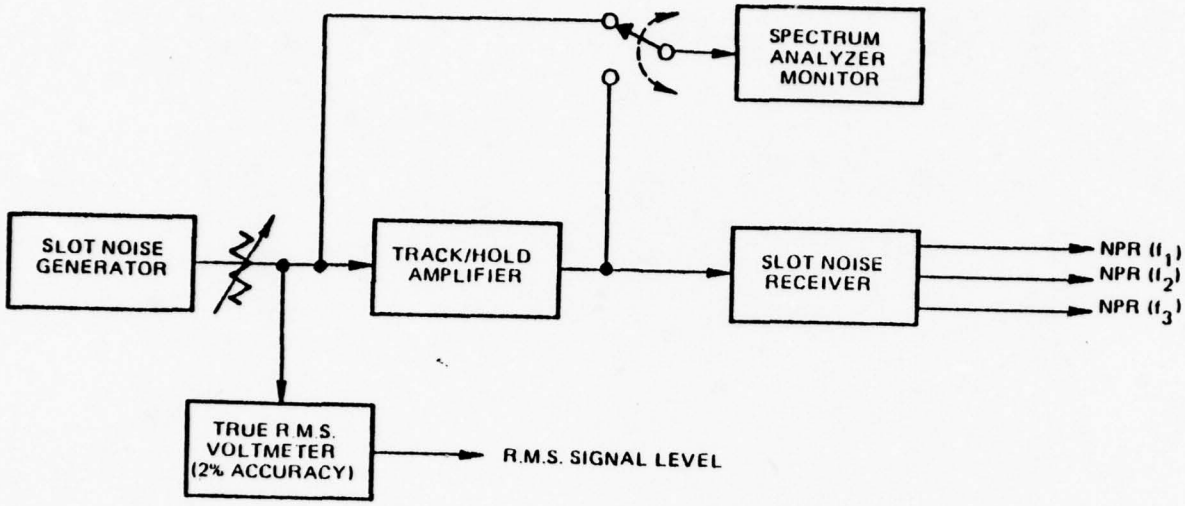

Figure 2-10. NPR Measurement Test Setup for a Sampler

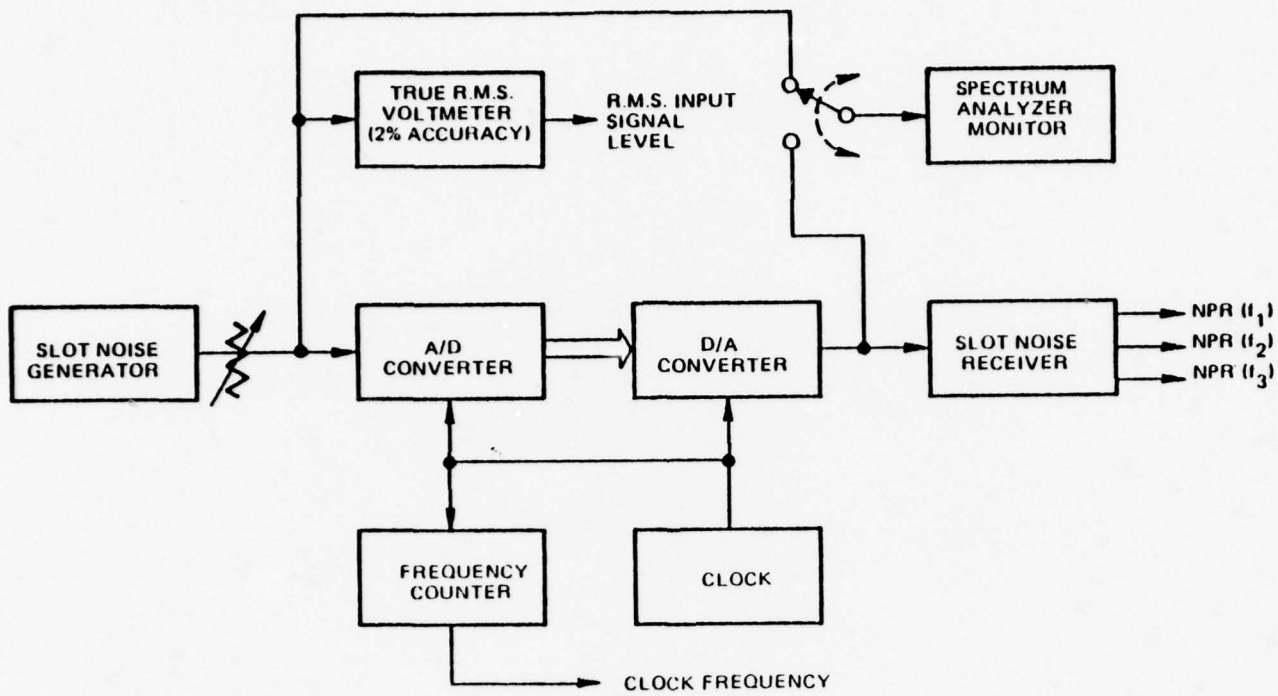

Figure 2-11. NPR Measurement Test Setup for an A-D-A System

5. Specification of Test Input Processes*.

In practice, the noise introduced by A-D-A systems is not uniformly distributed across the data band, but rather may vary with frequency by as much as 60 dB. The noise is also highly correlated with the signal. Consequently, careful selection of test input processes is required.

In all of our analyses the input signal spectrum is taken to be white noise filtered by an Nth order Butterworth or Chebyshev filter. In the limit as $N \to \infty$ these give an ideal low-pass (bandpass) spectrum. The Butterworth and Chebyshev spectrums are reasonable approximations for many signal spectrums and in particular for those of a baseband composed of frequency multiplexed audio channels when there are more than 16 active channels. They also permit an evaluation of the extent to which an input signal waveform must be filtered or bandlimited in order to reduce to tolerable level the noise due to aliasing error. As a result, it has become common practice to simulate traffic conditions on FDM telephone channels and in other systems with these spectrums. It is assumed that the desired signal (data band) ends at the 3 dB point of the spectrum. The sampling frequency is then referenced as some multiple of this maximum baseband frequency.

In order to complete the specification of the input, its amplitude statistics must be identified. Normally distributed amplitude statistics are particularly attractive because slot noise generators have normal outputs. Gaussian statistics are often a good model for many signals of interest. In particular, for signals composed of frequency multiplexed audio channels, the normal assumption is especially good for 16 or more active channels. However, at times the amplitude statistics of inputs are more nearly uniformly than

*Portions of this material are reprinted here with permission from: J.F. Holland, Statistical Analysis of Analog-Digital-Analog Systems, Ph.D. dissertation, Stanford University, March 1974.

normally distributed. For example, the amplitude statistics of the input might be multimodal. In the case of speech, the amplitude statistics are often modeled by a Laplace distribution. Consequently, the analytic determination of A-D-A system performance for uniformly and Laplacian distributed inputs is also useful.

6. Use of Design Curves

A compendium of design curves are given in the following sections. They include the effects quantization, aliasing, and other errors. Using equation (2-5), the SNSR for these different error sources may be added together to give the total system SNSR or NPR.

For example, from the design curves in Sections 3 and 5, a 10 bit system with 20% level errors set at the optimum crest factor of 4.5, with a 6 pole 1.0 dB ripple factor 2.0 MHz Chebyshev aliasing filter centered at 1.44 MHz, and with a 5.76 MHz sampling rate yields the NPR shown in Figure 2-12.

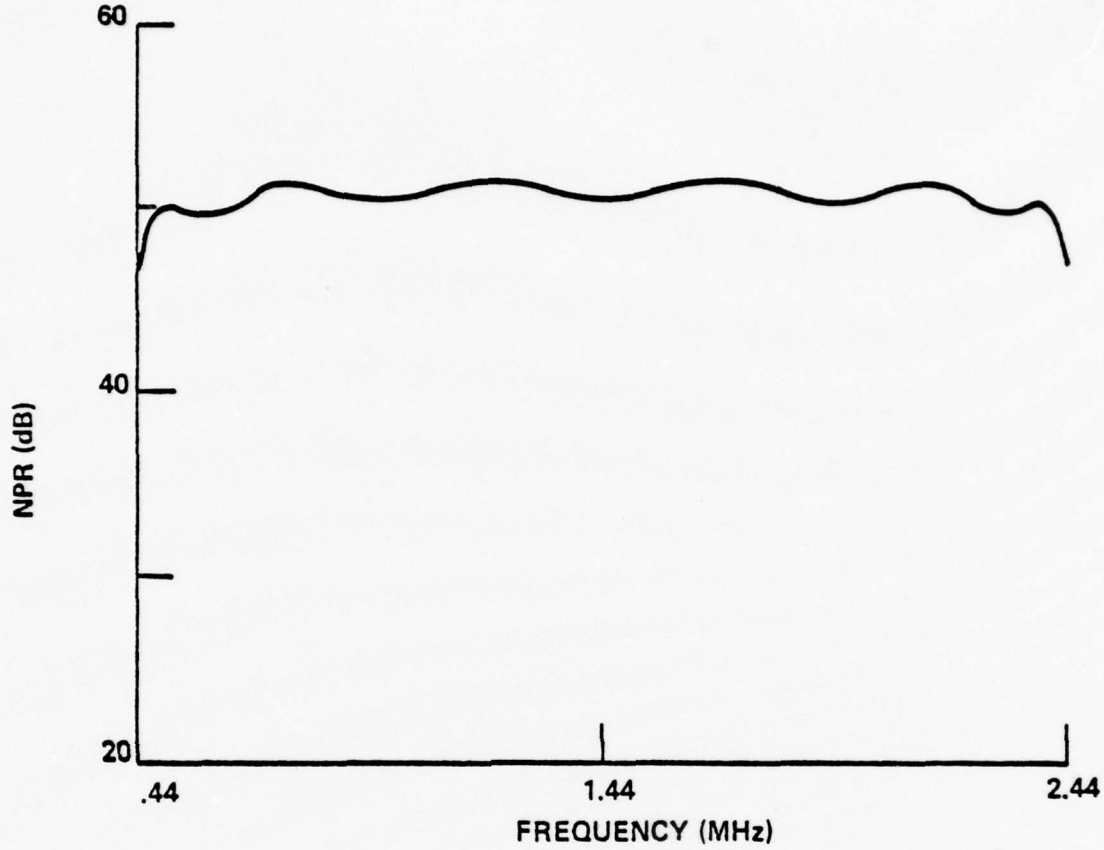

Figure 2-12. Total System NPR Versus Frequency.

- 10 Bits with 20% Level Errors and Optimum Crest Factor of 4.5
- 6 Pole 2.0 MHz Chebyshev Spectrum with 1.0 dB Ripple Factor and Center Frequency of 1.44 MHz
- 5.76 MHz Sampling Frequency

SECTION III

UNIFORM QUANTIZATION DESIGN CURVES

1. Introduction

This section gives equations and design curves for predicting the dynamic range limitations imposed by quantization and level error on a uniform (linearly companded) A/D converter. The results of this section are presented in terms of SNR since quantization and level error produce noises which are not strongly correlated with the input signal and whose power spectrums are approximately constant with frequency. Consequently,

$$SNSR(f) = \frac{S(f)}{T\sigma^2} \tag{3-1}$$

where S(f) is the signal power spectrum, T is the sampling period, and σ^2 is the quantization plus level error noise power. When the signal power spectrum is nearly constant with frequency,

$$S(f) = \frac{\sigma_s^2}{2B} \tag{3-2}$$

where σ_s^2 is the signal power and B is the 3dB signal bandwidth as defined in Figure 3-1. In this case the SNSR is nearly constant with frequency and equals

$$SNSR = \frac{SNR}{2BT} \tag{3-3}$$

where SNR is

$$SNR = \frac{\sigma_s^2}{\sigma^2} \tag{3-4}$$

This relationship is shown in Figure 3-2 as a function of normalized sampling rate.

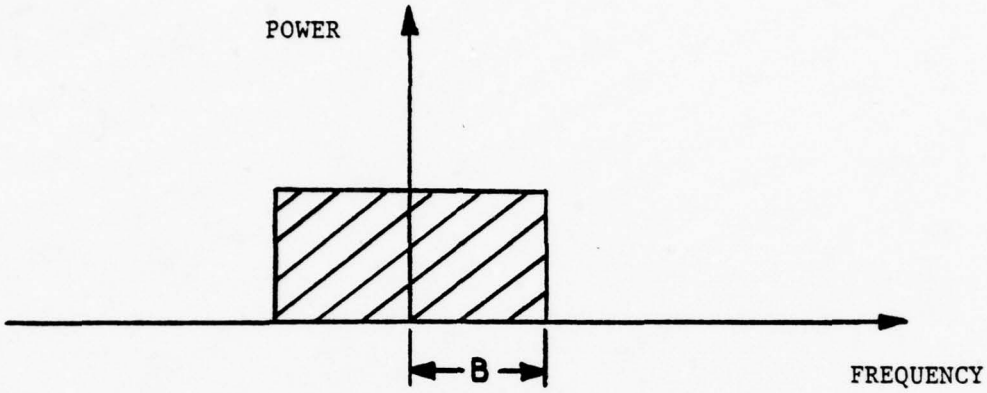

Definition of Bandwidth B - Lowpass Case

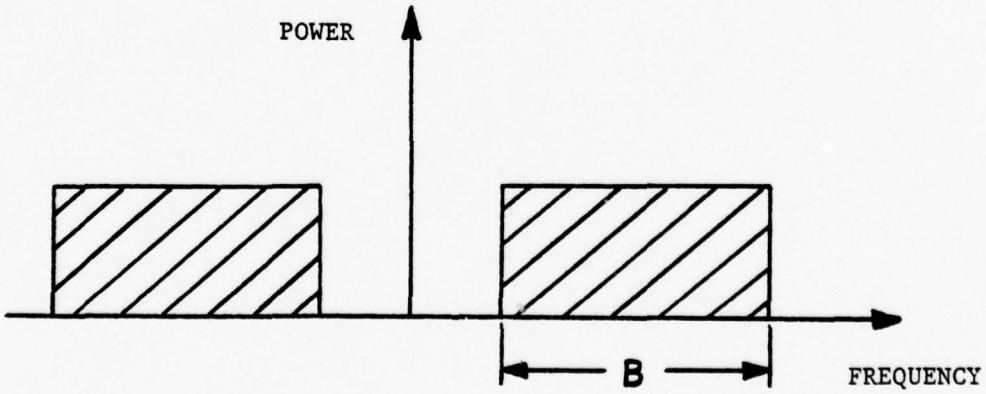

Definition of Bandwidth B - Bandpass Case

Figure 3-1. Definition of Signal Bandwidth

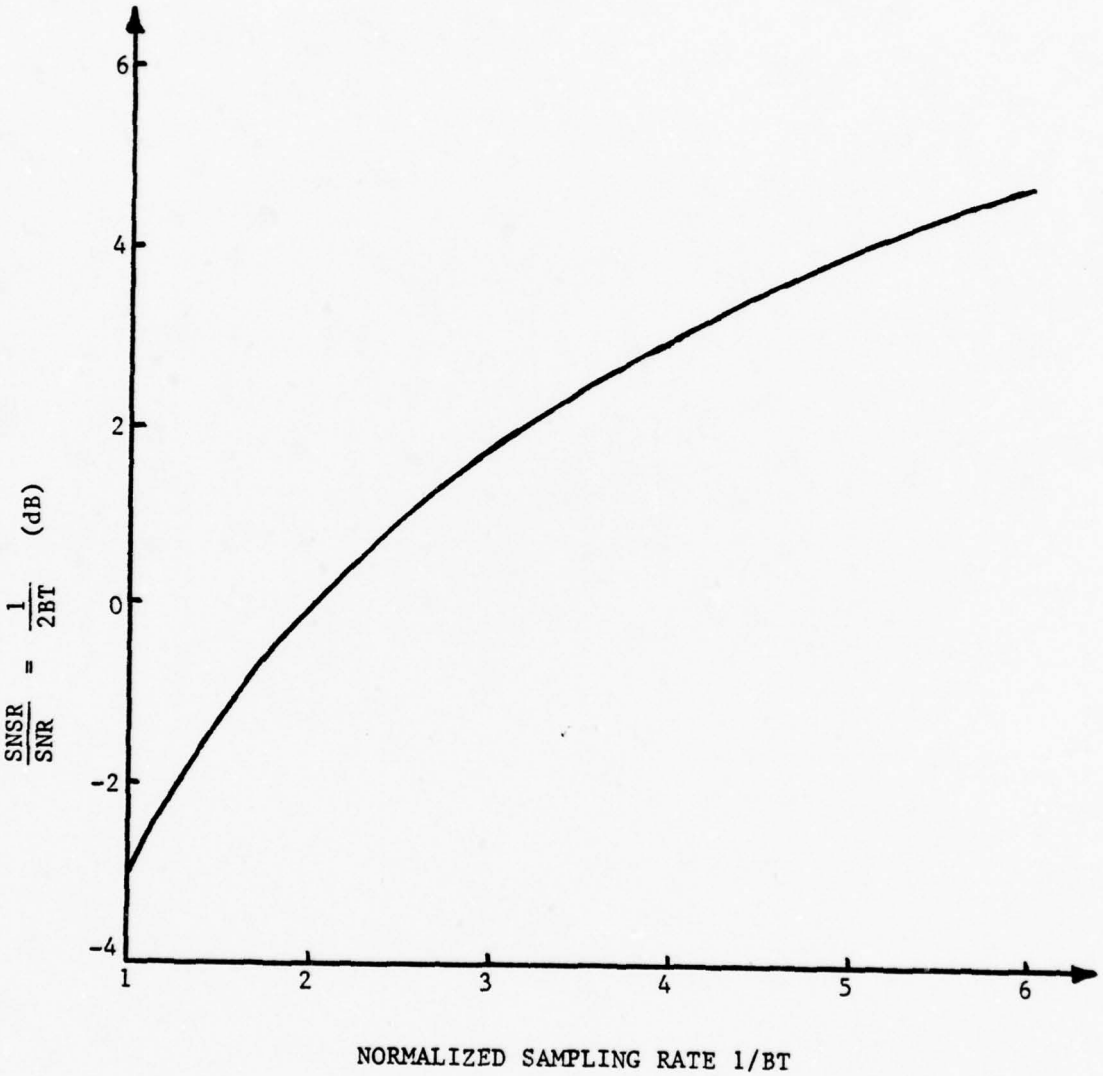

Figure 3-2. Relation Between SNSR And SNR Versus Normalized Sampling Rate.

For uniform quantization, the step size E is

$$E = 2^{-(q-1)}V = 2^{-(q-1)}\eta\sigma_s \tag{3-5}$$

where q is the number of bits, 2V is the peak to peak quantization range, and η is the crest factor (peak to RMS ratio).

$$\eta = \frac{V}{\sigma_s} \tag{3-6}$$

The noise power

$$\sigma^2 = \sigma_q^{\ 2} + E^2\sigma_T^{\ 2} \tag{3-7}$$

is the sum of the quantization noise power $\sigma_q^{\ 2}$ and the level error noise power $E^2\ \sigma_T^{\ 2}$. The parameter σ_T is the RMS value of the level error. Then

$$SNR = \frac{SNR_q}{1+SNR_q\eta^2\sigma_T^{\ 2}4^{-(q-1)}} \tag{3-8}$$

where SNR_q is the theoretical SNR associated with quantization.

$$SNR_q = \frac{\sigma_s^{\ 2}}{\sigma_q^{\ 2}} \tag{3-9}$$

Performance of an A/D converter depends on the amplitude statistics of the input signal. Two cases are considered here. The first is uniform statistics which gives an upper bound on performance and the second is Gaussian statistics which gives an estimate of typical performance for a great number of systems.

2. Uniform Amplitude Statistics

The uniform amplitude statistics case gives an upper bound on performance since the dynamic range of the input signal perfectly matches the quantization range. Hence, there is no overload error introduced by limiting the input signal. By definition the crest factor $\eta = \sqrt{3}$ and

$$SNR_q = 4^q = 6.02q(dB) \tag{3-10}$$

Equation (3-8) reduces to

$$SNR = \frac{4^q}{1+12\sigma_T^2} \tag{3-11}$$

which is plotted in Figure 3-3.

Observe the variation in performance with percent level errors. A manufacturer's specification of $\pm$ 1/2 LSB quantization error maximum, with a uniform distribution of level errors would produce $\sigma_T^2 = 1/12$. Thus, $\sigma_T = 1/\sqrt{12} =$ 29% results in a 3 dB loss in SNR from (3-11) which is equivalent to 1/2 bit less quantization resolution from (3-10). Table 3-1 summarizes the number of lost bits as a function of σ_T.

Table 3-1. Equivalent Number of Lost Bits

σ_T%	SNR dB lost	Number of Lost Bits
29	3	½
50	6	1
76	9	1½
112	12	2

3. Gaussian Amplitude Statistics

Performance predictions assuming Gaussian amplitude statistics are more nearly typical than for uniform statistics since actual signals are not received with their amplitudes hard limited. Since an A/D converter can only encode over the peak to peak voltage range of 2V, the signal will be limited by the A/D converter producing an overload noise. This additional noise degrades

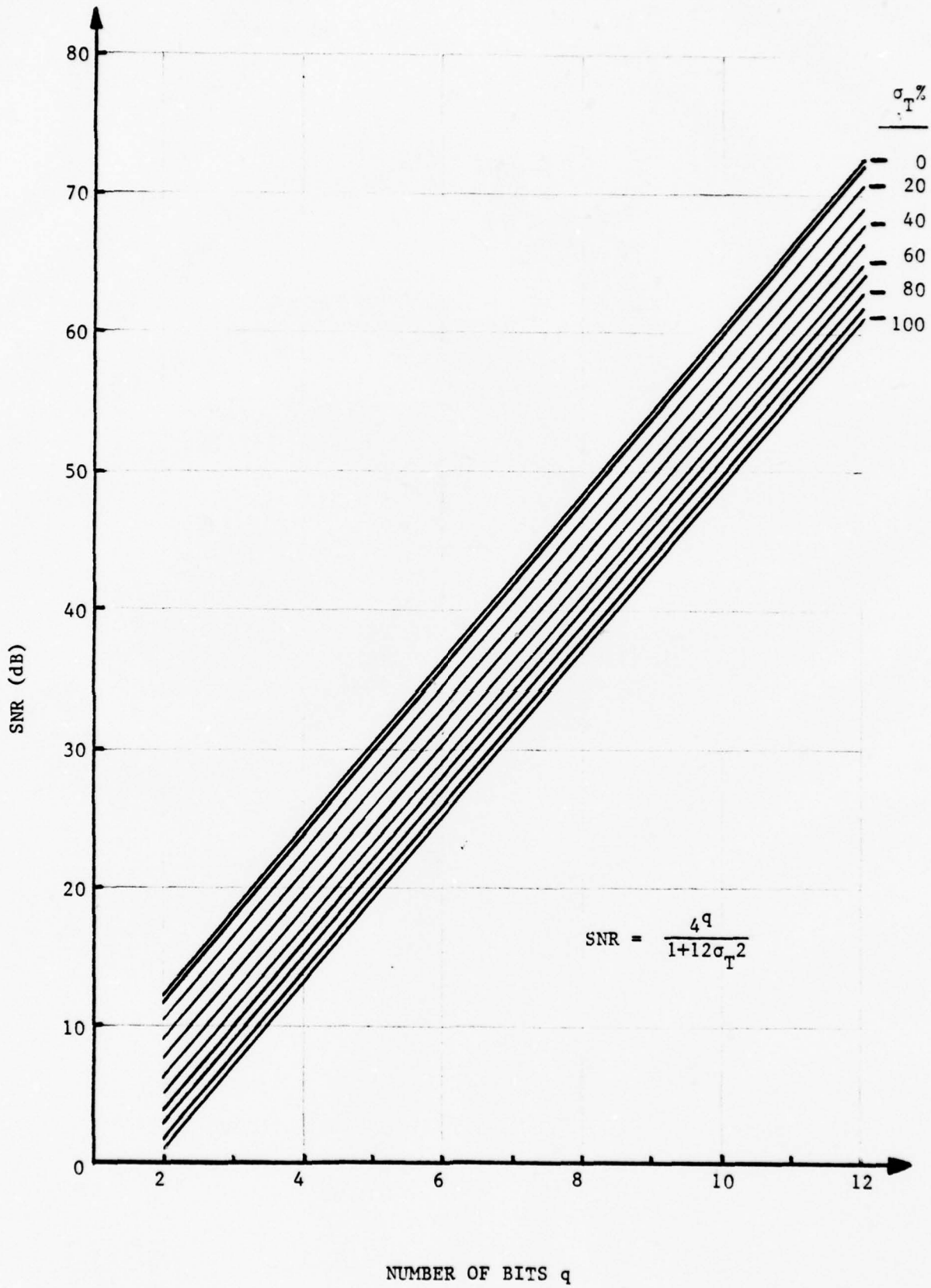

Figure 3-3. SNR Versus Number of Bits For Uniform Amplitude Statistics.

the performance of the A/D converter as a function of crest factor η. Too small a crest factor results in excessive overload noise while too large a crest factor results in a performance degradation because the full resolution of the A/D converter is not used. This is illustrated in Figure 3-4 for 10 bits.

There is thus an optimum crest factor for each number of bits q. This optimum crest factor is shown in Figure 3-5 for zero, 40%, and 90% level errors. Observe that the optimum crest factor increases almost linearly with the number of bits unlike the uniform amplitude statistics case. For this optimum crest factor, Figure 3-6 gives SNR versus the number of bits q.

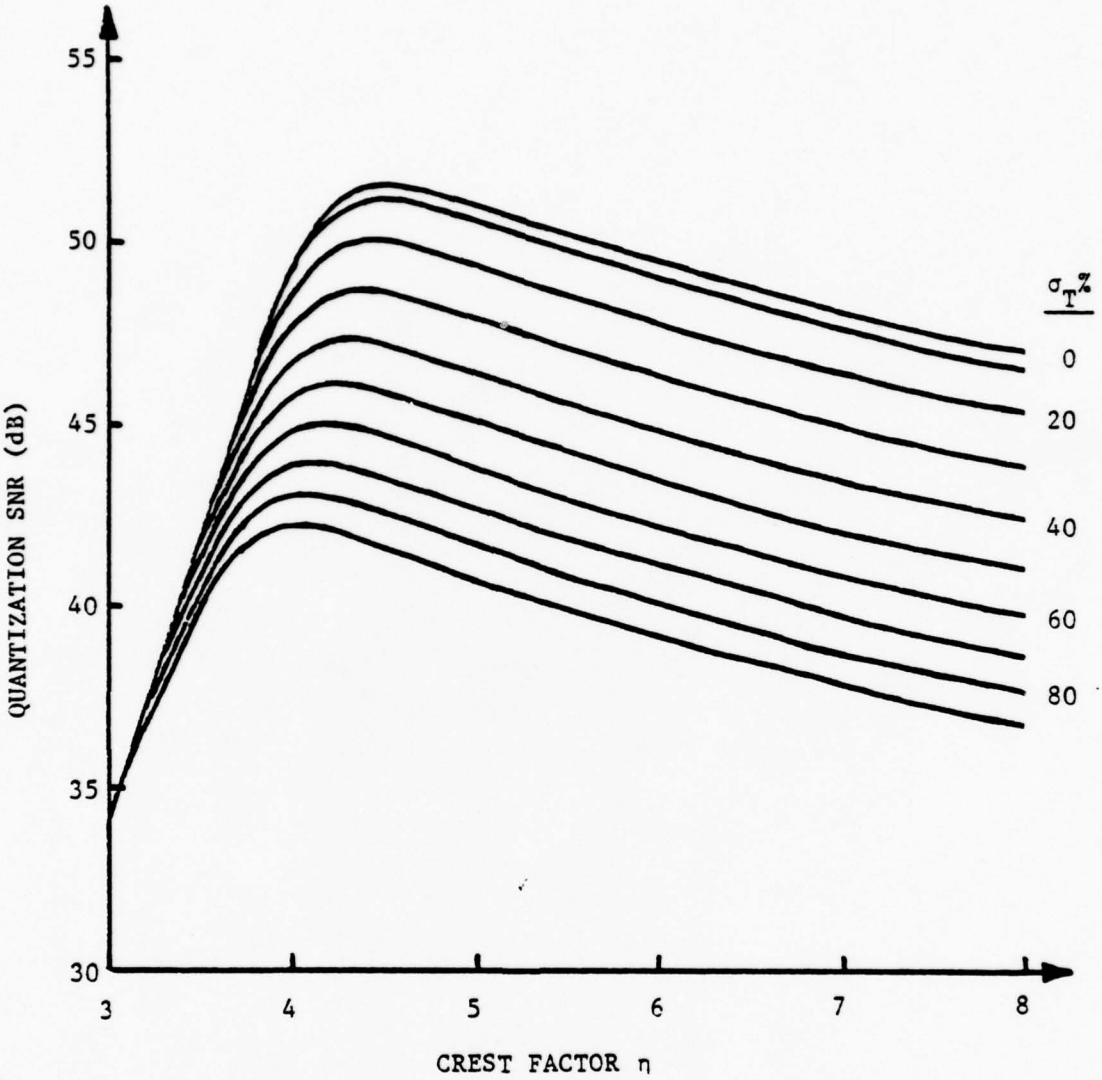

Figure 3-4. Quantization SNR Versus Crest Factor

For 10 bits and Gaussian Amplitude Statistics.

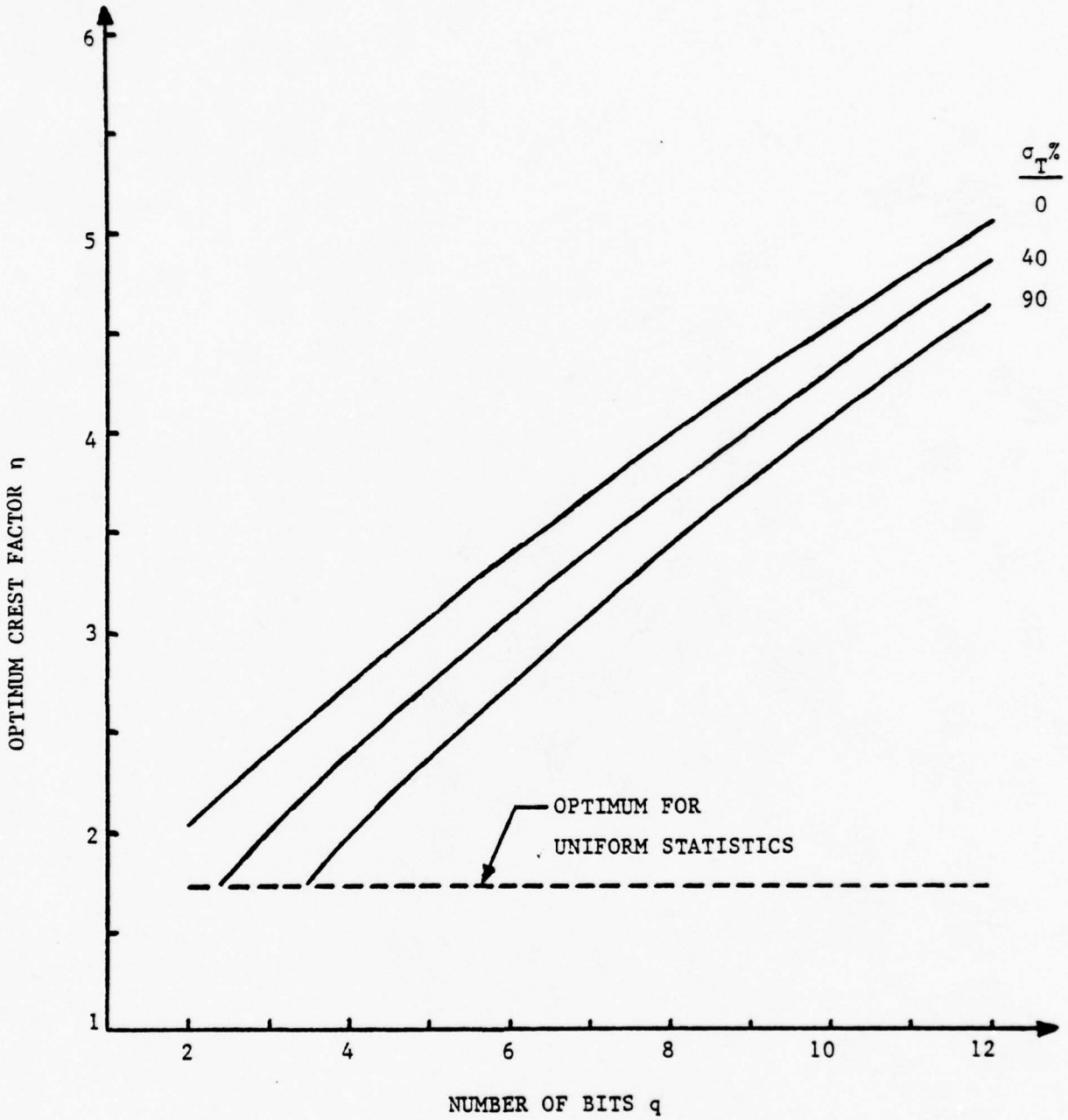

Figure 3-5. Optimum Crest Factor Versus Number of Bits for Gaussian Amplitude Statistics.

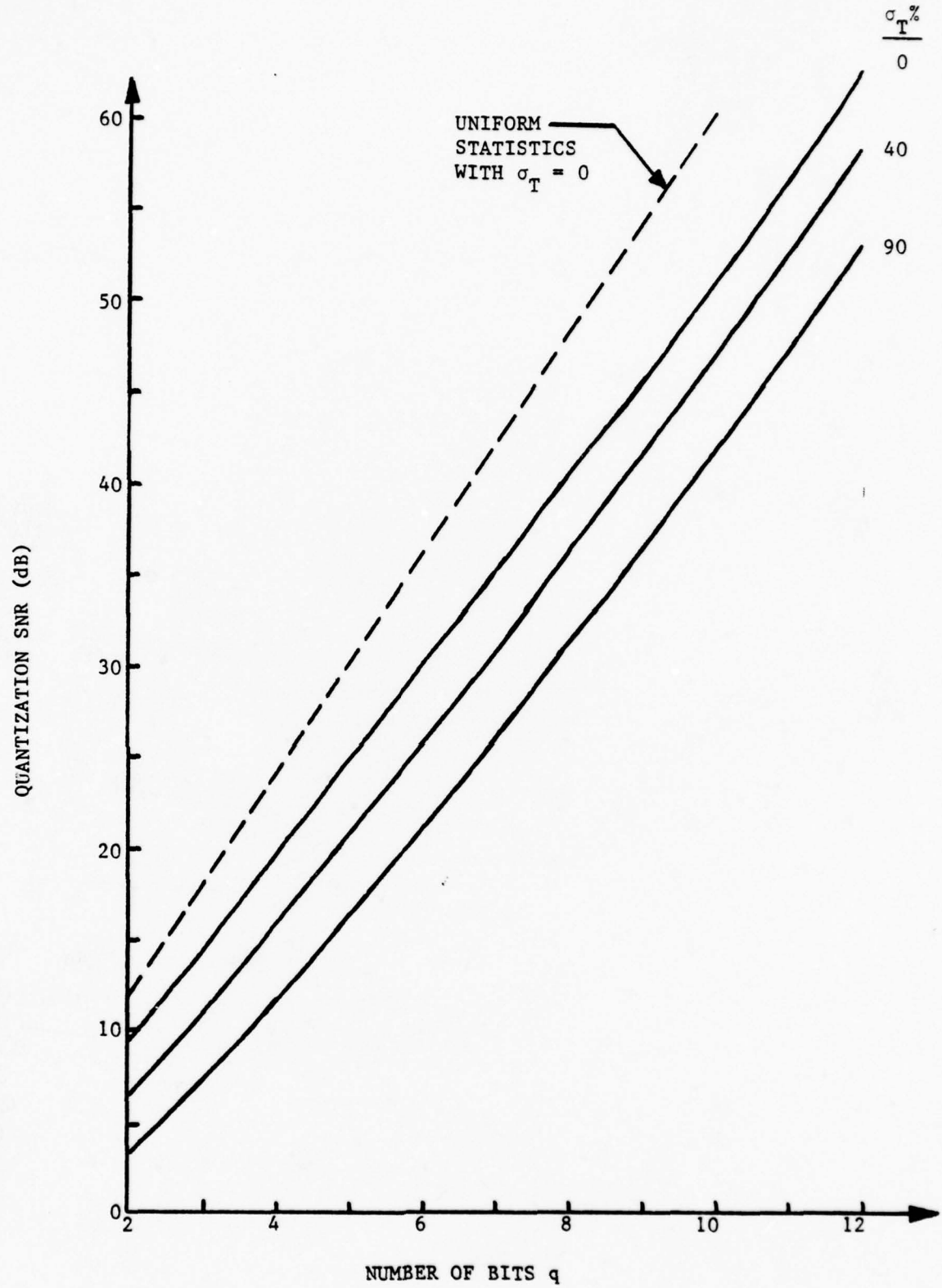

Figure 3-6. Quantization SNR Versus Number of Bits for Gaussian Amplitude Statistics.

4. Design Curves for Gaussian Statistics

Design curves of SNR as a function of crest factor for uniform quantizers and Gaussian amplitude statistics follow. They cover the range of 2 to 30 bits and are parametric in RMS level errors. These curves were obtained from the equations given in Appendix A.

For example, a 10 bit A/D converter with 40% level error has a SNR = 47.3 dB at the optimum crest factor of n = 4.3. With a normalized sampling rate of 2.5, the SNSR = 48.3 dB in the center of the band and 3 dB less at band edge.

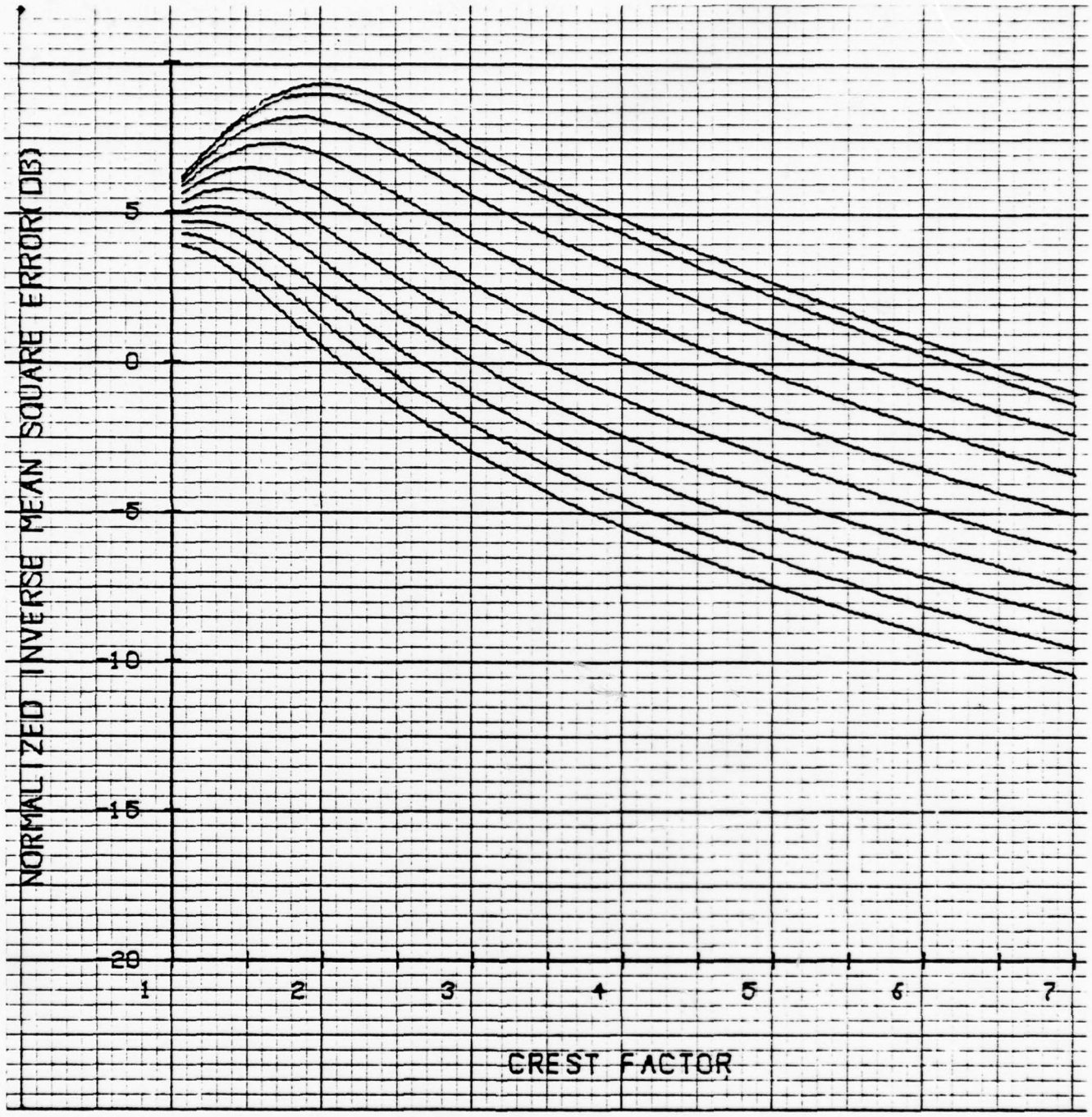

Uniform Quantization SNR Versus Crest Factor for 2 Bits and 0, 10, ... 80, 90 Percent Normalized Level Errors.

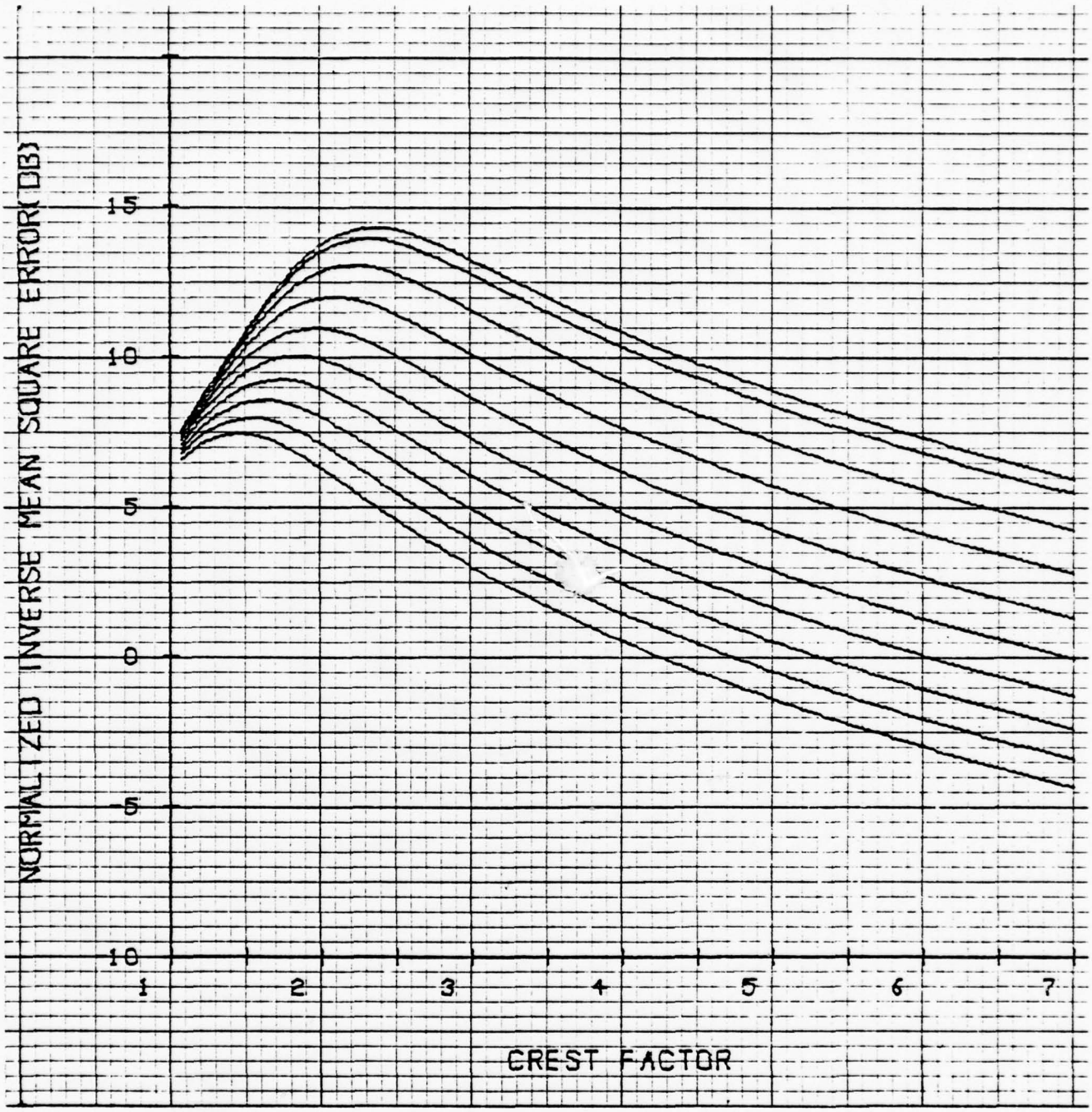

Uniform Quantization SNR Versus Crest Factor for 3 Bits and 0, 10, ... 80, 90 Percent Normalized Level Errors.

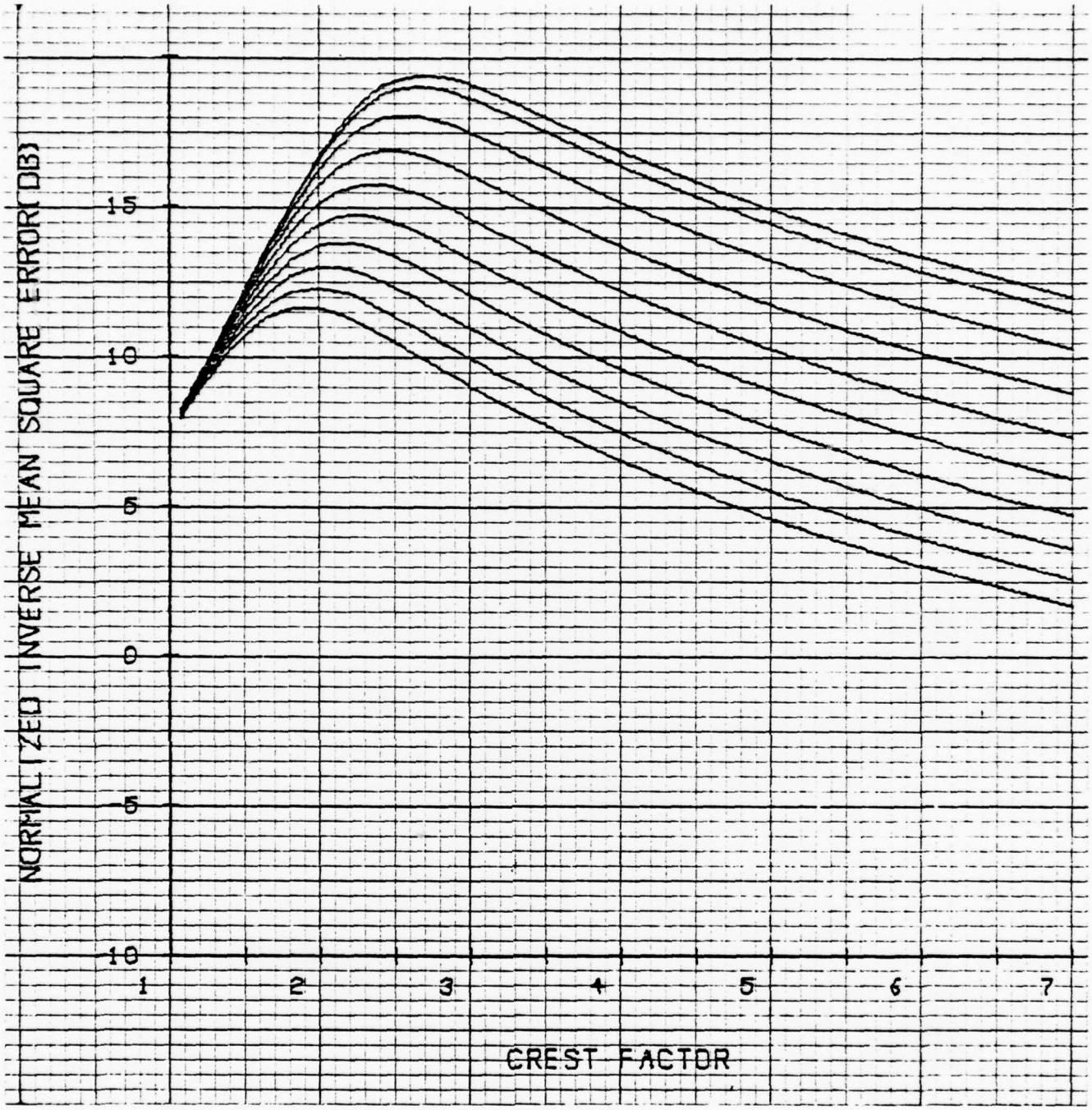

Uniform Quantization SNR Versus Crest Factor for 4 Bits and

0, 10, ... 80, 90 Percent Normalized Level Errors.

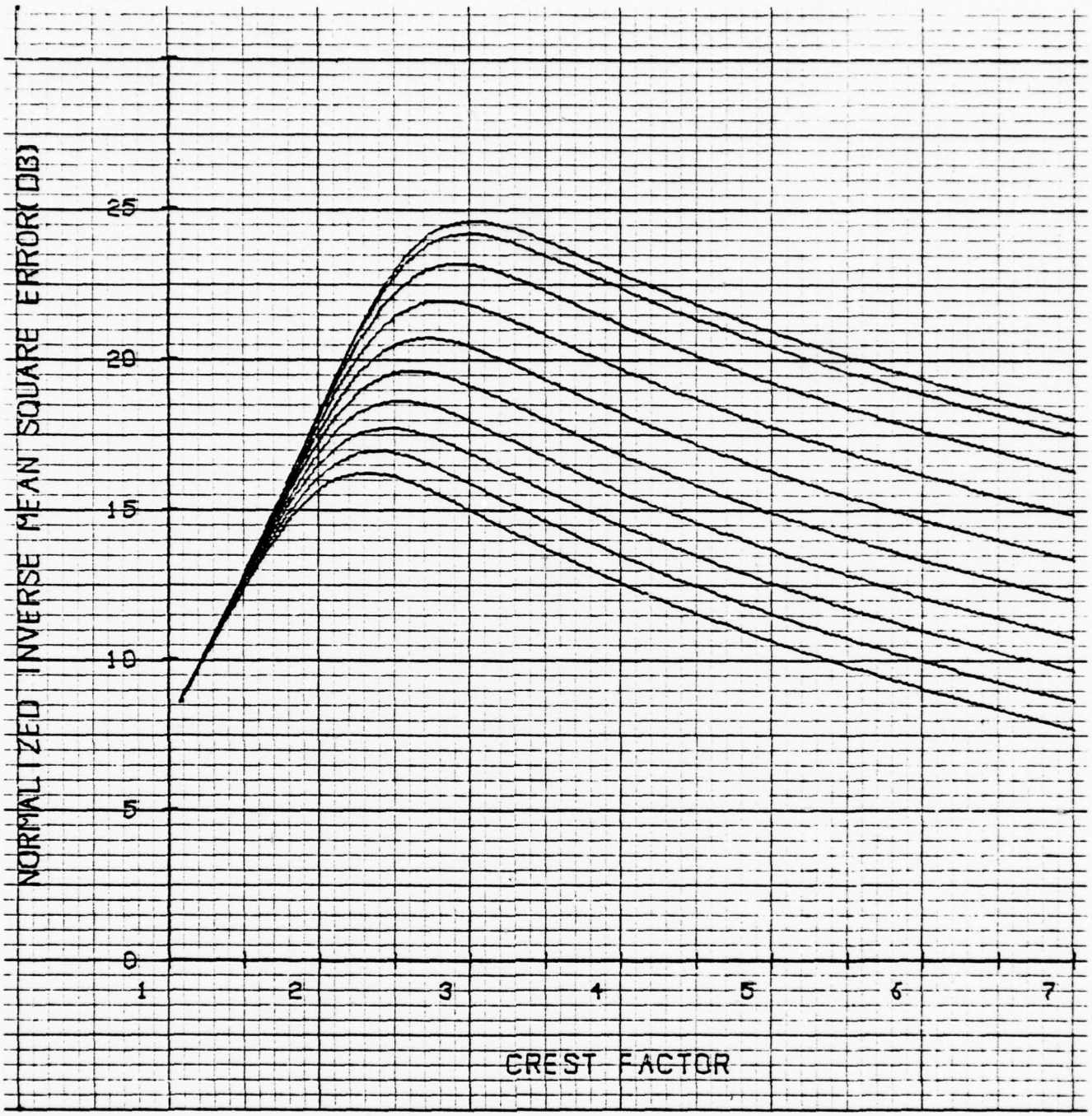

Uniform Quantization SNR Versus Crest Factor for 5 Bits and

0, 10, ... 80, 90 Percent Normalized Level Errors.

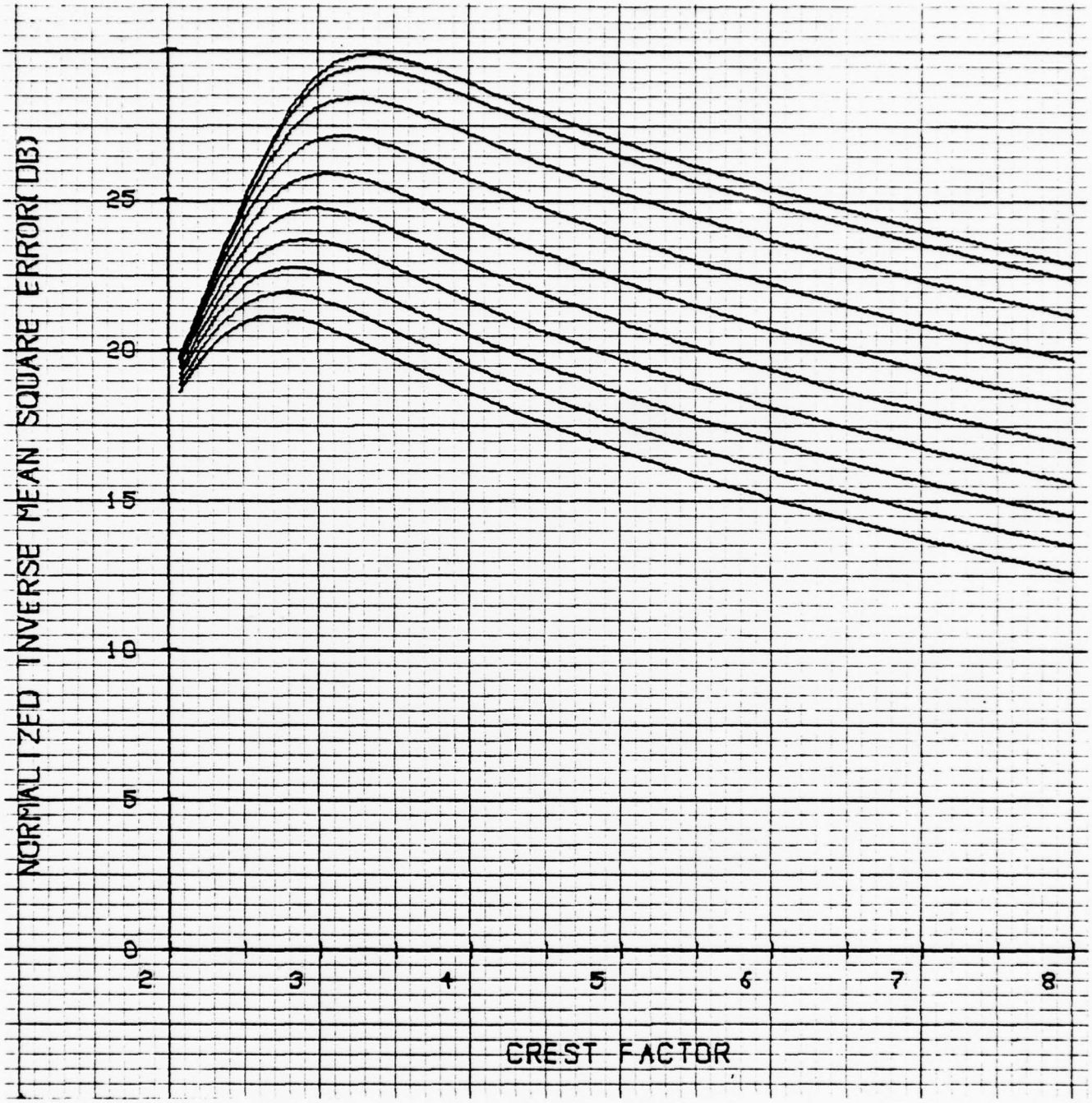

Uniform Quantization SNR Versus Crest Factor for 6 Bits and

0, 10, ... 80, 90 Percent Normalized Level Errors.

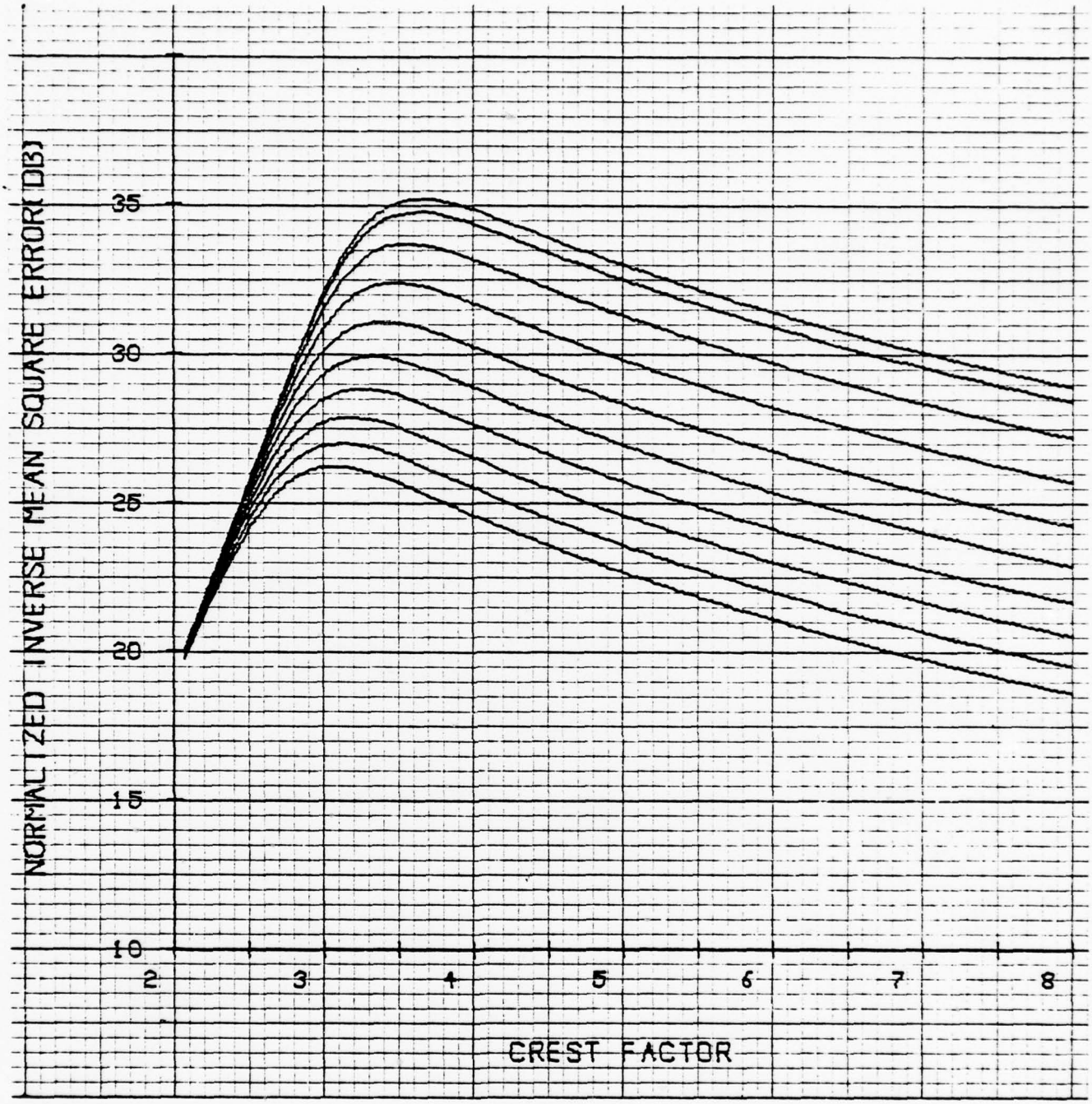

Uniform Quantization SNR Versus Crest Factor for 7 Bits and 0, 10, ... 80, 90 Percent Normalized Level Errors.

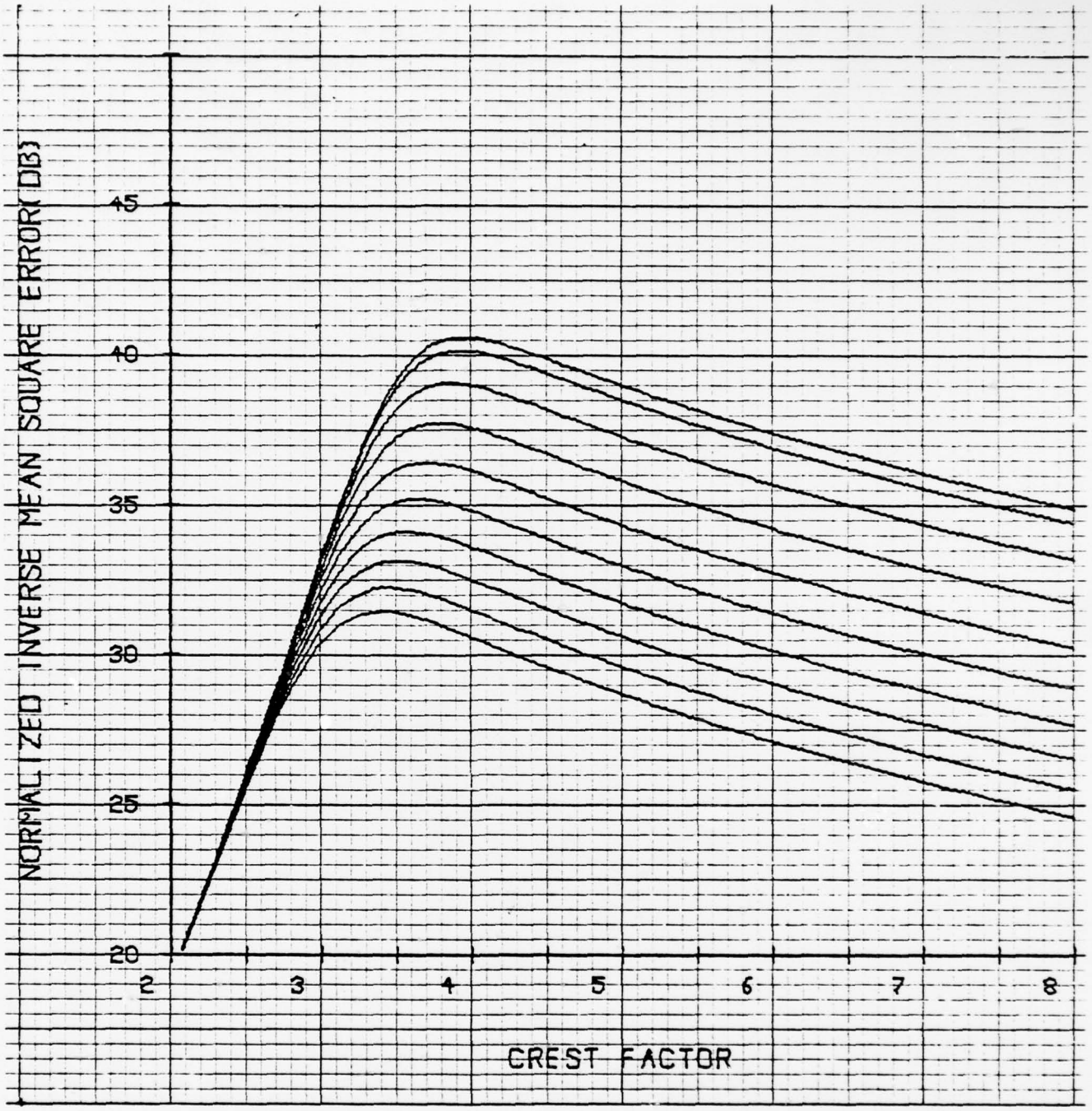

Uniform Quantization SNR Versus Crest Factor for 8 **Bits and**

0, 10, ... 80, 90 Percent Normalized Level Errors.

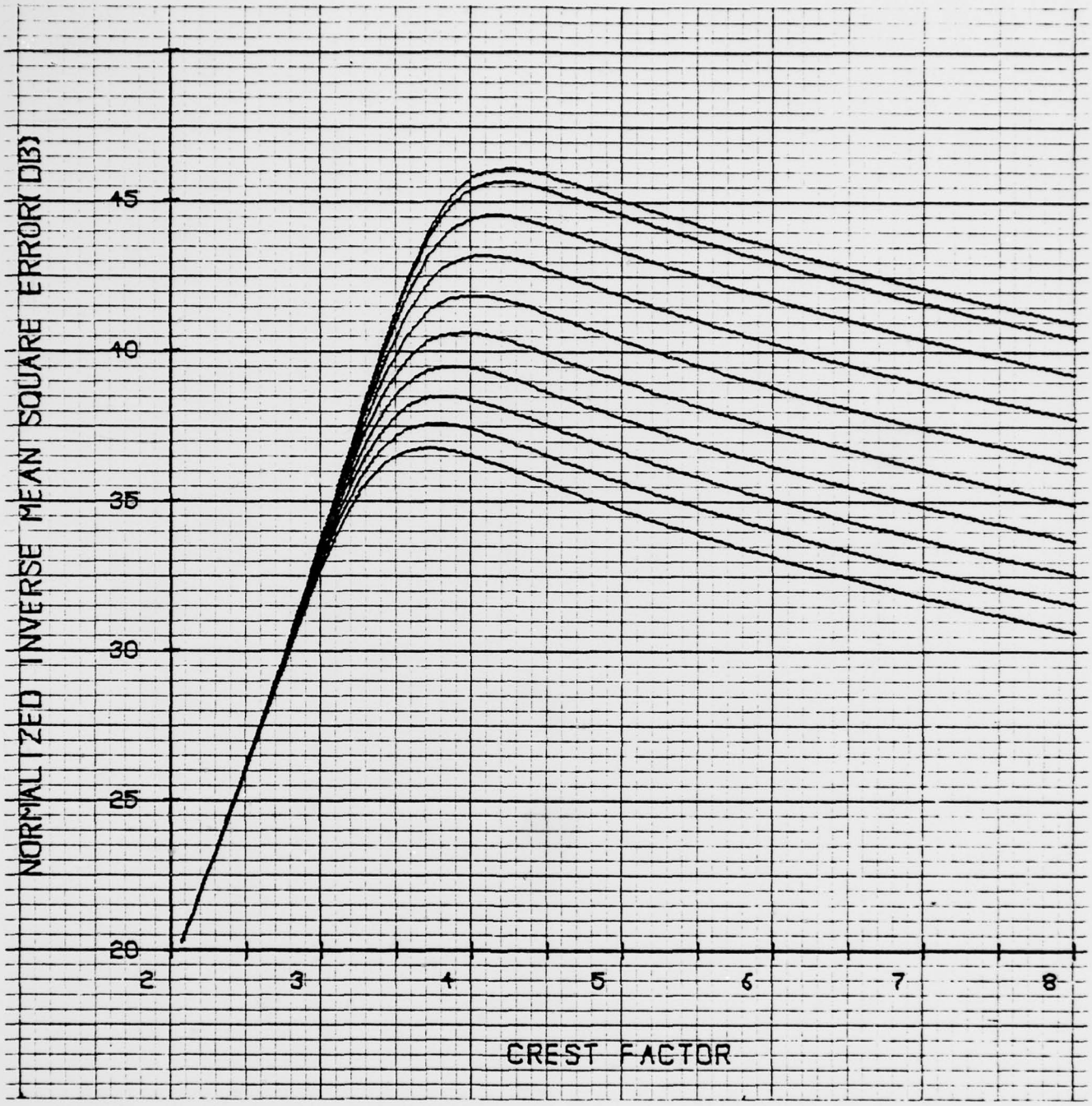

Uniform Quantization SNR Versus Crest Factor for 9 Bits and 0, 10, ... 80, 90 Percent Normalized Level Errors.

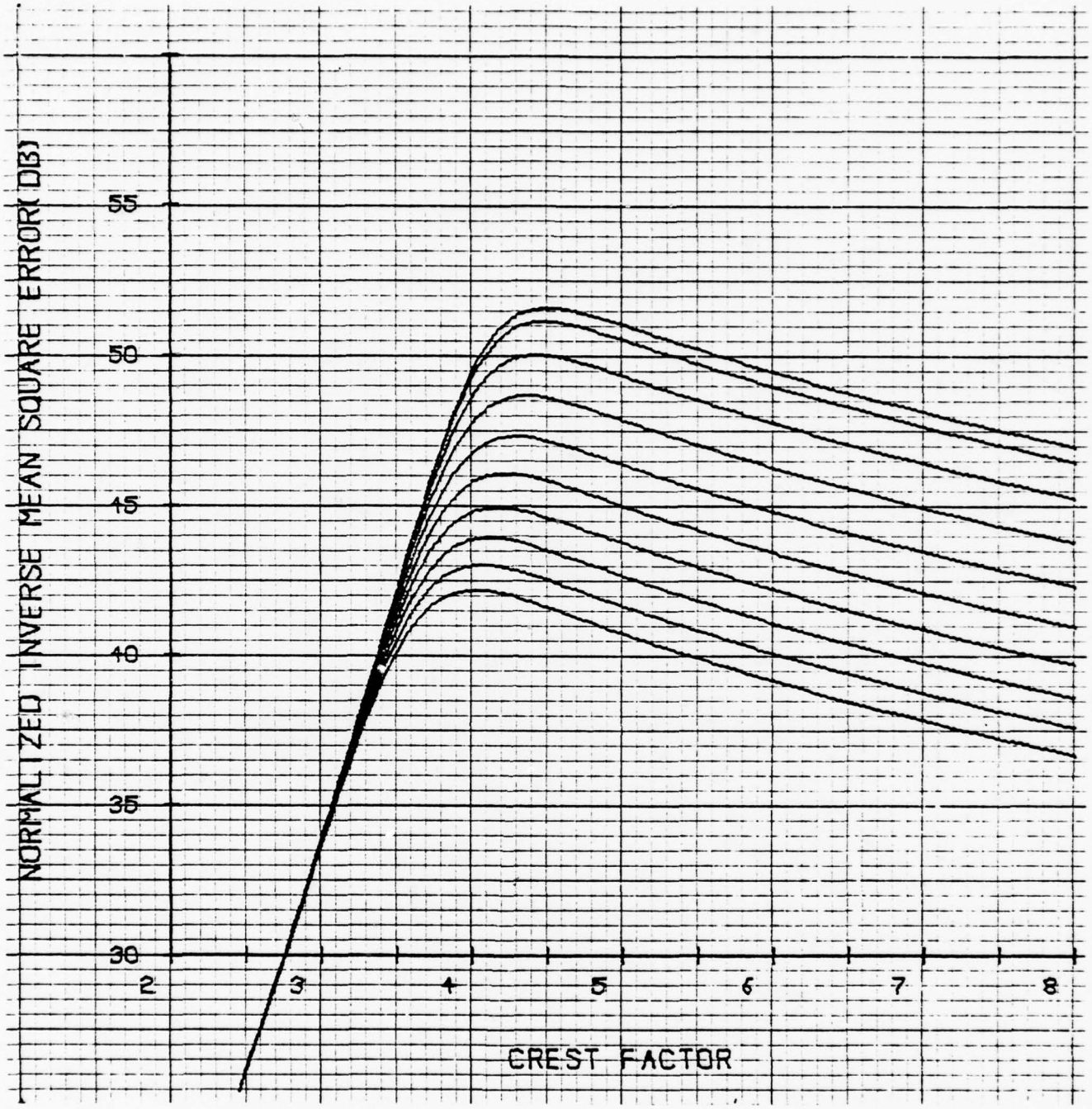

Uniform Quantization SNR Versus Crest Factor for 10 Bits and

0, 10, ... 80, 90 Percent Normalized Level Errors.

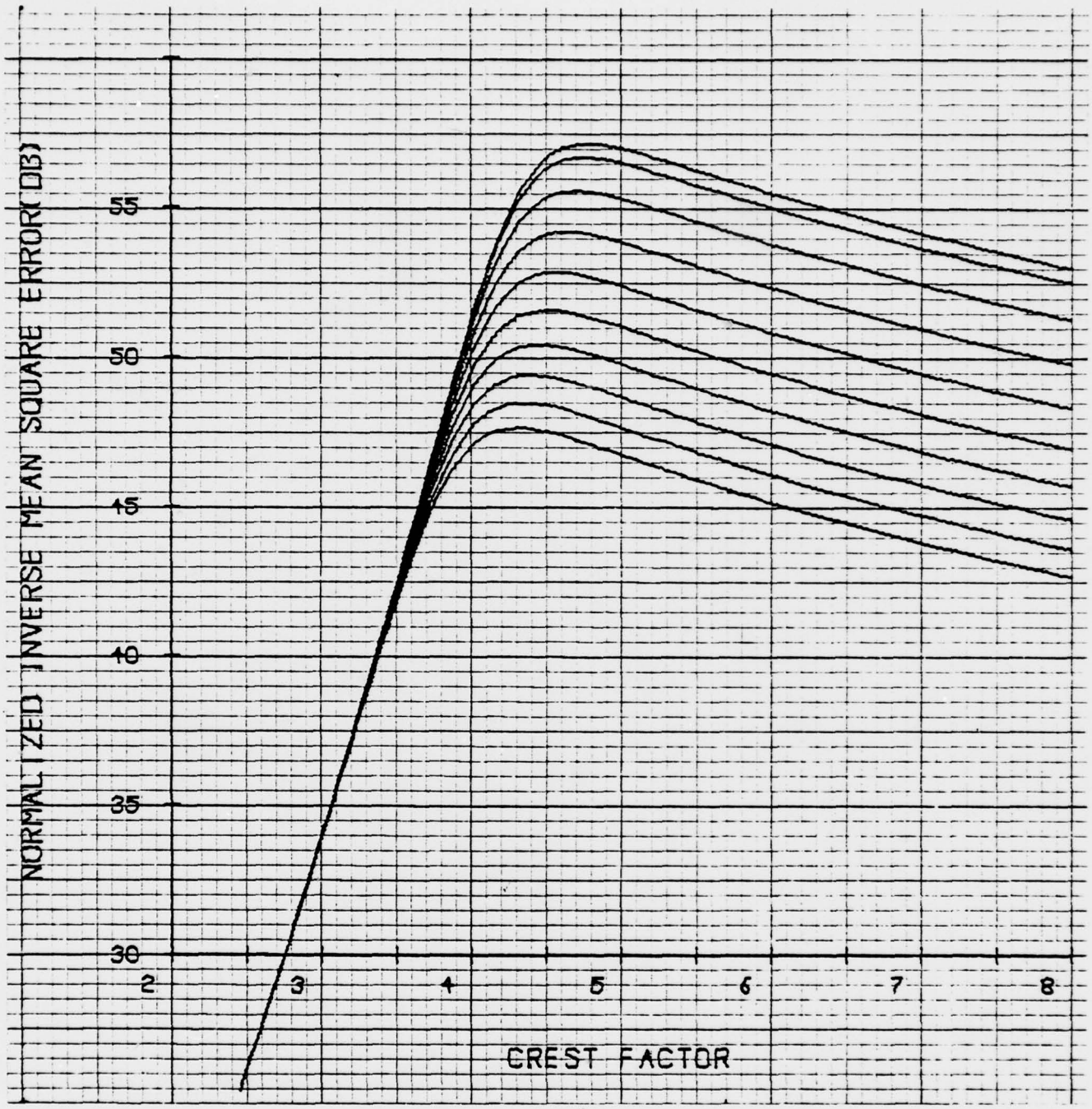

Uniform Quantization SNR Versus Crest Factor for 11 Bits and

0, 10, ... 80, 90 Percent Normalized Level Errors.

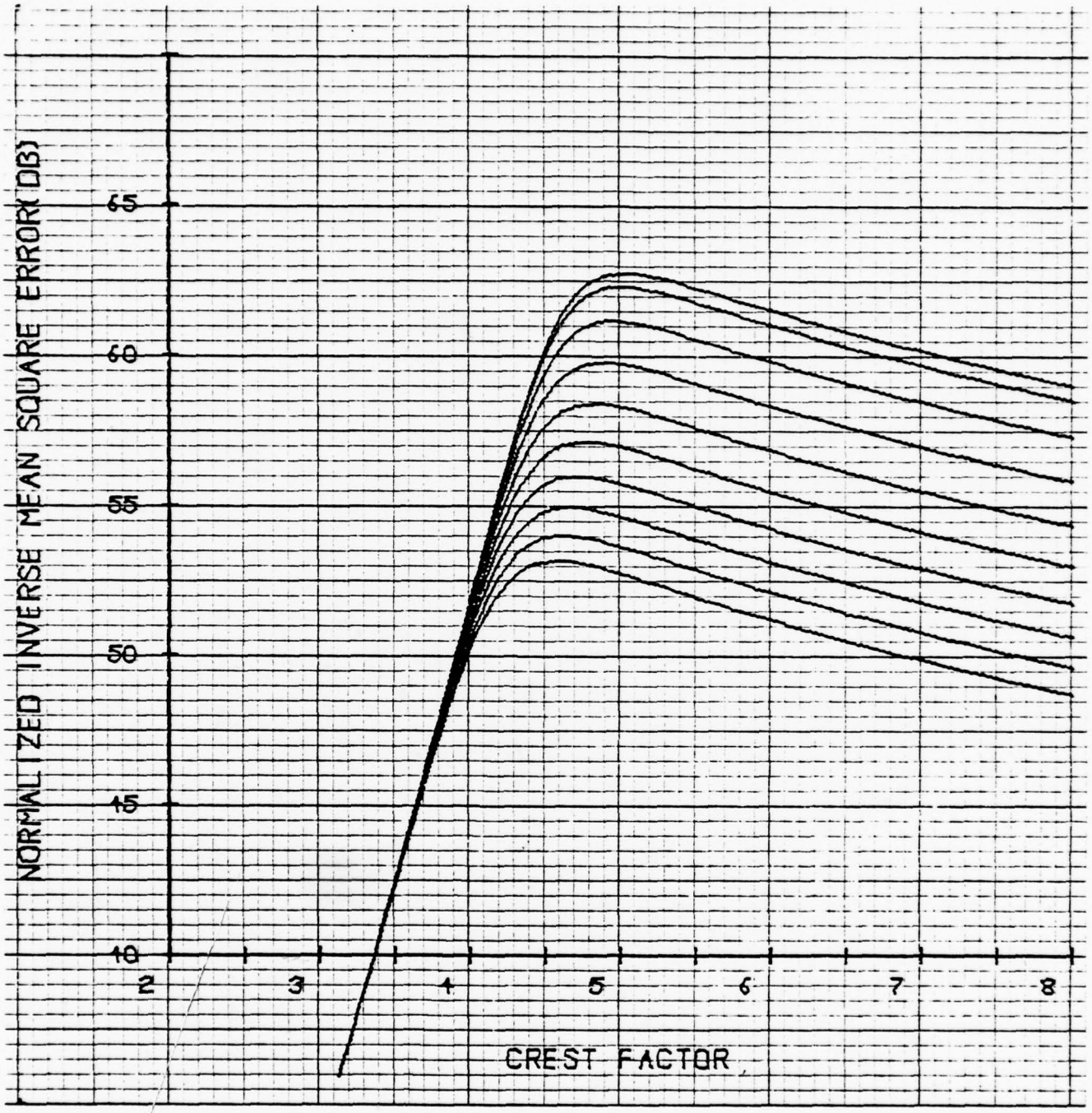

Uniform Quantization SNR Versus Crest Factor for 12 Bits and 0, 10, ... 80, 90 Percent Normalized Level Errors.

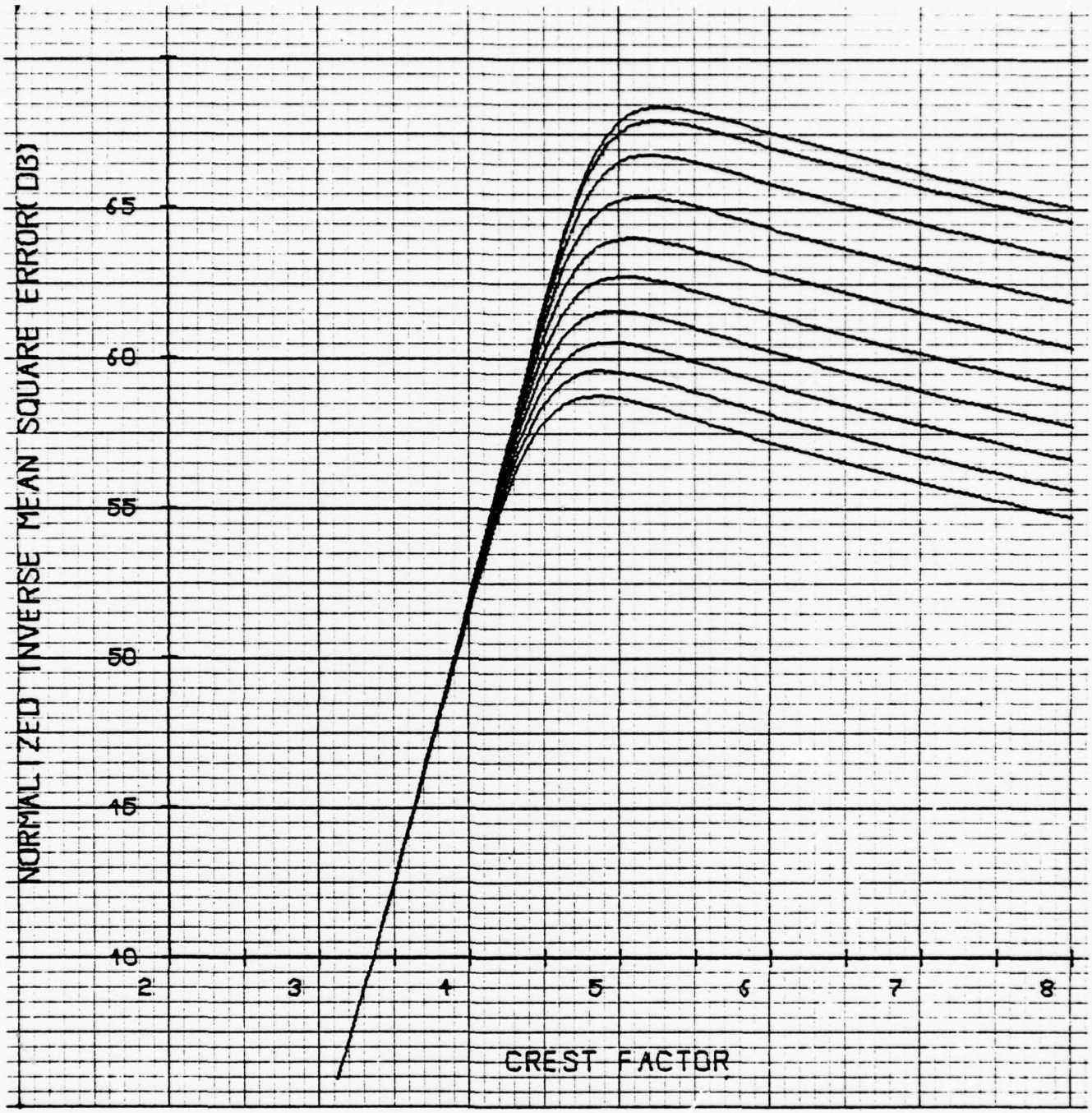

Uniform Quantization SNR Versus Crest Factor for 13 Bits and 0, 10, ... 80, 90 Percent Normalized Level Errors.

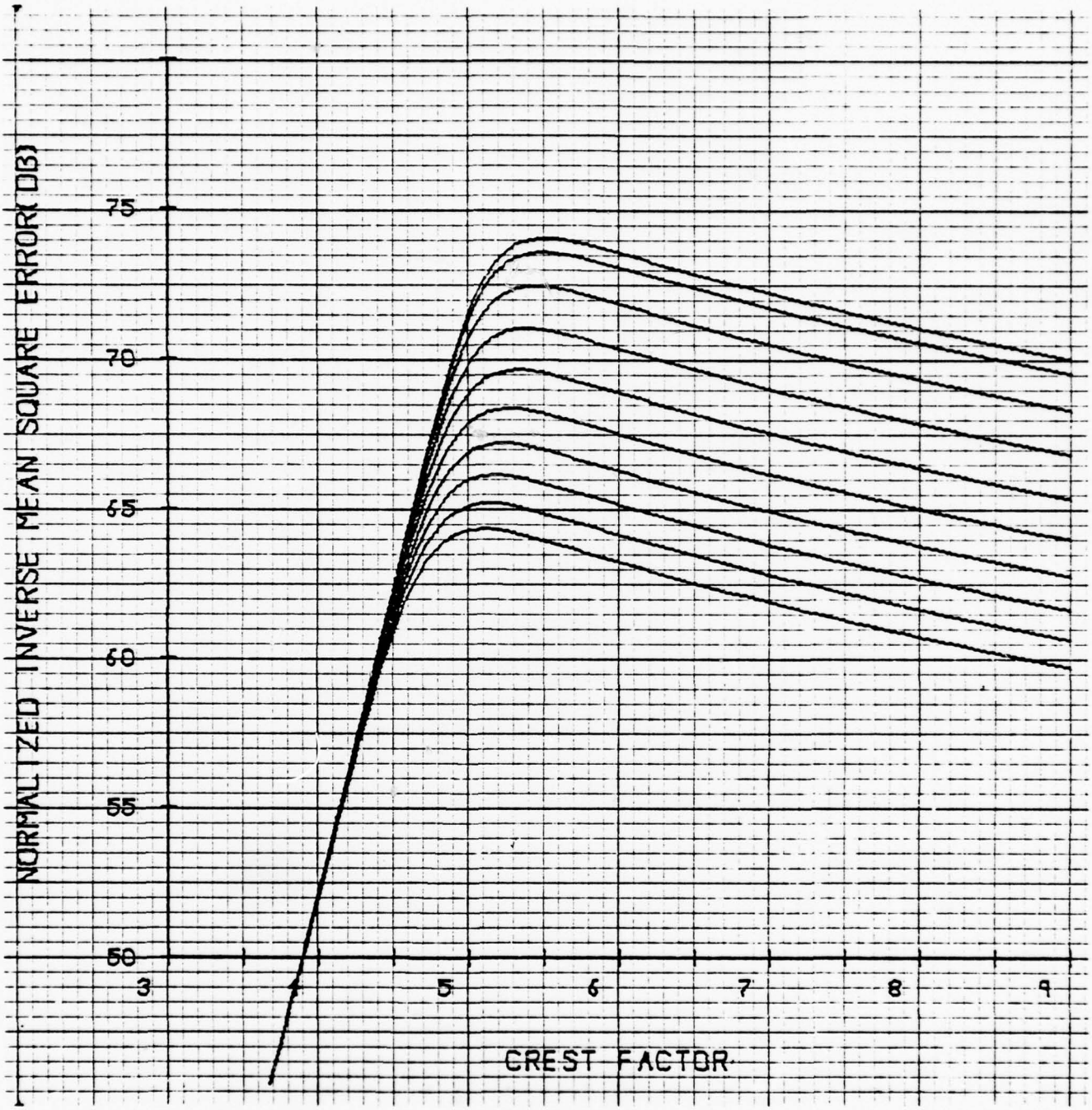

Uniform Quantization SNR Versus Crest Factor for 14 Bits and 0, 10, ... 80, 90 Percent Normalized Level Errors.

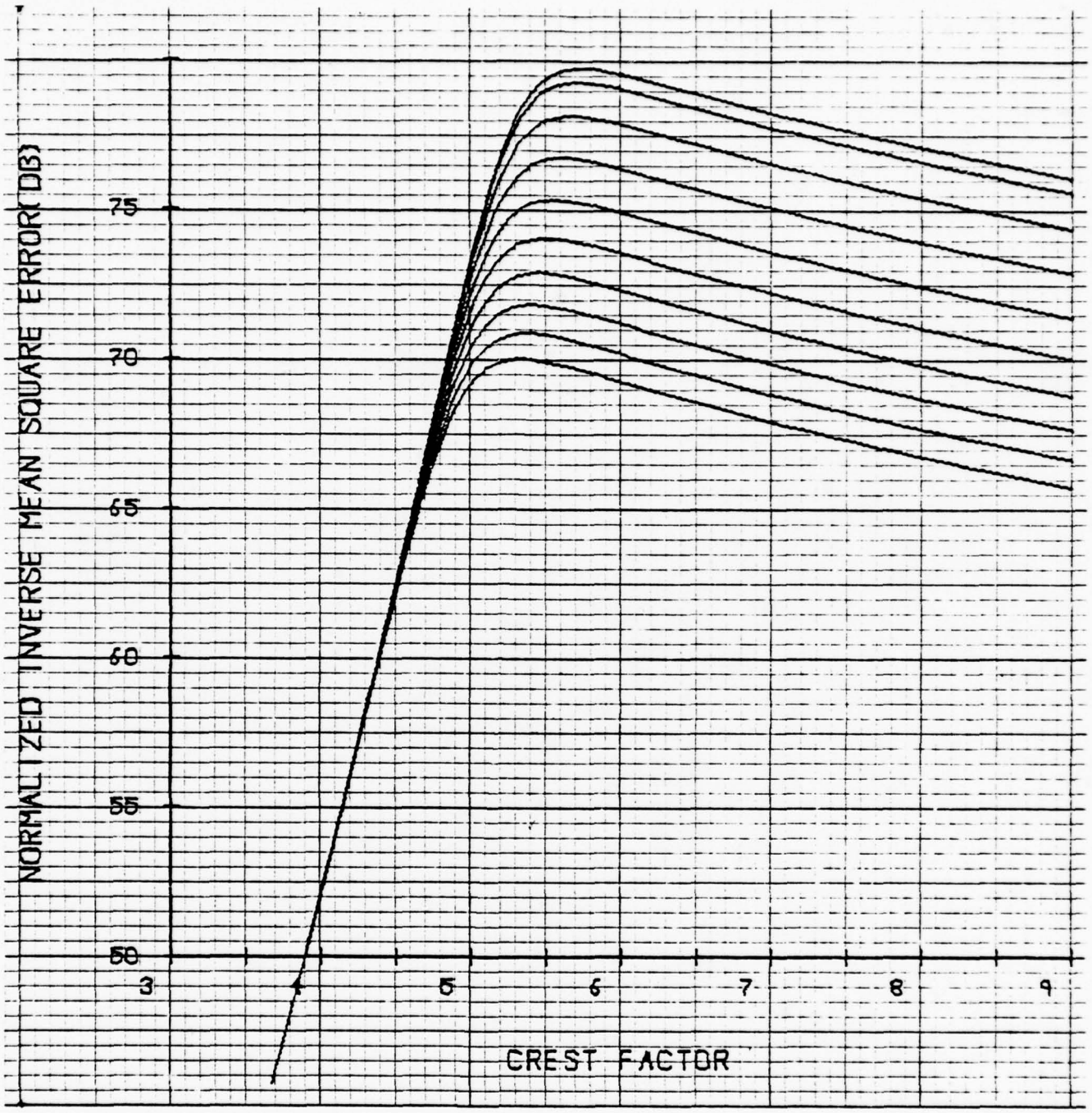

Uniform Quantization SNR Versus Crest Factor for 15 Bits and 0, 10, ... 80, 90 Percent Normalized Level Errors.

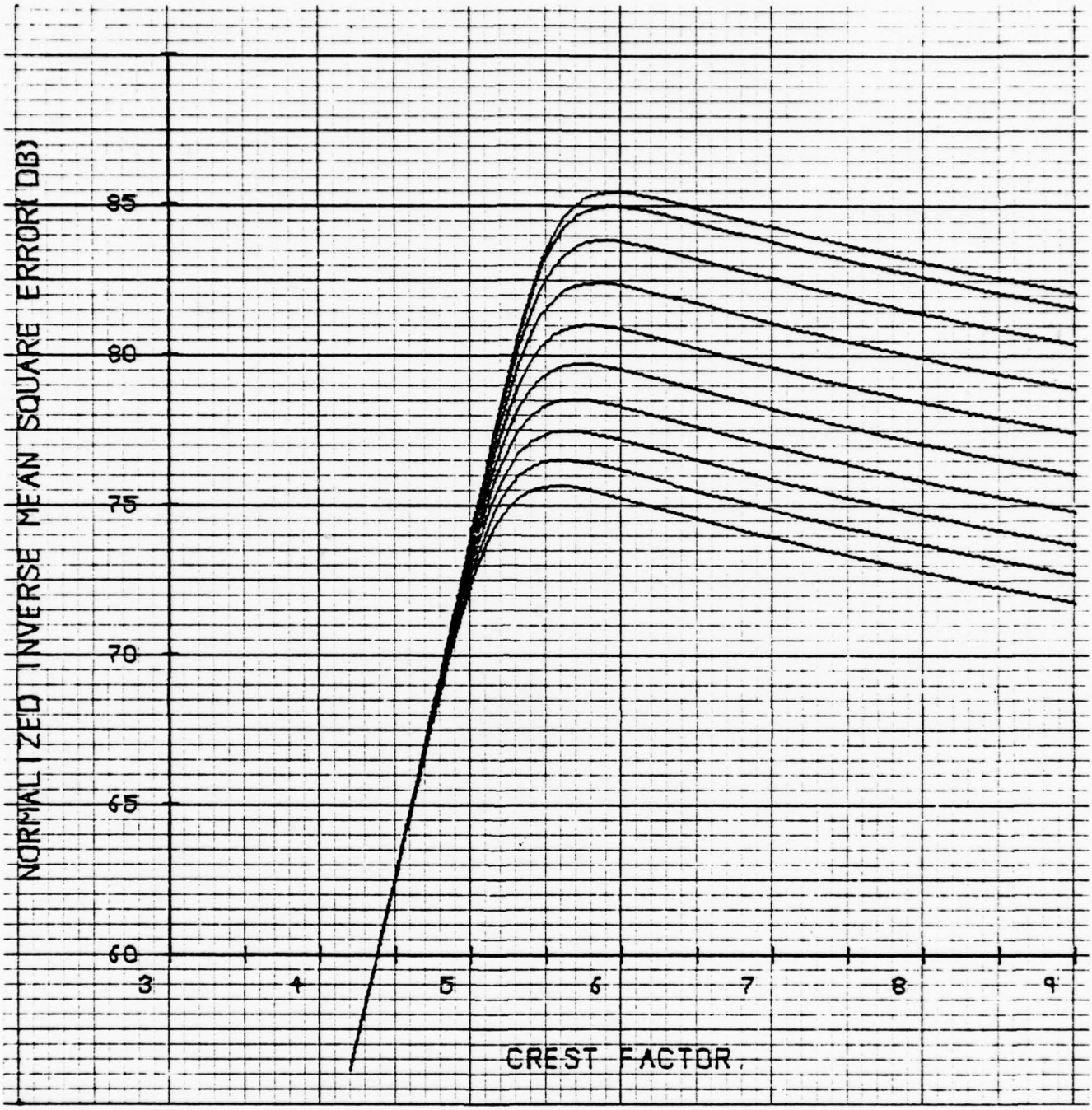

Uniform Quantization SNR Versus Crest Factor for 16 Bits and

0, 10, ... 80, 90 Percent Normalized Level Errors.

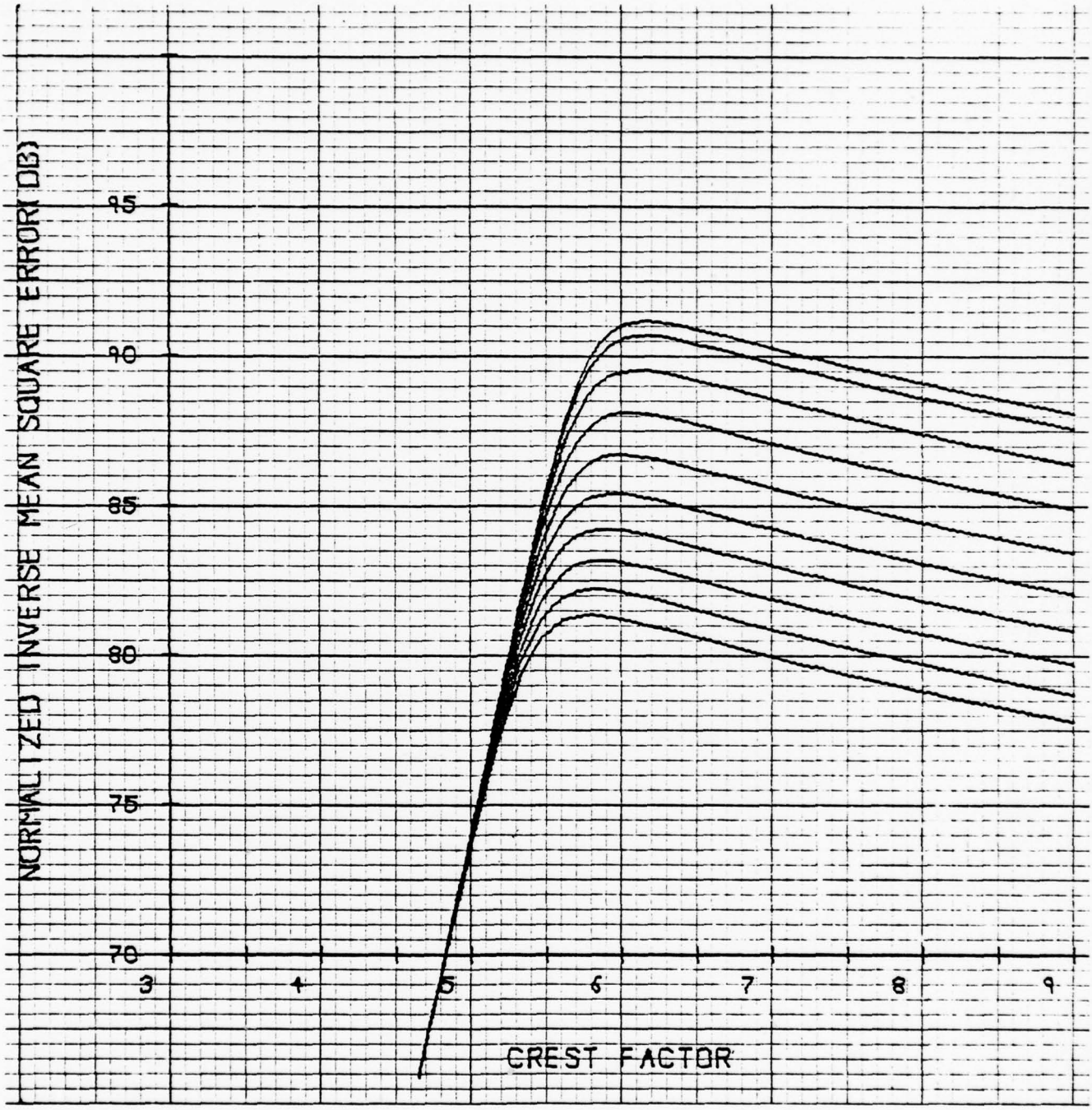

Uniform Quantization SNR Versus Crest Factor for 17 Bits and 0, 10, ... 80, 90 Percent Normalized Level Errors.

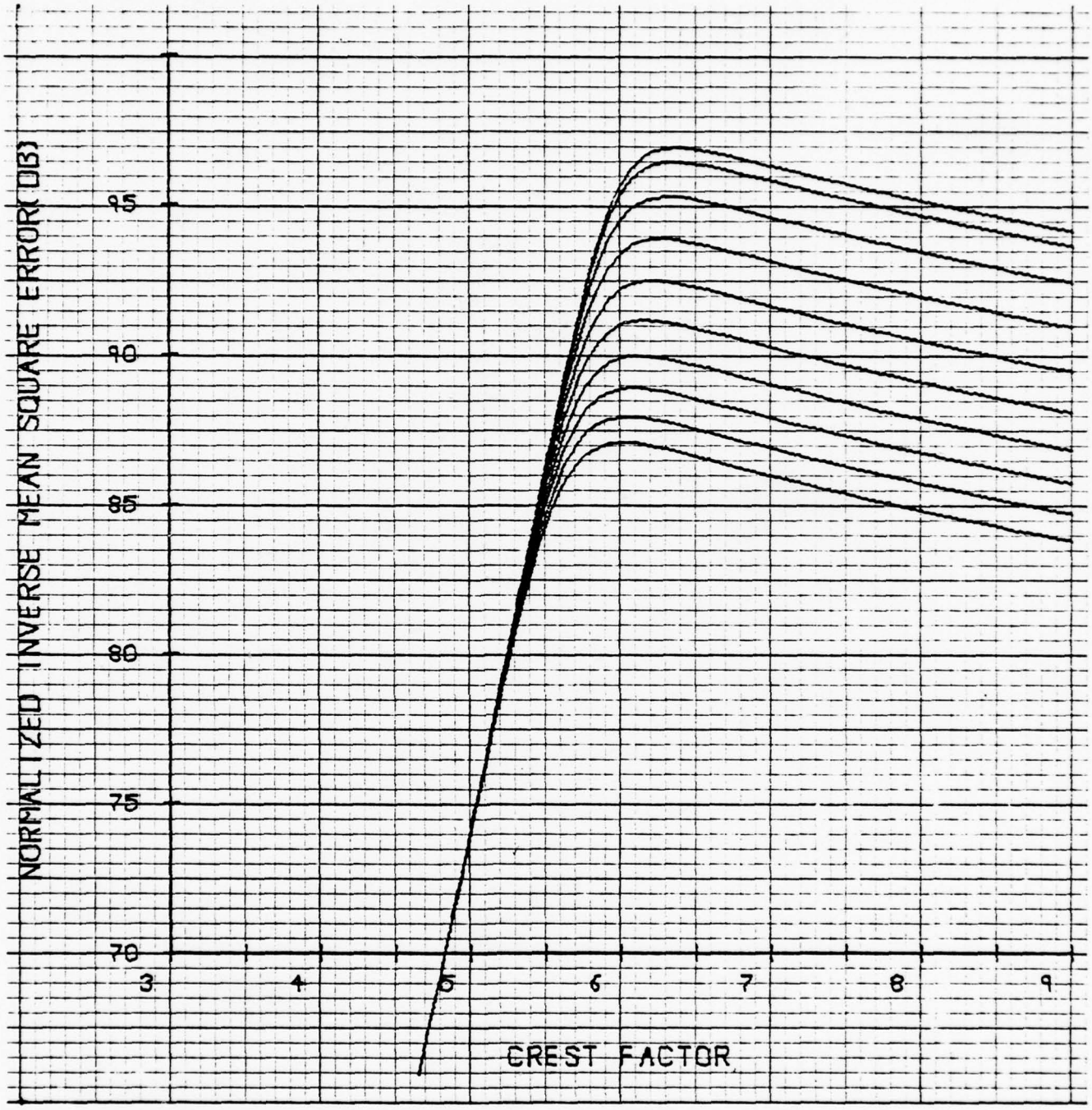

Uniform Quantization SNR Versus Crest Factor for 18 Bits and 0, 10, ... 80, 90 Percent Normalized Level Errors.

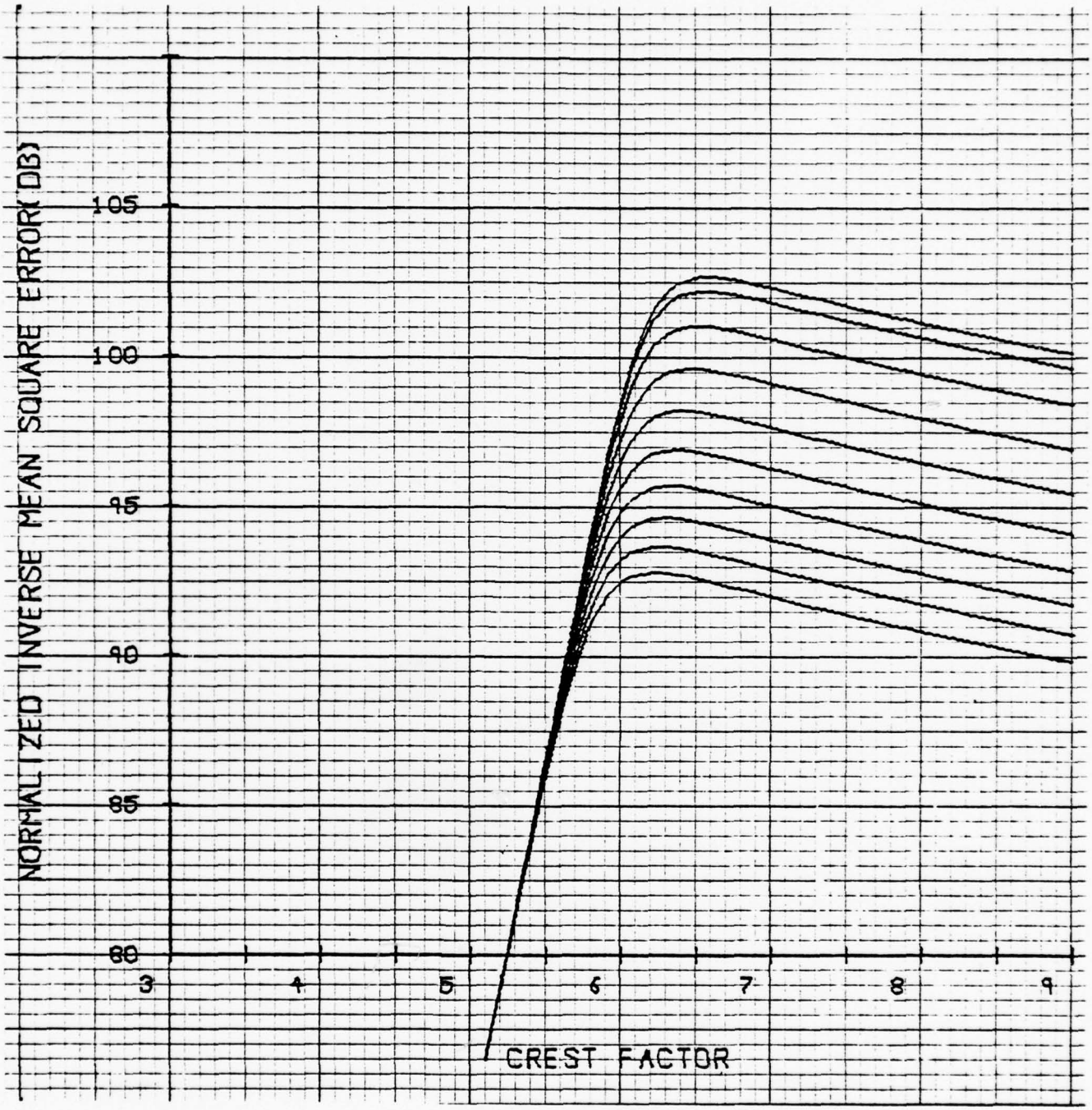

Uniform Quantization SNR Versus Crest Factor for 19 Bits and 0, 10, ... 80, 90 Percent Normalized Level Errors.

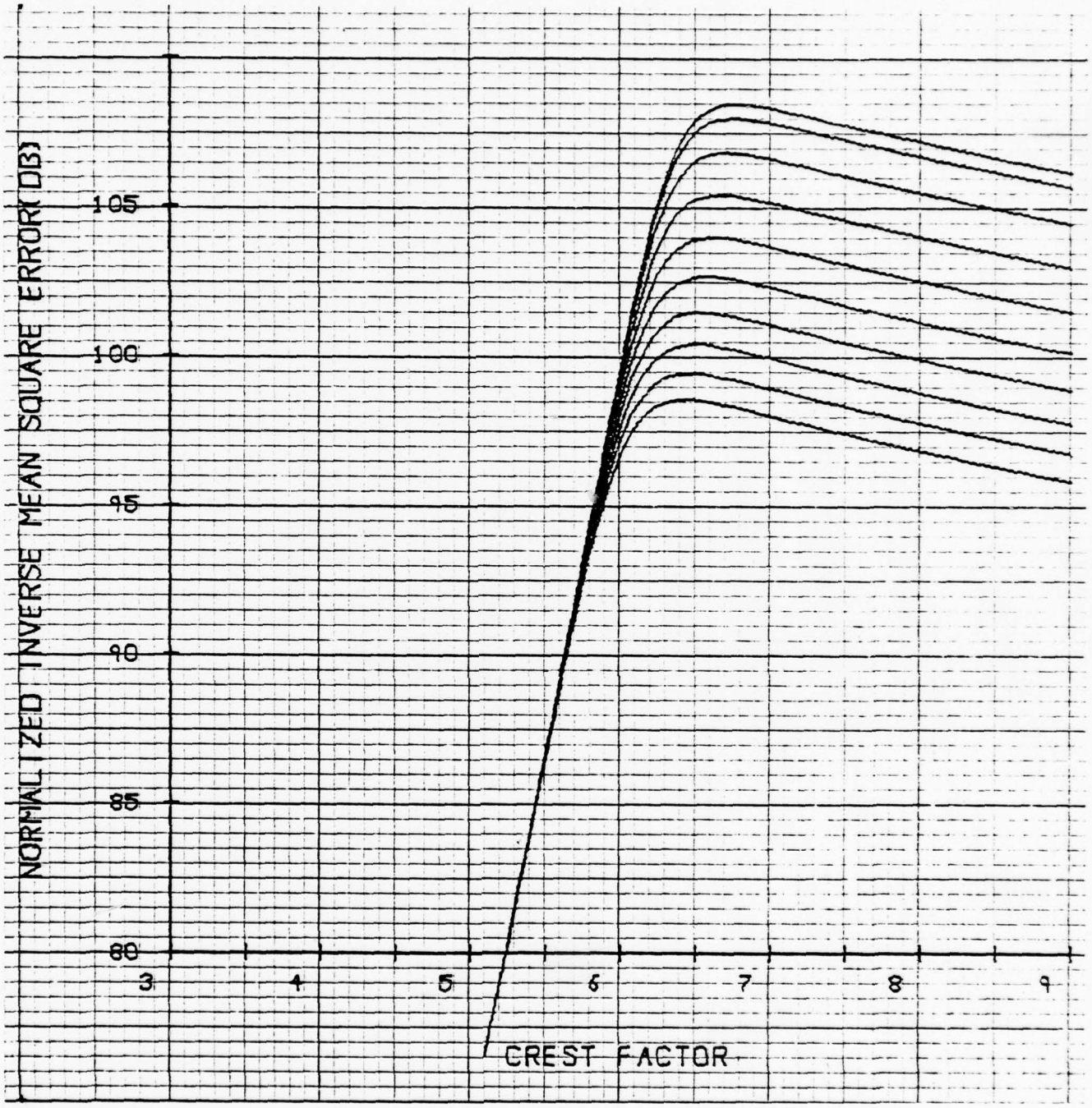

Uniform Quantization SNR Versus Crest Factor for 20 Bits and

0, 10, ... 80, 90 Percent Normalized Level Errors.

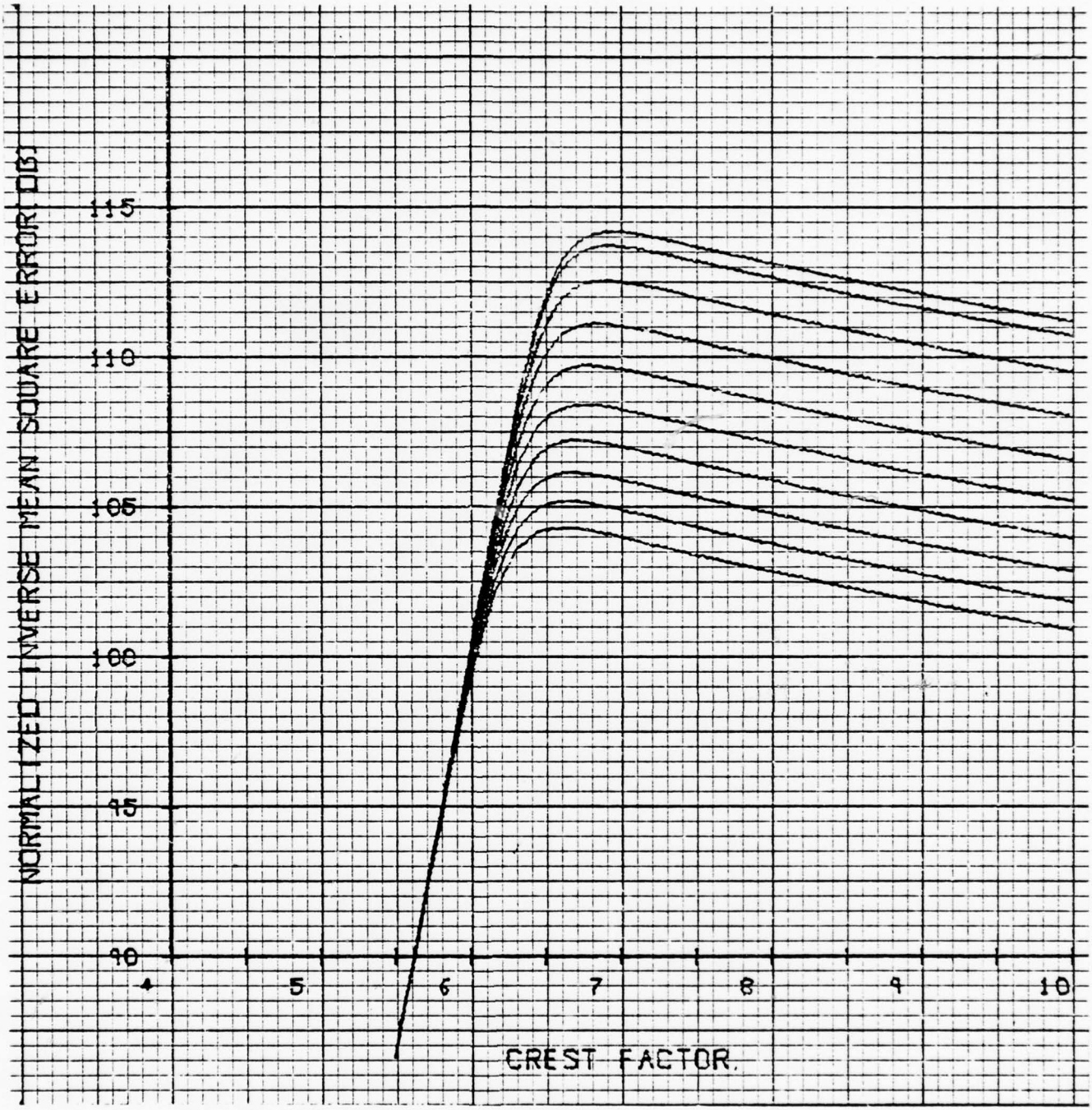

Uniform Quantization SNR Versus Crest Factor for 21 Bits and 0, 10, ... 80, 90 Percent Normalized Level Errors.

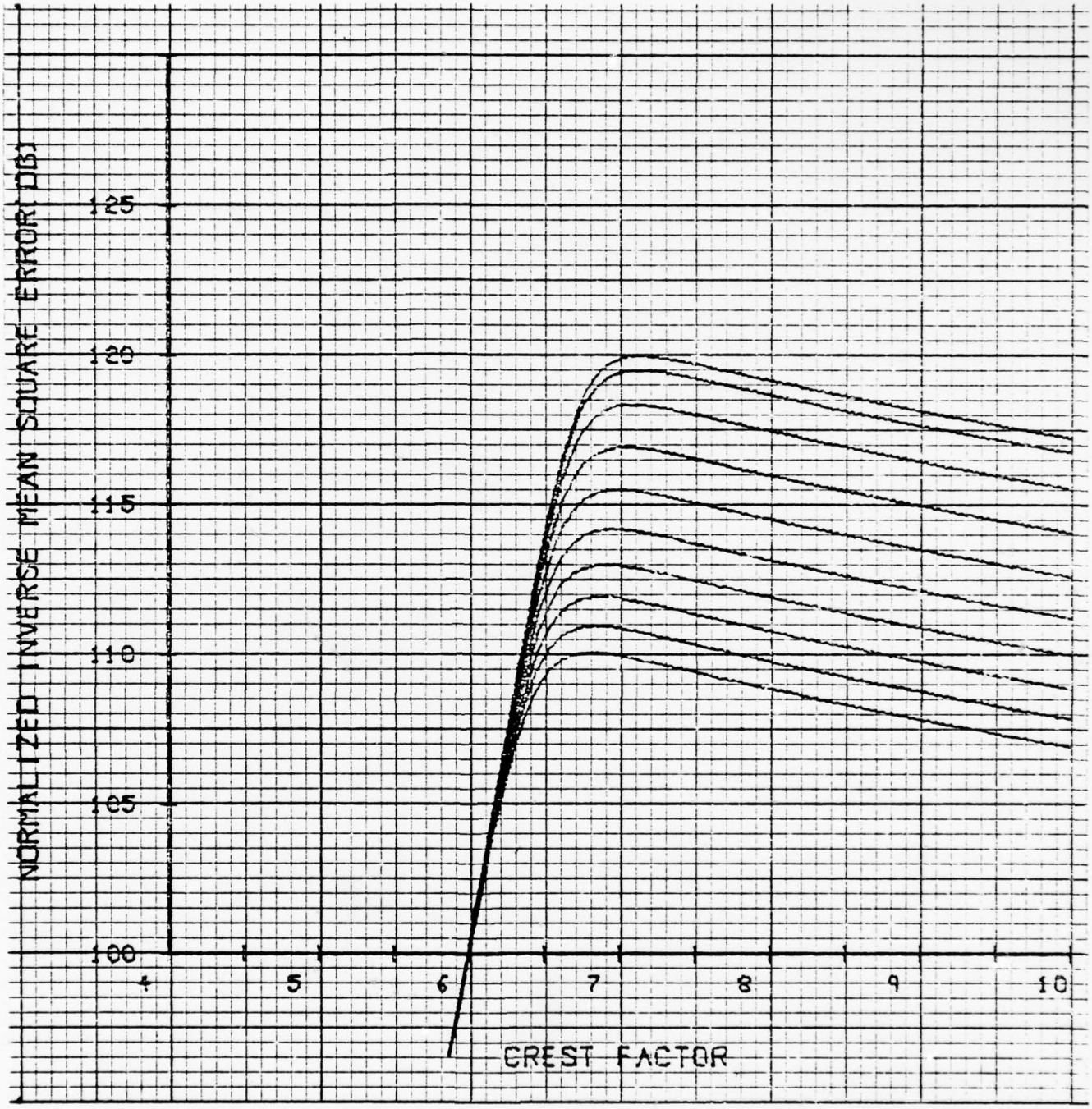

Uniform Quantization SNR Versus Crest Factor for 22 Bits and 0, 10, ... 80, 90 Percent Normalized Level Errors.

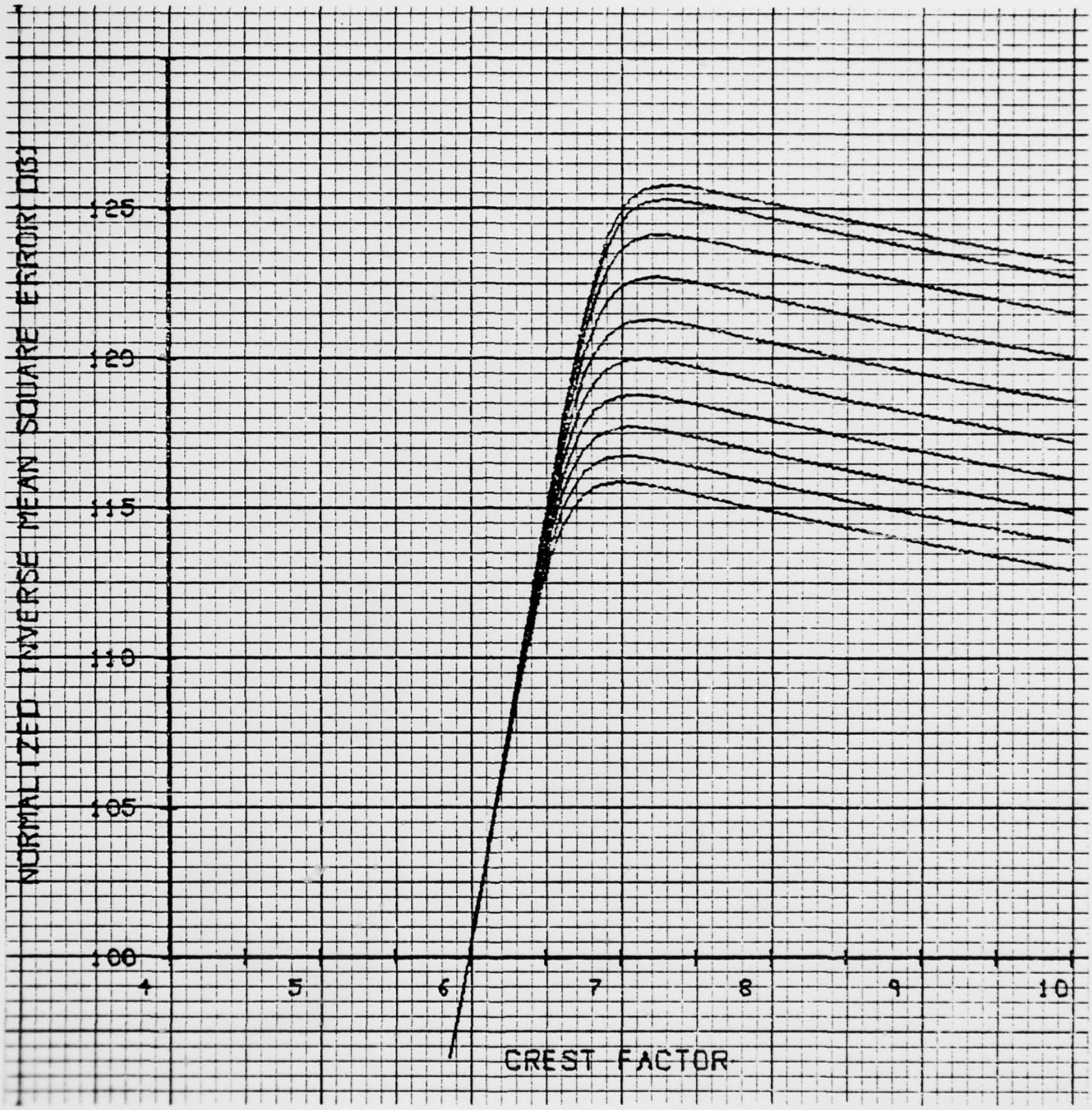

Uniform Quantization SNR Versus Crest Factor for 23 Bits and

0, 10, ... 80, 90 Percent Normalized Level Errors.

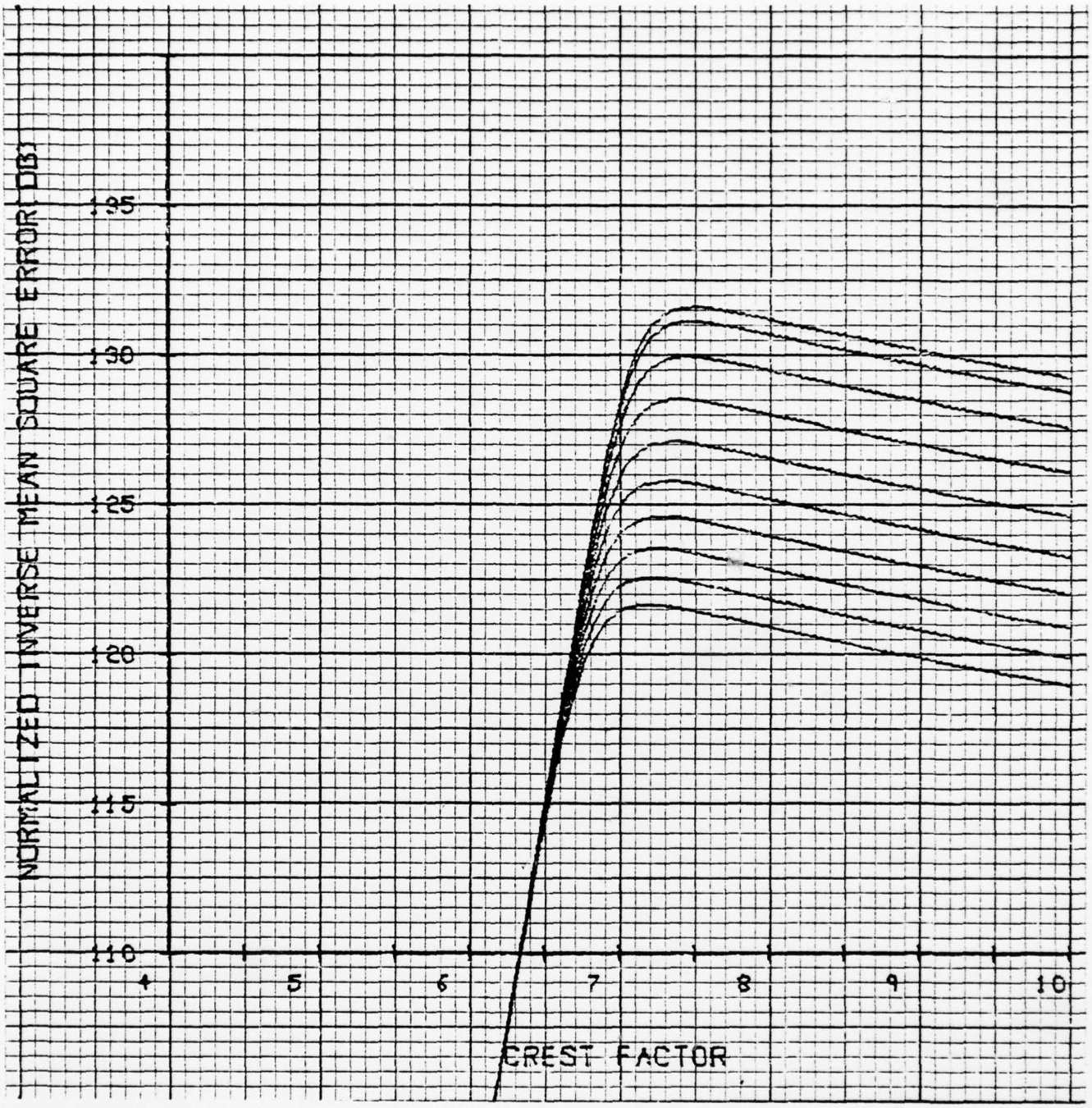

Uniform Quantization SNR Versus Crest Factor for 24 Bits and 0, 10, ... 80, 90 Percent Normalized Level Errors.

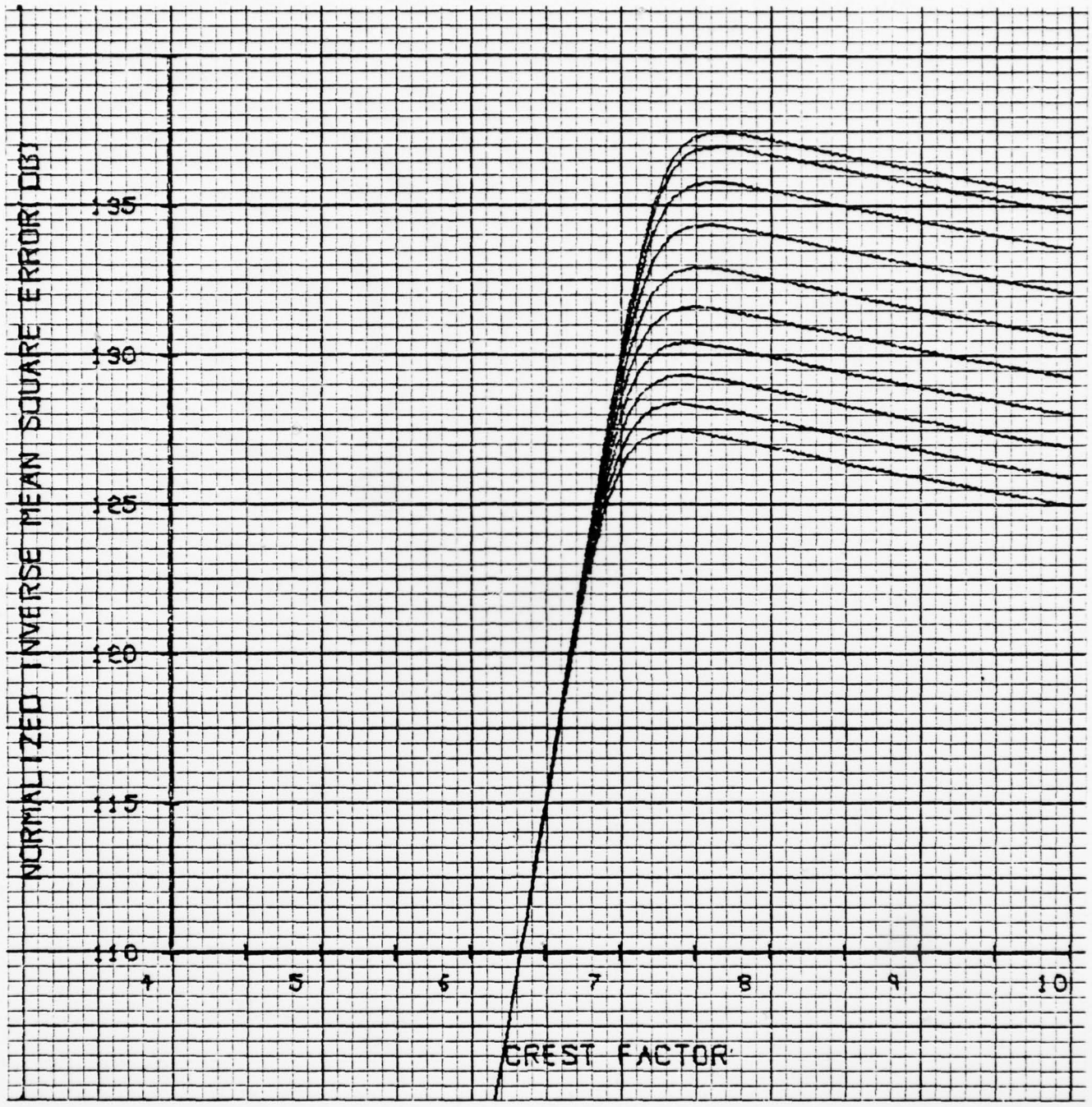

Uniform Quantization SNR Versus Crest Factor for 25 Bits and 0, 10, ... 80, 90 Percent Normalized Level Errors.

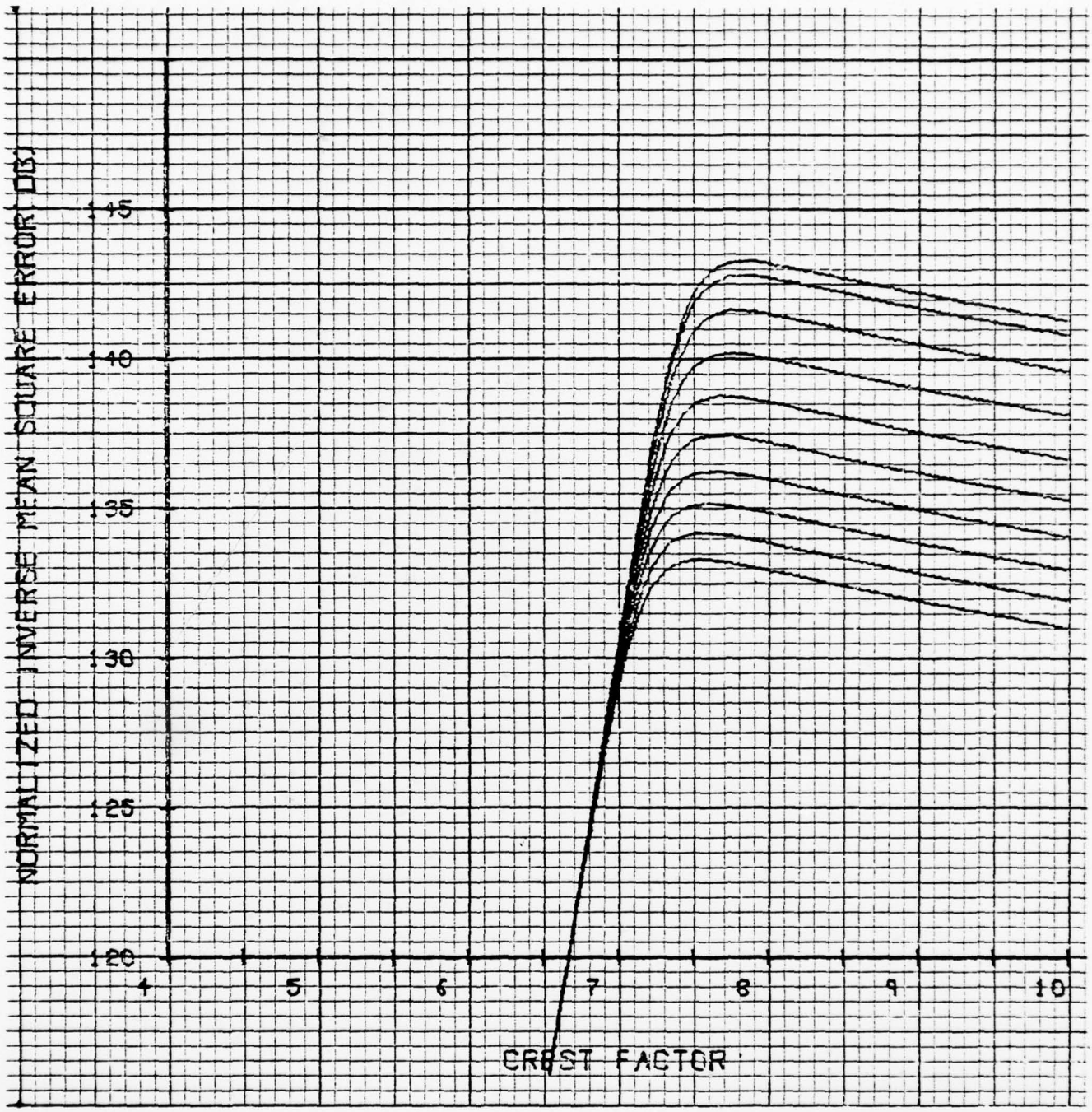

Uniform Quantization SNR Versus Crest Factor for 26 Bits and 0, 10, ... 80, 90 Percent Normalized Level Errors.

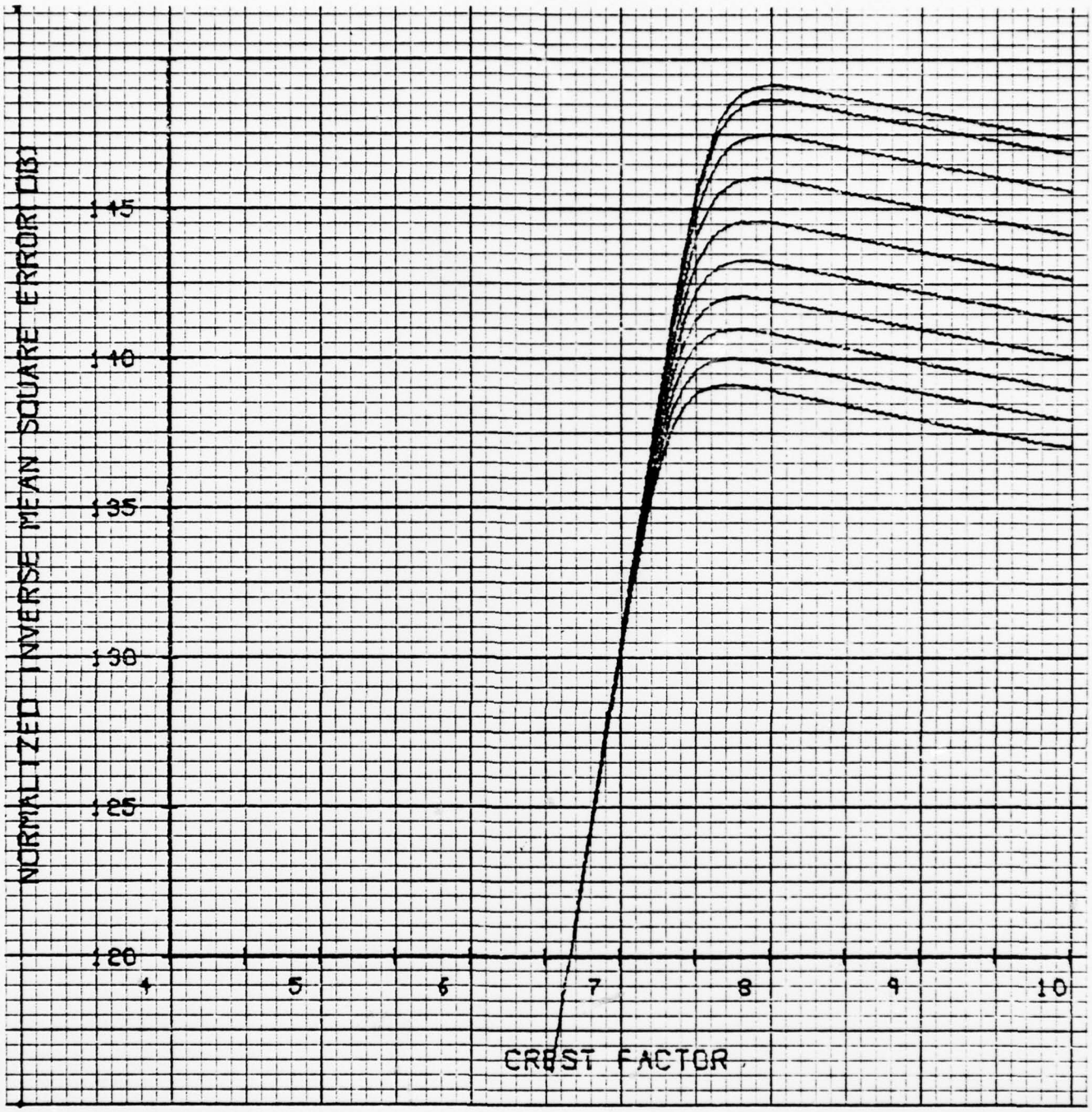

Uniform Quantization SNR Versus Crest Factor for 27 Bits and 0, 10, ... 80, 90 Percent Normalized Level Errors.

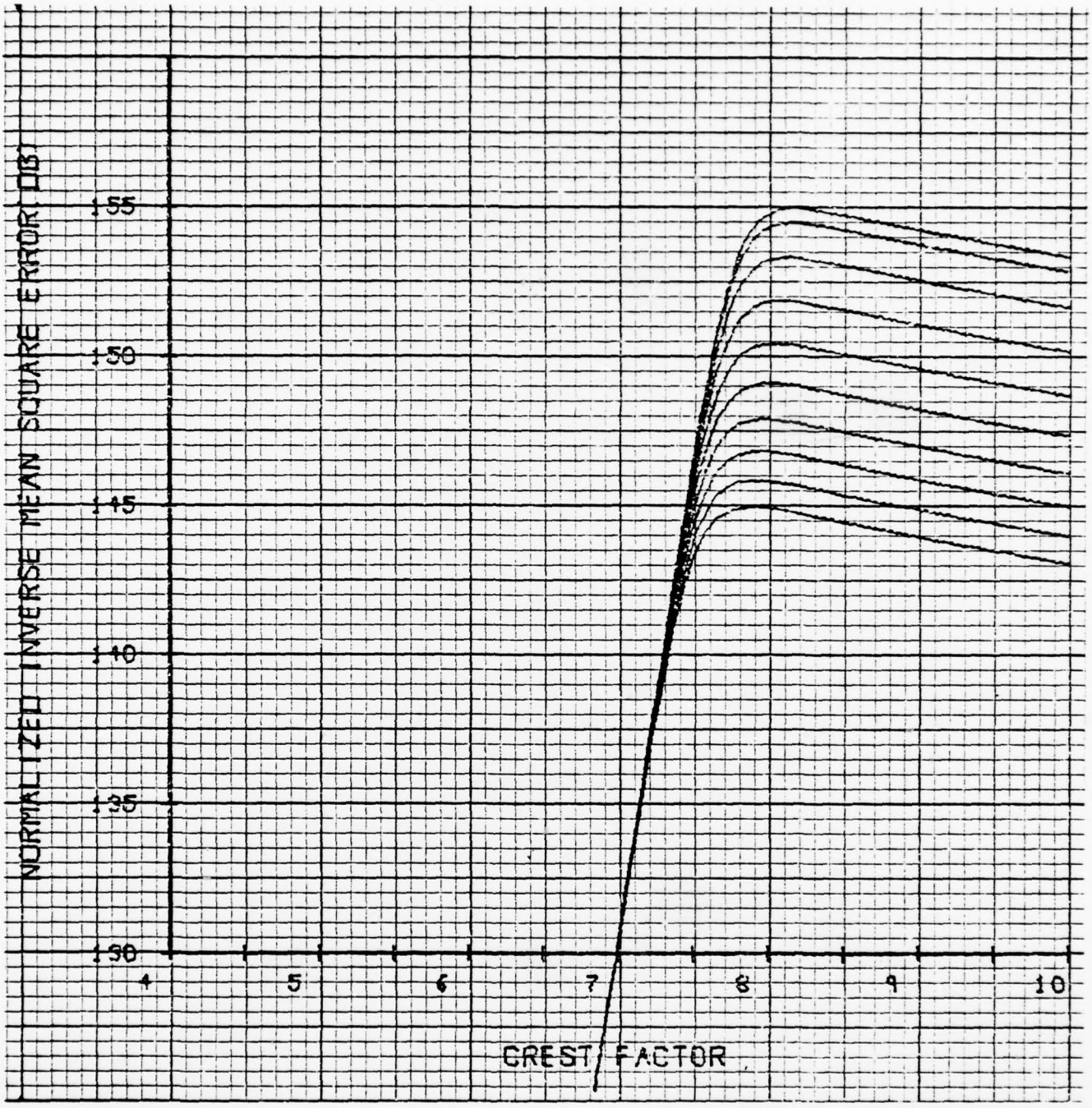

Uniform Quantization SNR Versus Crest Factor for 28 Bits and 0, 10, ... 80, 90 Percent Normalized Level Errors.

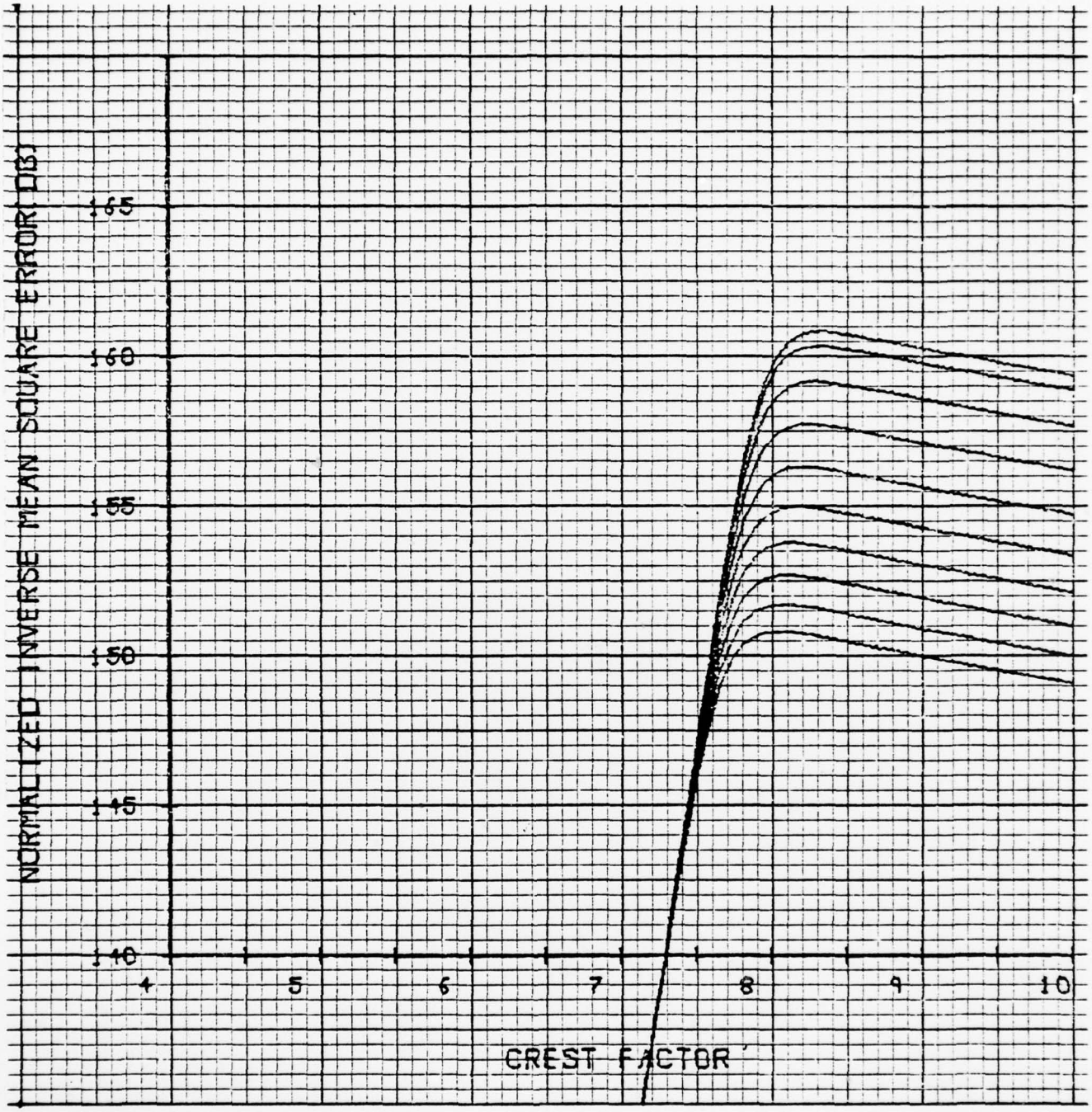

Uniform Quantization SNR Versus Crest Factor for 29 Bits and 0, 10, ... 80, 90 Percent Normalized Level Errors.

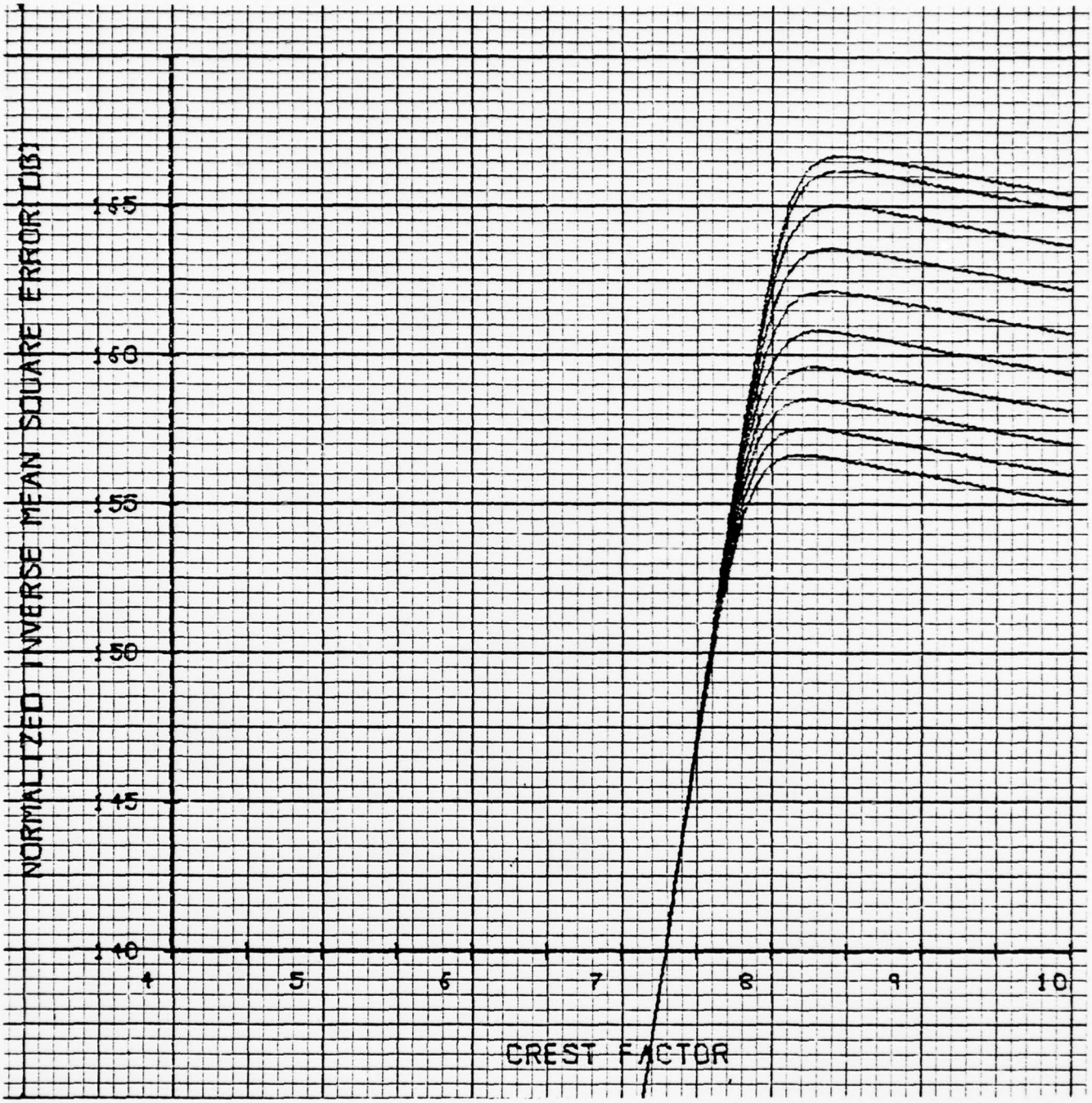

Uniform Quantization SNR Versus Crest Factor for 30 Bits and 0, 10, ... 80, 90 Percent Normalized Level Errors.

SECTION IV

LOGARITHMIC QUANTIZATION DESIGN CURVES

1. Introduction

This section gives design curves for predicting the dynamic range limitations imposed by quantization on a logarithmically companded A/D converter. The basic theory is the same as presented in Section 3 except that the quantization is no longer uniform. Consequently, only a discussion of logarithmic companding is included in this section. Both Gaussian and Laplacian amplitude statistics are considered and the equations from which these curves were obtained are given in Appendix A.

2. Logarithmic Companding

As discussed in Section 3, uniform quantization is only optimum when the input signal has uniformly distributed amplitude statistics. For other amplitude statistics nonuniform quantization gives better theoretical performance. Quantization of a compressed version of the input signal is logically equivalent to nonuniform quantization and is generally easier to implement in hardware. Signal compression achieves the same goal as nonuniform quantization by amplifying weak portions of the signal more than strong portions without altering the quantization step size.

Figure 4-1 gives a block diagram of a logarithmically companded A-D-A system. It consists of a logarithmic compressor, a uniform quantization A-D-A system, and an exponential expander. The expander is chosen to have the inverse characteristic of the compressor in order to restore the proper amplitude statistics to the output signal. Let $x(t)$ and $y(t)$ be the input and

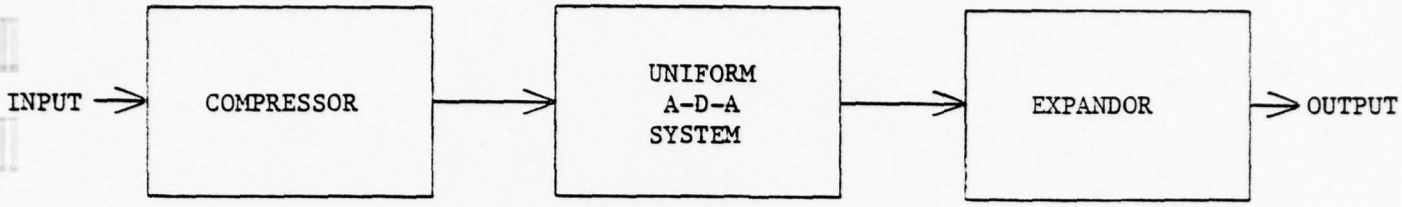

Figure 4-1. Logarithmically Companded A-D-A System.

output of the compressor, respectively. Then the logarithmic compressor is defined by

$$y(t) = \begin{cases} V \dfrac{\ln\left[1 + \mu x(t)/V\right]}{\ln\left[1 + \mu\right]} & x(t) \geq 0 \\ -V \dfrac{\ln\left[1 - \mu x(t)/V\right]}{\ln\left[1 + \mu\right]} & x(t) \leq 0 \end{cases} \tag{4-1}$$

where μ is the compression factor and 2V is the peak to peak quantization range. This equation is plotted in Figure 4-2 for several values of μ. Generally speaking, the slower the input signal probability density function goes to zero as the magnitude of the input goes to infinity, the more logarithmic compression will improve performance relative to SNR. This is exemplified in Figure 4-3 and 4-4 where SNR versus crest factor is plotted. In both figures the second curve gives the optimum SNR for all values of compression factor μ. With Gaussian amplitude statistics the optimum $\mu = 2.5$ whereas with Laplacian amplitude statistics the optimum $\mu = 8.0$. Observe the optimum companding only improves performance over no companding ($\mu = 0$) by 1.0 dB with Gaussian amplitude statistics. However, with

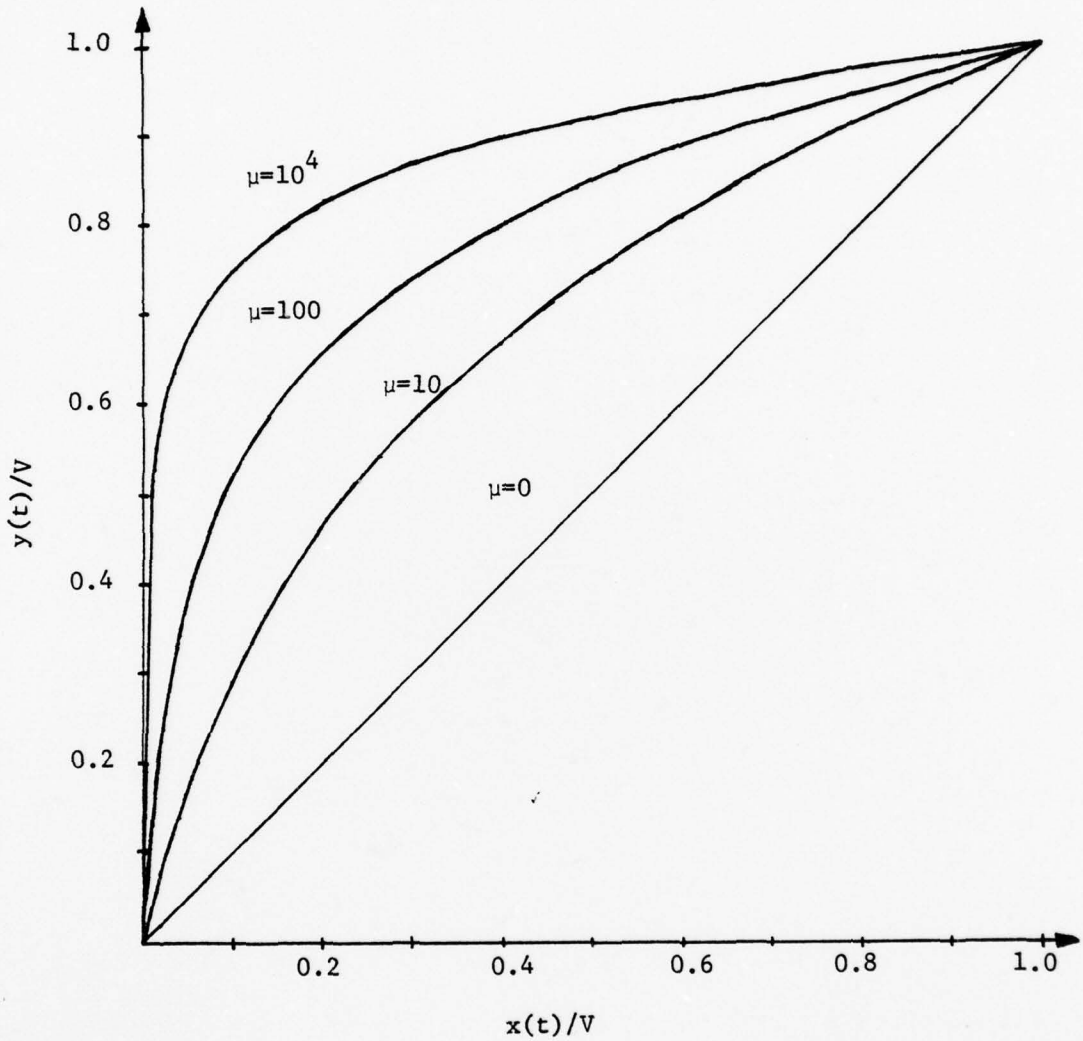

Figure 4-2. Logarithmic Compressor Characteristic.

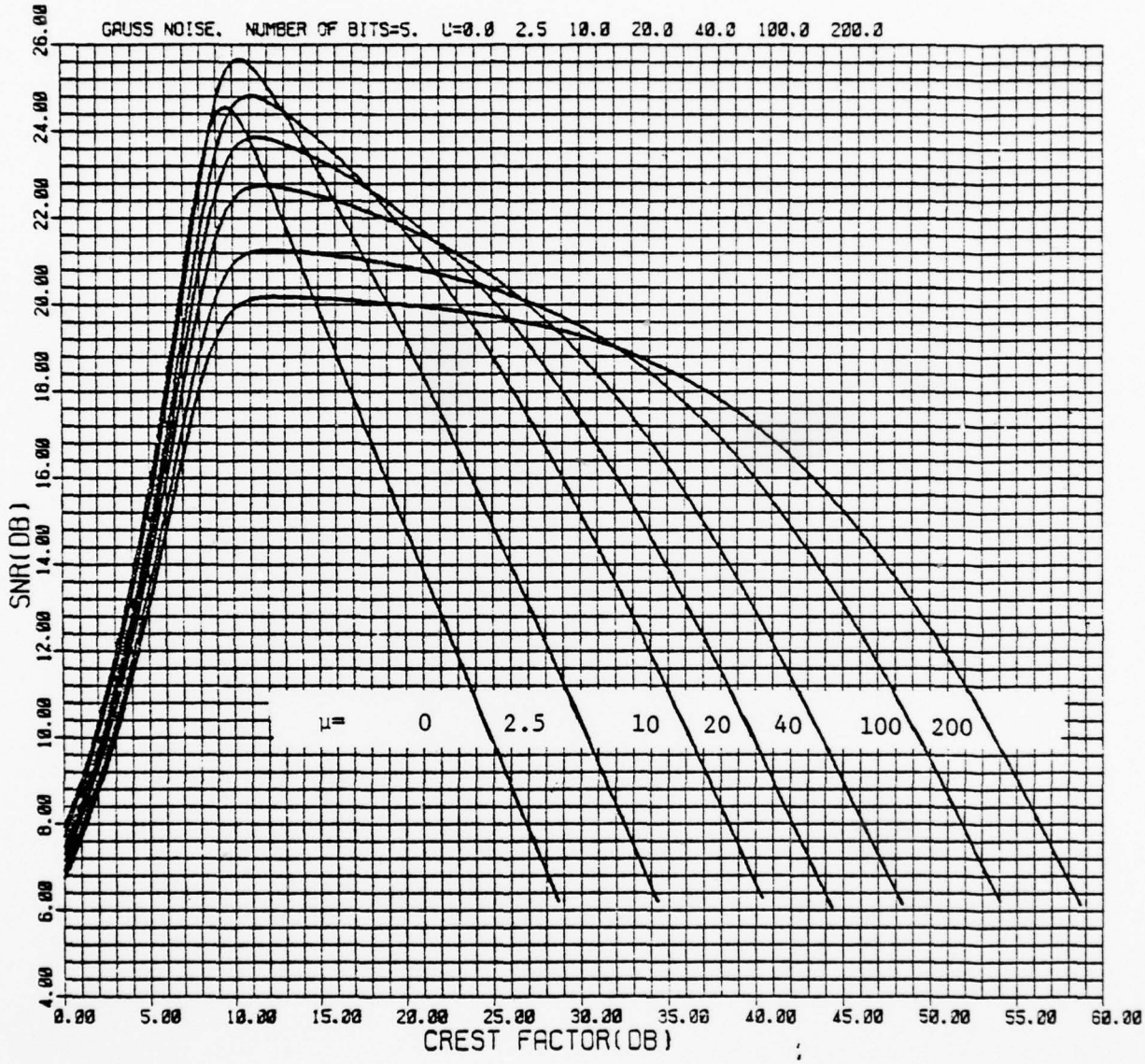

Figure 4-3. SNR Versus Crest Factor For 5 Bits And Gaussian Amplitude Statistics.

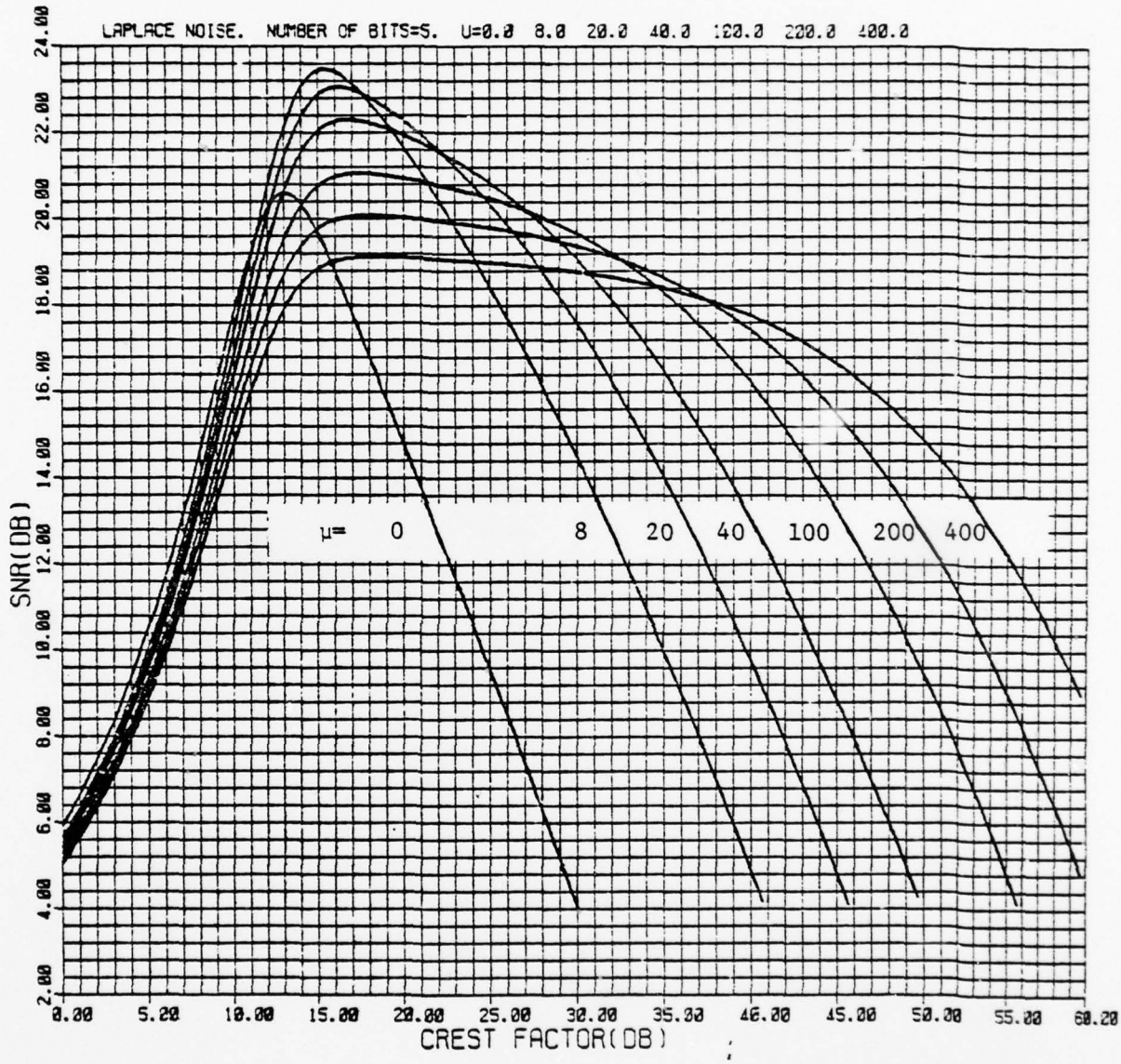

Figure 4-4. SNR Versus Crest Factor For 5 Bits And Laplacian Amplitude Statistics.

Laplacian amplitude statistics there is over 3.0 dB improvement. Nevertheless, the Gaussian case with no companding yields a higher SNR than the Laplacian case with optimum companding.

From these curves, optimum SNR is only maintained over a small range of crest factor or alternatively over a small range of input signal power. It is often desirable to maintain a minimum SNR (say 20 dB) over some range of input signal powers. With a compression factor $\mu = 100$, this minimum SNR is maintained with Gaussian amplitude statistics for crest factors between 9 and 27 dB. Similarly, it is achieved with Laplacian amplitude statistics for crest factors between 13 and 28 dB. Thus, the larger the compression factor beyond the optimum value the lower the maximum SNR, but the larger the range in crest factor or signal power. The no companding case gives the least range in crest factor.

AD-A060 430 SPERRY SYSTEMS MANAGEMENT RESTON VA F/G 9/5

A STATISTICAL DESIGN MANUAL FOR HIGH SPEED ANALOG-DIGITAL-ANALO--ETC(U)

1974 J F HOLLAND N00039-77-C-0124

UNCLASSIFIED NL

2 OF 3

AD
A060430

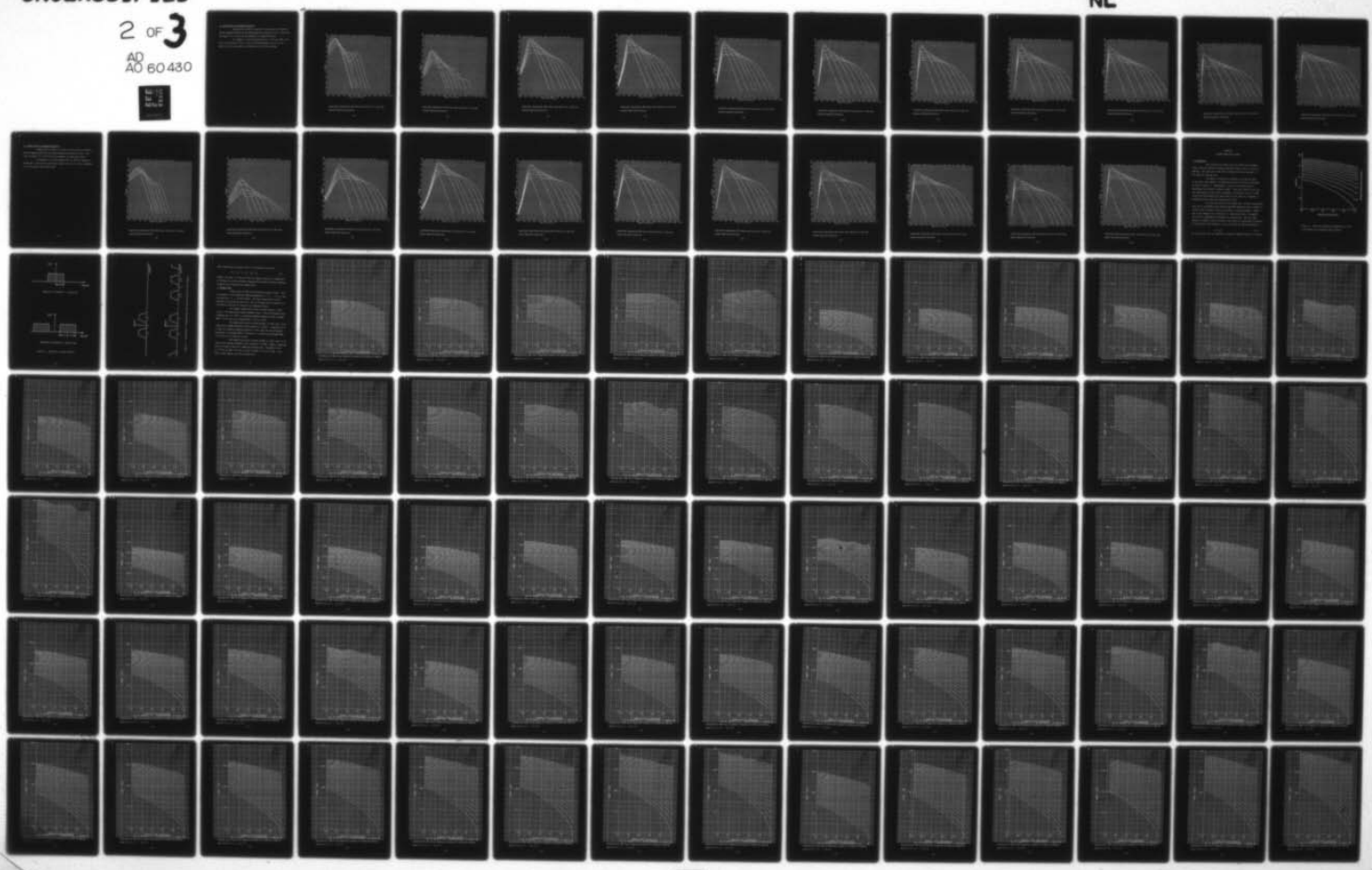

2 OF 3

AD
AO 60430

3. Design Curves for Gaussian Statistics

Design curves of SNR as a function of crest factor for logarithmically companded quantizers and Gaussian amplitude statistics follow. They cover the range of 2 to 12 bits and are parametric in compression factor.

For example, a 10 bit A/D converter with $\mu = 200$ has a SNR = 50.2 dB at a crest factor of 15 dB. With a normalized sampling rate of 2.5, the SNSR = 51.2 dB in the center of the band and 3 dB less at band edge.

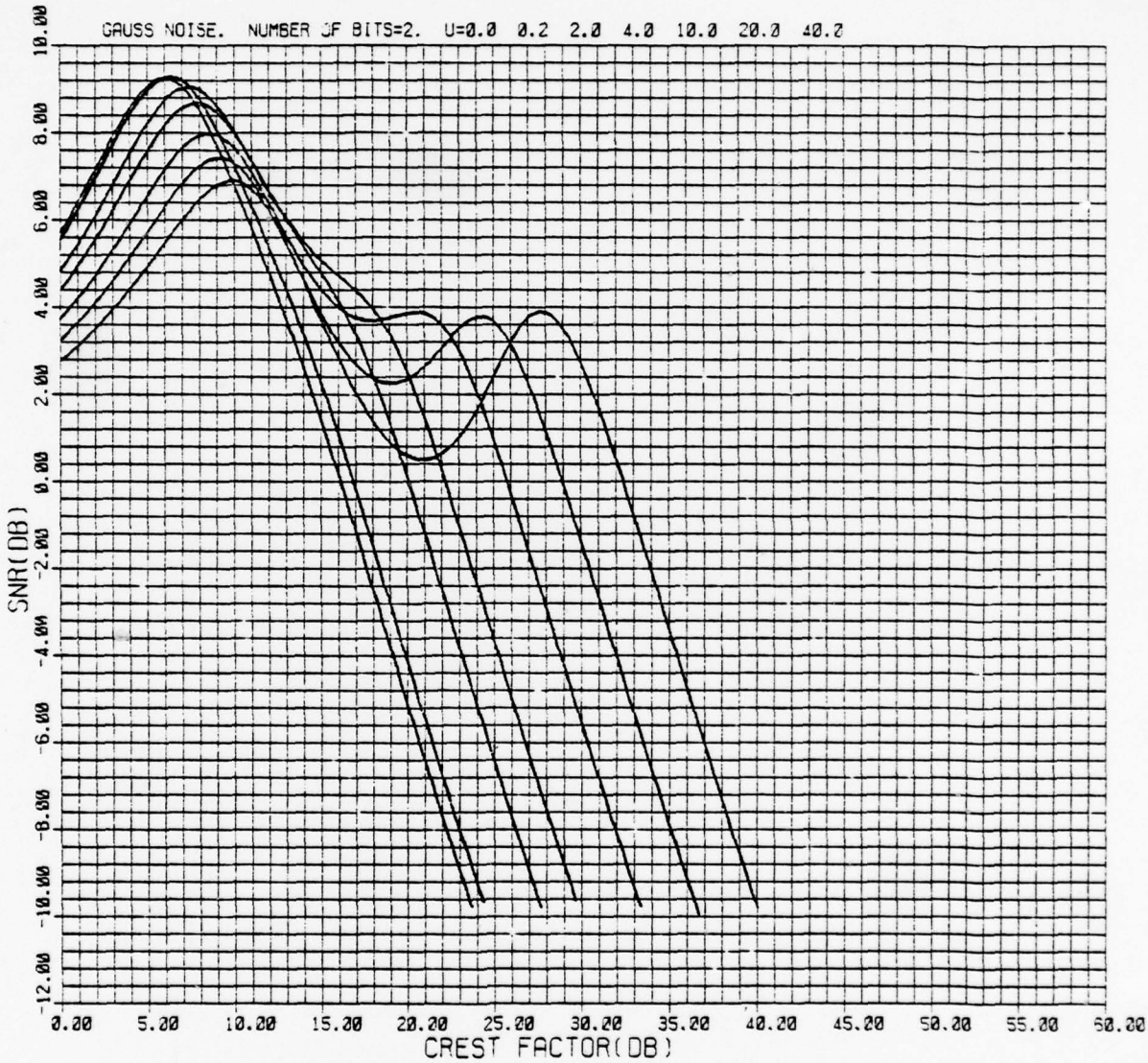

Logarithmic Quantization SNR Versus Crest Factor For 2 Bits and Gaussian Amplitude Statistics.

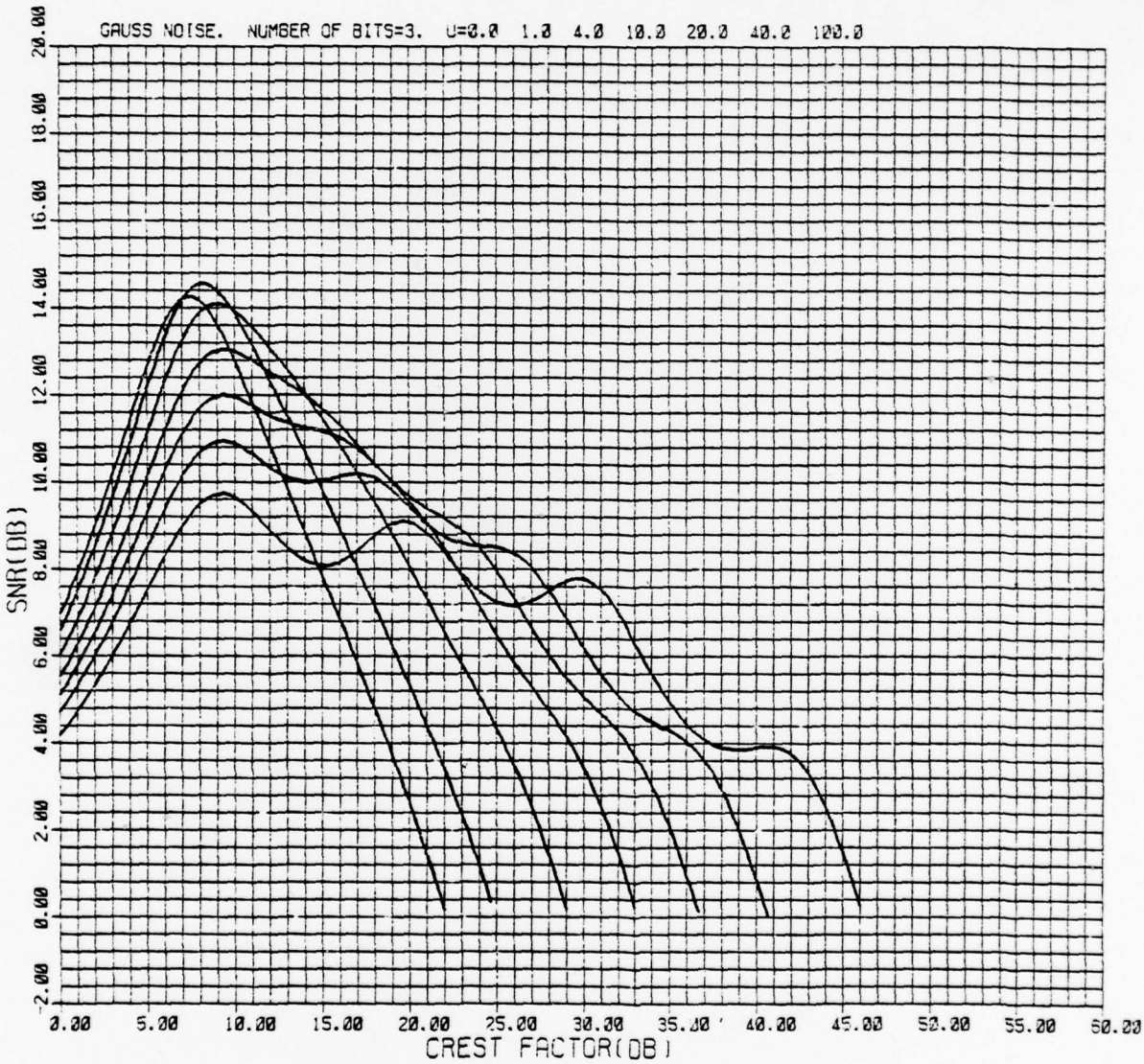

Logarithmic Quantization SNR Versus Crest Factor For 3 Bits And Gaussian Amplitude Statistics.

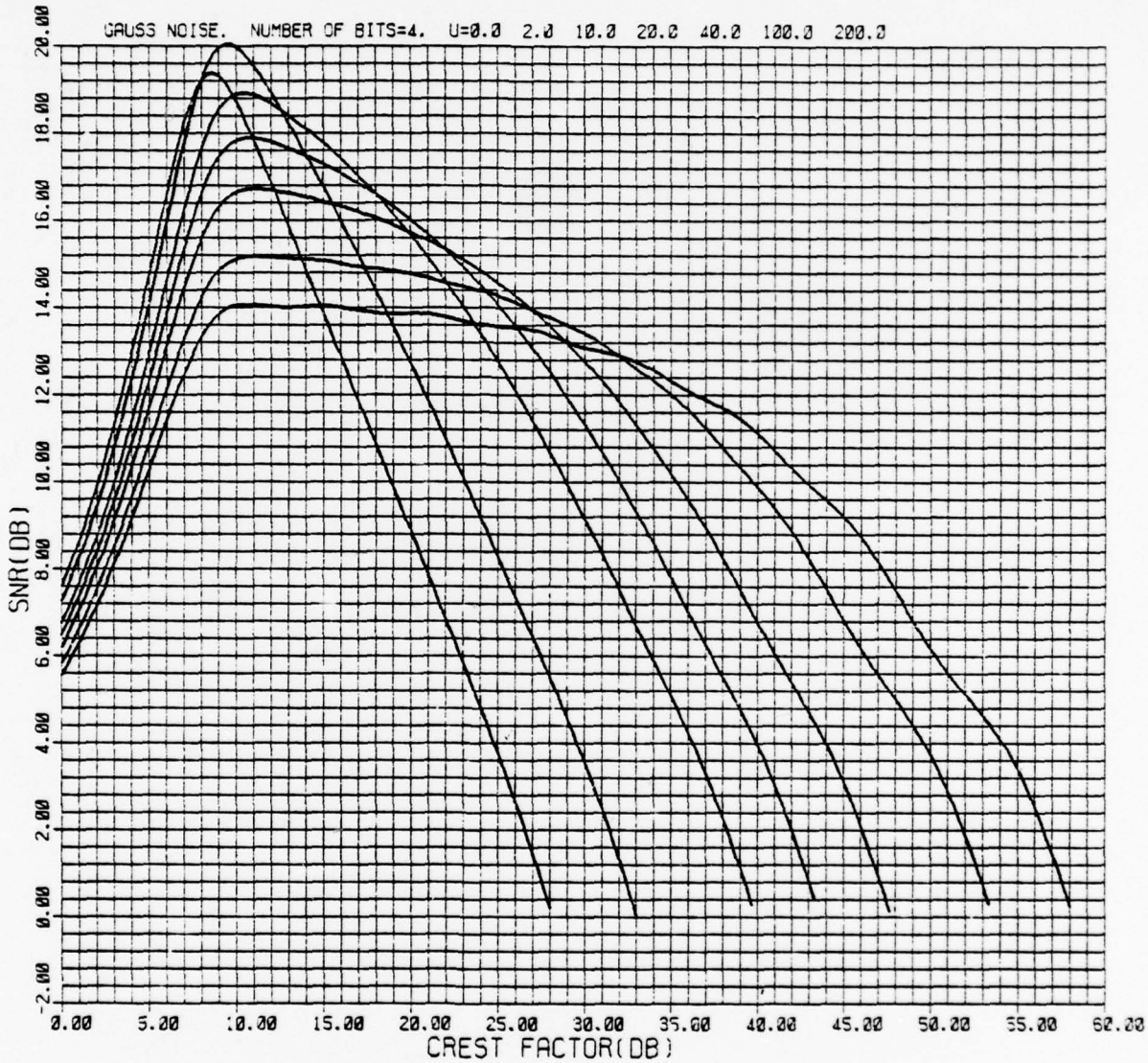

Logarithmic Quantization SNR Versus Crest Factor For 4 Bits And Gaussian Amplitude Statistics.

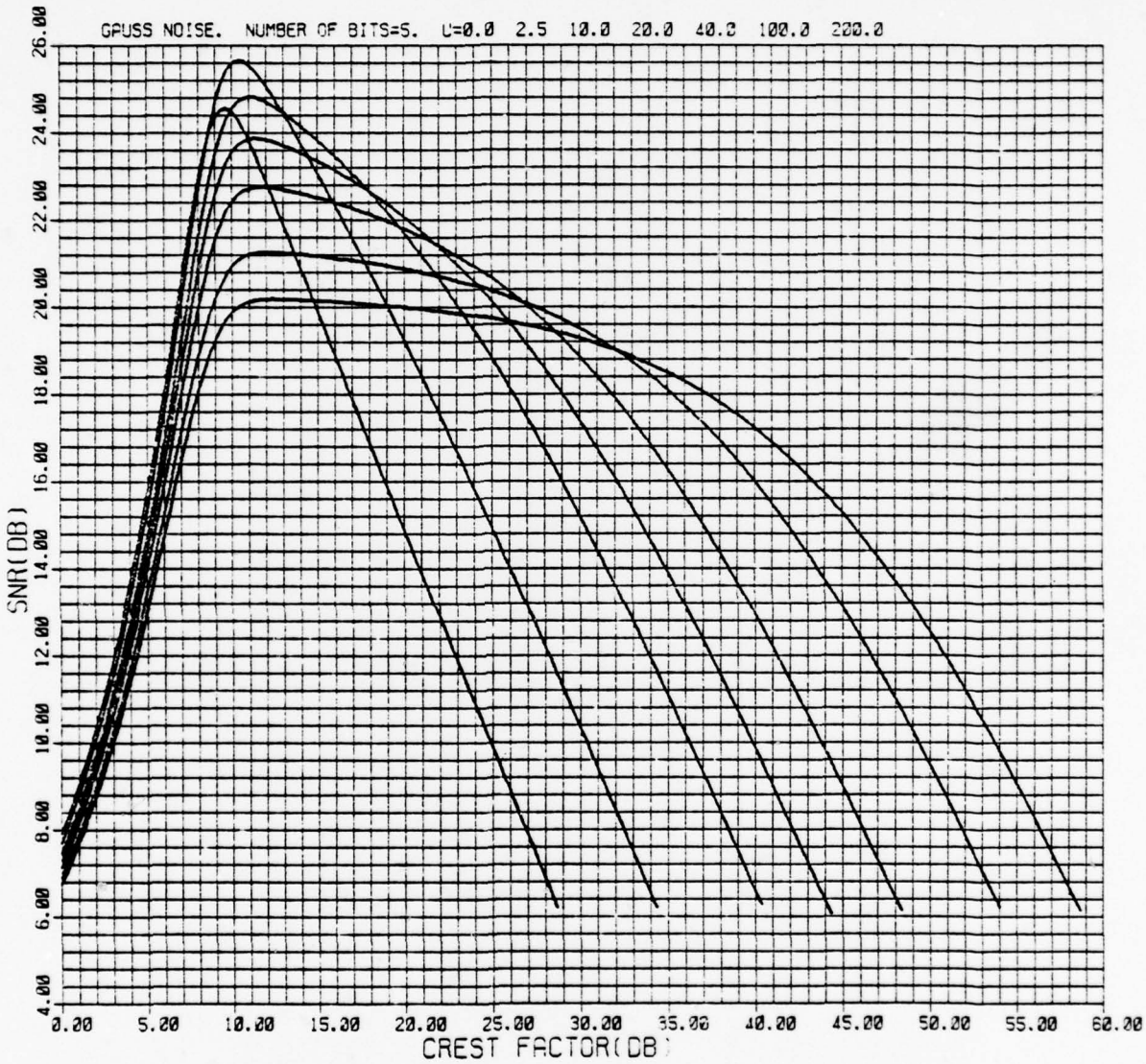

Logarithmic Quantization SNR Versus Crest Factor For 5 Bits And Gaussian Amplitude Statistics.

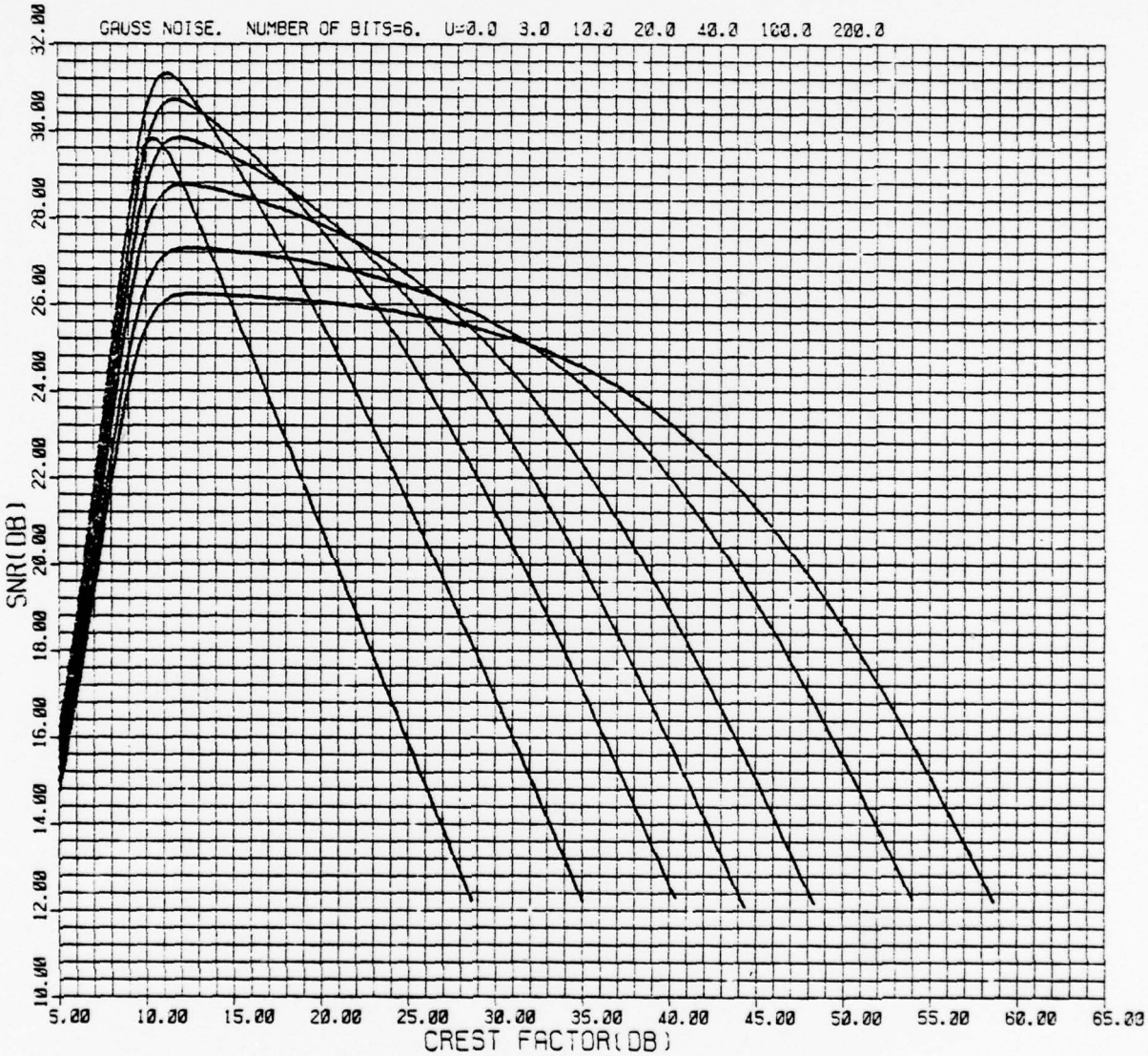

Logarithmic Quantization SNR Versus Crest Factor For 6 Bits And Gaussian Amplitude Statistics.

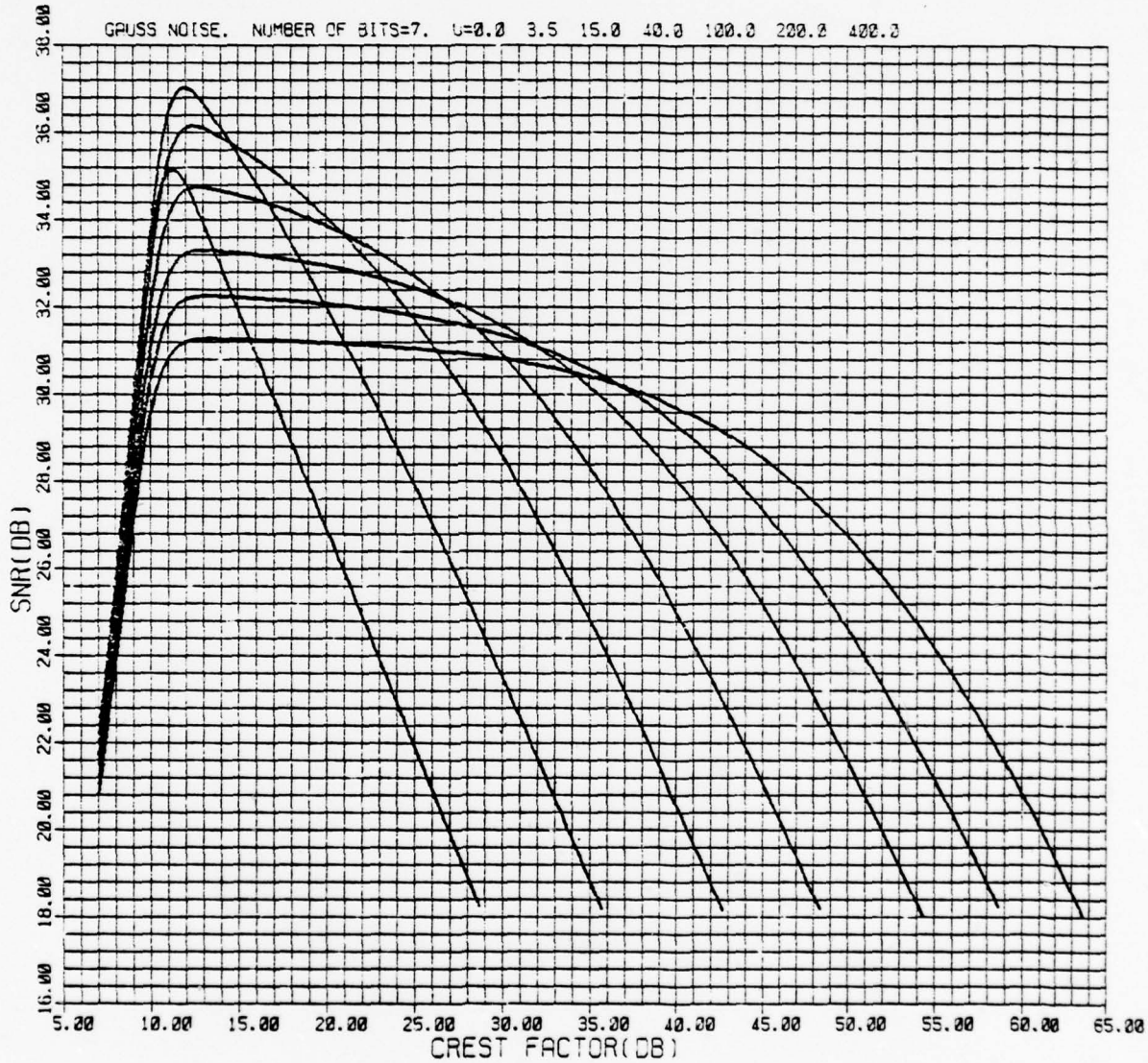

Logarithmic Quantization SNR Versus Crest Factor For 7 Bits And Gaussian Amplitude Statistics.

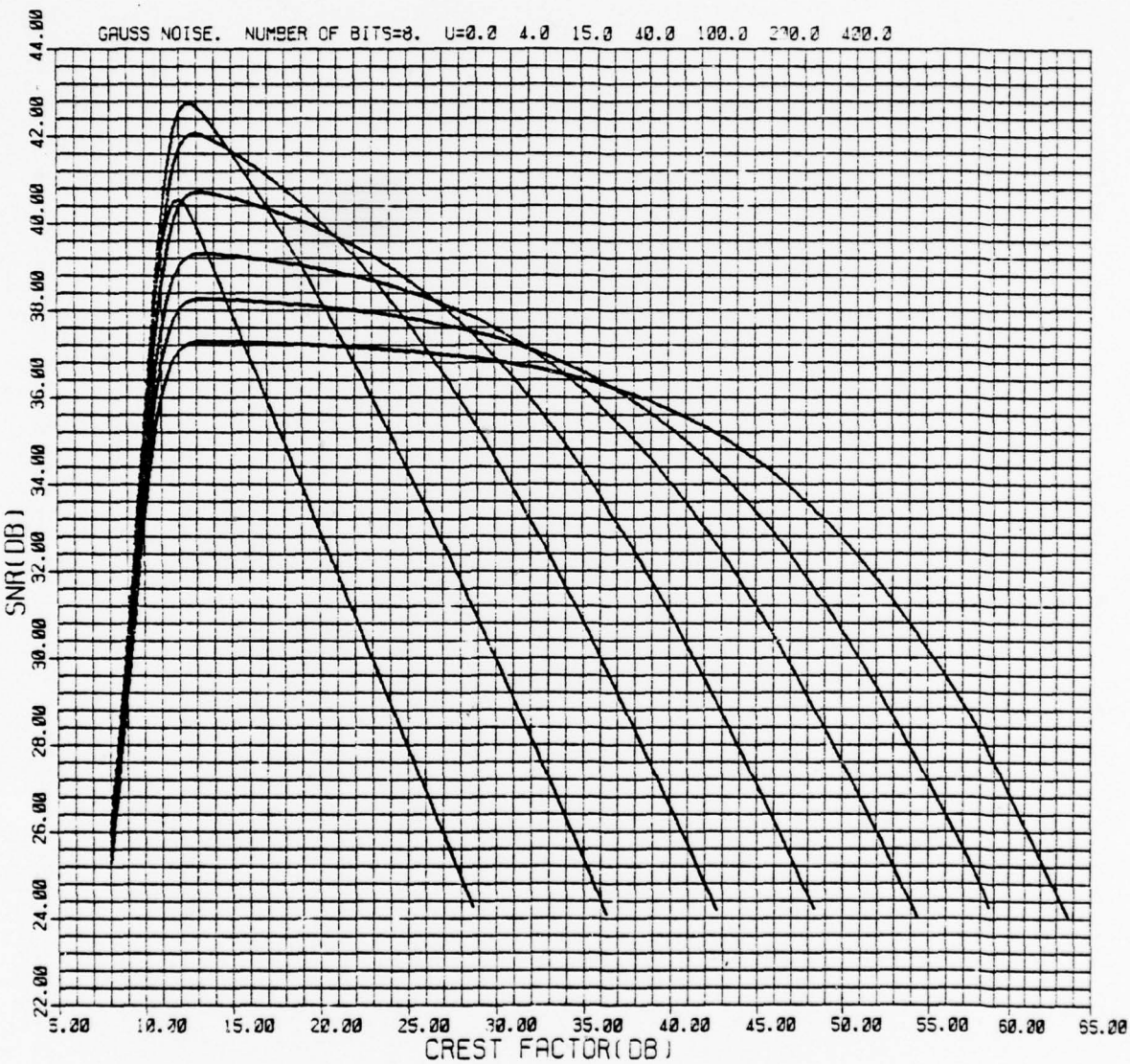

Logarithmic Quantization SNR Versus Crest Factor For 8 Bits And Gaussian Amplitude Statistics.

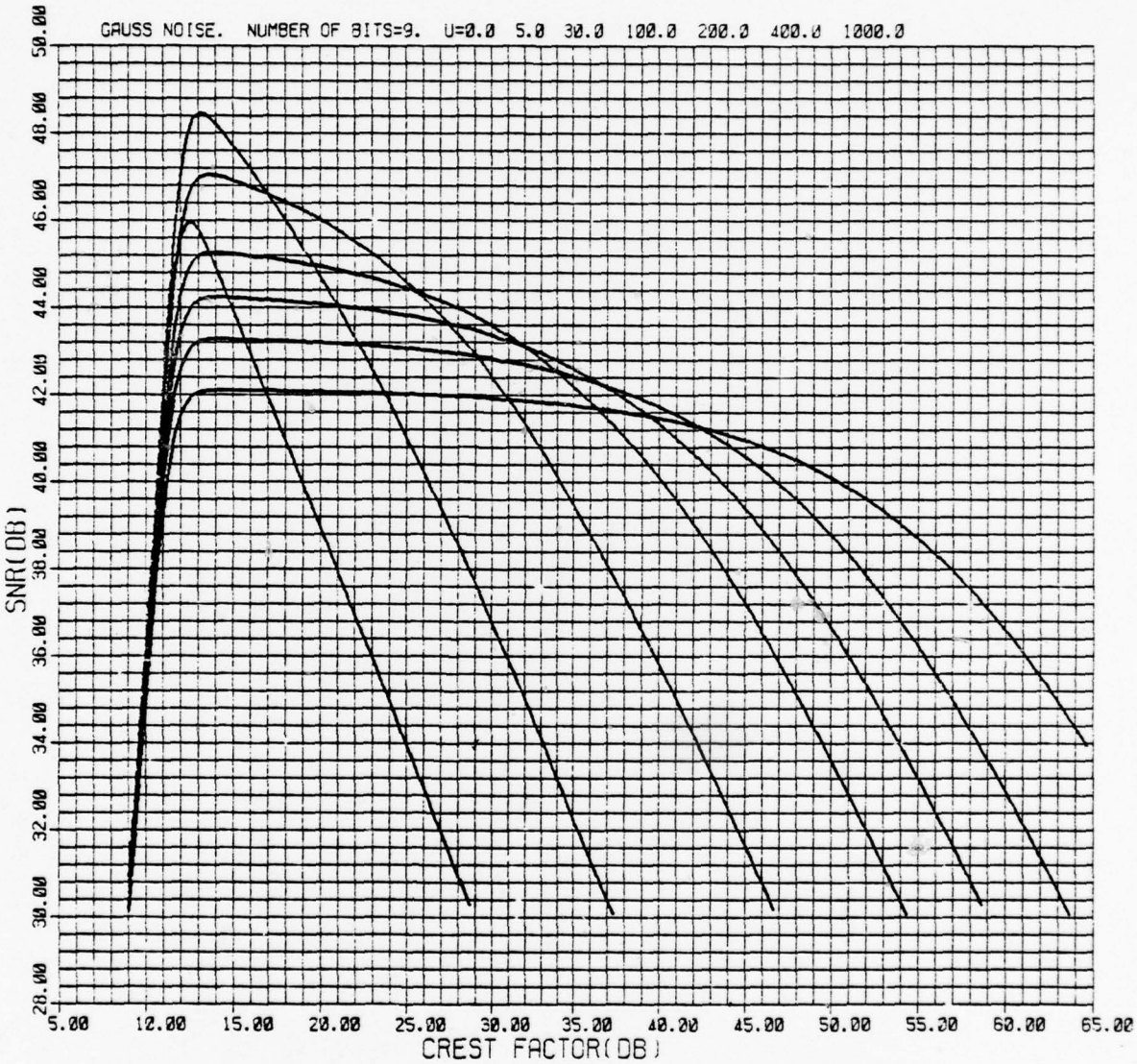

Logarithmic Quantization SNR Versus Crest Factor For 9 Bits And Gaussian Amplitude Statistics.

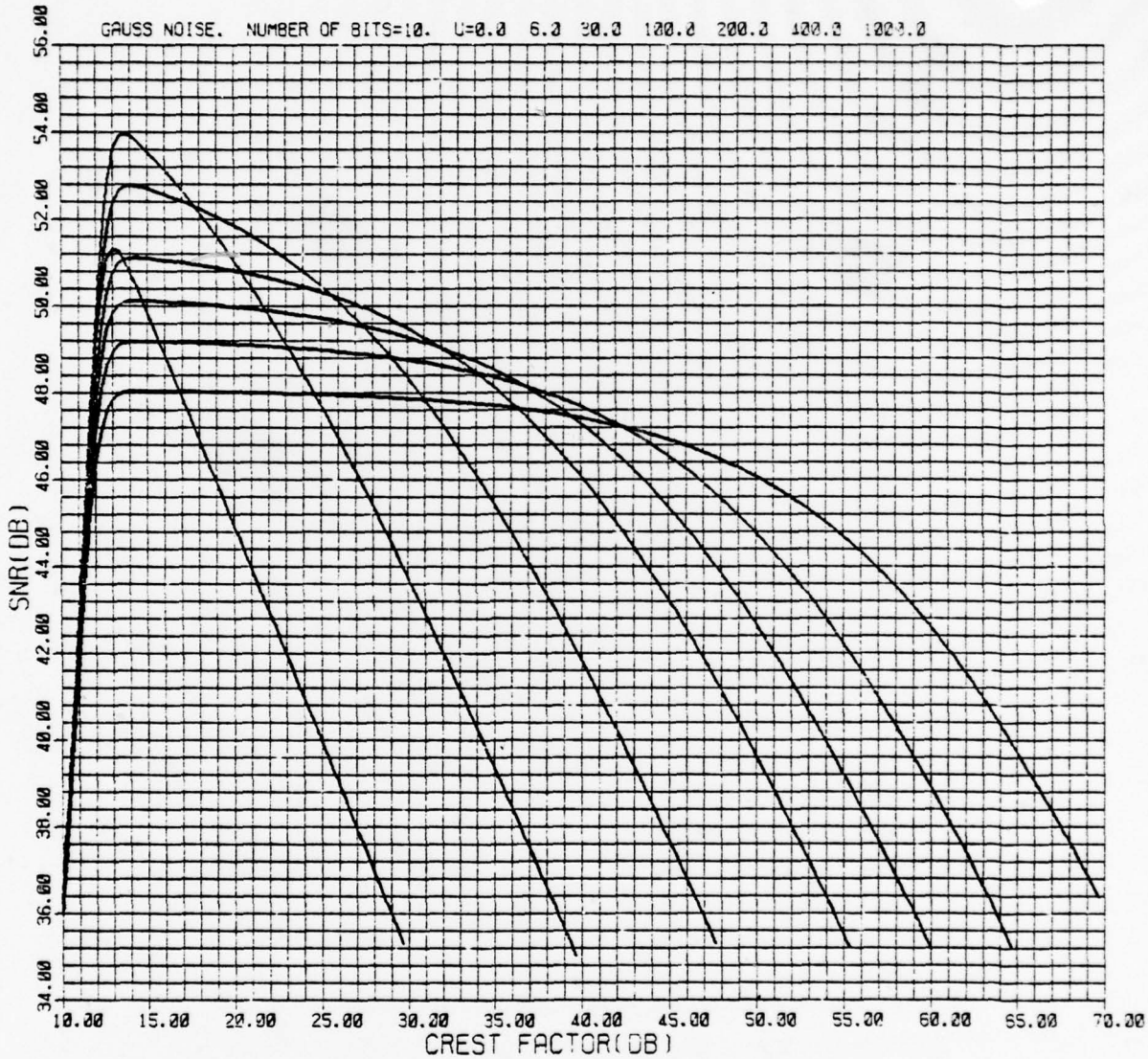

Logarithmic Quantization SNR Versus Crest Factor For 10 Bits And Gaussian Amplitude Statistics.

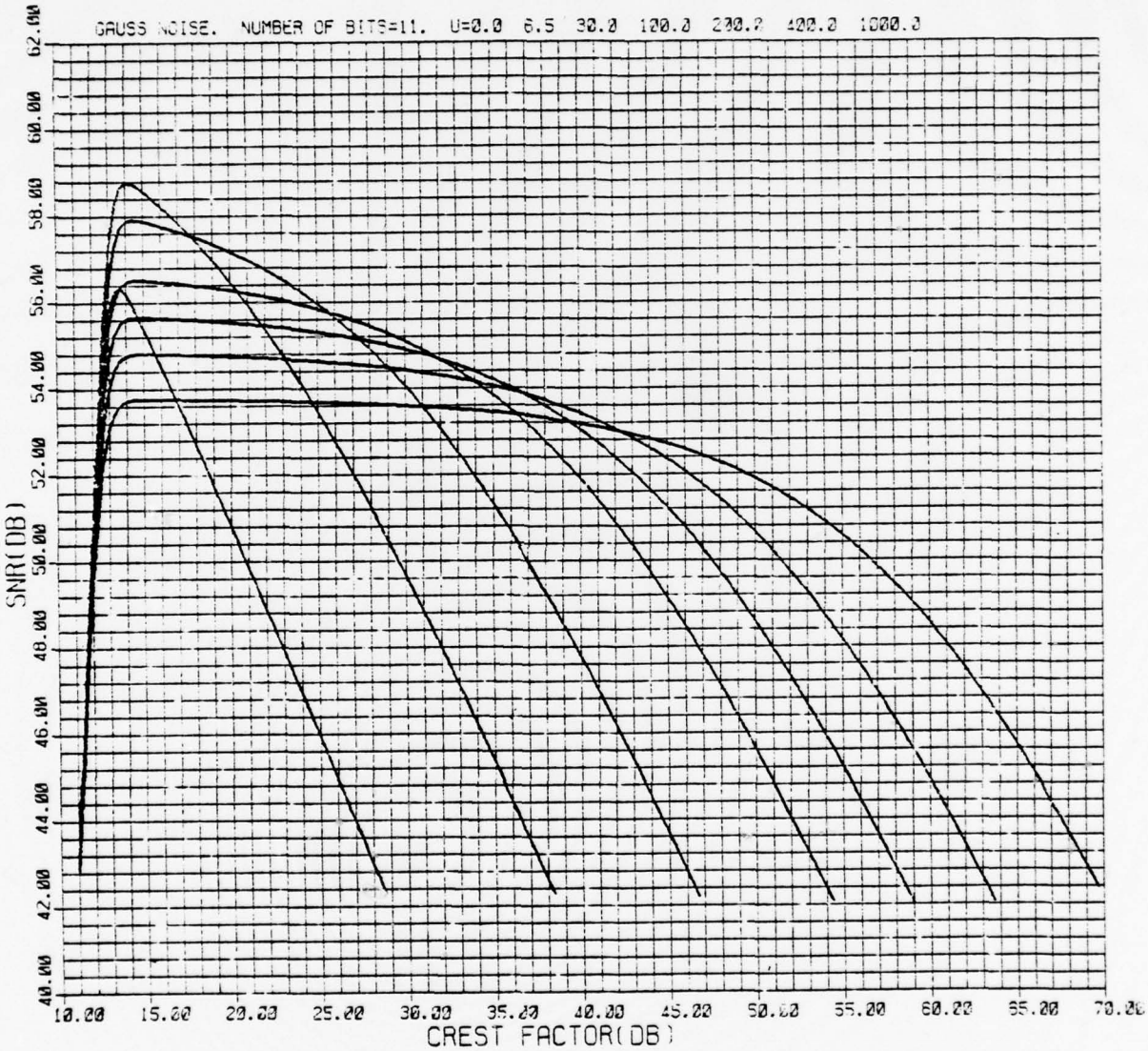

Logarithmic Quantization SNR Versus Crest Factor For 11 Bits And Gaussian Amplitude Statistics.

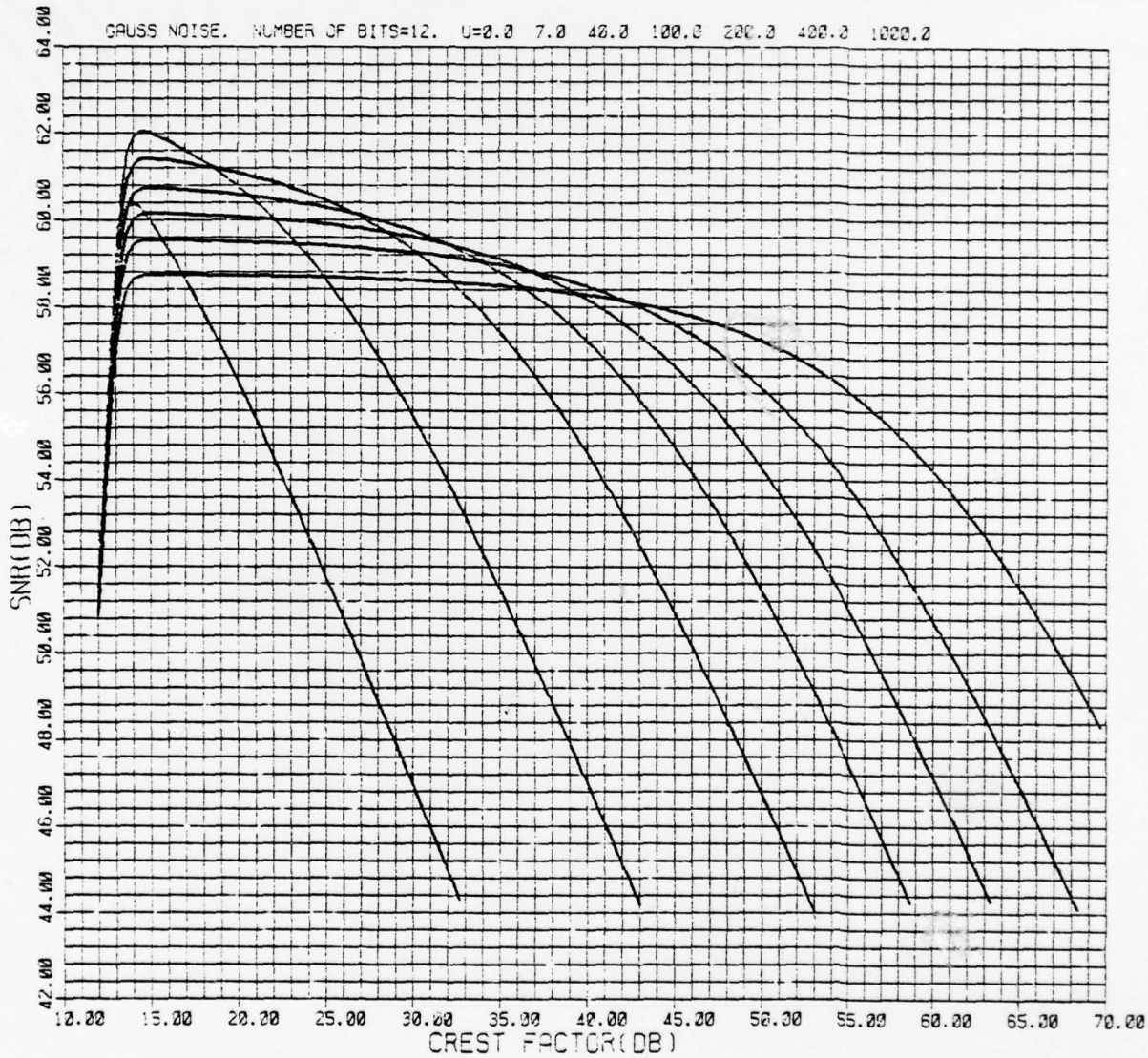

Logarithmic Quantization SNR Versus Crest Factor For 12 Bits And Gaussian Amplitude Statistics.

4. Design Curves for Laplacian Statistics

Design curves of SNR as a function of crest factor for logarithmically companded quantizers and Laplacian amplitude statistics follow. They cover the range of 2 to 12 bits and are parametric in compression factor.

For example a 7 bit A/D converter with $\mu = 1000$ will maintain a minimum SNR = 28 dB over the crest factor range 15 dB to 51 dB. This corresponds to a 36 dB range in input signal power.

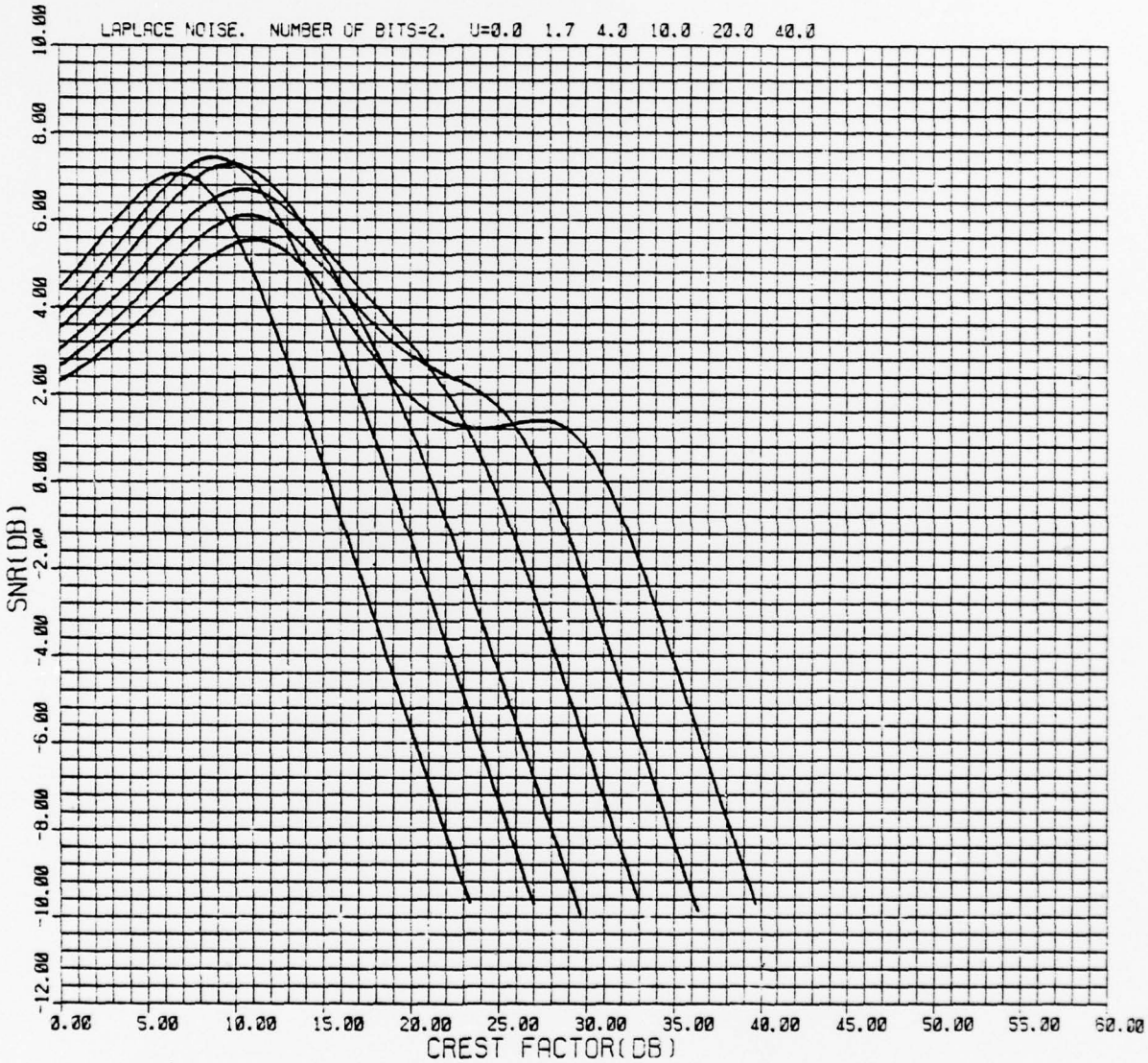

Logarithmic Quantization SNR Versus Crest Factor For 2 Bits And Laplace Amplitude Statistics.

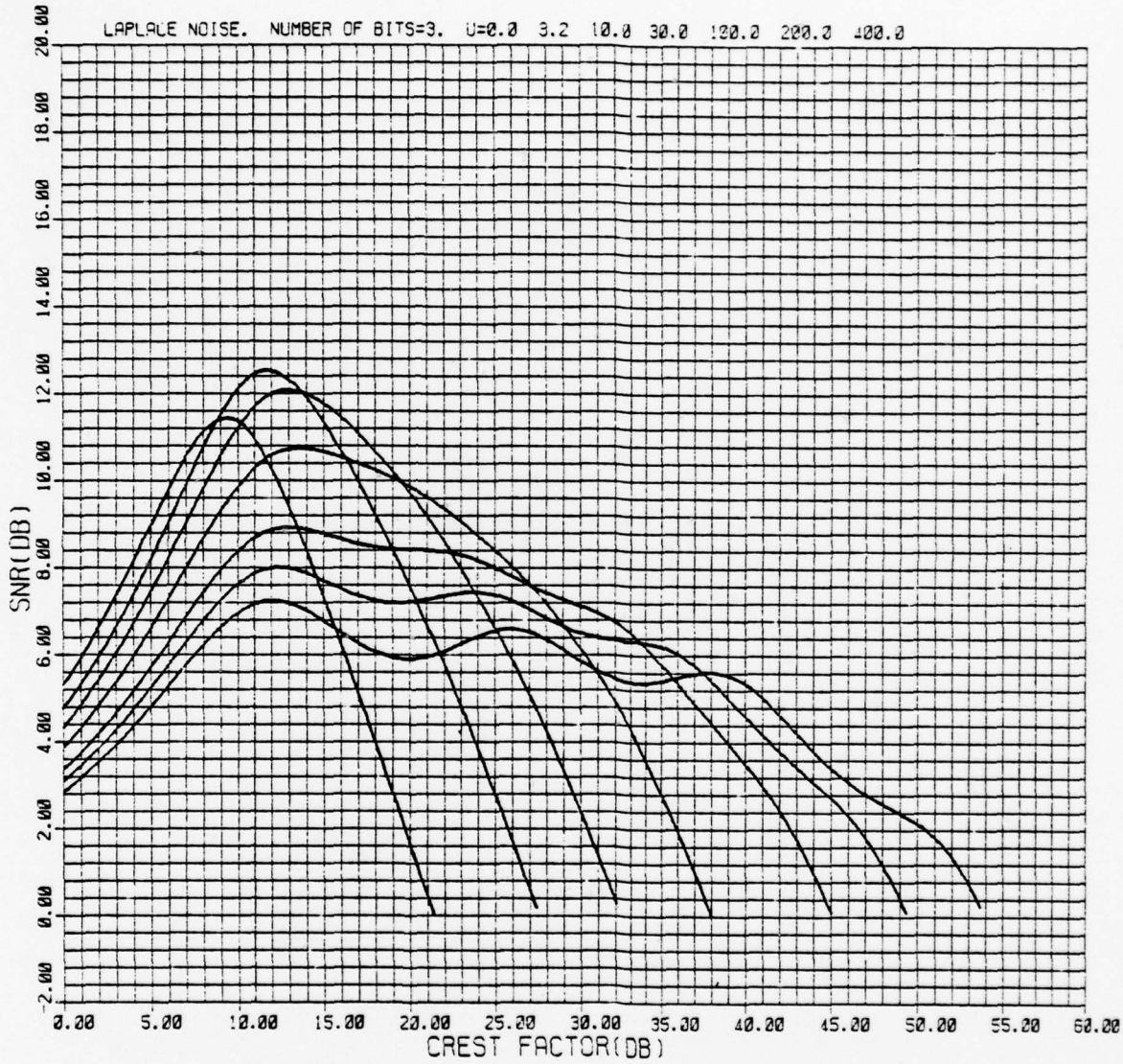

Logarithmic Quantization SNR Versus Crest Factor For 3 Bits And Laplace Amplitude Statistics.

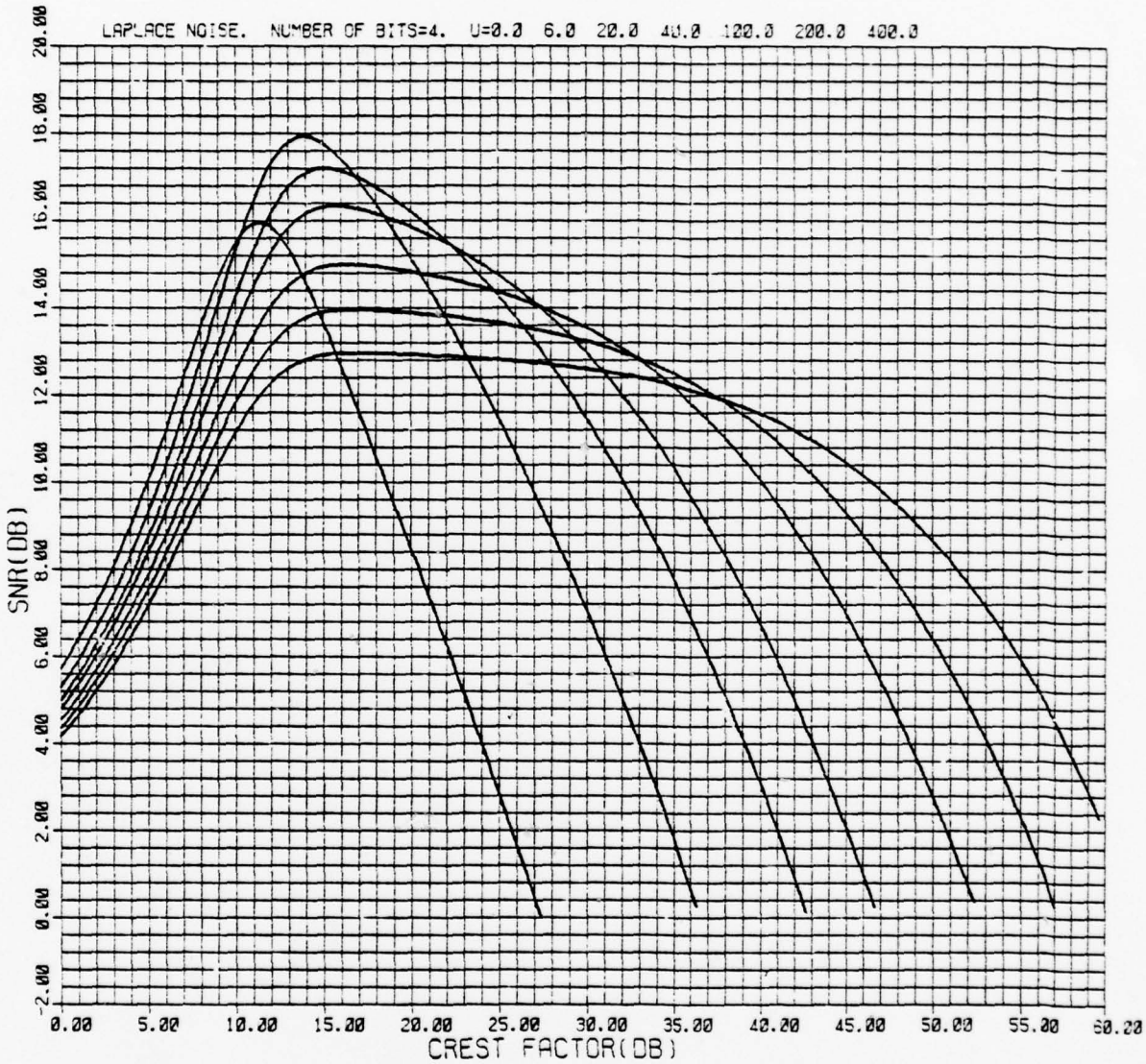

Logarithmic Quantization SNR Versus Crest Factor For 4 Bits And Laplace Amplitude Statistics.

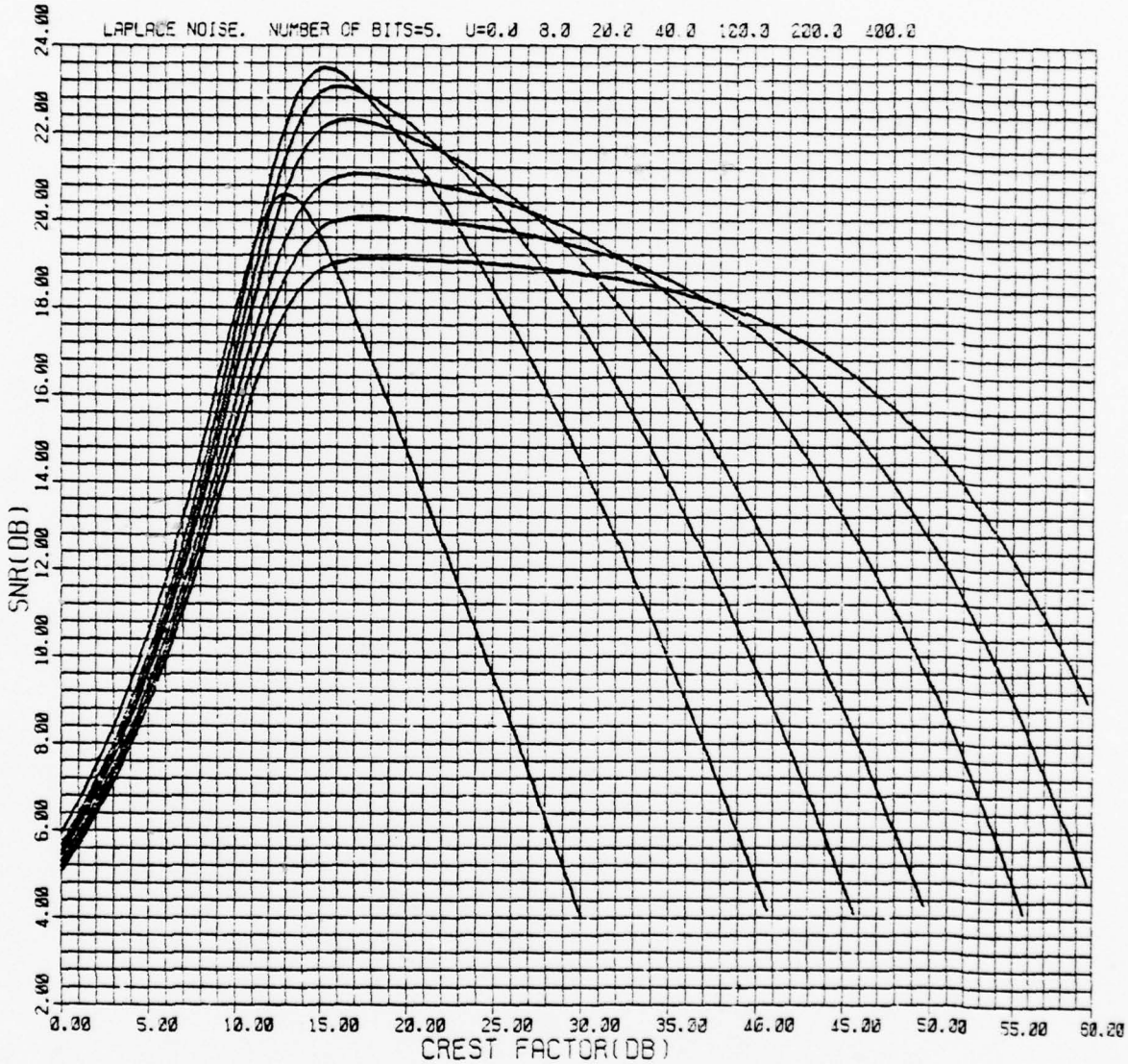

Logarithmic Quantization SNR Versus Crest Factor For 5 Bits And Laplace Amplitude Statistics.

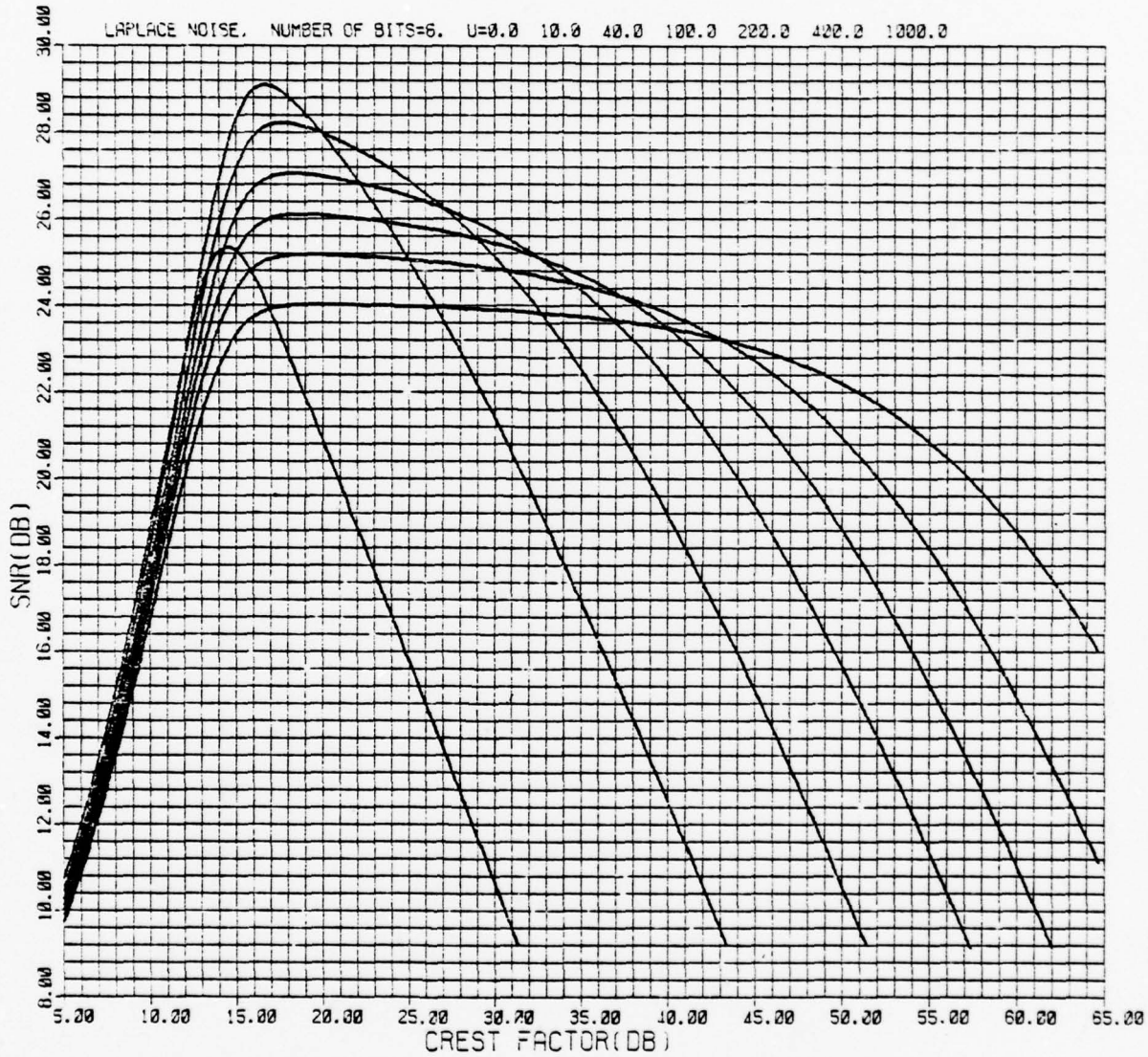

Logarithmic Quantization SNR Versus Crest Factor For 6 Bits And Laplace Amplitude Statistics.

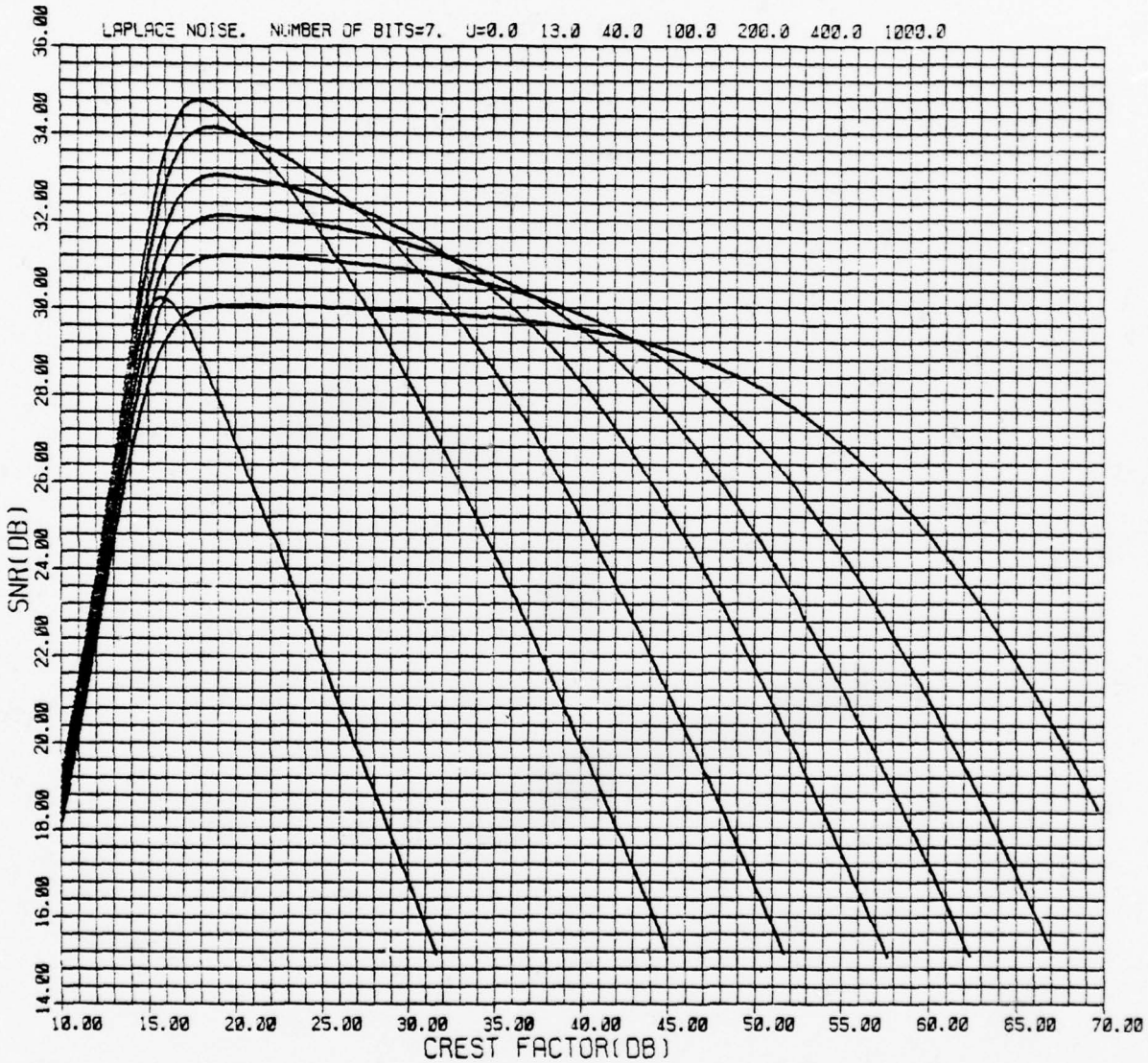

Logarithmic Quantization SNR Versus Crest Factor For 7 Bits And Laplace Amplitude Statistics.

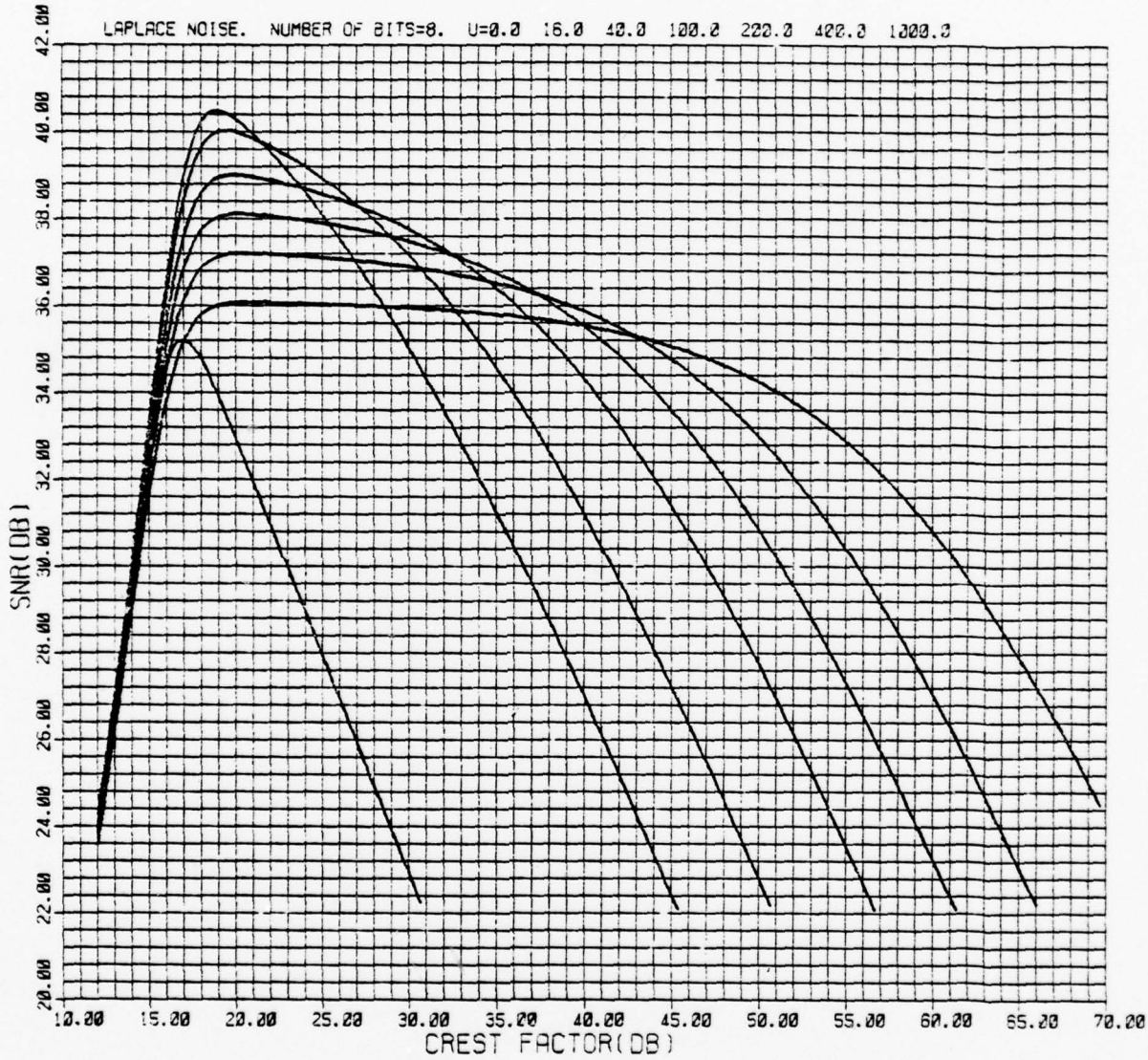

Logarithmic Quantization SNR Versus Crest Factor For 8 Bits And Laplace Amplitude Statistics.

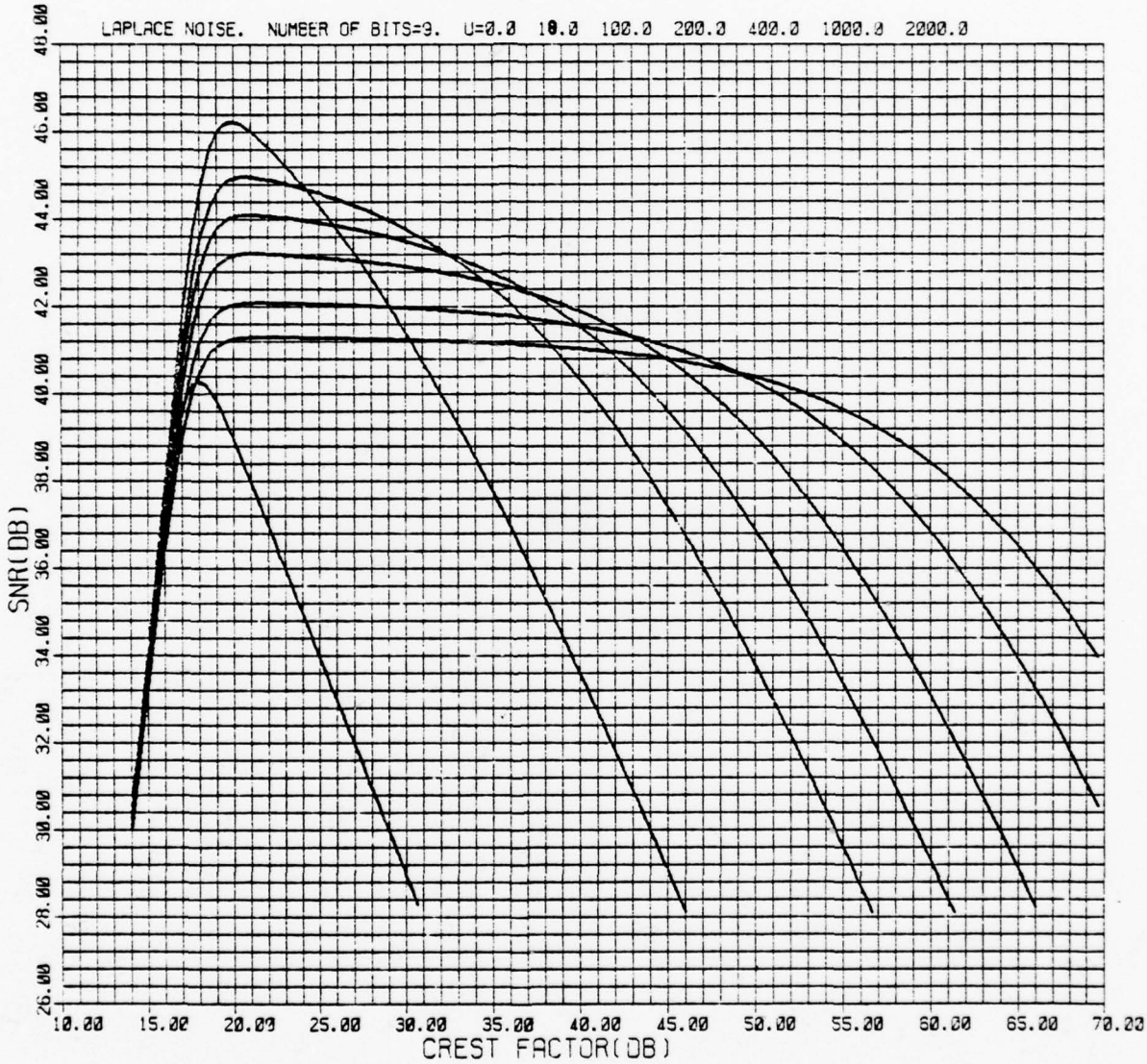

Logarithmic Quantization SNR Versus Crest Factor For 9 Bits And Laplace Amplitude Statistics.

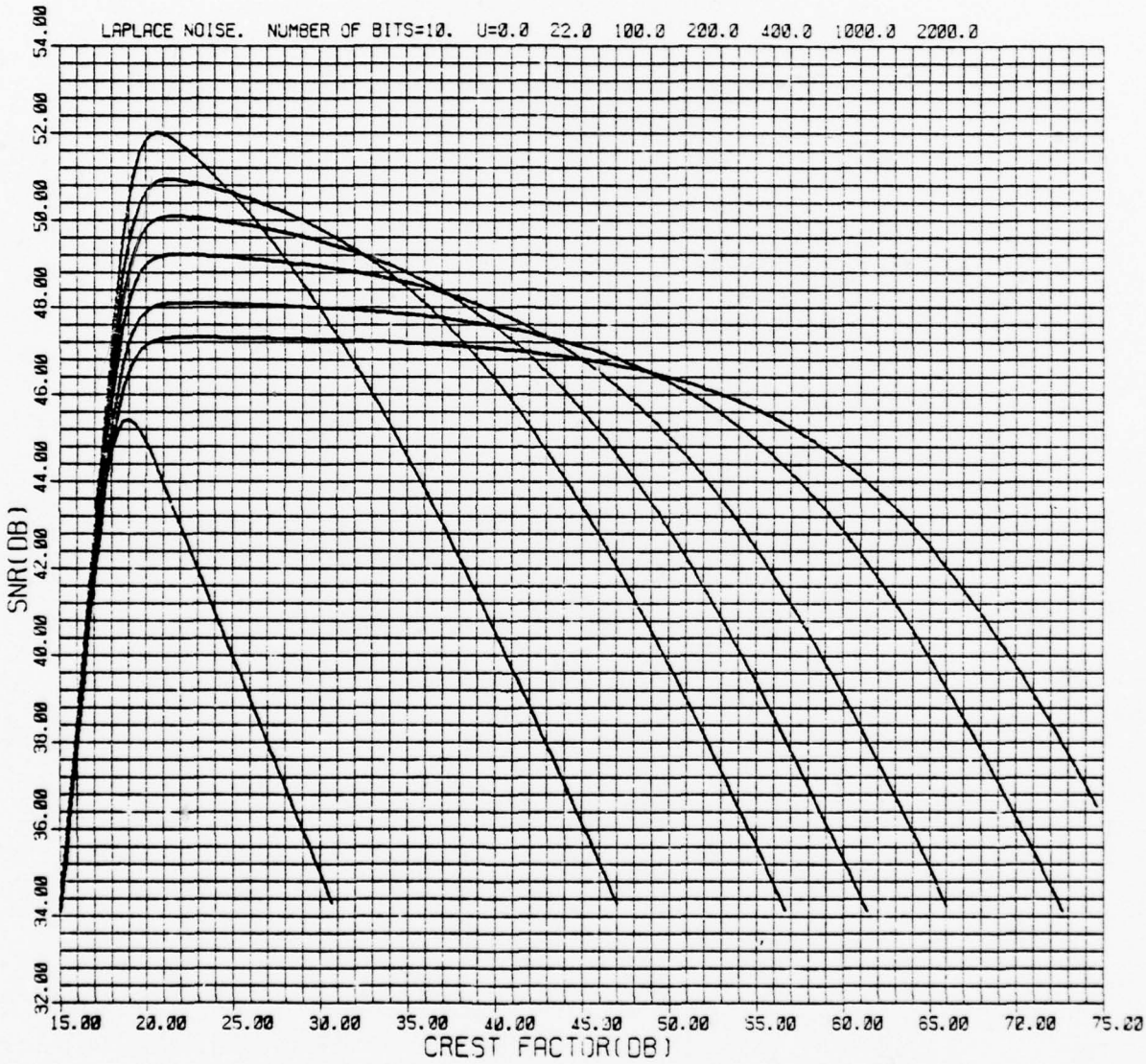

Logarithmic Quantization SNR Versus Crest Factor For 10 Bits And Laplace Amplitude Statistics.

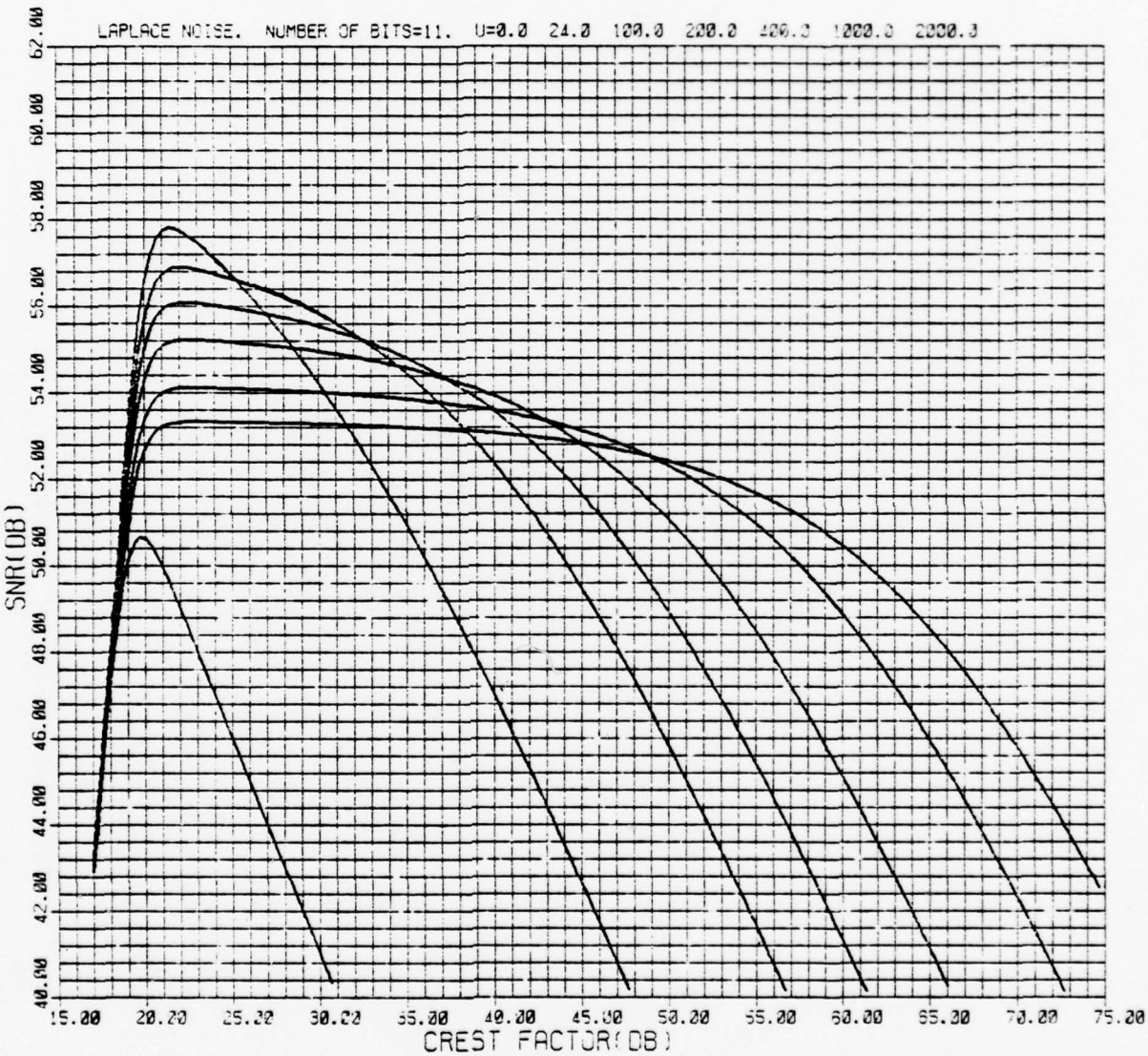

Logarithmic Quantization SNR Versus Crest Factor For 11 Bits And Laplace Amplitude Statistics.

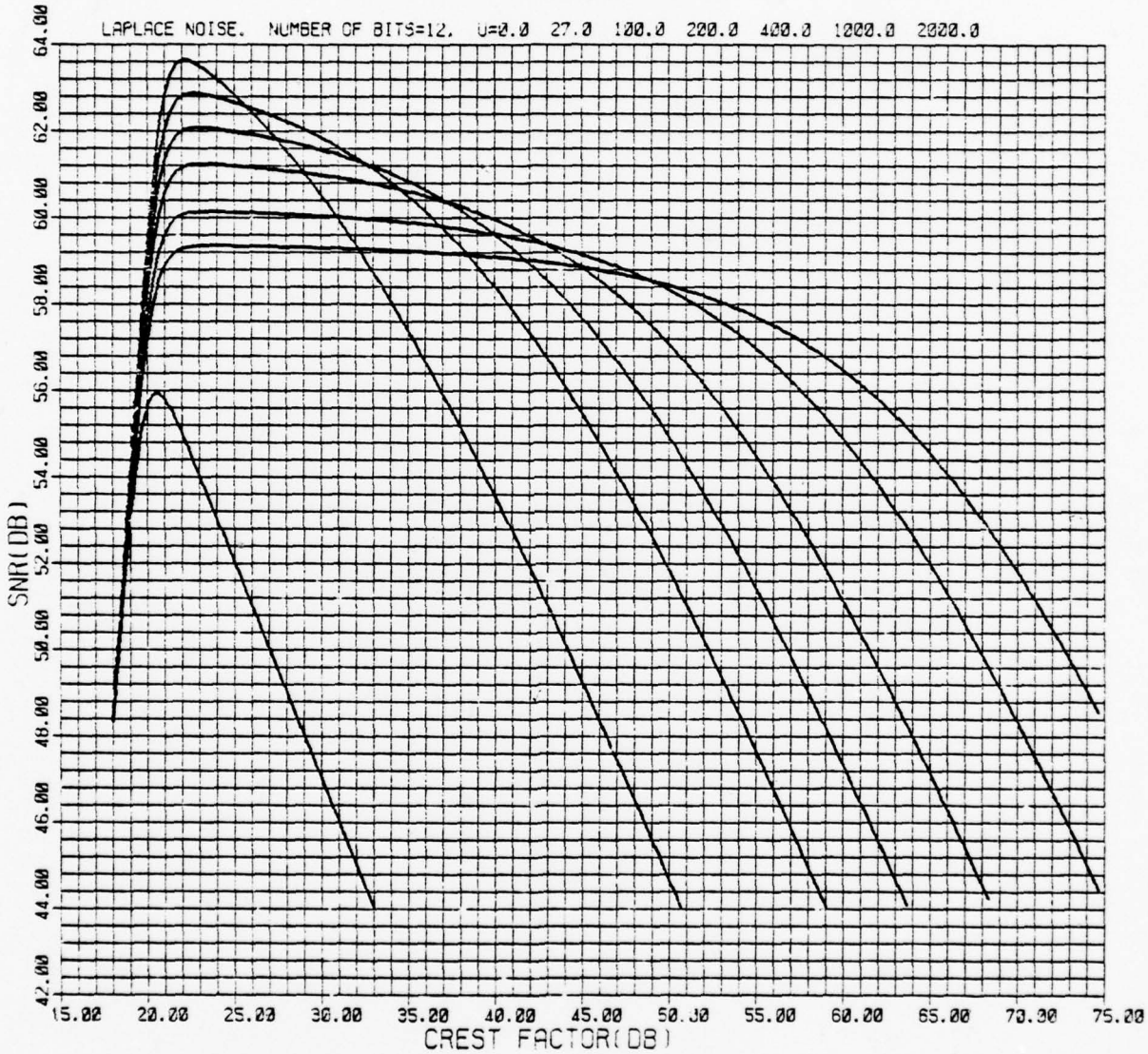

Logarithmic Quantization SNR Versus Crest Factor For 12 Bits And Laplace Amplitude Statistics.

SECTION V

ALIASING ERROR DESIGN CURVES

1. Introduction

This section gives design curves for predicting the dynamic range limitations imposed by aliasing (spectral folding) error as a result of sampling. The curves are of SNSR versus normalized frequency parametric in the normalized sampling rate.

The amount of aliasing error depends on the spectral shape of the signal being sampled. Aliasing error may vary 50 dB over the passband as shown in Figure 5-1. Consequently, a variety of curves are given to approximate the multitude of spectral shapes. Since most aliasing filters are well approximated at band edge by a Chebyshev or Butterworth filter, the SNSR curves have been generated for signals which are the output of a Chebyshev or Butterworth filter driven with Gaussian white noise.

The curves are given for the lowpass case, but may be extrapolated with care to any bandpass case using the bandwidth definition shown in Figure 5-2. Pictures such as Figure 5-3 can be very helpful in avoiding mistakes. Observe that in the bandpass case in addition to aliasing error there is an imaging error which is mathematically analogous to aliasing error. When the signal spectrum is symmetric about the carrier, both errors are simultaneously minimized by choosing the center frequency f_c to be one fourth the sampling frequency f_s.

$$f_c = f_s/4 \tag{5-1}$$

For this special case, no correction in normalized sampling frequency is required

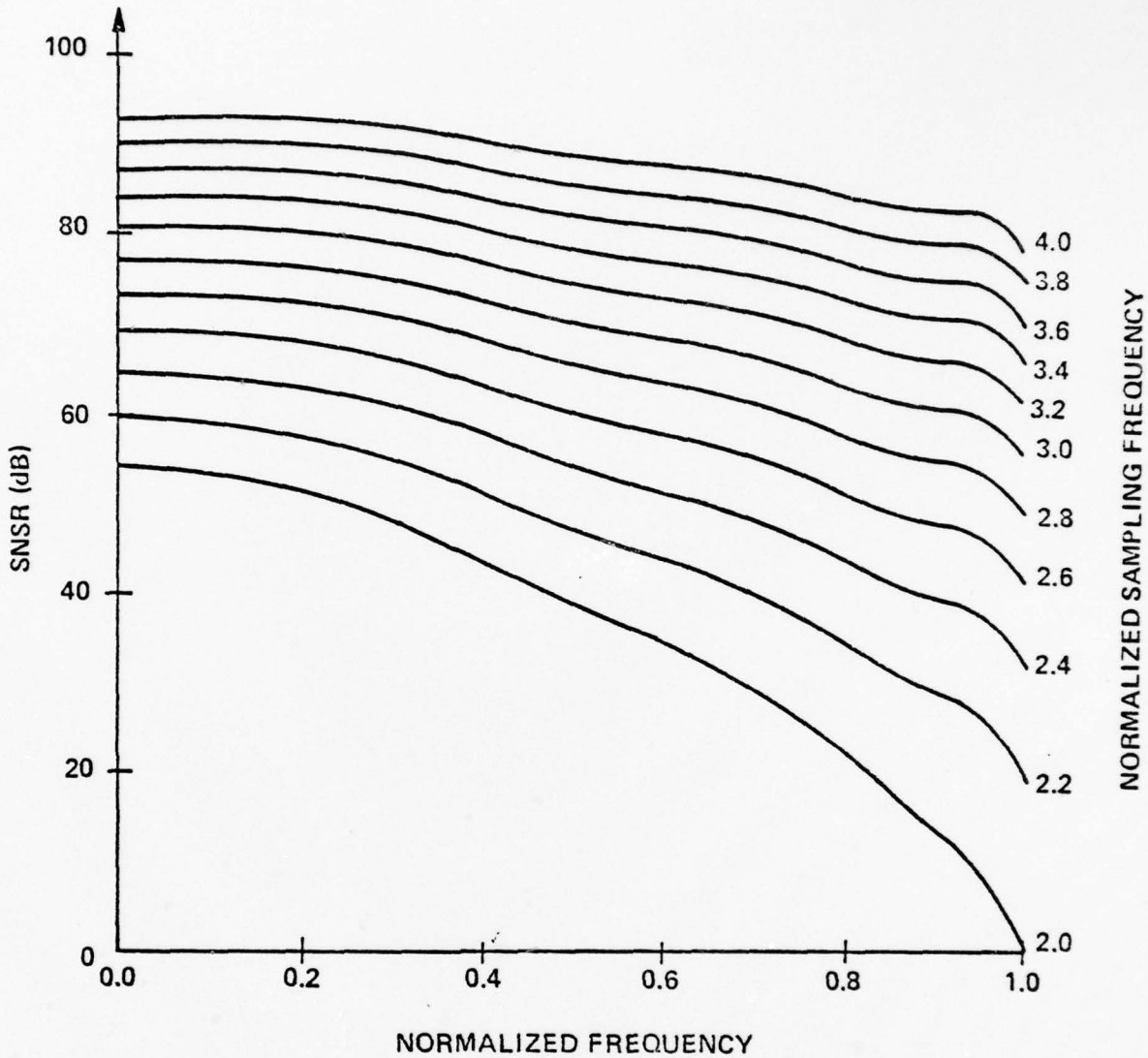

Figure 5-1. SNSR Versus Normalized Frequency for a 6 Pole 1.0 dB Ripple Factor Chebyshev Signal Spectrum.

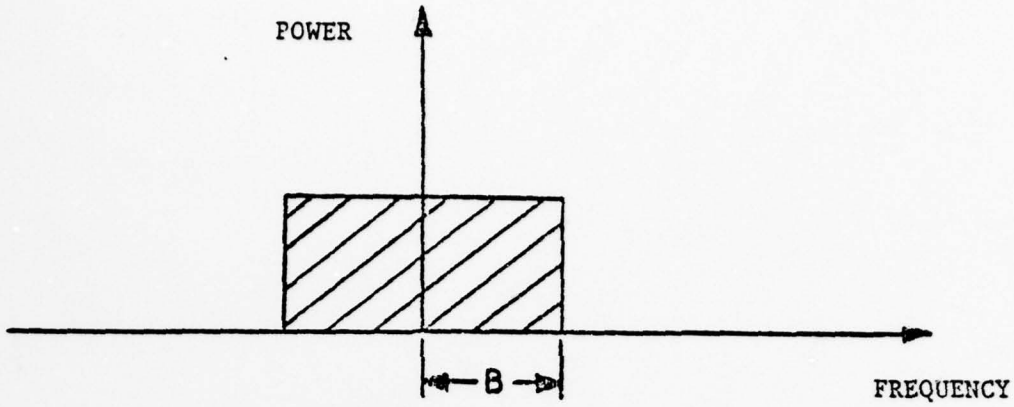

Definition of Bandwidth B - Lowpass Case

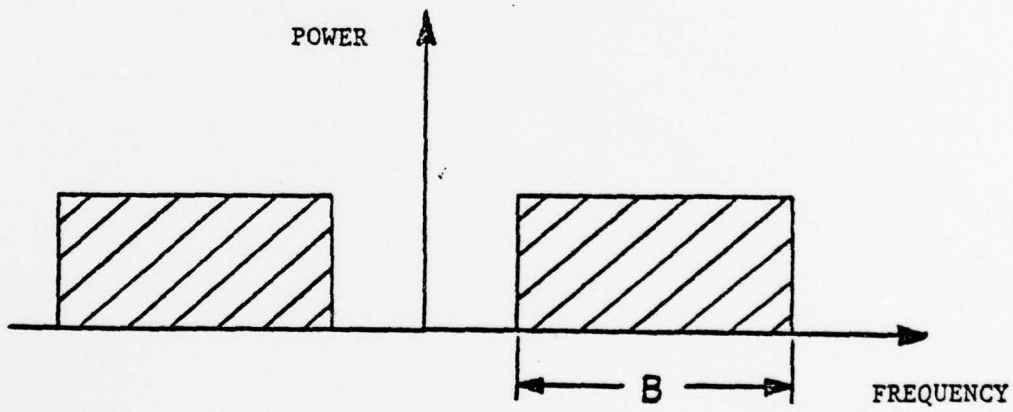

Definition of Bandwidth B - Bandpass Case

Figure 5-2. Definition of Signal Bandwidth

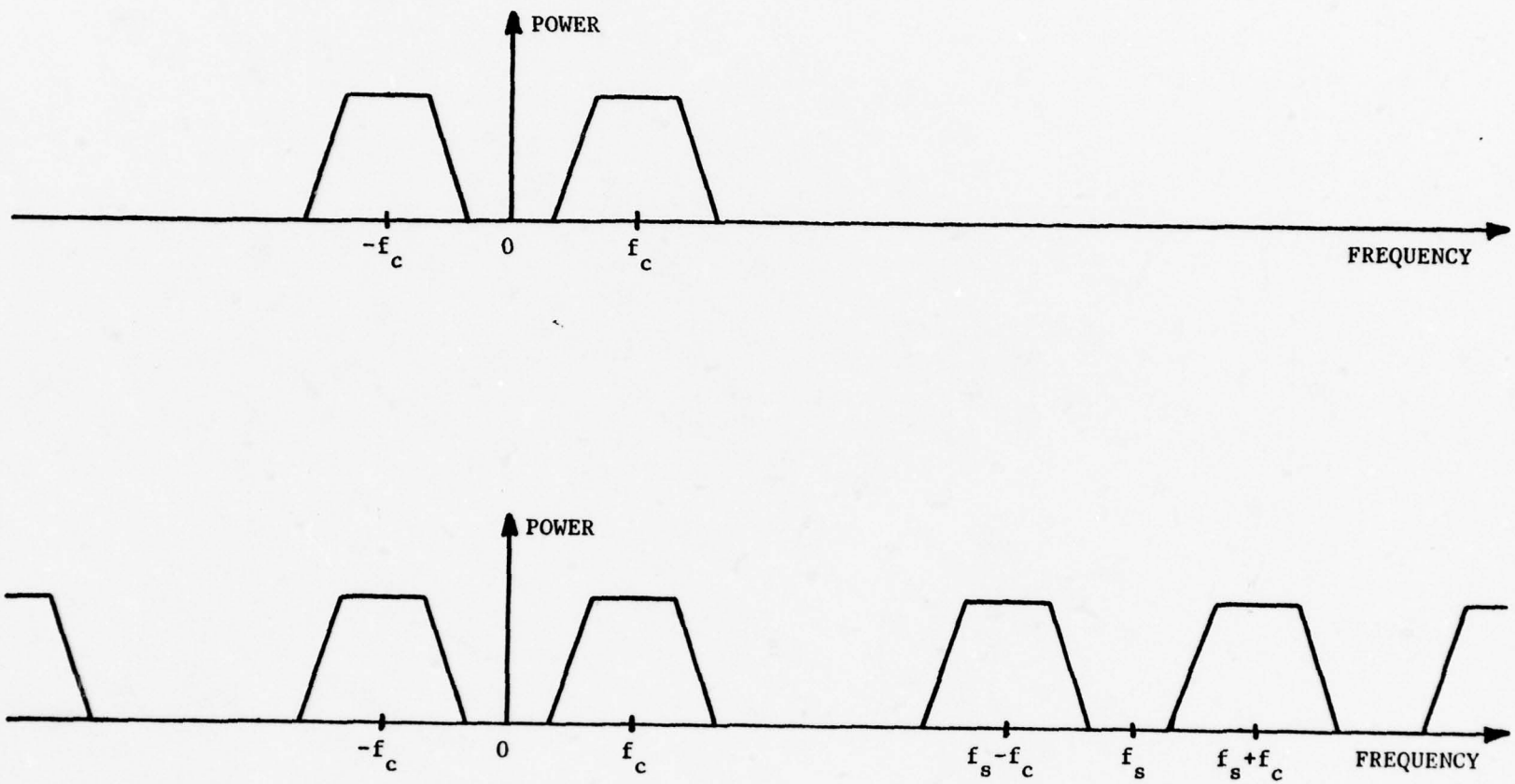

Figure 5-3. Illustration of a Bandpass Signal Power Spectrum Before and After Sampling.

when extrapolating the lowpass curves to the bandpass case because

$$(f_s - f_c) - f_c = f_s - 2f_c = 2f_c \qquad (5\text{-}2)$$

However, even when (5-1) does not hold, the lowpass curves may be extrapolated by drawing a picture and carefully computing the equivalent normalized sampling frequency for the aliasing and imaging errors.

2. Design Curves

Design curves of SNSR versus normalized frequency follow. They are parametric in the normalized sampling frequencies 2.0, 2.1, ... 3.9, 4.0 and are given for 2, 3, ... 10 pole filters. The filter ripple factor in dB is specified at the bottom of each curve. The 0.0 dB ripple factor curves are for Butterworth filters and the others are for Chebyshev filters.

For example, suppose white noise is passed through a 1.0 MHz 6 pole 1.0 dB ripple factor lowpass Chebyshev filter. From the following curves a sampling rate of 2.5 MHz (2.5 normalized sampling frequency) yields a maximum SNSR = 67 dB at zero and a minimum SNSR = 37 dB at 1.0 MHz.

Now suppose white noise is passed through a 2.0 MHz 6 pole 1.0 dB ripple factor bandpass Chebyshev filter centered at 1.25 MHz. A sampling rate of 5.0 MHz (2.5 normalized sampling frequency) is four times the center frequency. Consequently, the maximum SNSR = 67 dB occurs at 1.25 MHz and the minimum SNSR = 37 dB occurs at 0.25 MHz and 2.25 MHz.

Next suppose white noise is passed through a 2.0 MHz 6 pole 1.0 dB ripple factor bandpass Chebyshev filter centered at 1.25 MHz. However, a sampling rate of 6.0 MHz is chosen (3.0 normalized sampling rate). Then SNSR = 37 dB at 0.25 MHz and SNSR = 67 dB at 1.25 MHz, but SNSR = 55 dB at 2.25 MHz. Thus, there is more imaging error than aliasing error.

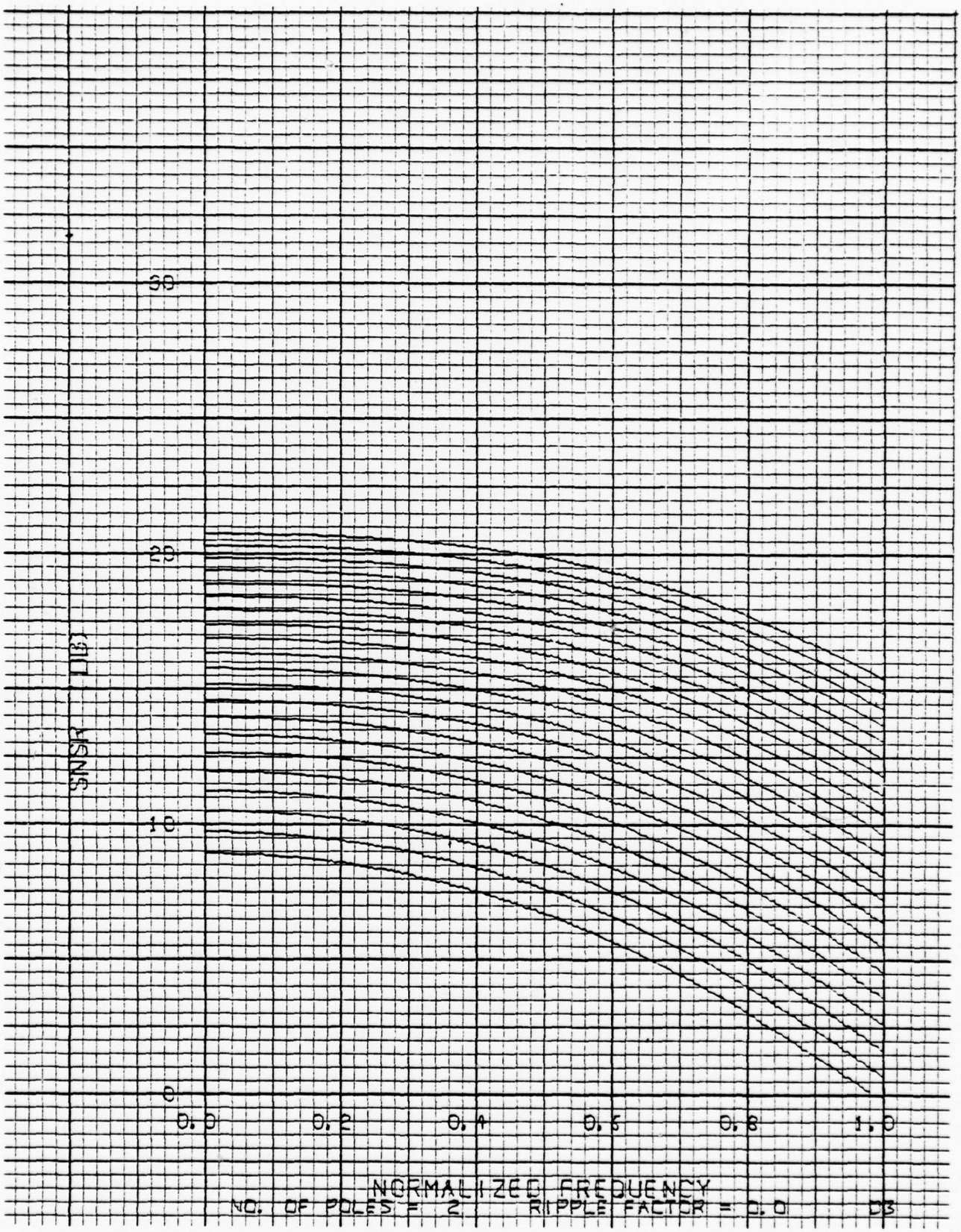

Aliasing Error SNSR Versus Normalized Frequency For Normalized Sampling Rates of 2.0, 2.1, ... 3.9, 4.0.

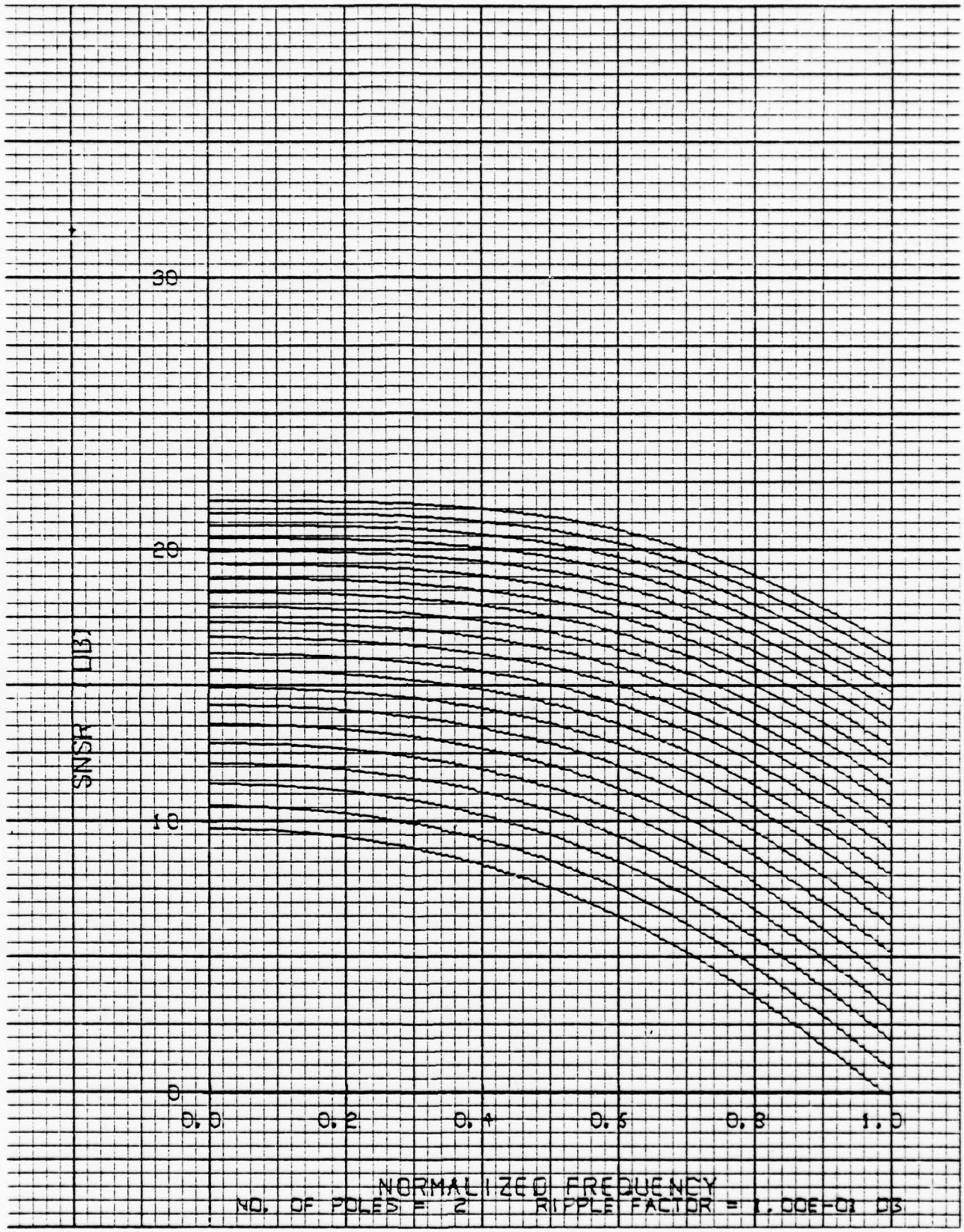

Aliasing Error SNSR Versus Normalized Frequency For Normalized Sampling Rates of 2.0, 2.1, ... 3.9, 4.0.

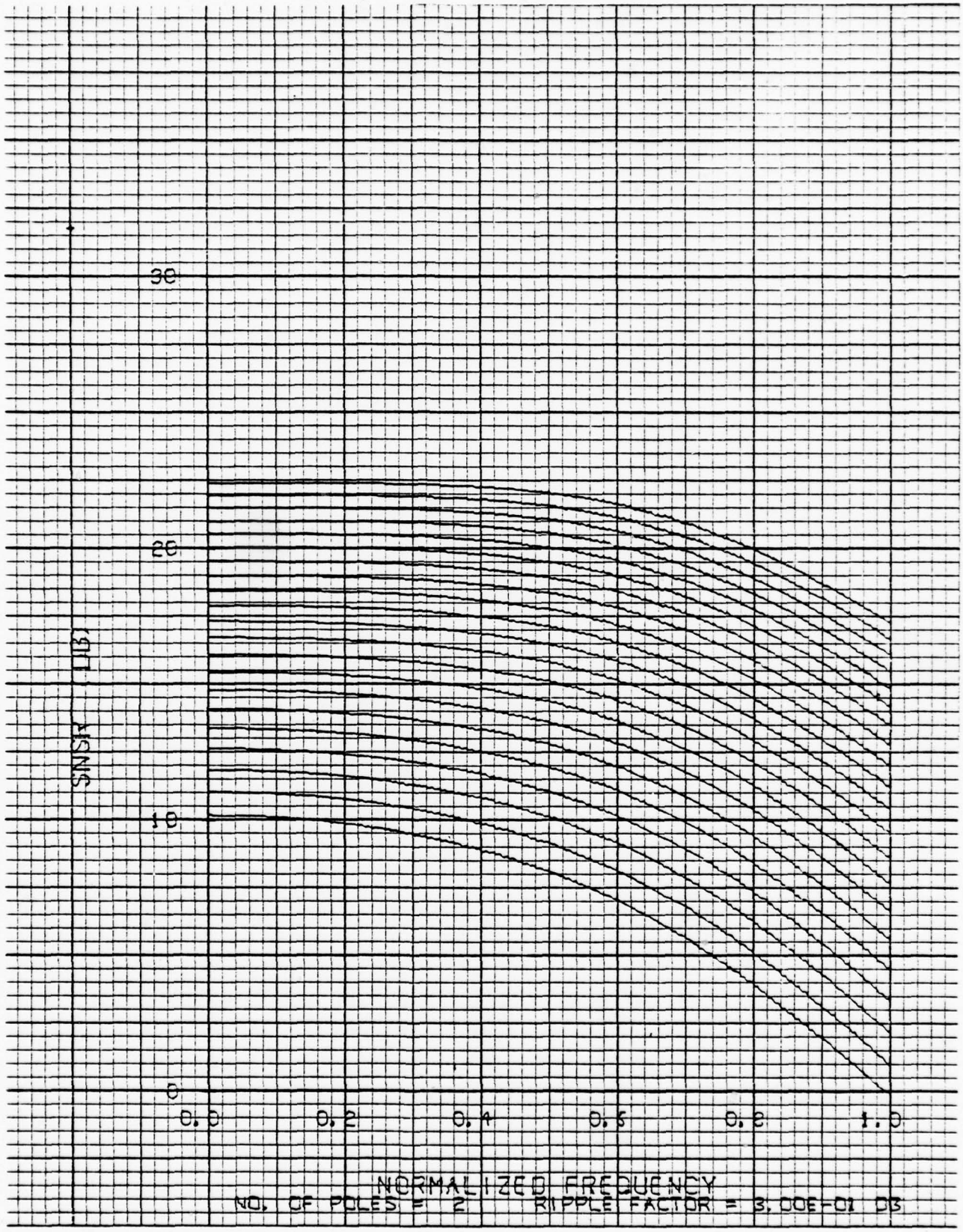

Aliasing Error SNSR Versus Normalized Frequency For Normalized Sampling Rates of 2.0, 2.1, ... 3.9, 4.0.

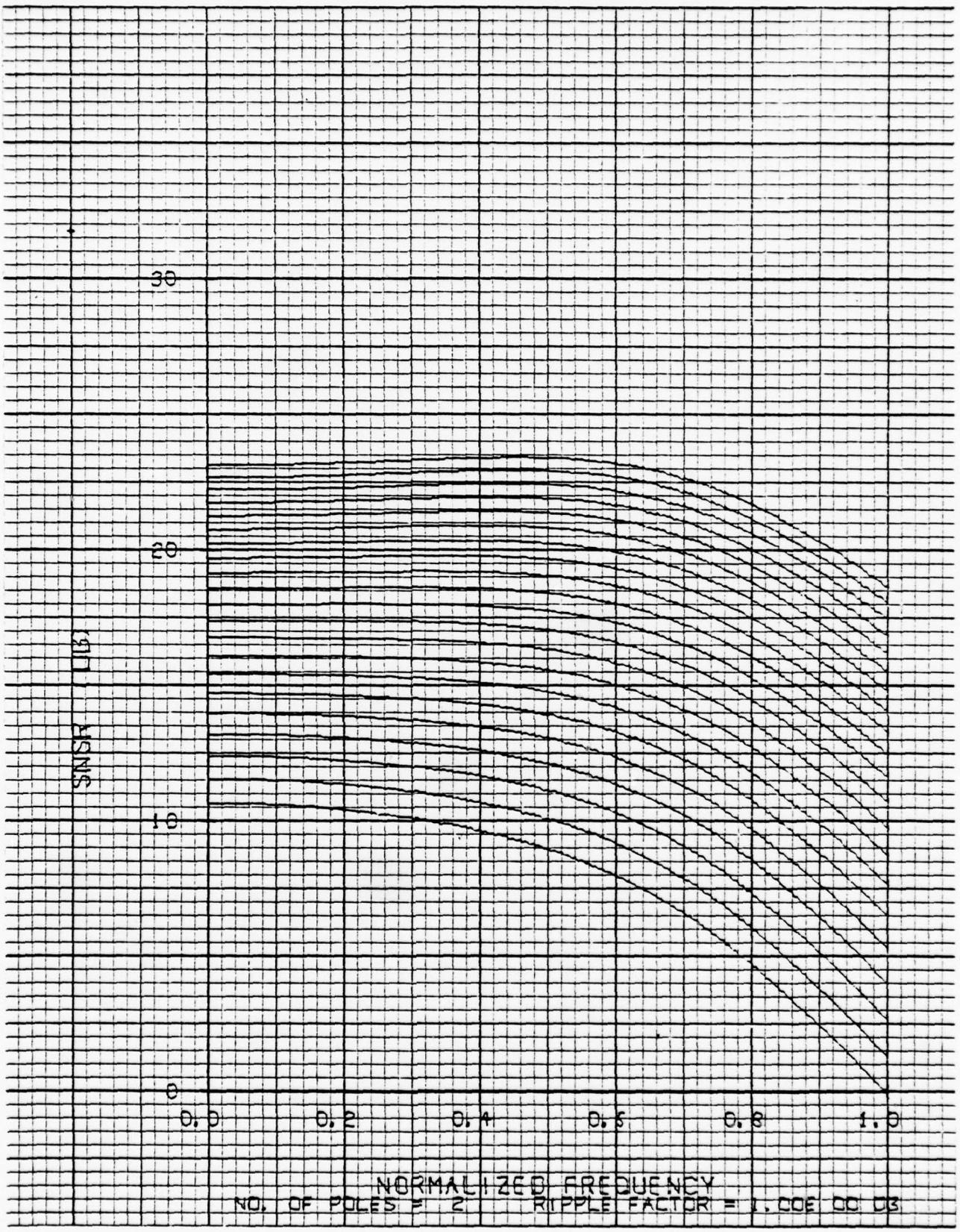

Aliasing Error SNSR Versus Normalized Frequency For Normalized Sampling Rates of 2.0, 2.1, ... 3.9, 4.0.

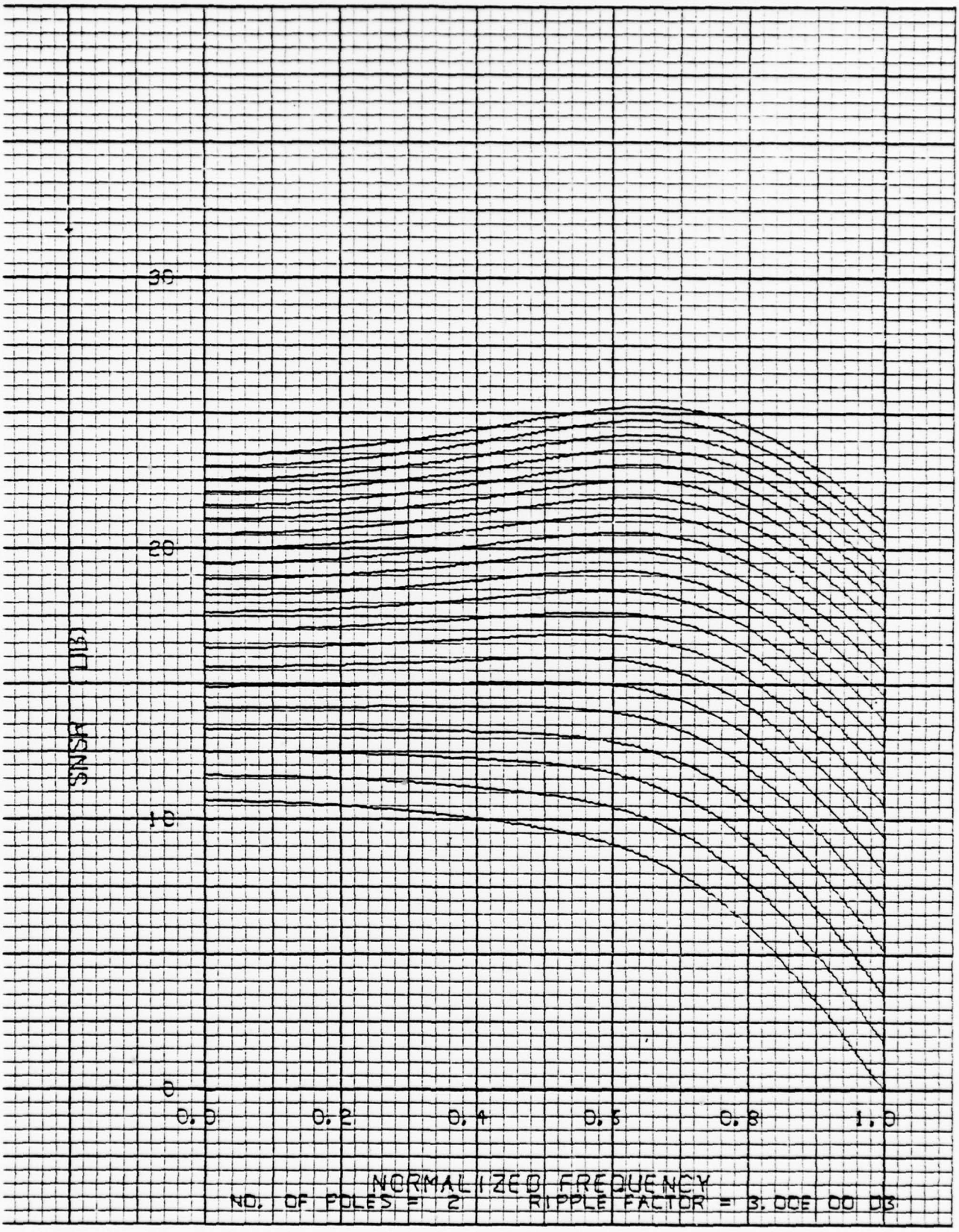

Aliasing Error SNSR Versus Normalized Frequency For Normalized Sampling Rates of 2.0, 2.1, ... 3.9, 4.0.

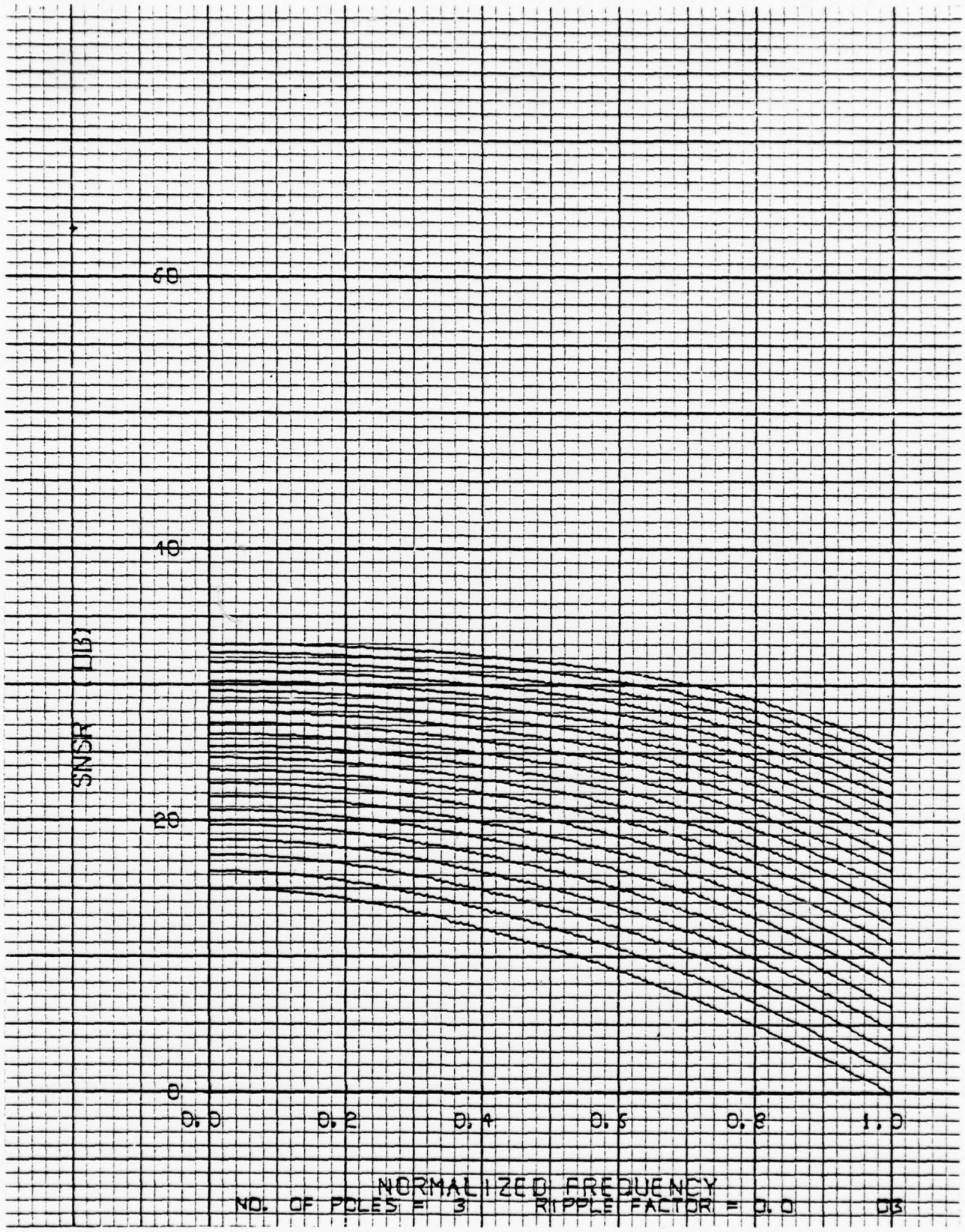

Aliasing Error SNSR Versus Normalized Frequency For Normalized Sampling Rates of 2.0, 2.1, ... 3.9, 4.0.

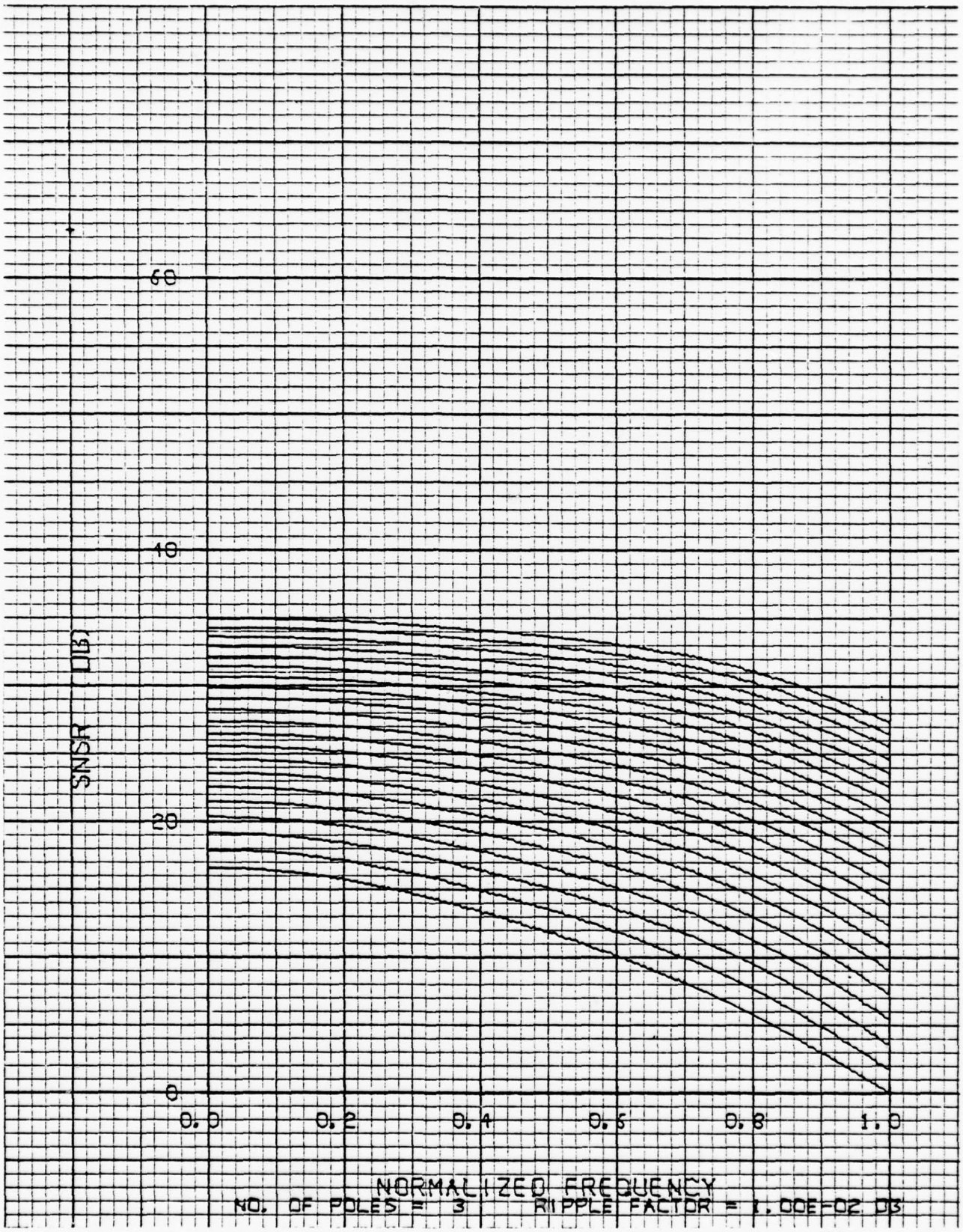

Aliasing Error SNSR Versus Normalized Frequency For Normalized Sampling Rates of 2.0, 2.1, ... 3.9, 4.0.

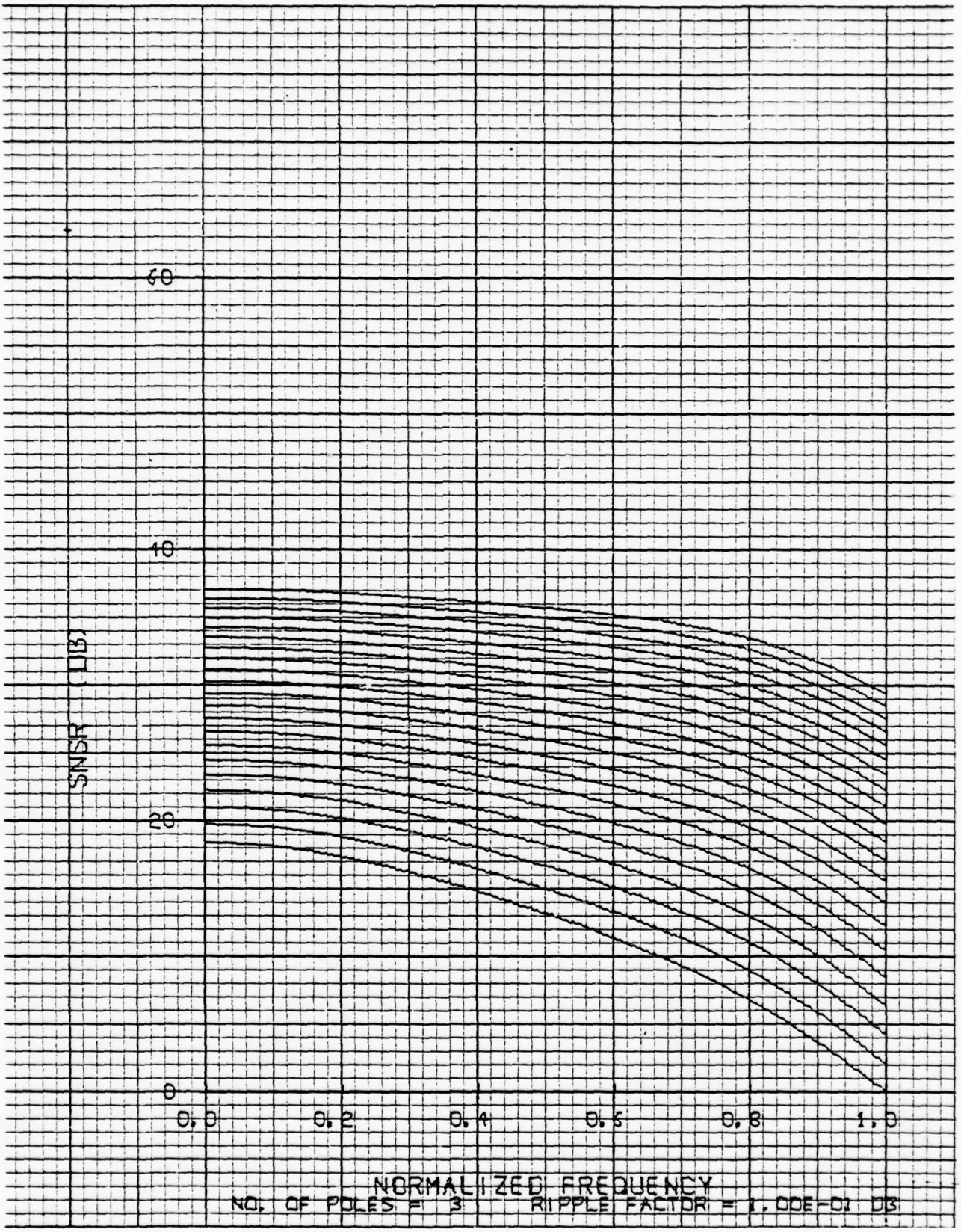

Aliasing Error SNSR Versus Normalized Frequency For Normalized Sampling Rates of 2.0, 2.1, ... 3.9, 4.0.

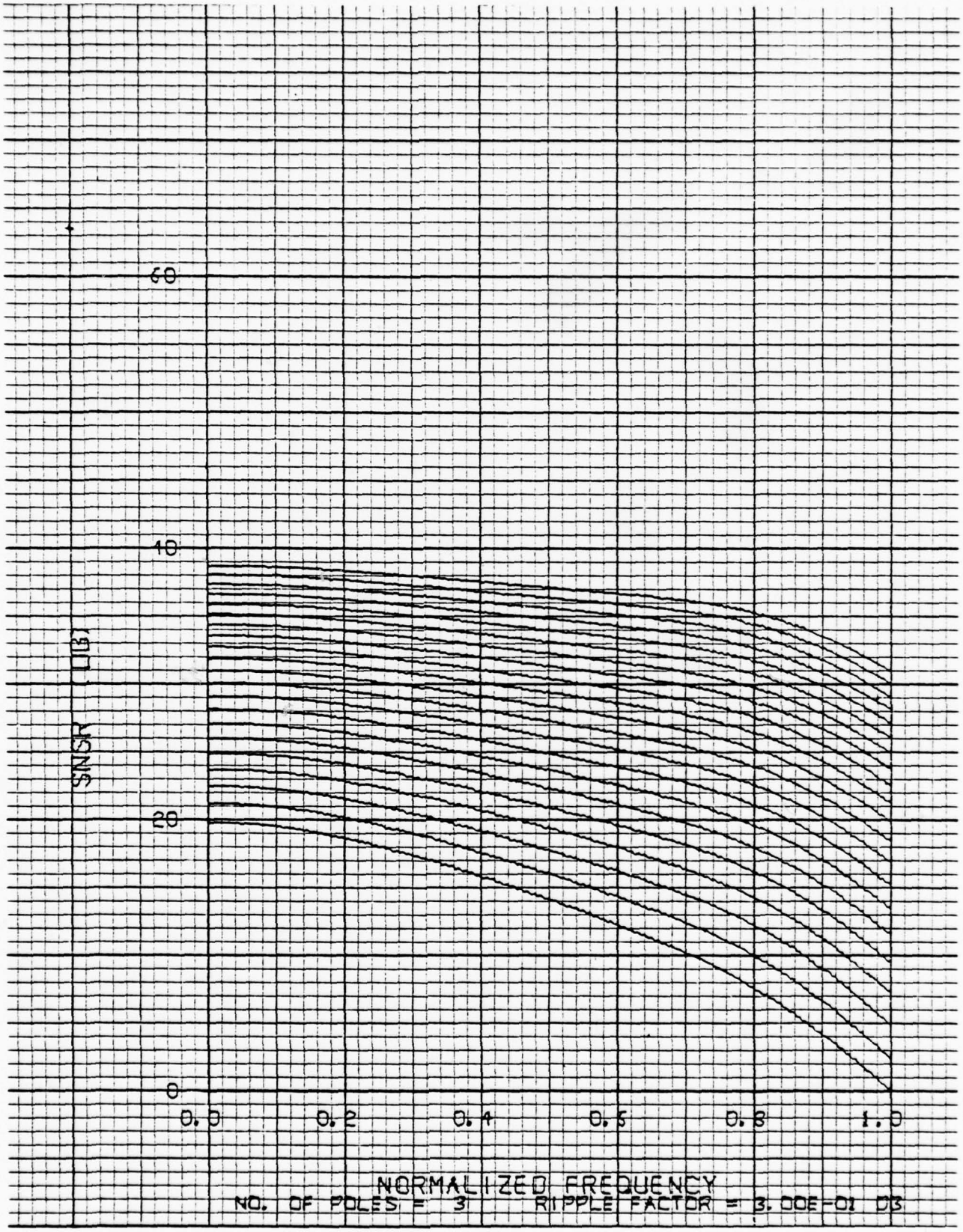

Aliasing Error SNSR Versus Normalized Frequency For Normalized Sampling Rates of 2.0, 2.1, ... 3.9, 4.0.

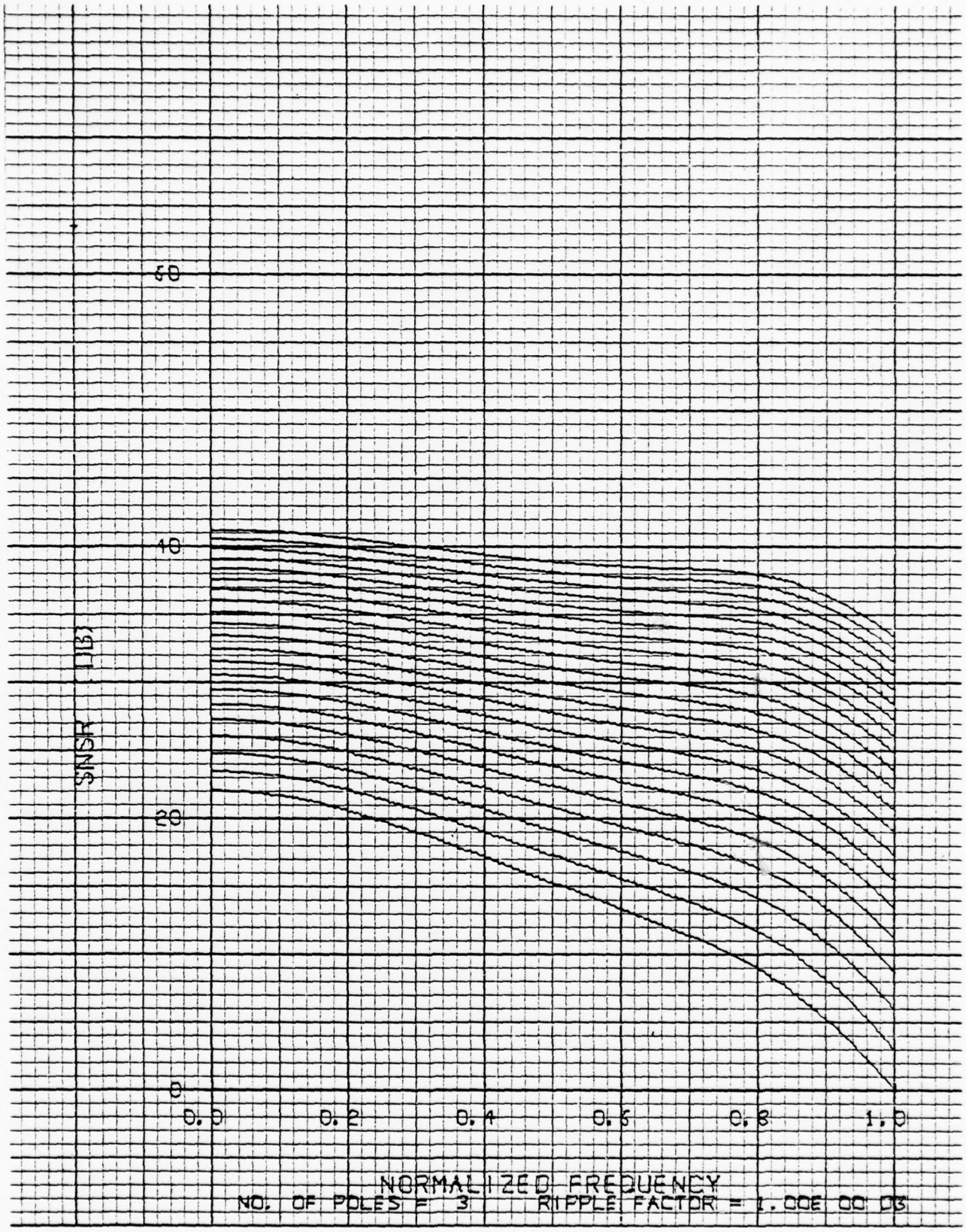

Aliasing Error SNSR Versus Normalized Frequency For Normalized Sampling Rates of 2.0, 2.1, ... 3.9, 4.0.

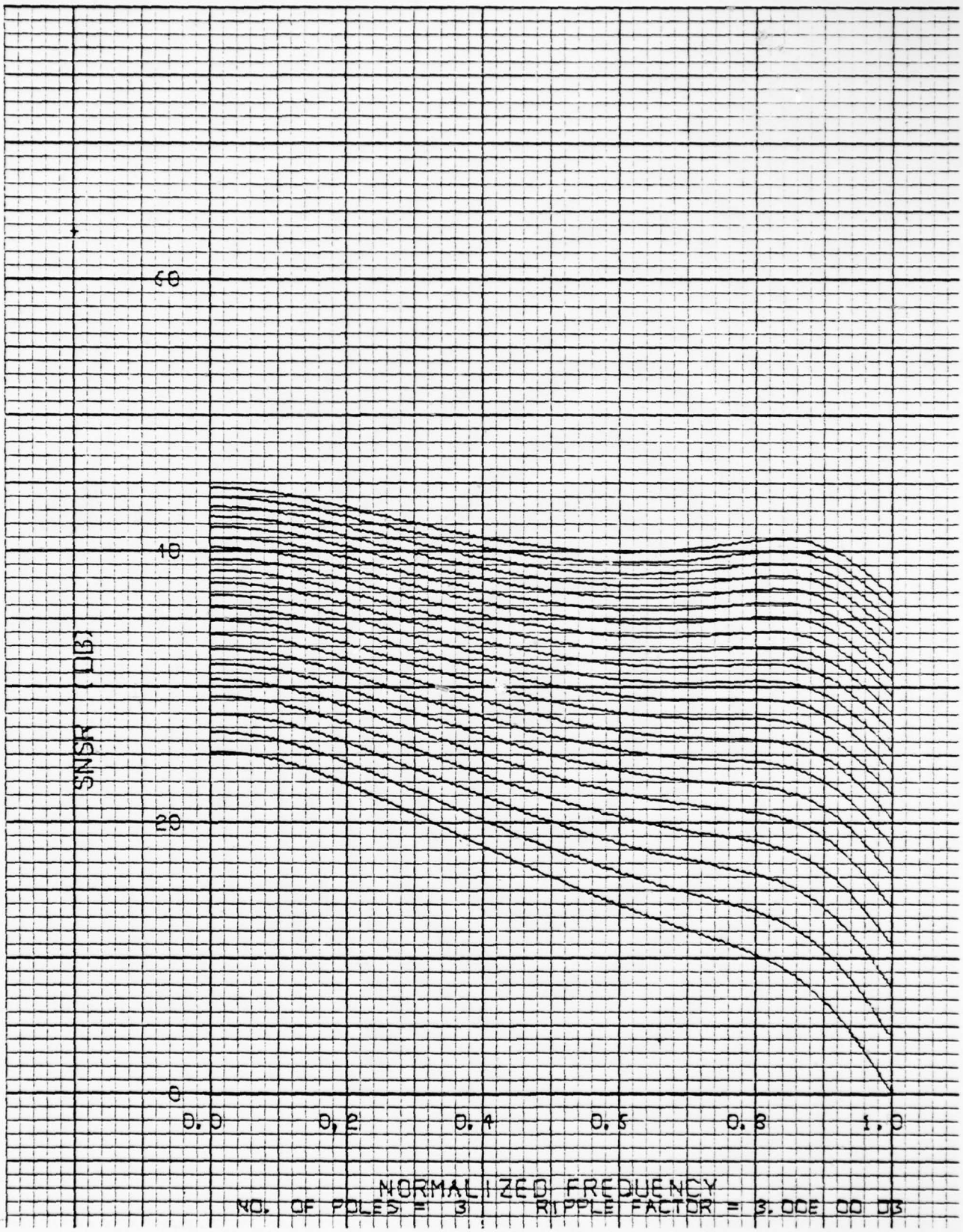

Aliasing Error SNSR Versus Normalized Frequency For Normalized Sampling Rates of 2.0, 2.1, ... 3.9, 4.0.

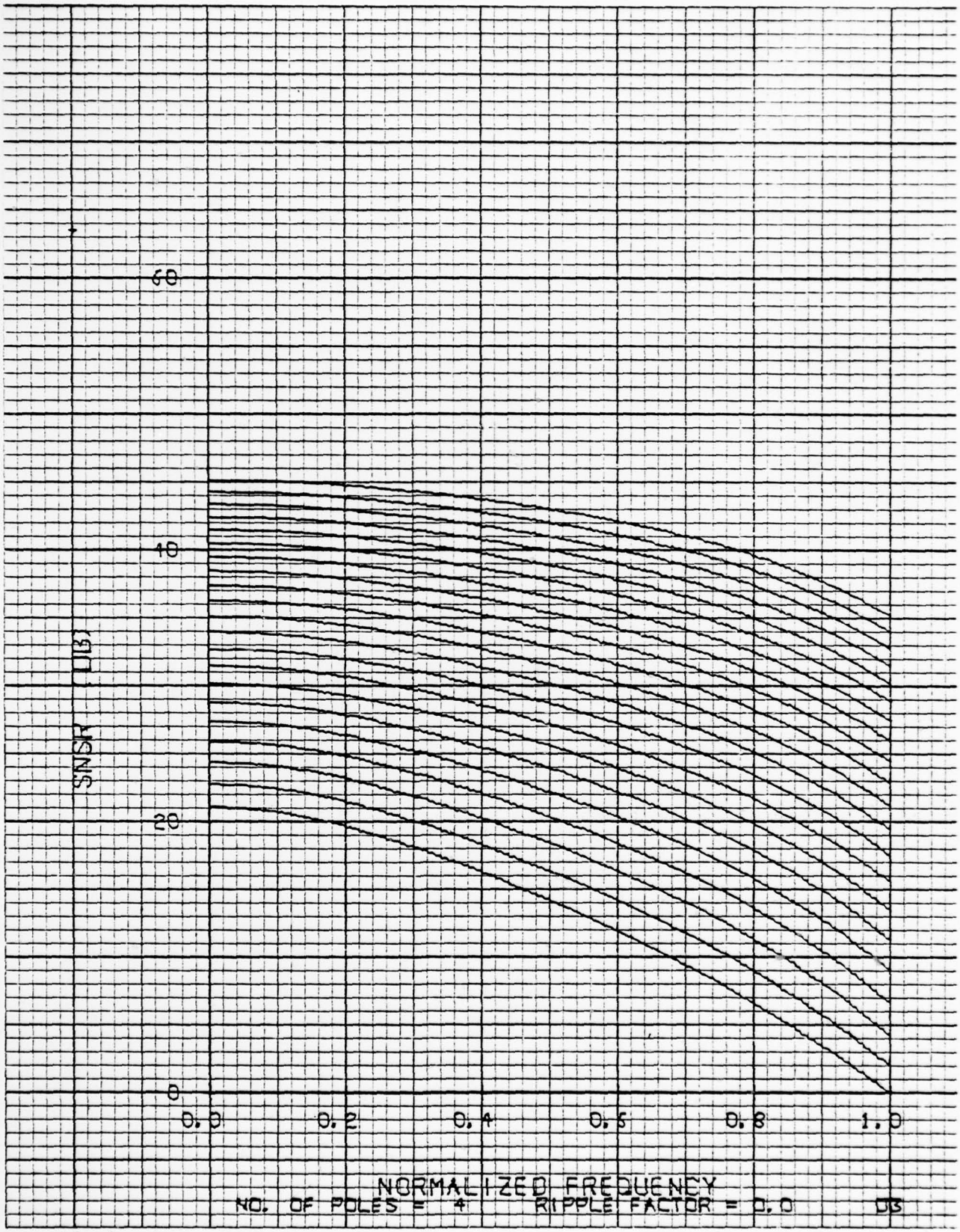

Aliasing Error SNSR Versus Normalized Frequency For Normalized Sampling Rates of 2.0, 2.1, ... 3.9, 4.0.

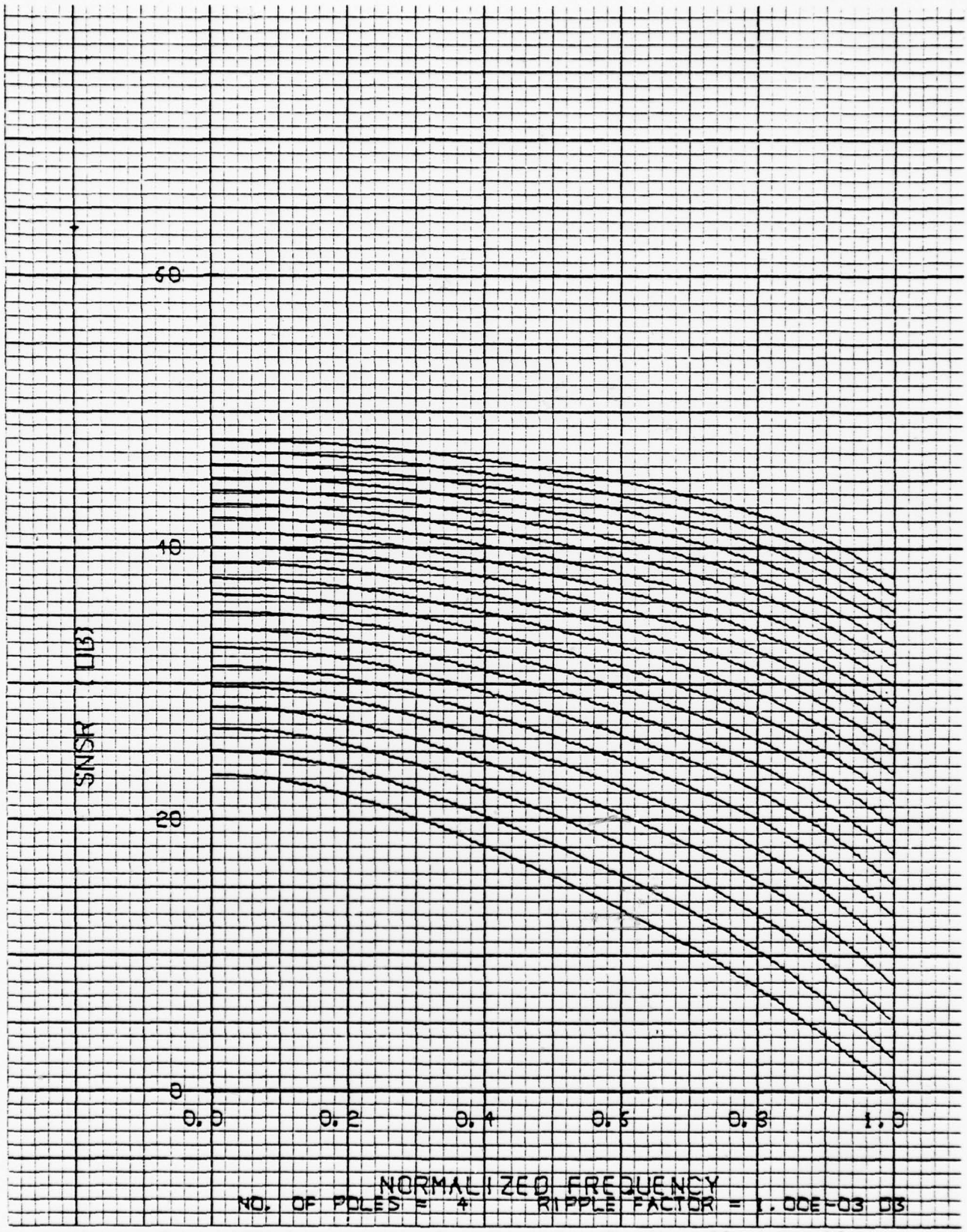

Aliasing Error SNSR Versus Normalized Frequency For Normalized Sampling Rates of 2.0, 2.1, ... 3.9, 4.0.

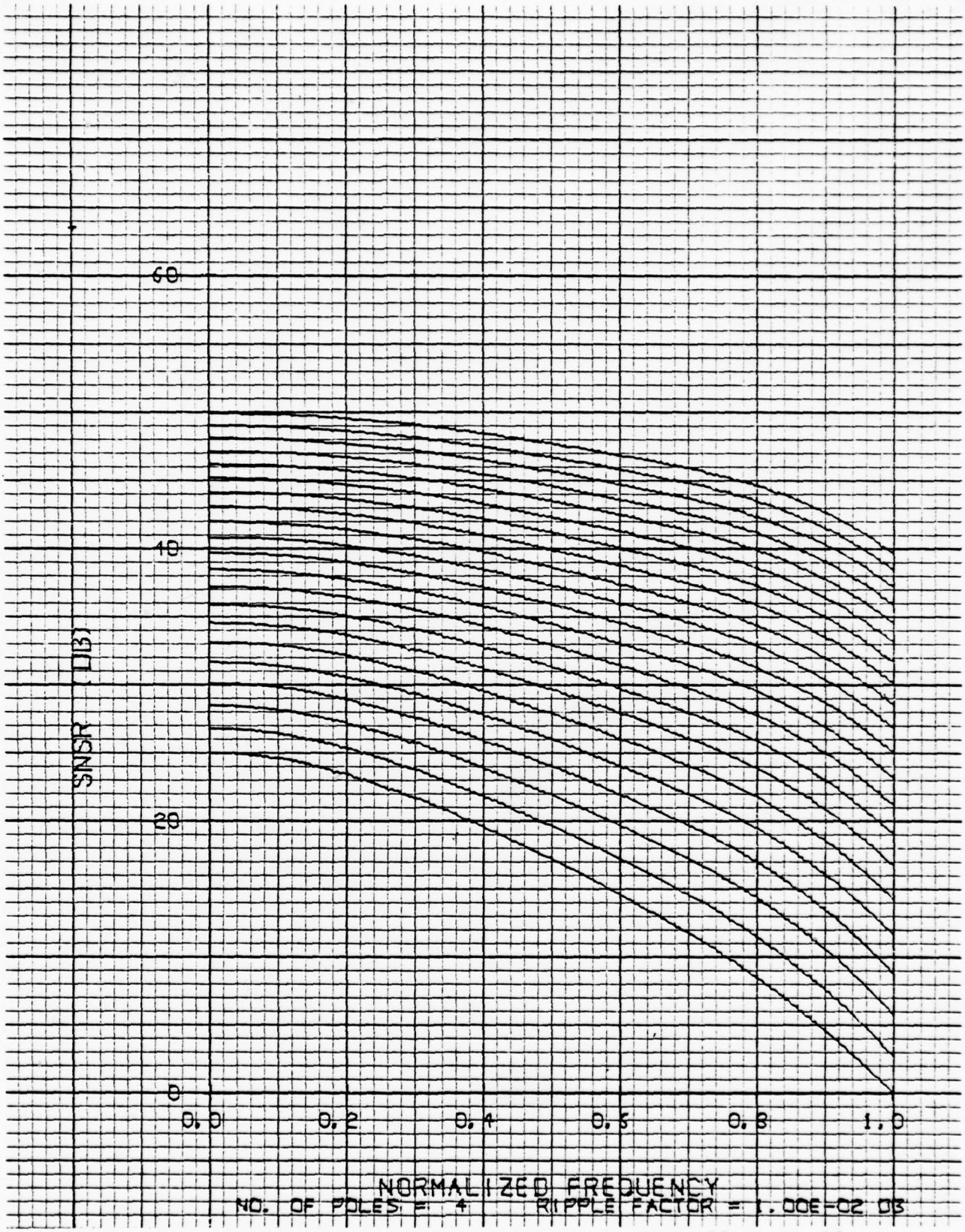

Aliasing Error SNSR Versus Normalized Frequency For Normalized Sampling Rates of 2.0, 2.1, ... 3.9, 4.0.

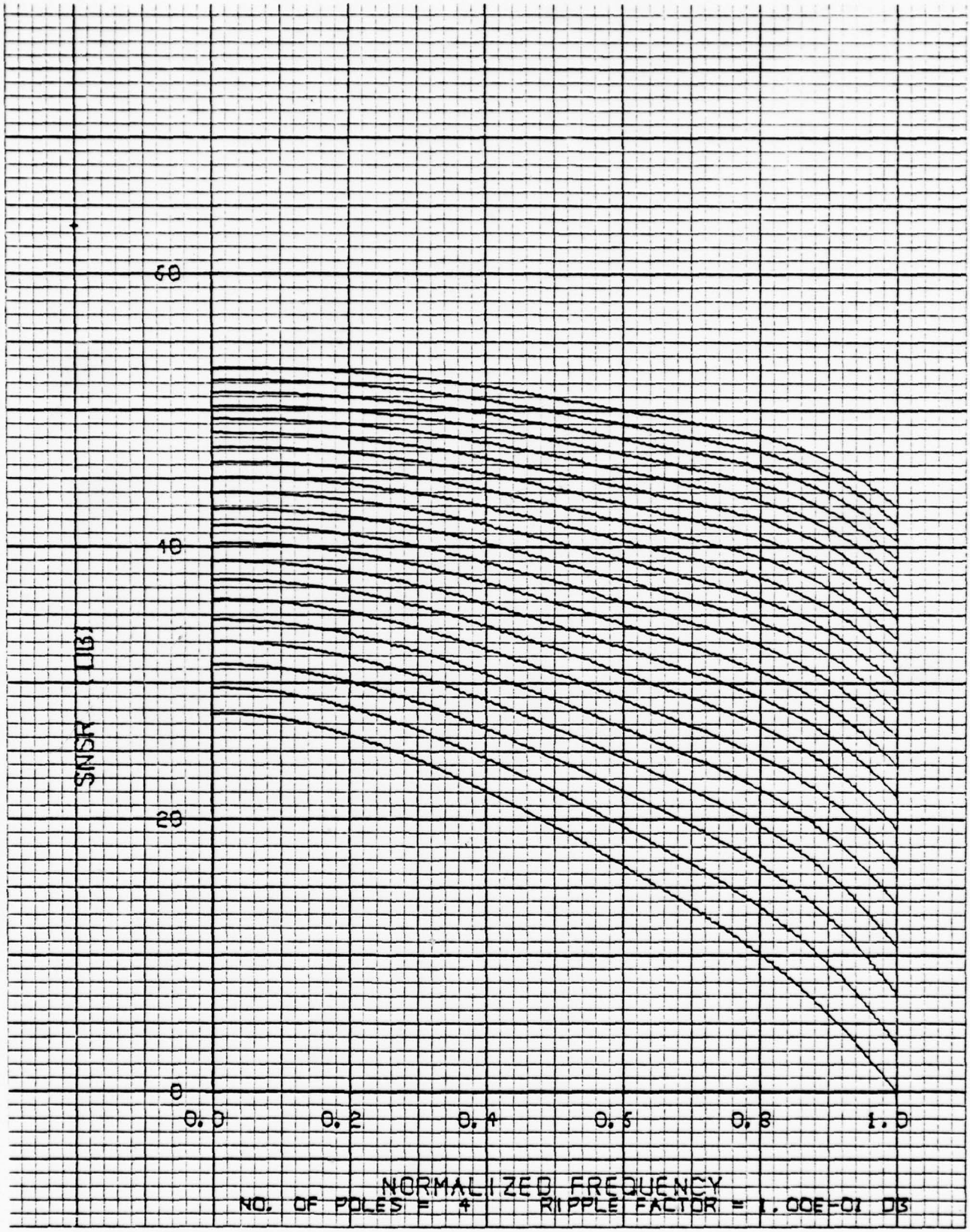

Aliasing Error SNSR Versus Normalized Frequency For Normalized Sampling Rates of 2.0, 2.1, ... 3.9, 4.0.

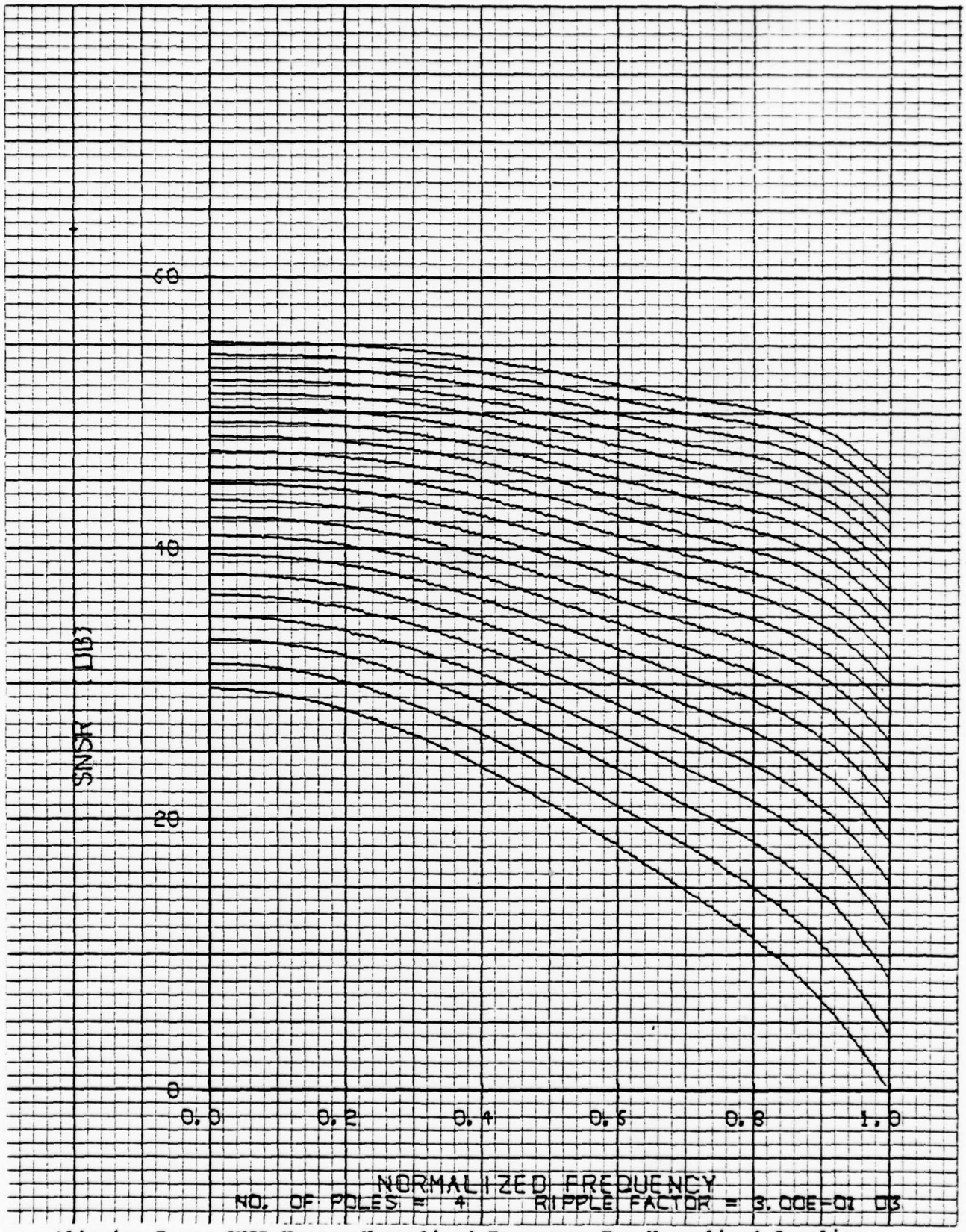

Aliasing Error SNSR Versus Normalized Frequency For Normalized Sampling Rates of 2.0, 2.1, ... 3.9, 4.0.

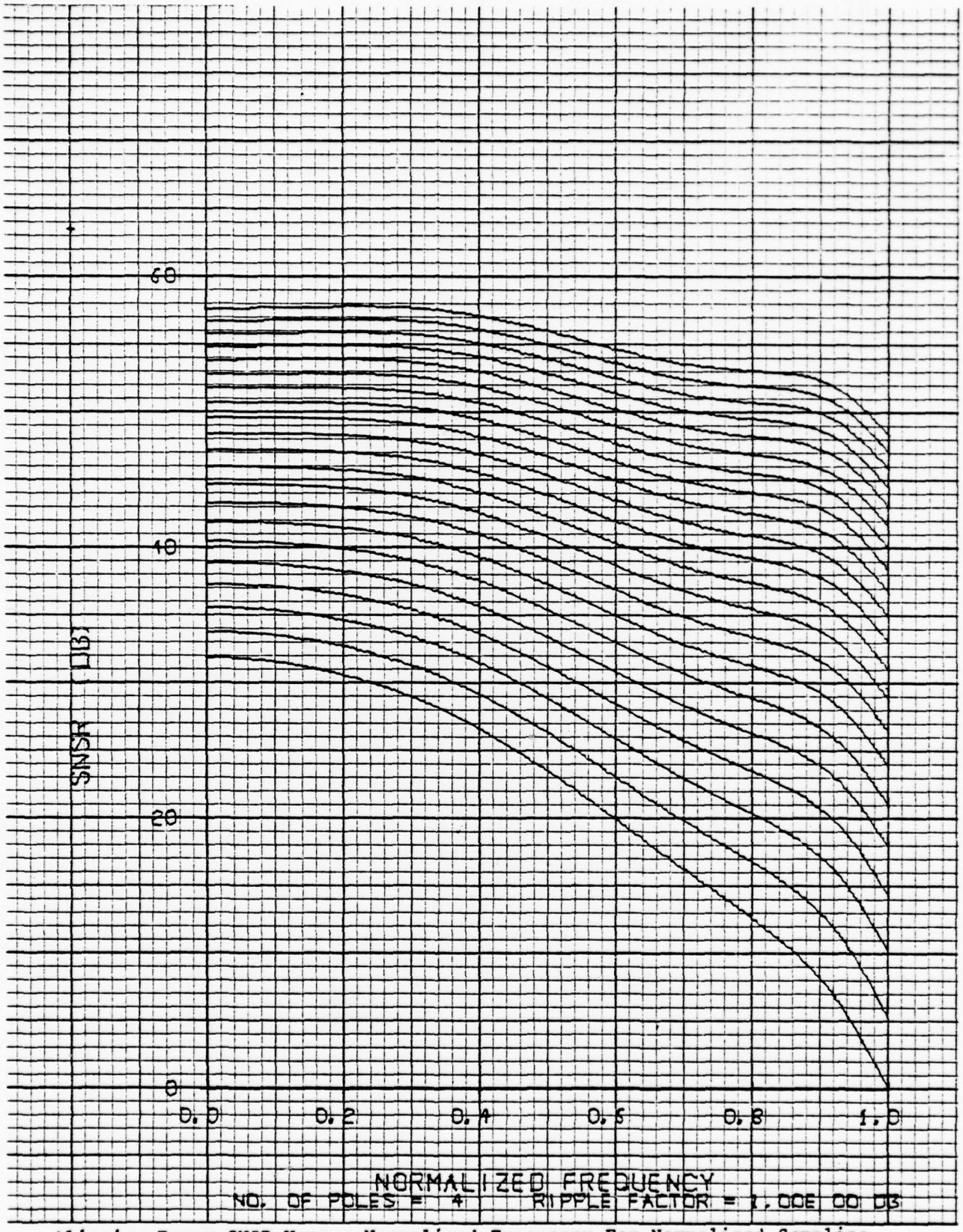

Aliasing Error SNSR Versus Normalized Frequency For Normalized Sampling Rates of 2.0, 2.1, ... 3.9, 4.0.

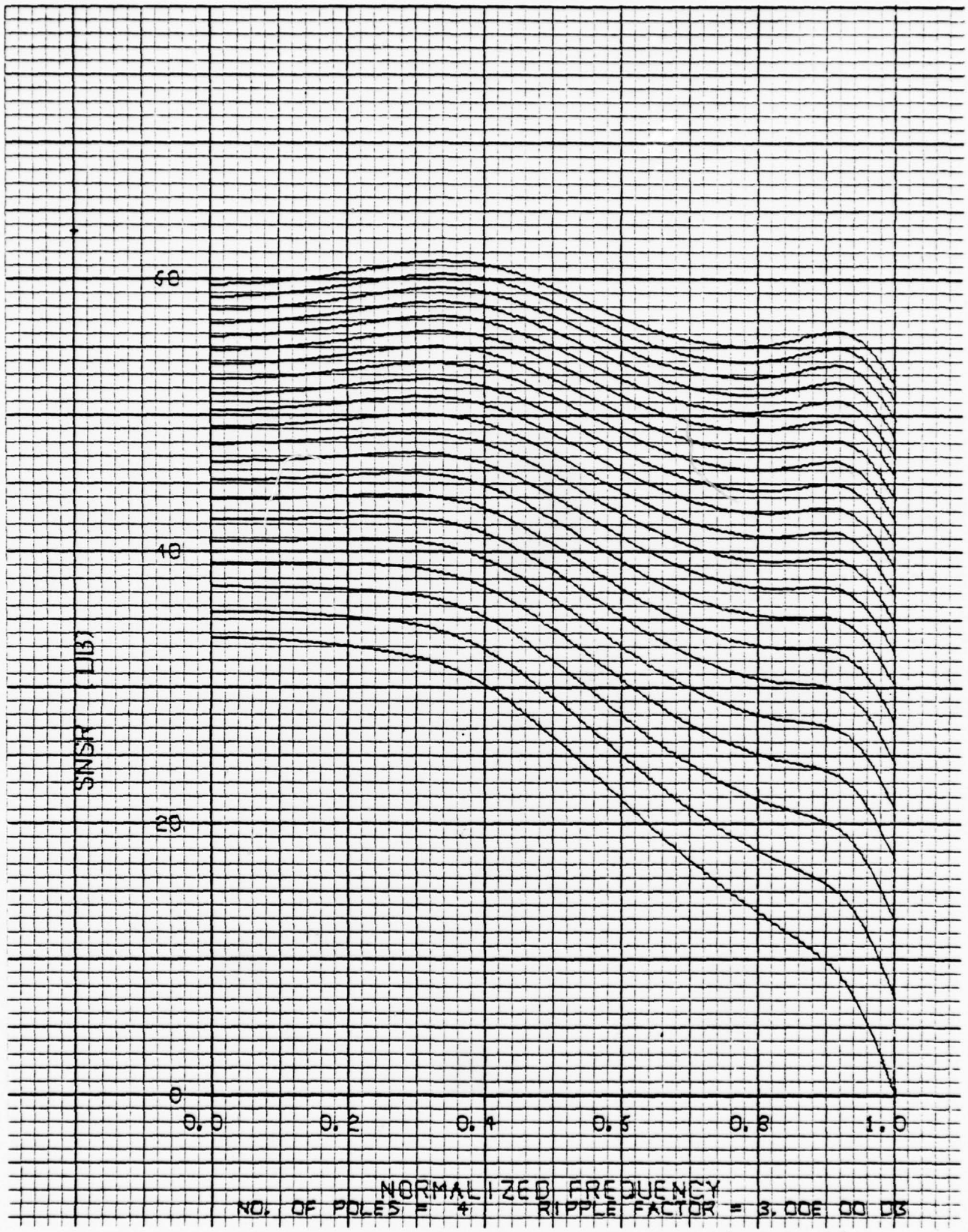

Aliasing Error SNSR Versus Normalized Frequency For Normalized Sampling Rates of 2.0, 2.1, ... 3.9, 4.0.

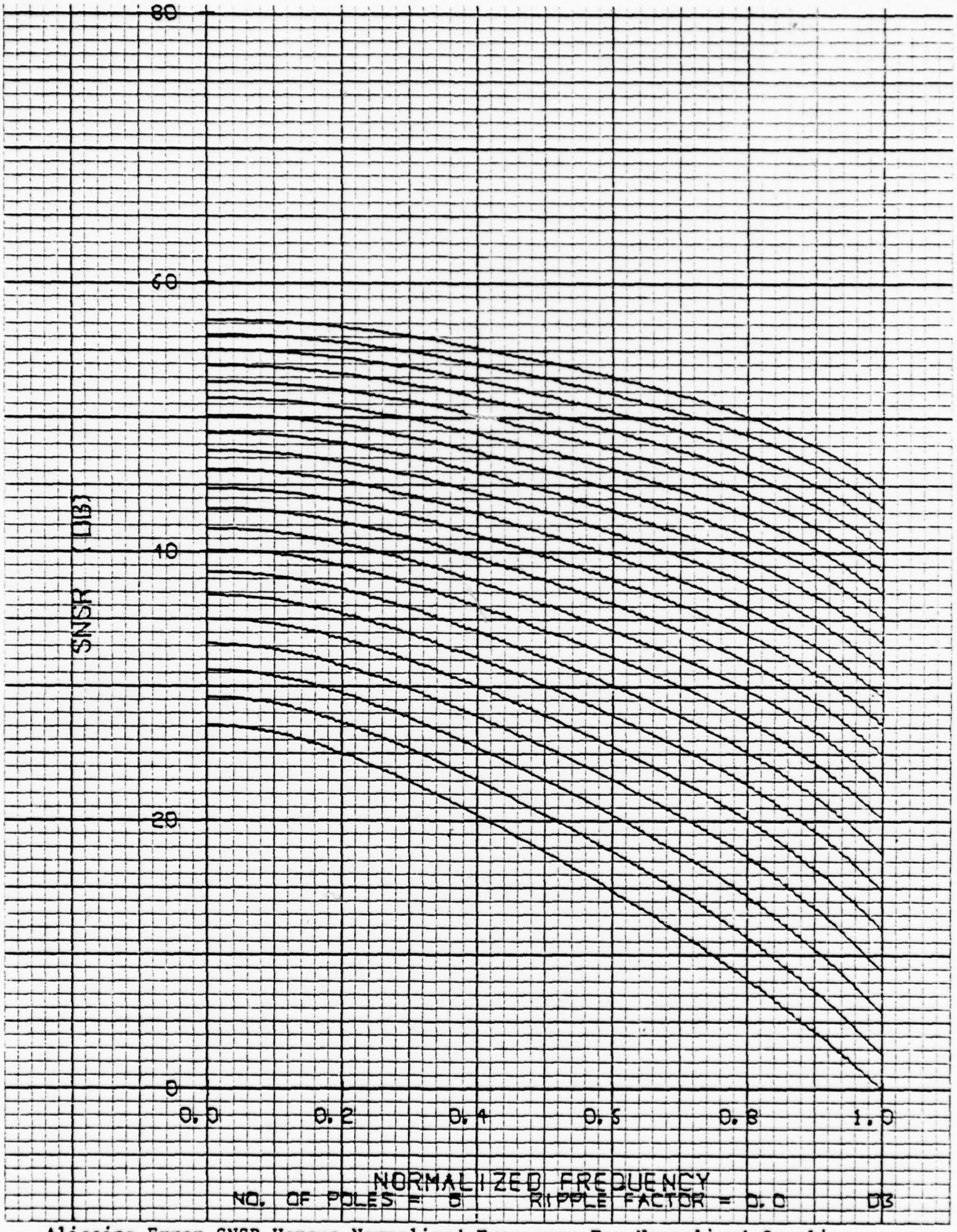

Aliasing Error SNSR Versus Normalized Frequency For Normalized Sampling Rates of 2.0, 2.1, ... 3.9, 4.0.

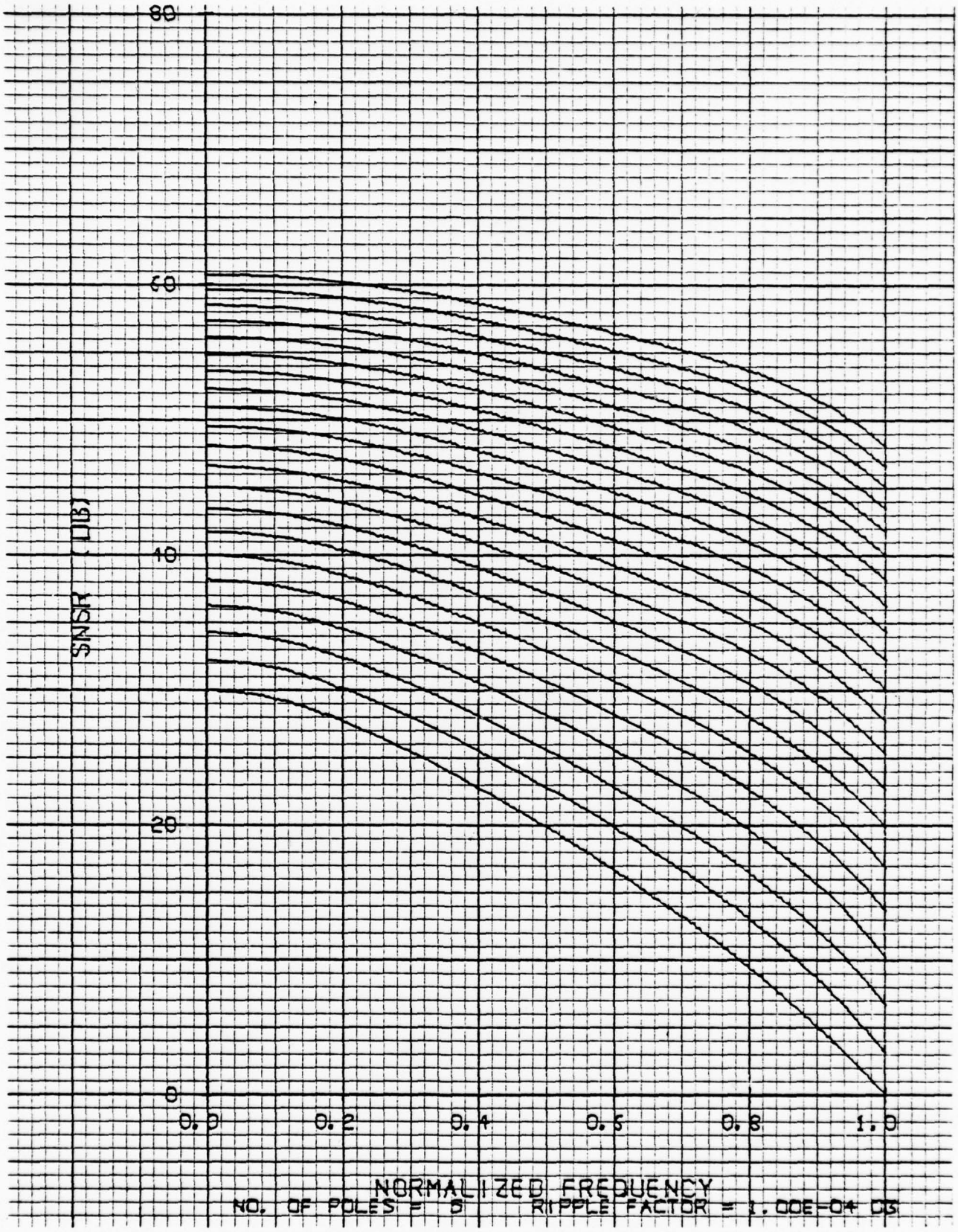

Aliasing Error SNSR Versus Normalized Frequency For Normalized Sampling Rates of 2.0, 2.1, ... 3.9, 4.0.

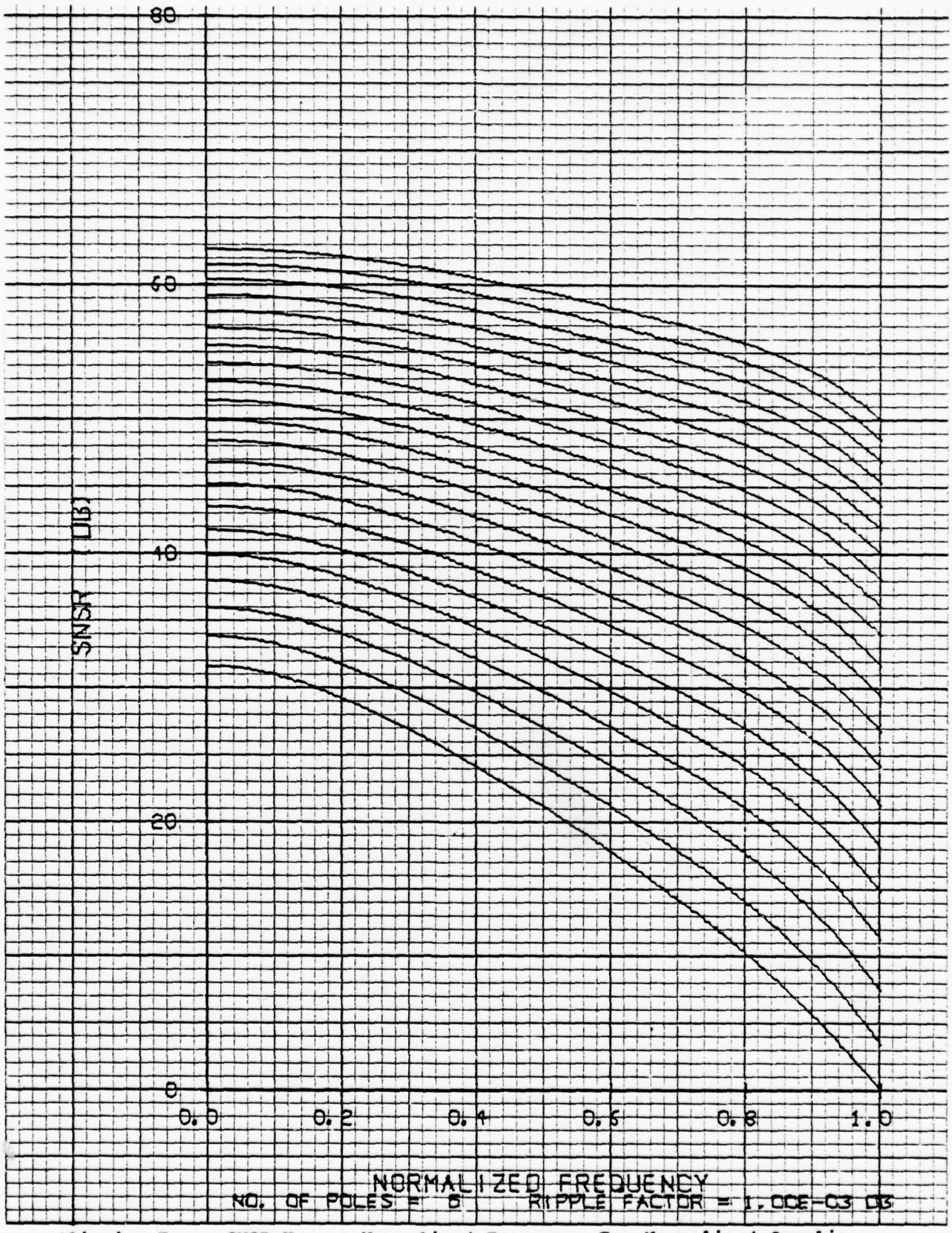

Aliasing Error SNSR Versus Normalized Frequency For Normalized Sampling Rates of 2.0, 2.1, ... 3.9, 4.0.

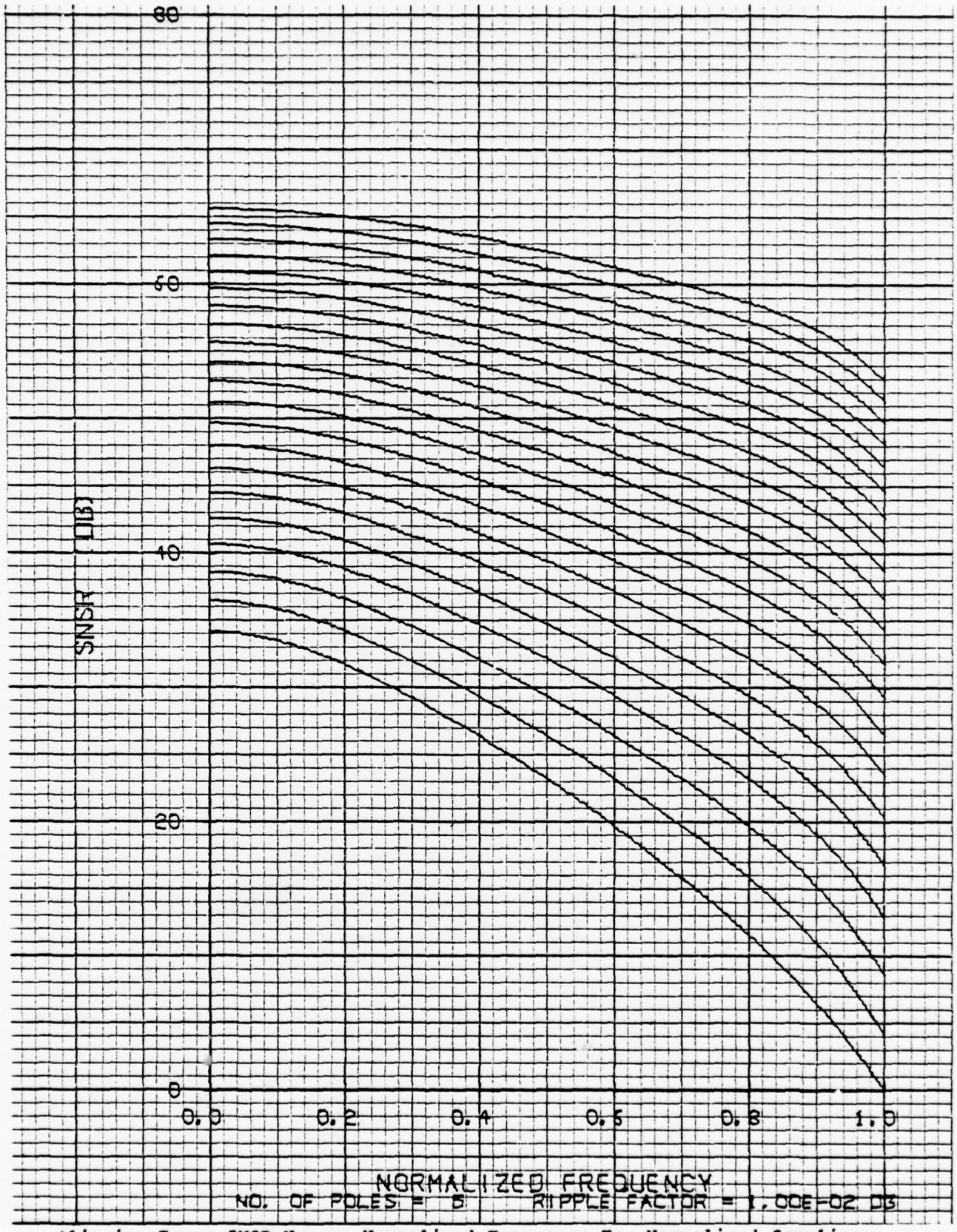

Aliasing Error SNSR Versus Normalized Frequency For Normalized Sampling Rates of 2.0, 2.1, ... 3.9, 4.0.

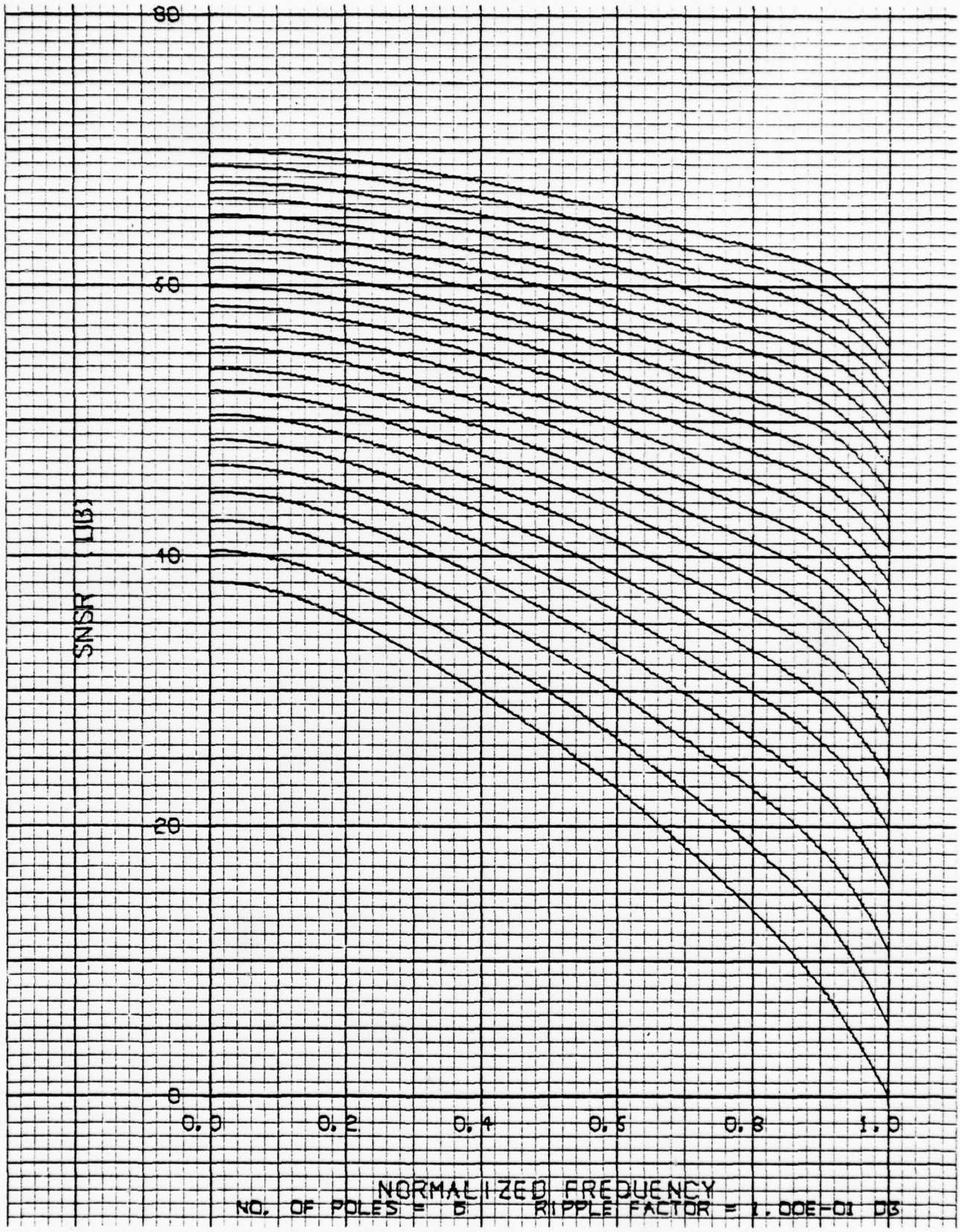

Aliasing Error SNSR Versus Normalized Frequency For Normalized Sampling Rates of 2.0, 2.1, ... 3.9, 4.0.

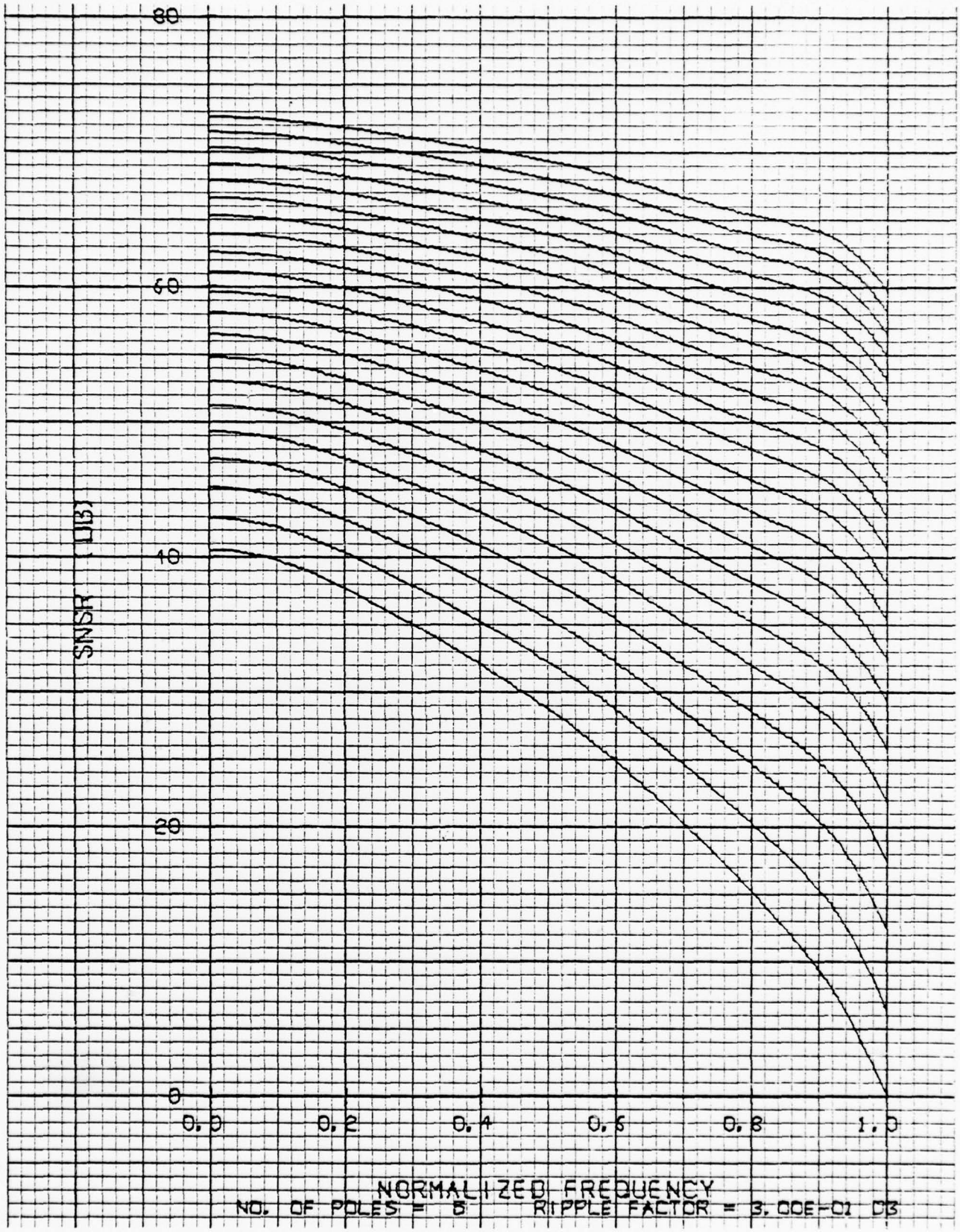

Aliasing Error SNSR Versus Normalized Frequency For Normalized Sampling Rates of 2.0, 2.1, ... 3.9, 4.0.

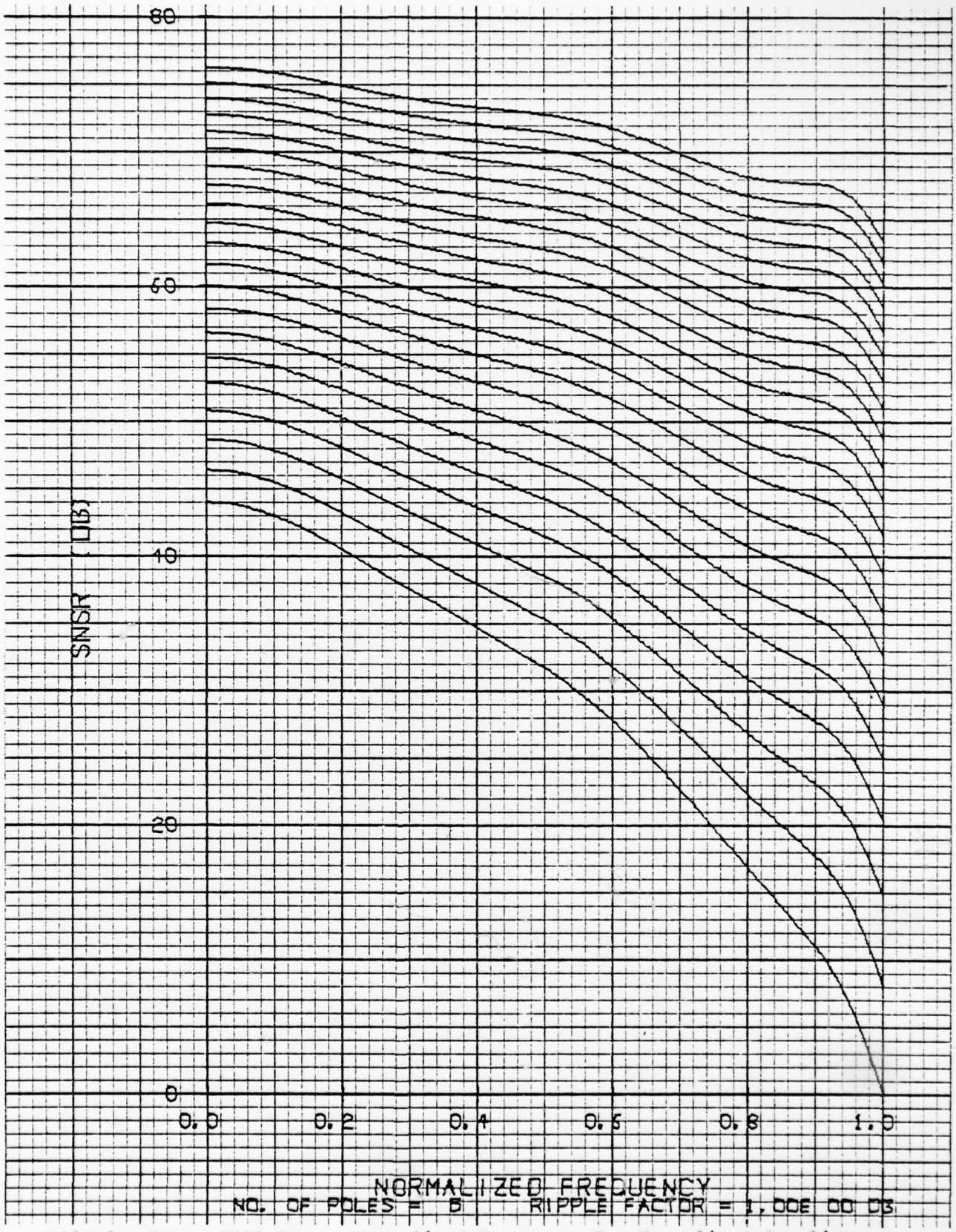

Aliasing Error SNSR Versus Normalized Frequency For Normalized Sampling Rates of 2.0, 2.1, ... 3.9, 4.0.

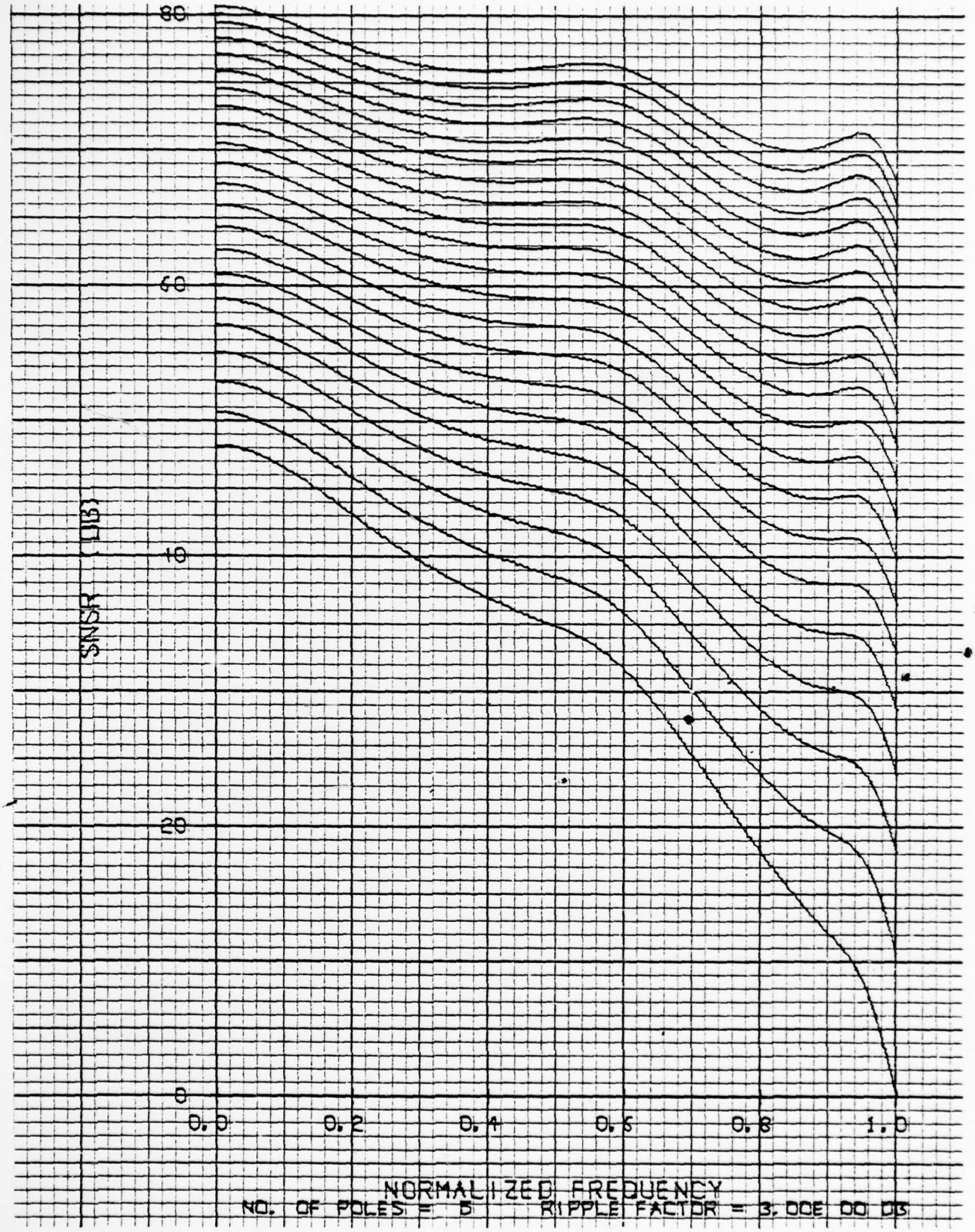

Aliasing Error SNSR Versus Normalized Frequency For Normalized Sampling Rates of 2.0, 2.1, ... 3.9, 4.0.

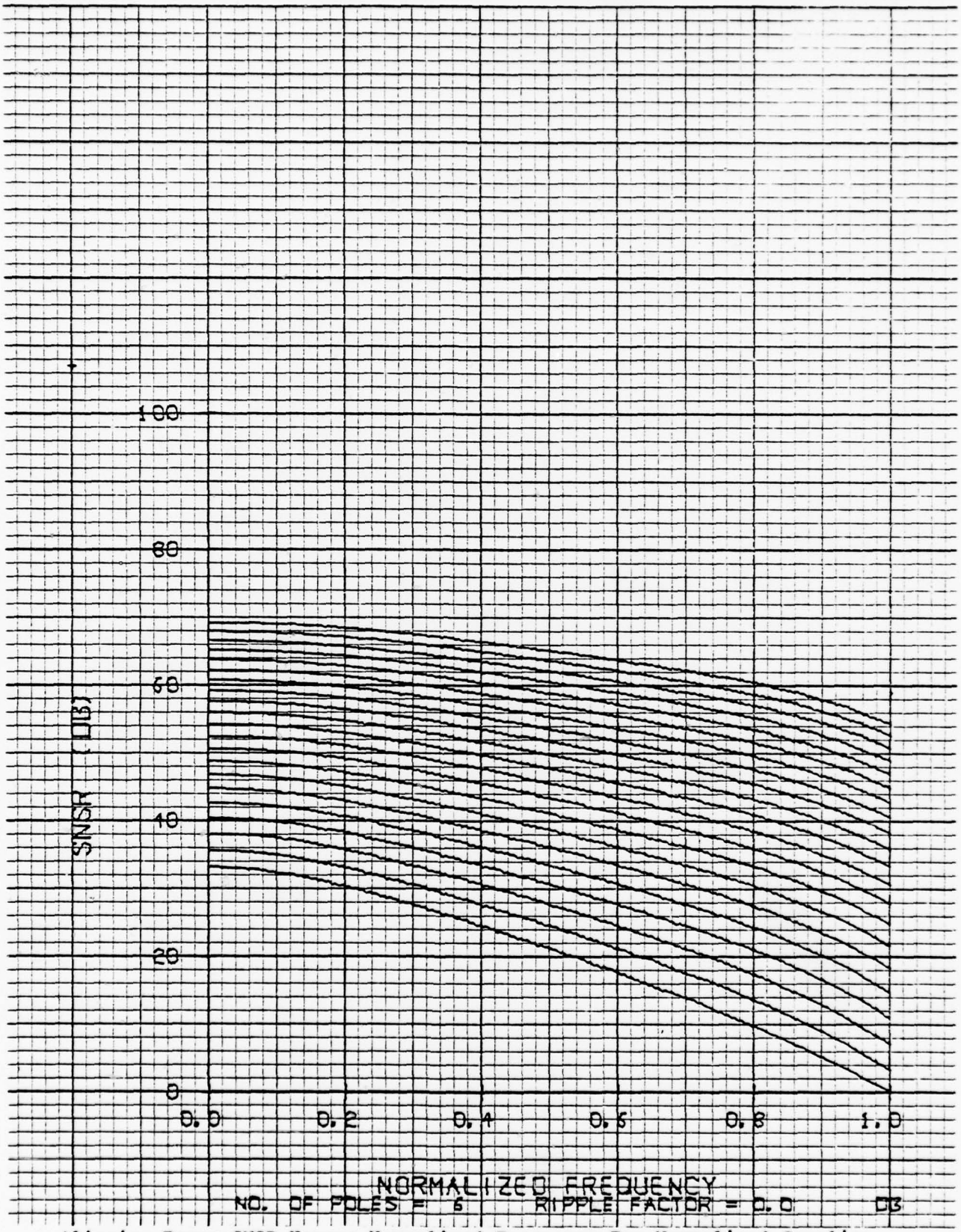

Aliasing Error SNSR Versus Normalized Frequency For Normalized Sampling Rates of 2.0, 2.1, ... 3.9, 4.0.

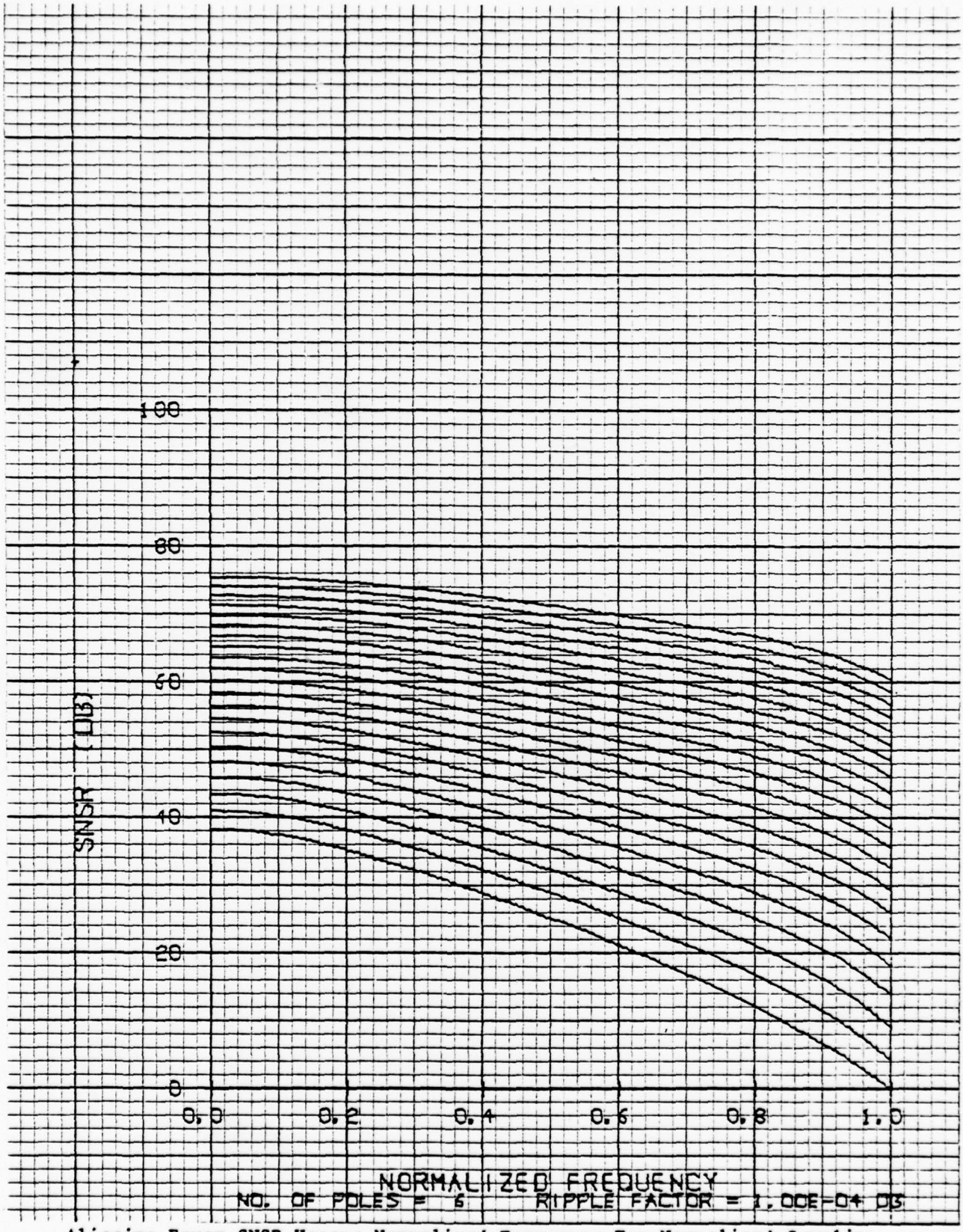

Aliasing Error SNSR Versus Normalized Frequency For Normalized Sampling Rates of 2.0, 2.1, ... 3.9, 4.0.

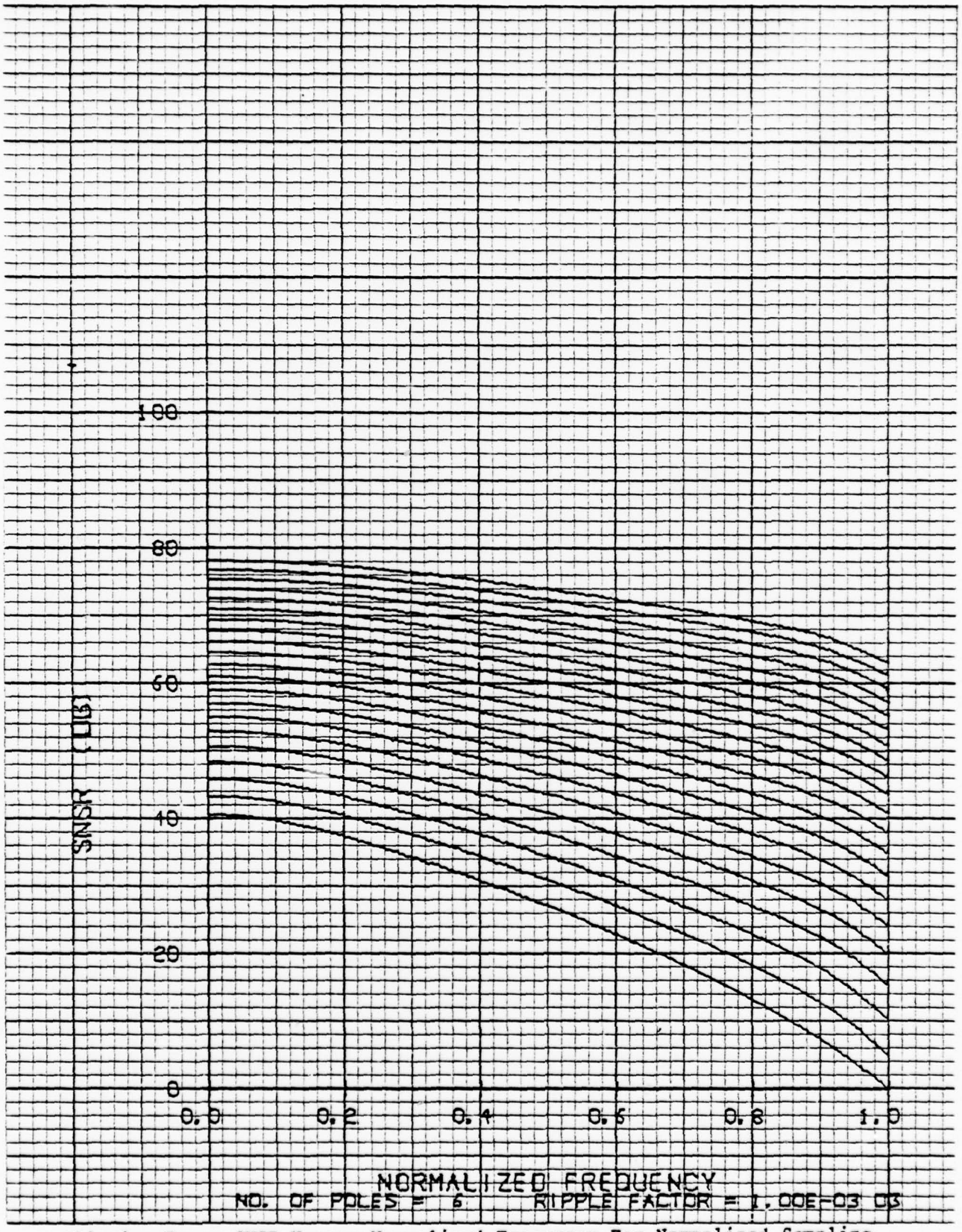

Aliasing Error SNSR Versus Normalized Frequency For Normalized Sampling Rates of 2.0, 2.1, ... 3.9, 4.0.

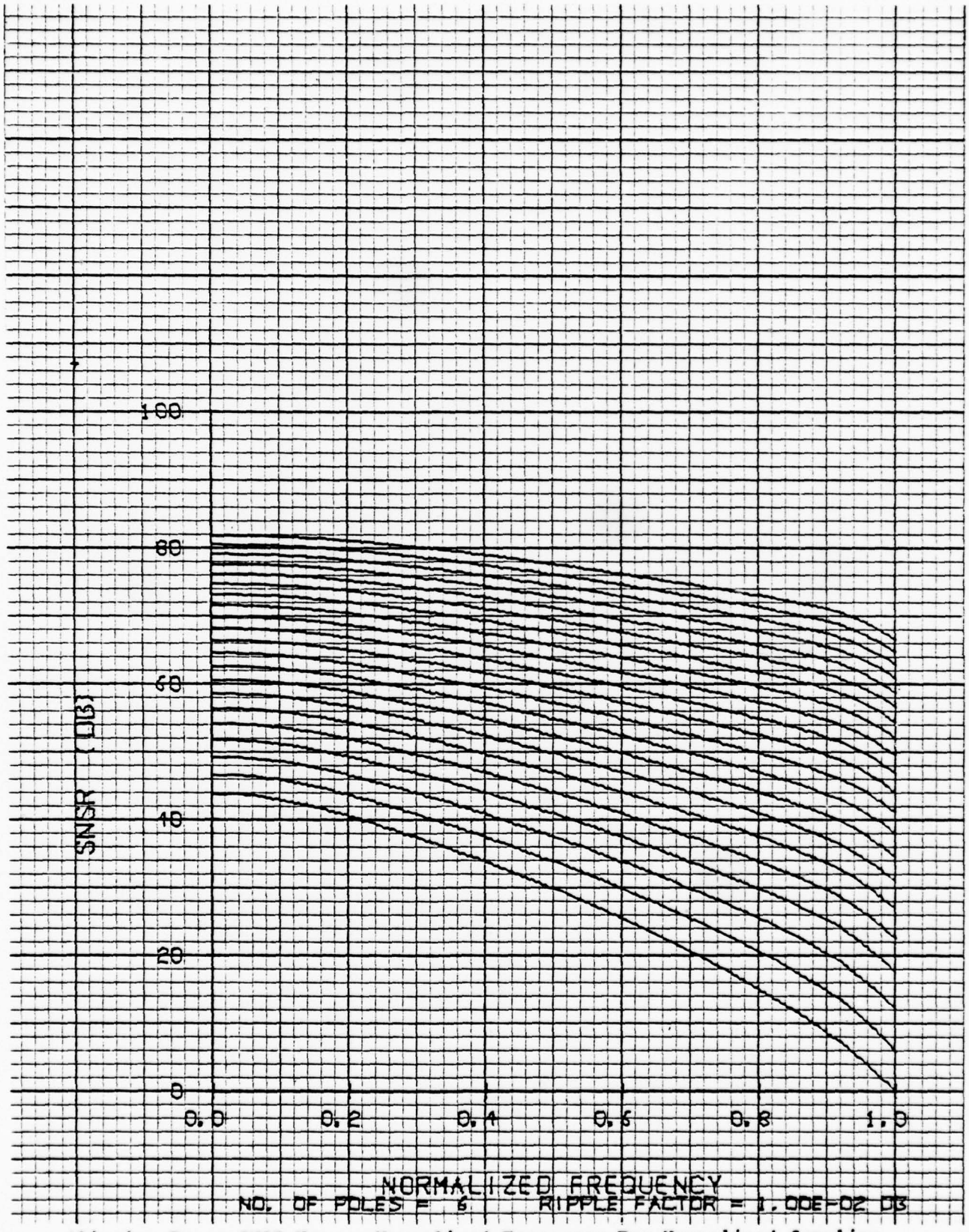

Aliasing Error SNSR Versus Normalized Frequency For Normalized Sampling Rates of 2.0, 2.1, ... 3.9, 4.0.

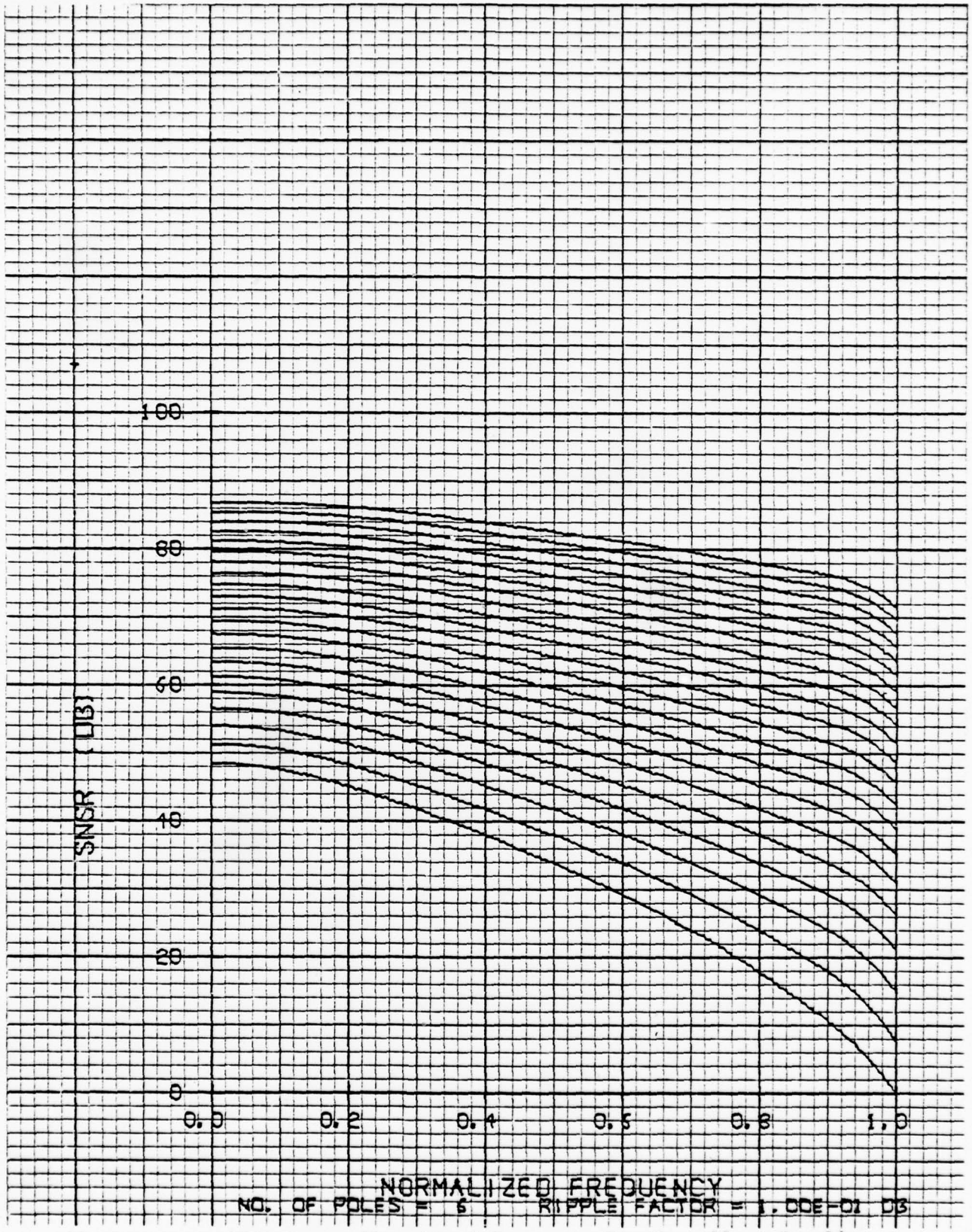

Aliasing Error SNSR Versus Normalized Frequency For Normalized Sampling Rates of 2.0, 2.1, ... 3.9, 4.0.

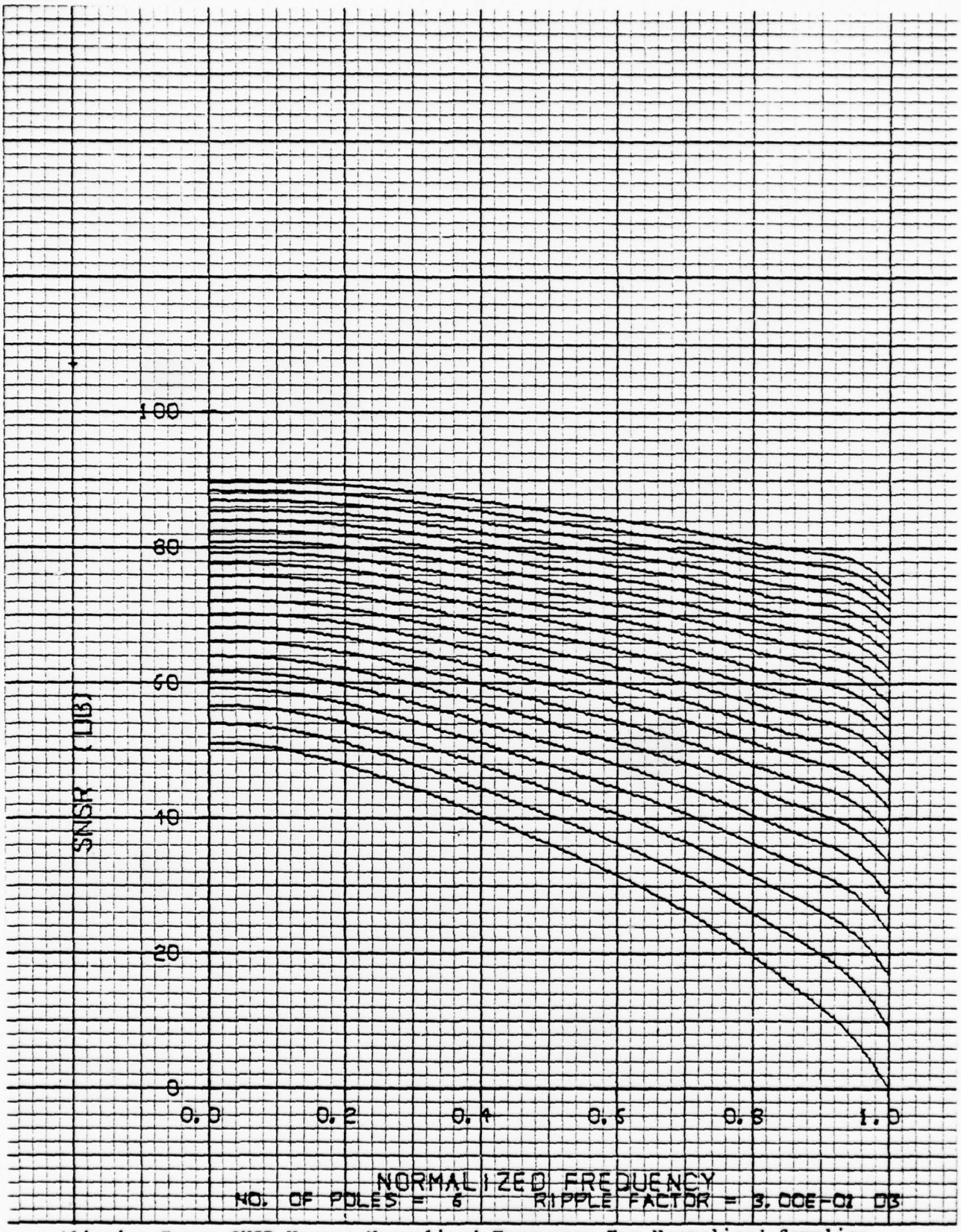

Aliasing Error SNSR Versus Normalized Frequency For Normalized Sampling Rates of 2.0, 2.1, ... 3.9, 4.0.

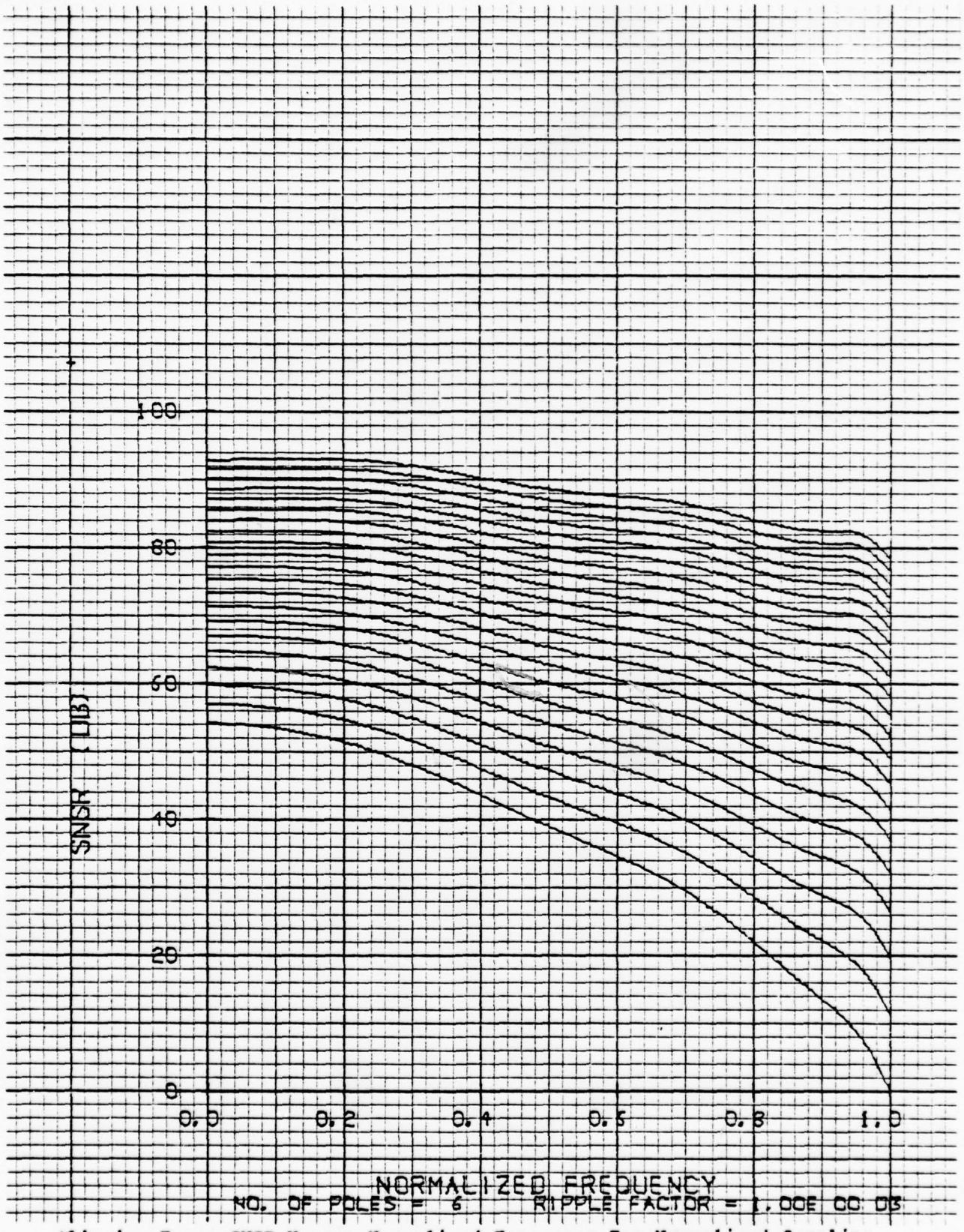

Aliasing Error SNSR Versus Normalized Frequency For Normalized Sampling Rates of 2.0, 2.1, ... 3.9, 4.0.

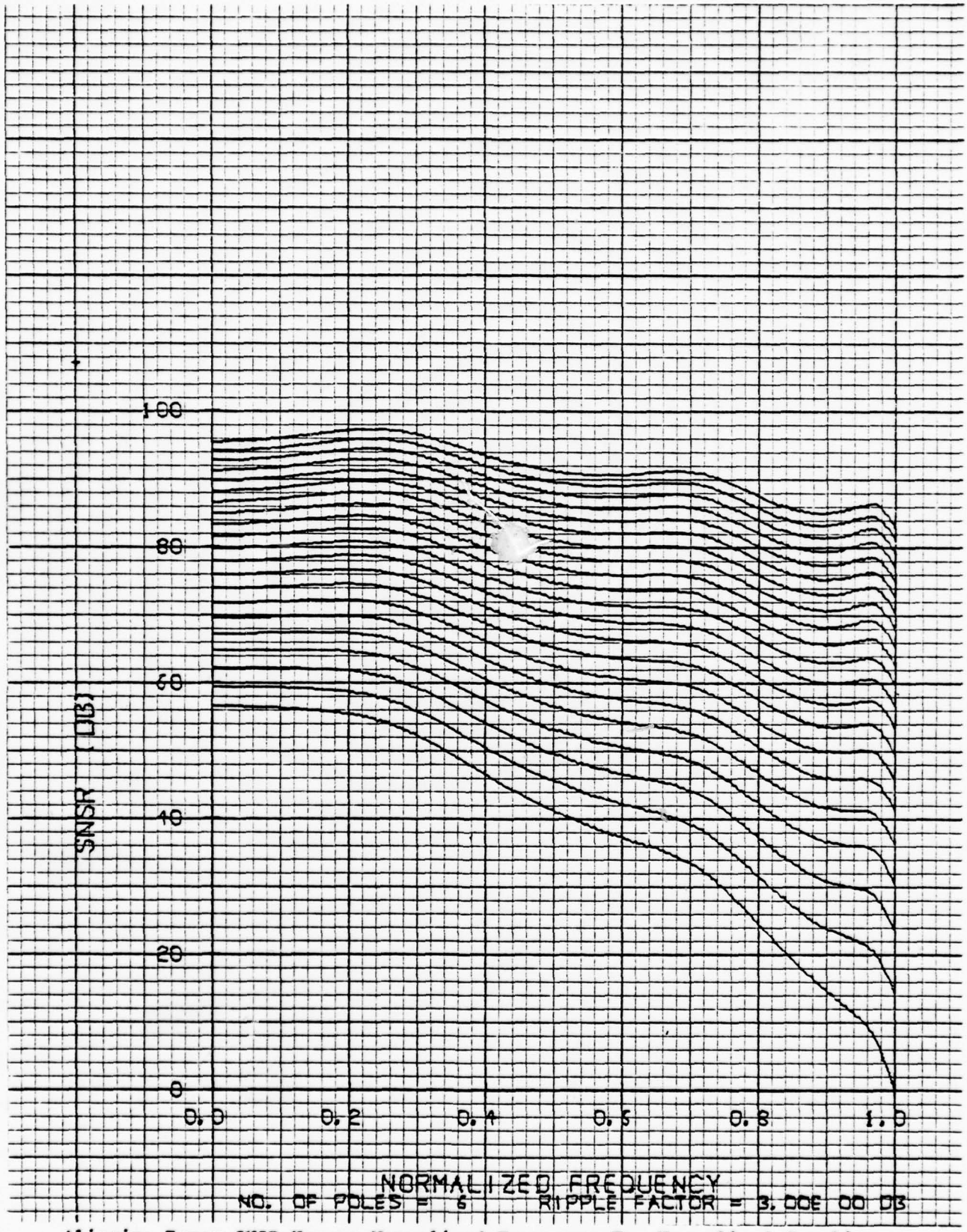

Aliasing Error SNSR Versus Normalized Frequency For Normalized Sampling Rates of 2.0, 2.1, ... 3.9, 4.0.

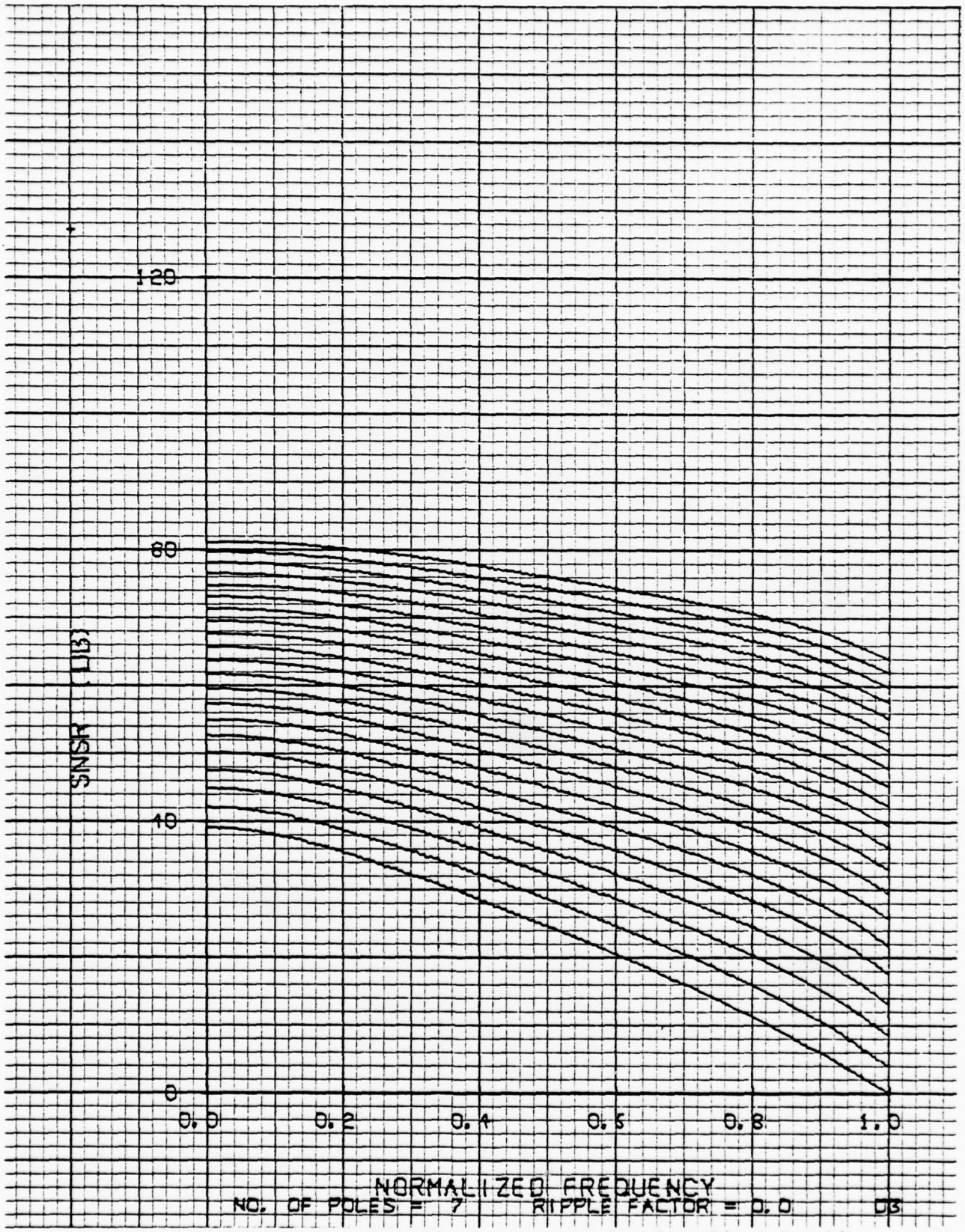

Aliasing Error SNSR Versus Normalized Frequency For Normalized Sampling Rates of 2.0, 2.1, ... 3.9, 4.0.

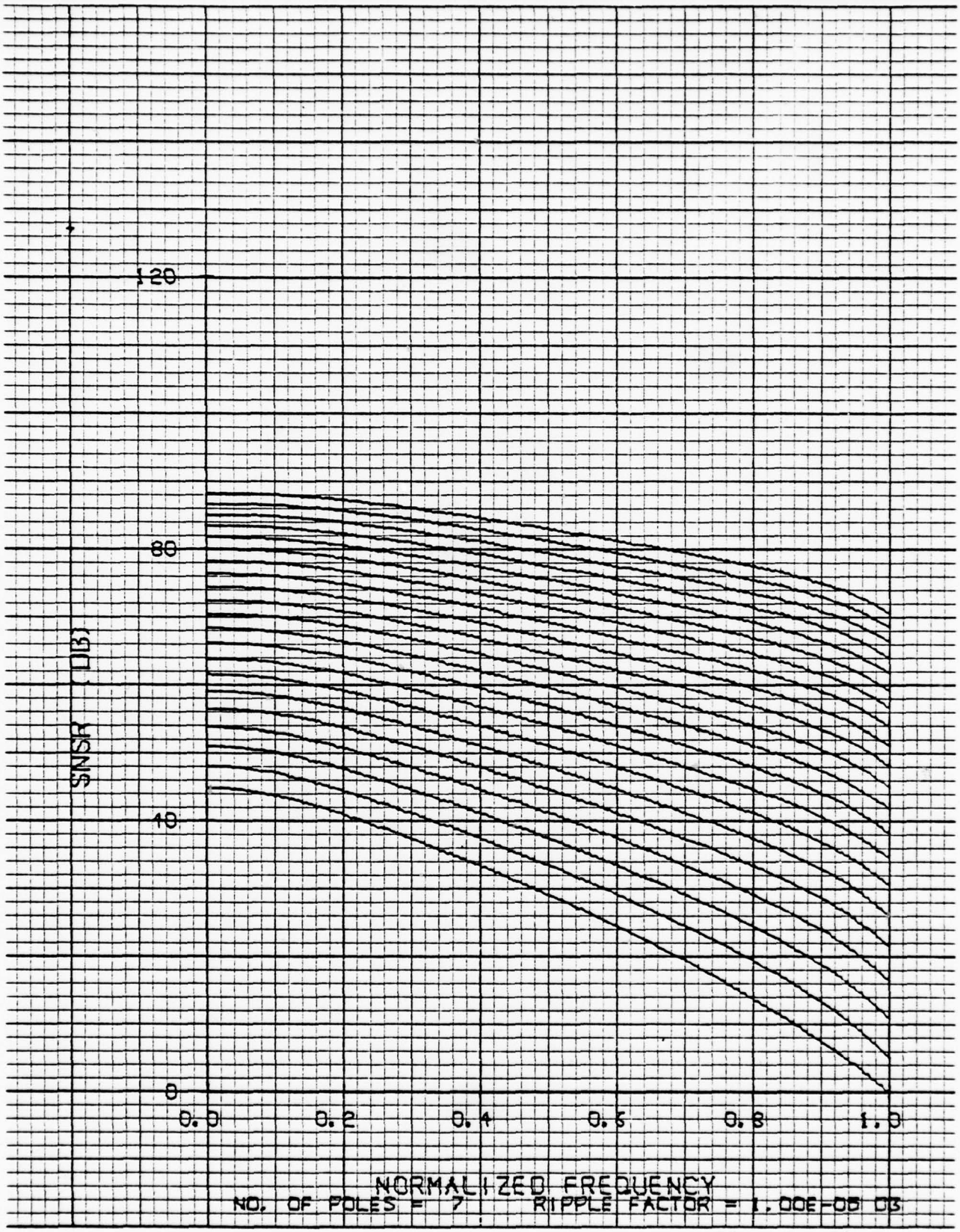

Aliasing Error SNSR Versus Normalized Frequency For Normalized Sampling Rates of 2.0, 2.1, ... 3.9, 4.0.

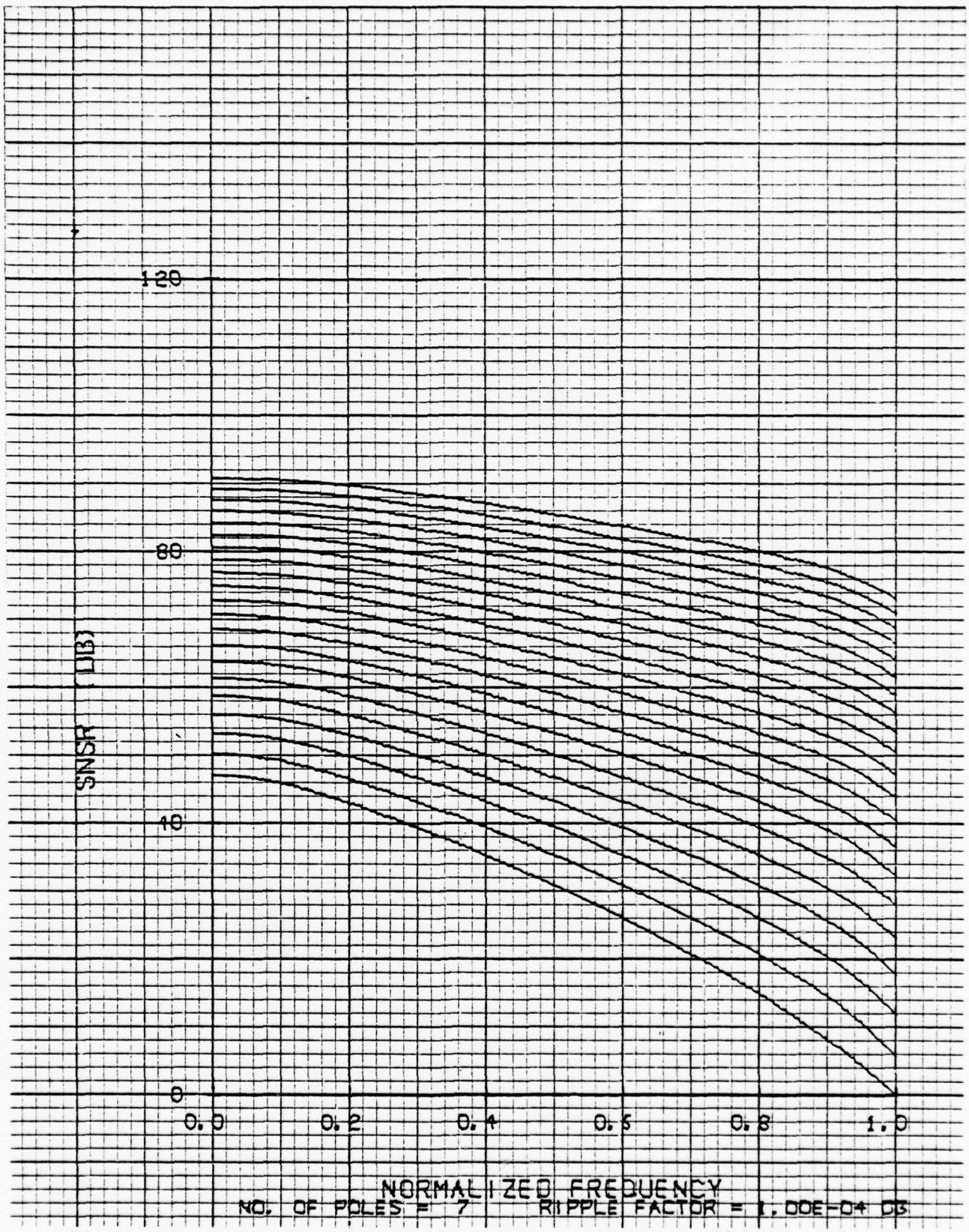

Aliasing Error SNSR Versus Normalized Frequency For Normalized Sampling Rates of 2.0, 2.1, ... 3.9, 4.0.

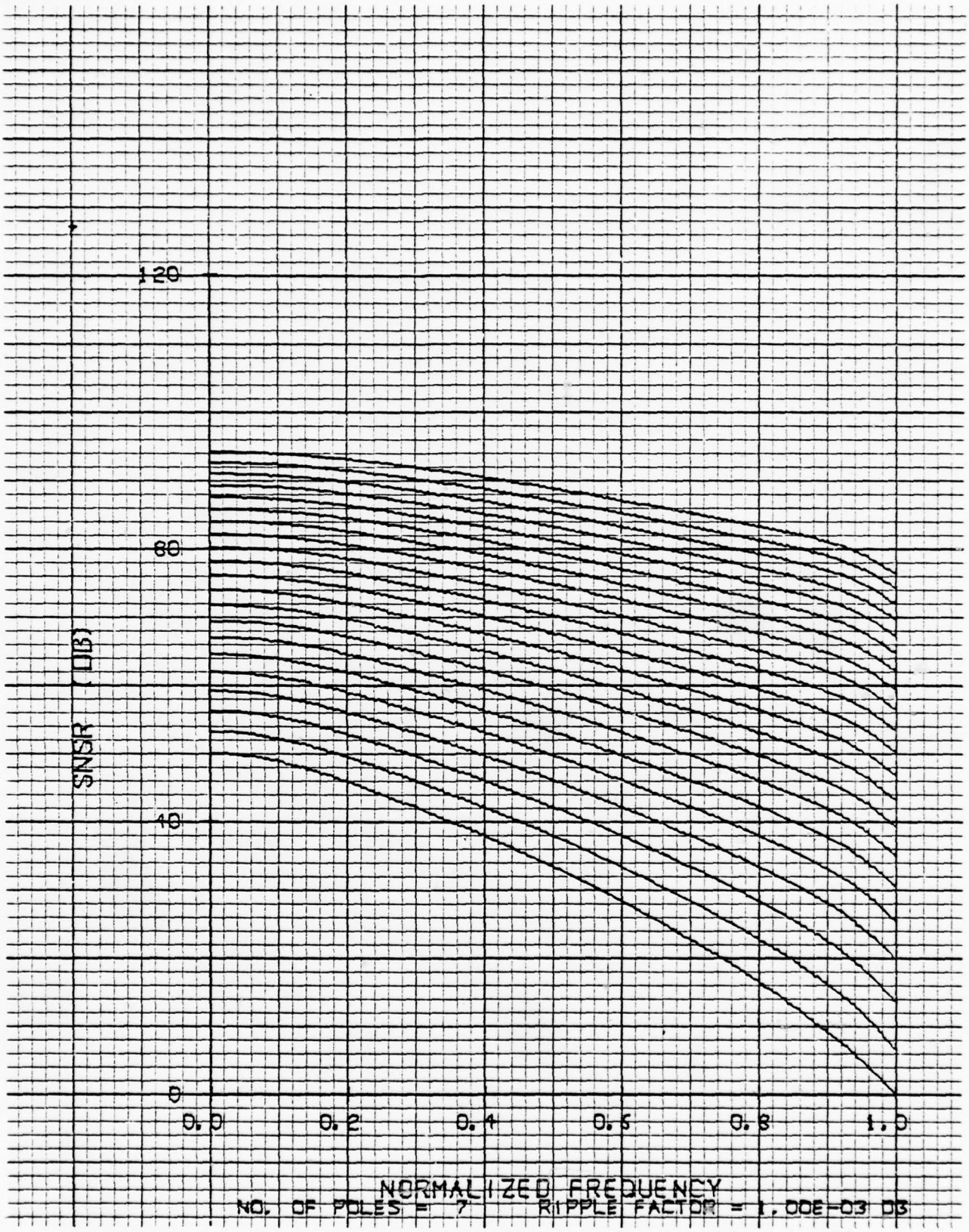

Aliasing Error SNSR Versus Normalized Frequency For Normalized Sampling Rates of 2.0, 2.1, ... 3.9, 4.0.

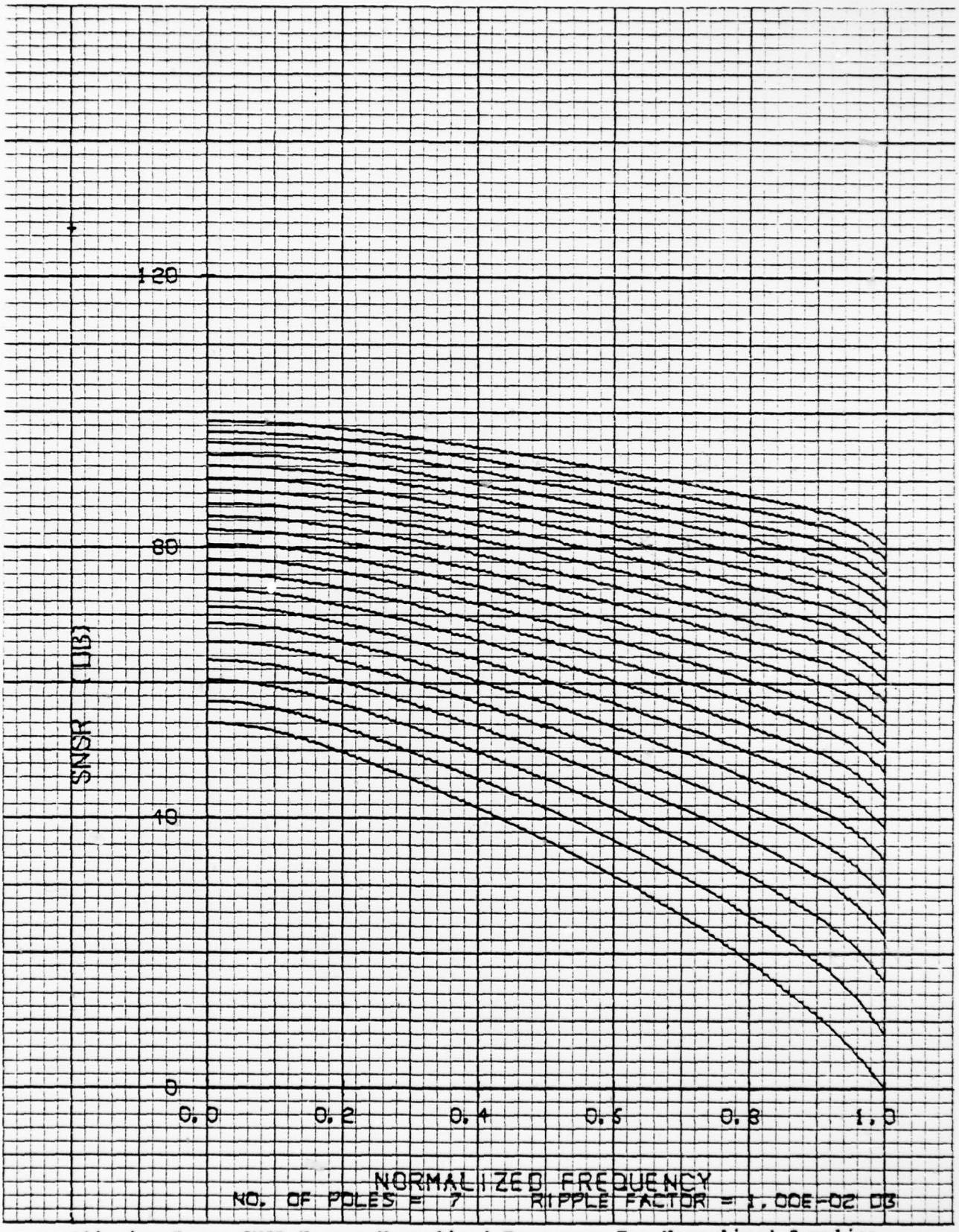

Aliasing Error SNSR Versus Normalized Frequency For Normalized Sampling Rates of 2.0, 2.1, ... 3.9, 4.0.

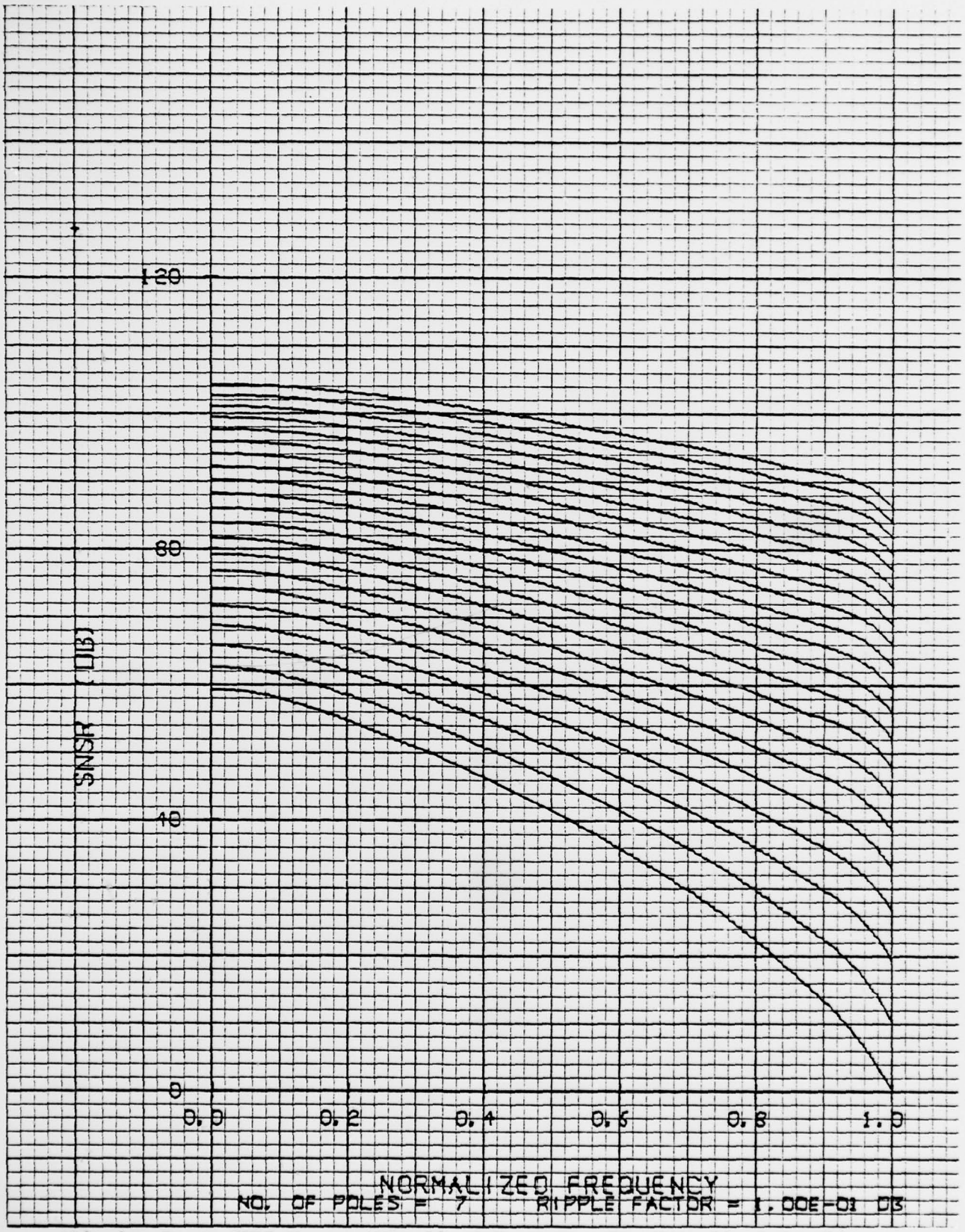

Aliasing Error SNSR Versus Normalized Frequency For Normalized Sampling Rates of 2.0, 2.1, ... 3.9, 4.0.

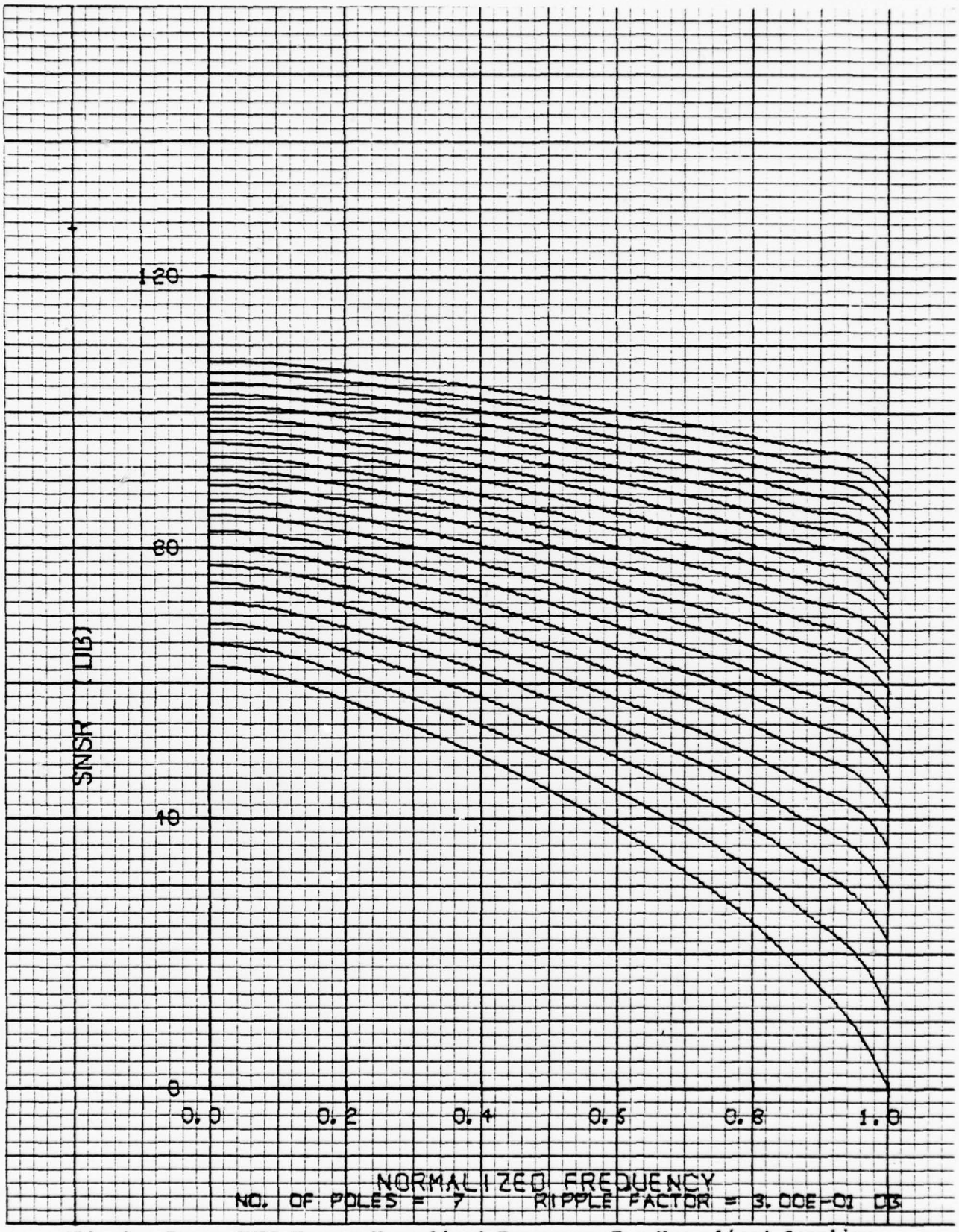

Aliasing Error SNSR Versus Normalized Frequency For Normalized Sampling Rates of 2.0, 2.1, ... 3.9, 4.0.

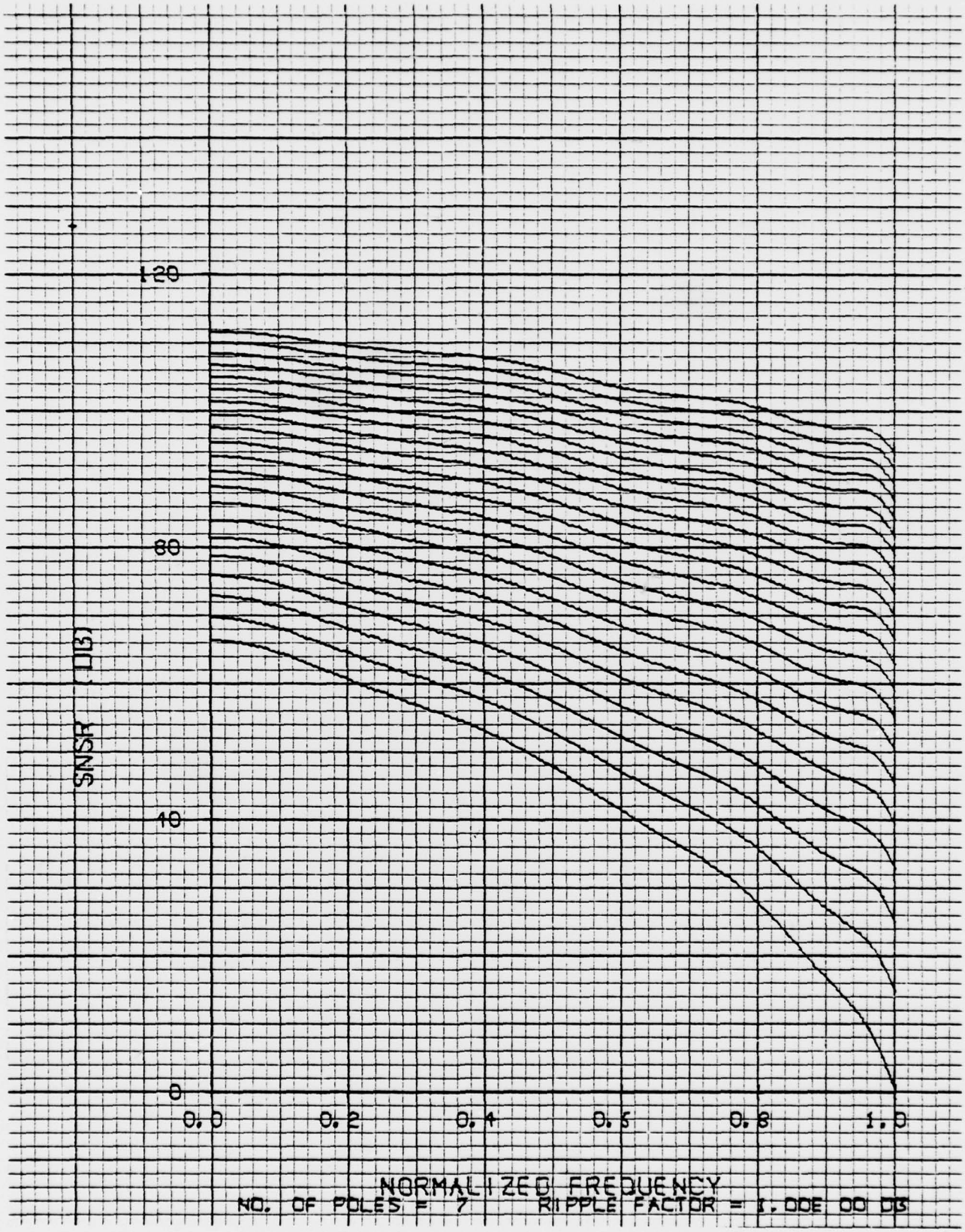

Aliasing Error SNSR Versus Normalized Frequency For Normalized Sampling Rates of 2.0, 2.1, ... 3.9, 4.0.

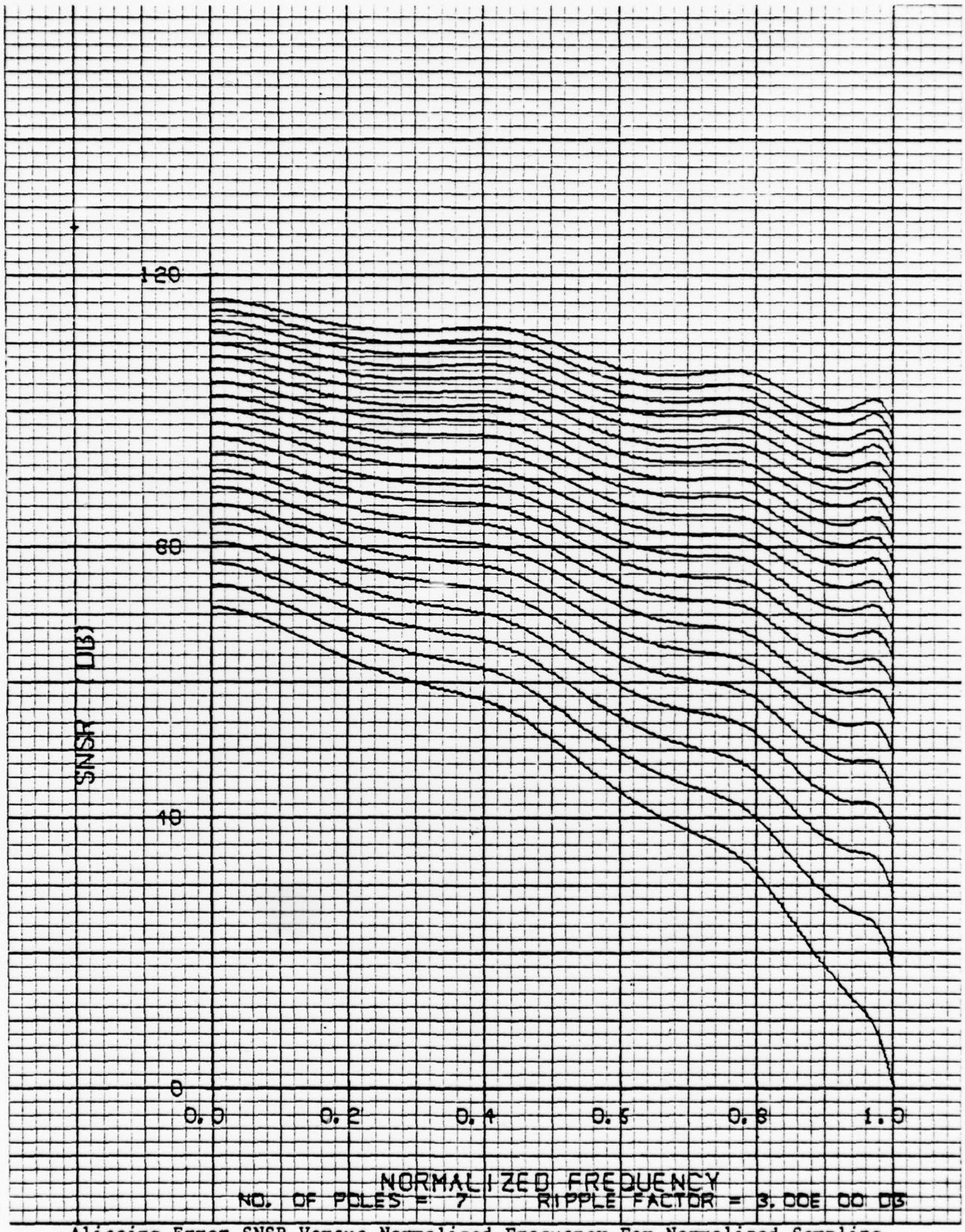

Aliasing Error SNSR Versus Normalized Frequency For Normalized Sampling Rates of 2.0, 2.1, ... 3.9, 4.0.

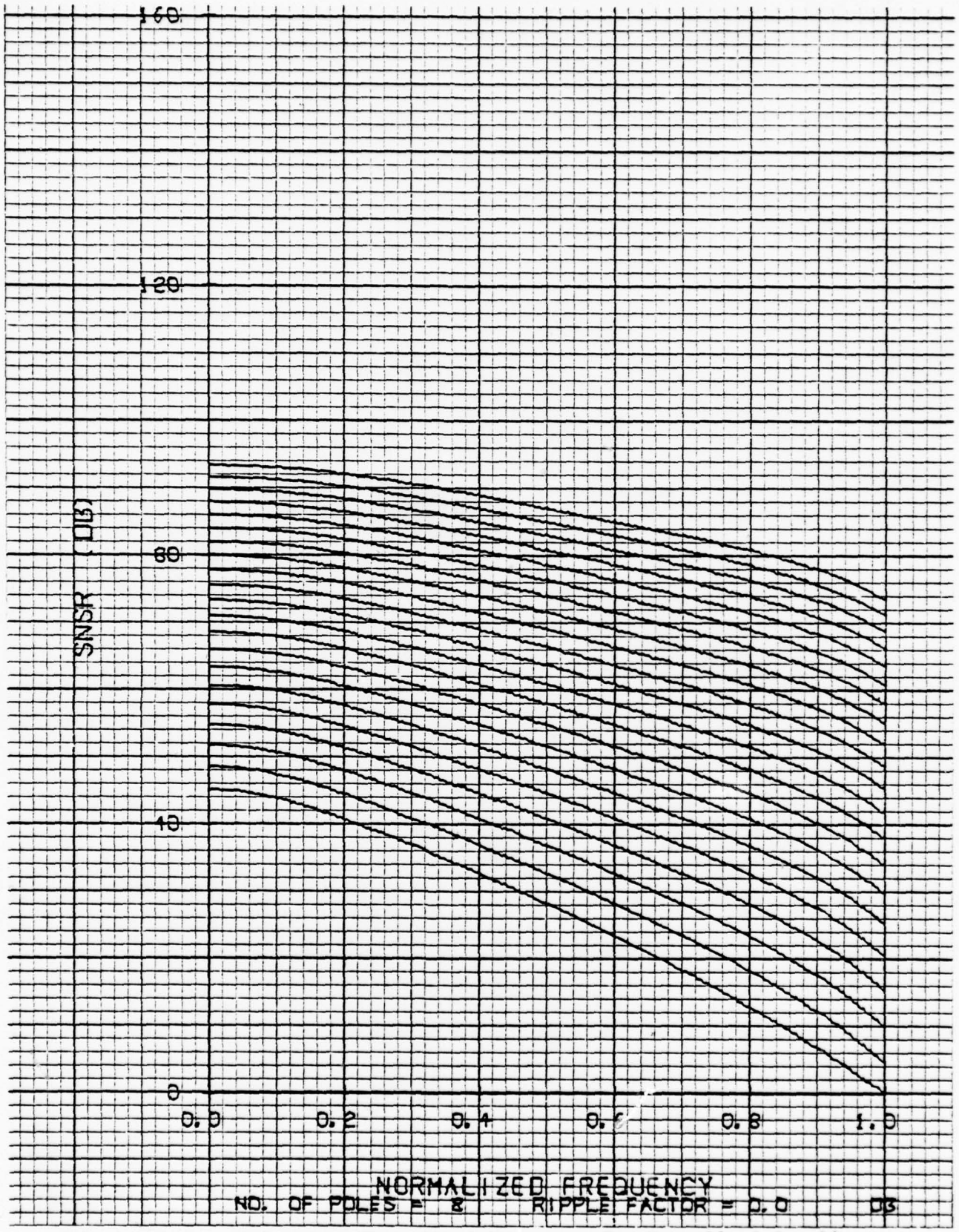

Aliasing Error SNSR Versus Normalized Frequency For Normalized Sampling Rates of 2.0, 2.1, ... 3.9, 4.0.

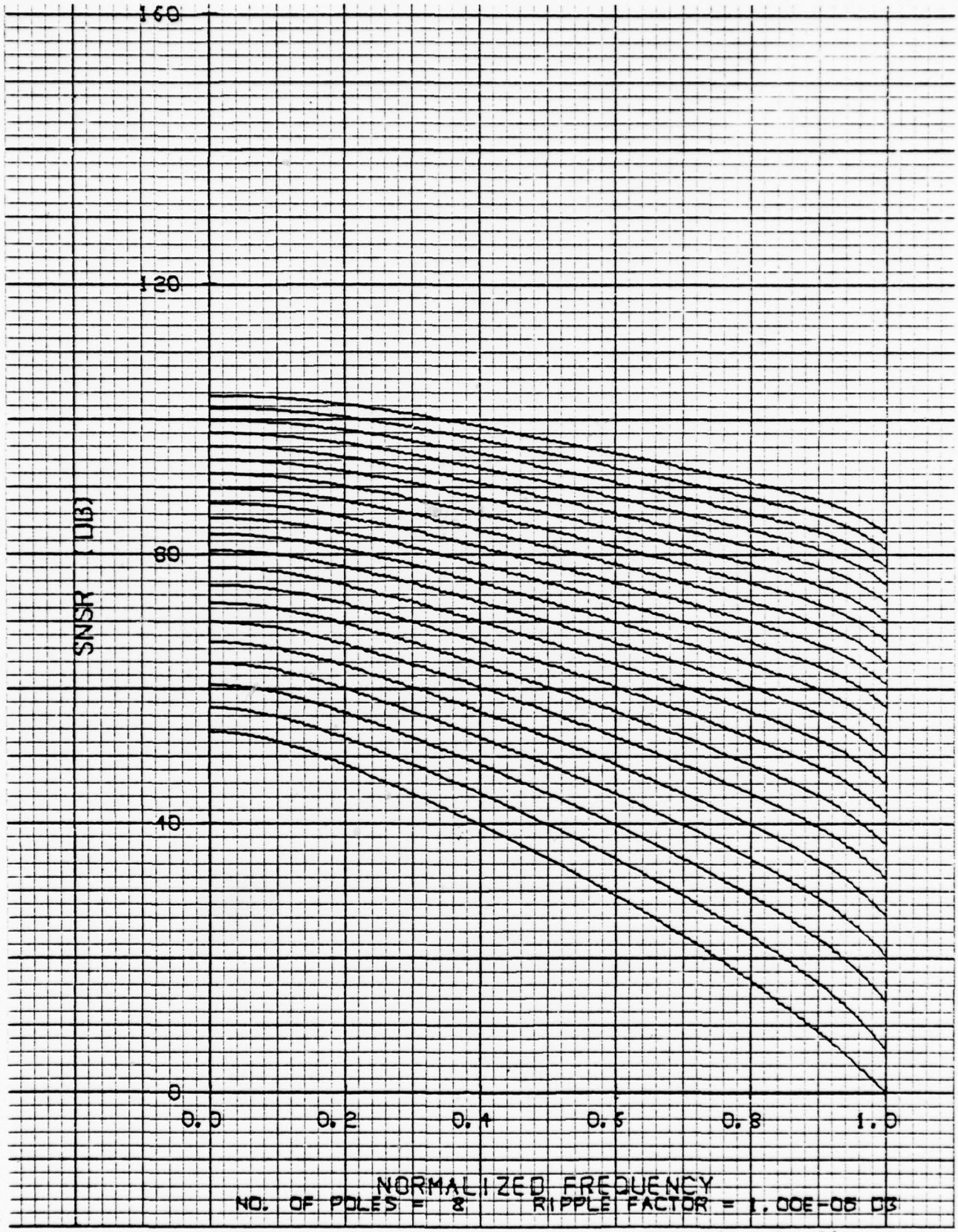

Aliasing Error SNSR Versus Normalized Frequency For Normalized Sampling Rates of 2.0, 2.1, ... 3.9, 4.0.

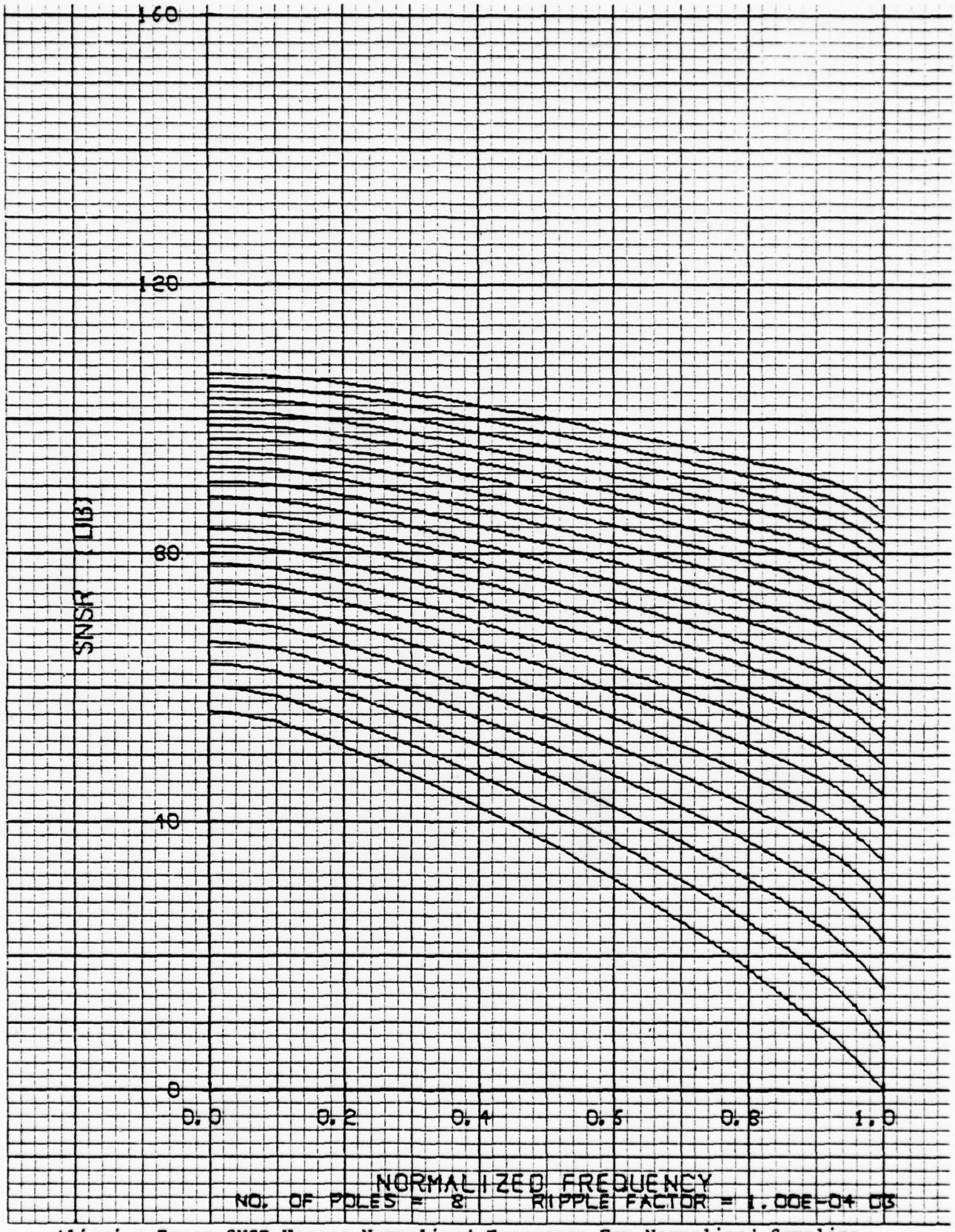

Aliasing Error SNSR Versus Normalized Frequency For Normalized Sampling Rates of 2.0, 2.1, ... 3.9, 4.0.

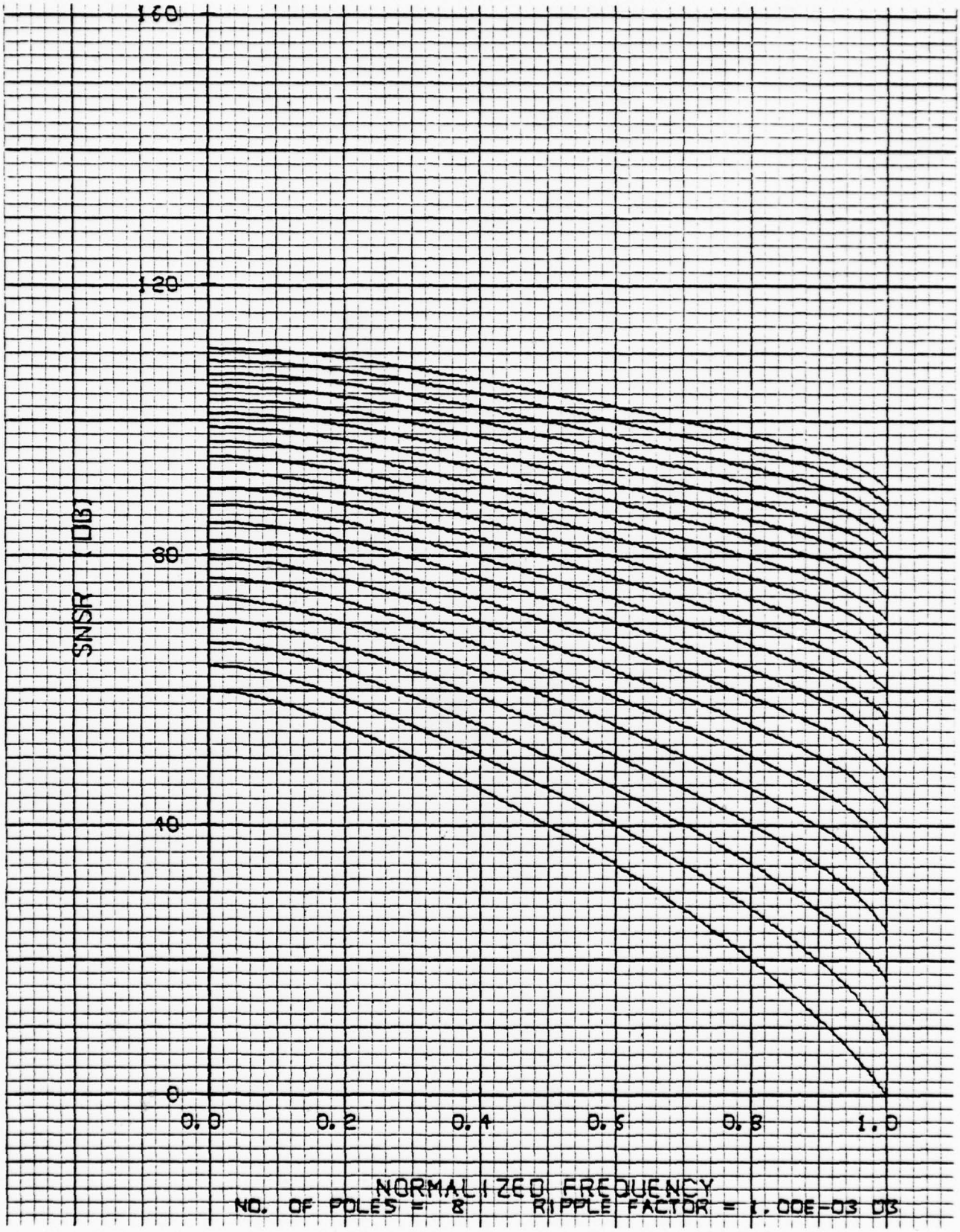

Aliasing Error SNSR Versus Normalized Frequency For Normalized Sampling Rates of 2.0, 2.1, ... 3.9, 4.0.

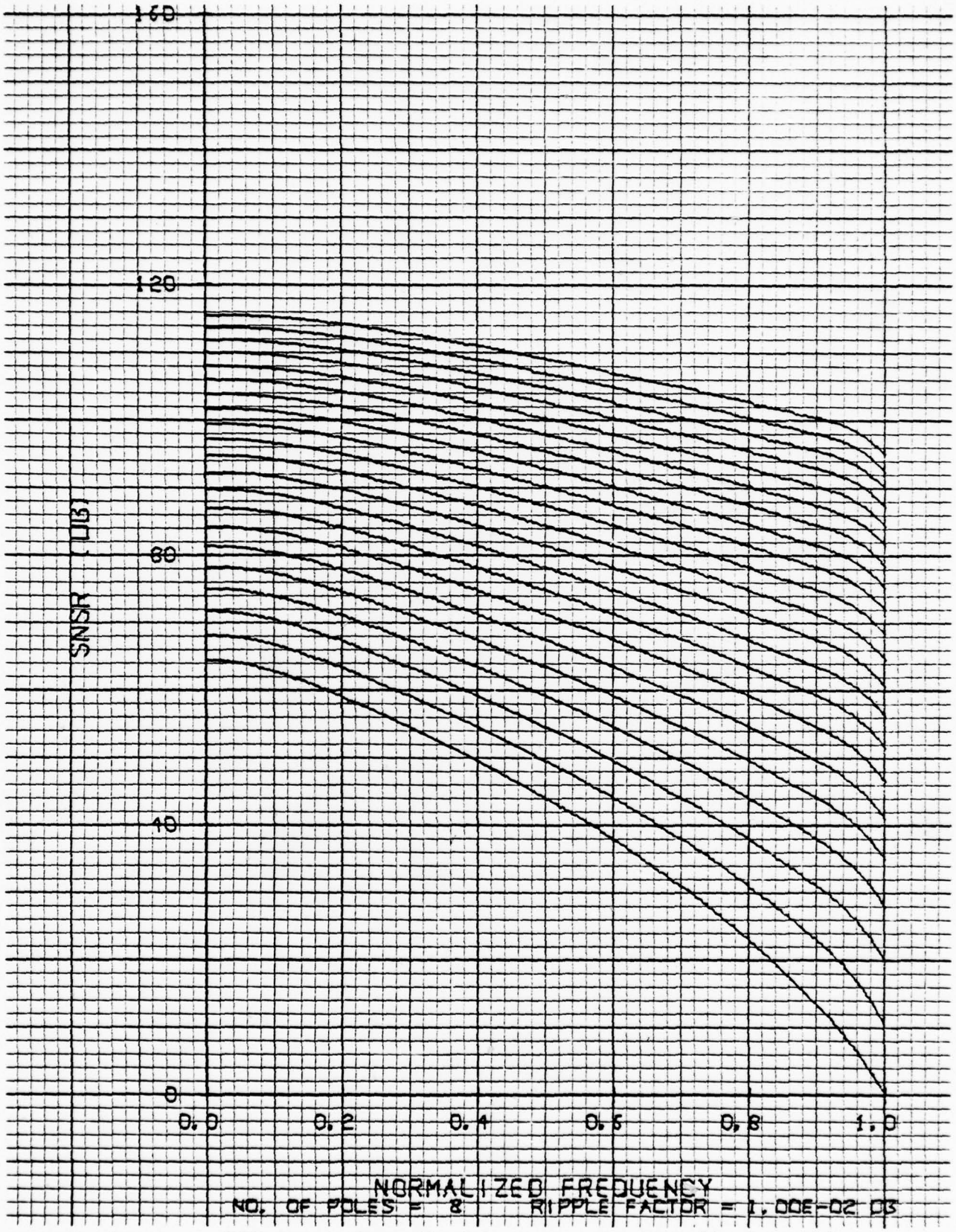

Aliasing Error SNSR Versus Normalized Frequency For Normalized Sampling Rates of 2.0, 2.1, ... 3.9, 4.0.

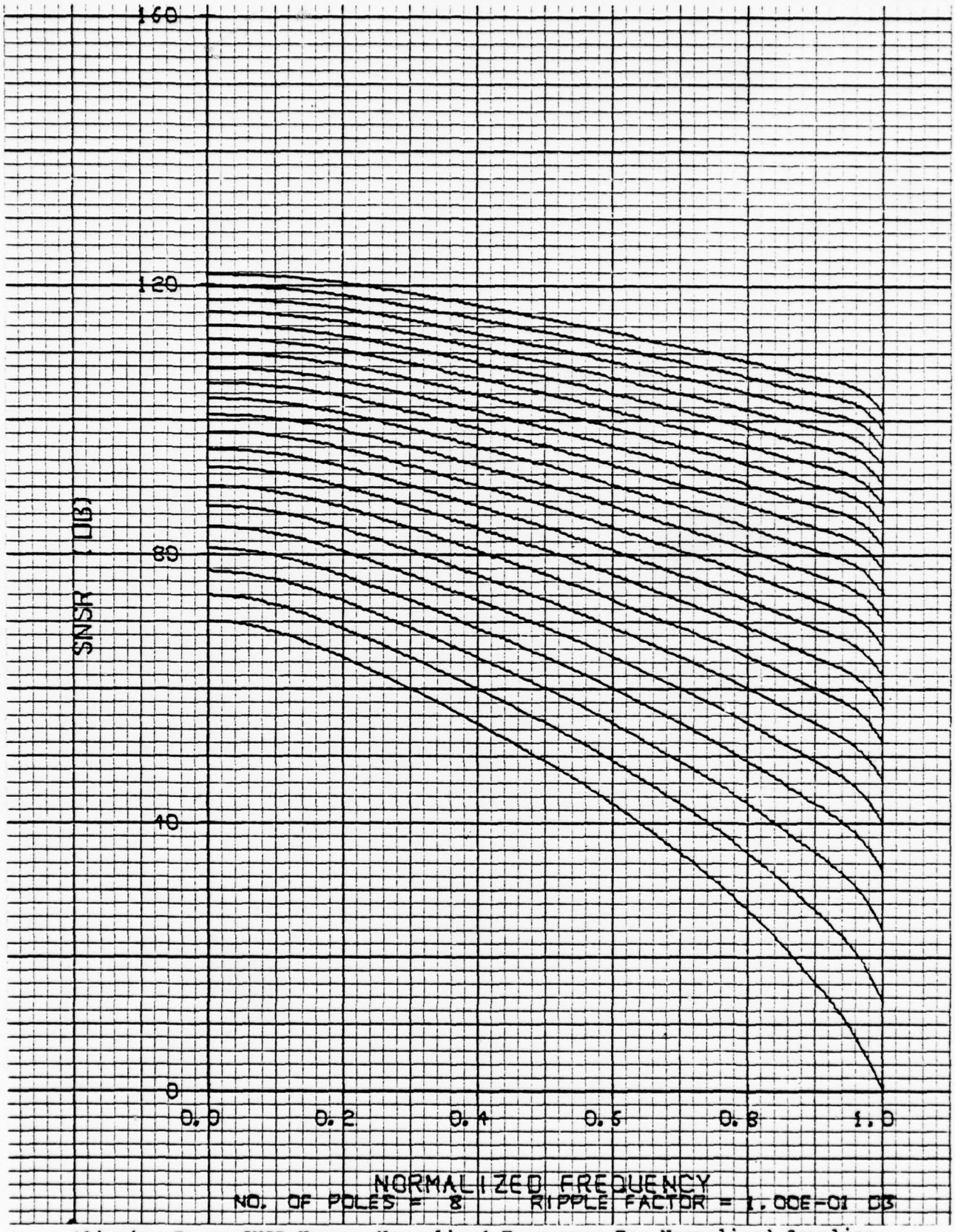

Aliasing Error SNSR Versus Normalized Frequency For Normalized Sampling Rates of 2.0, 2.1, ... 3.9, 4.0.

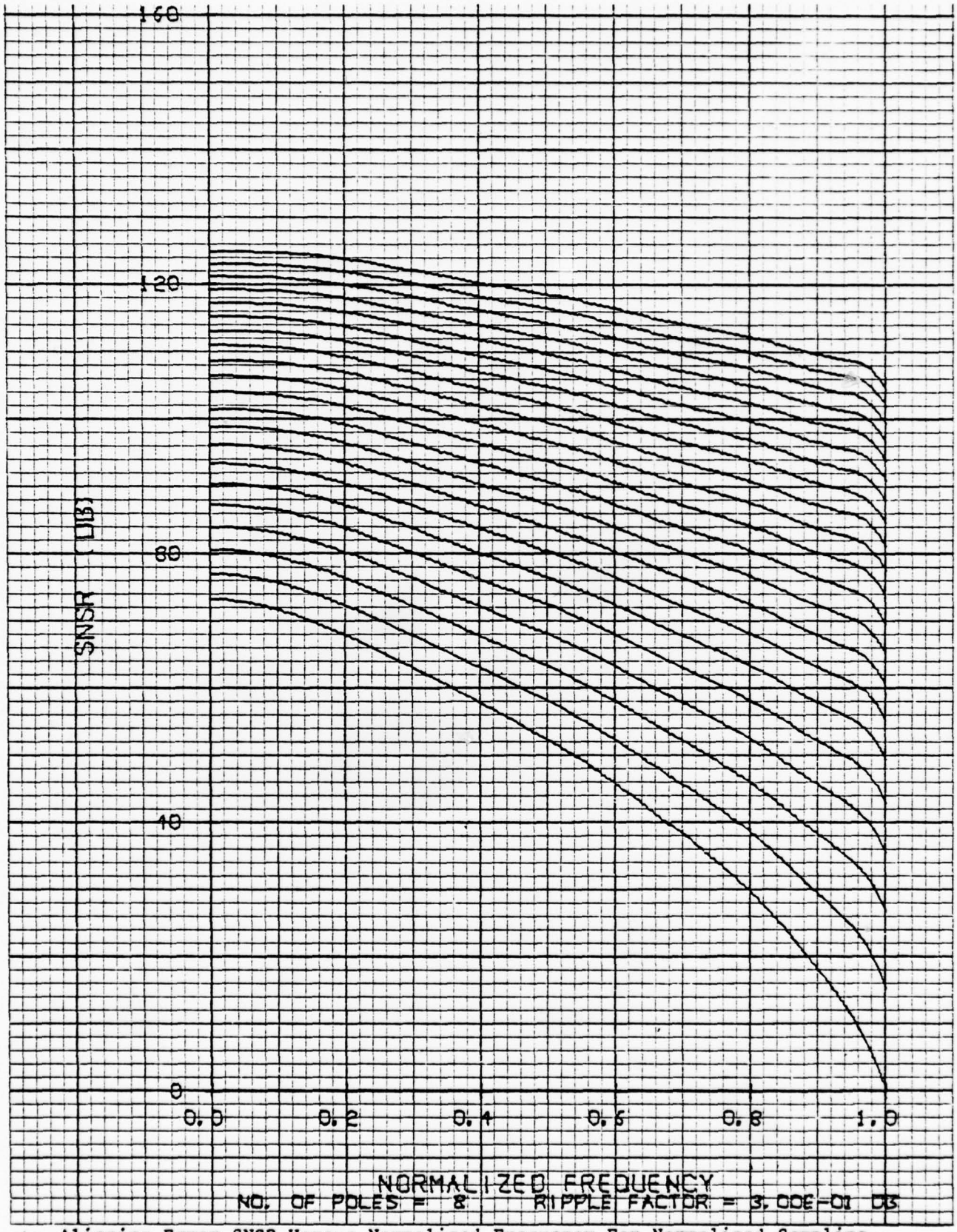

Aliasing Error SNSR Versus Normalized Frequency For Normalized Sampling Rates of 2.0, 2.1, ... 3.9, 4.0.

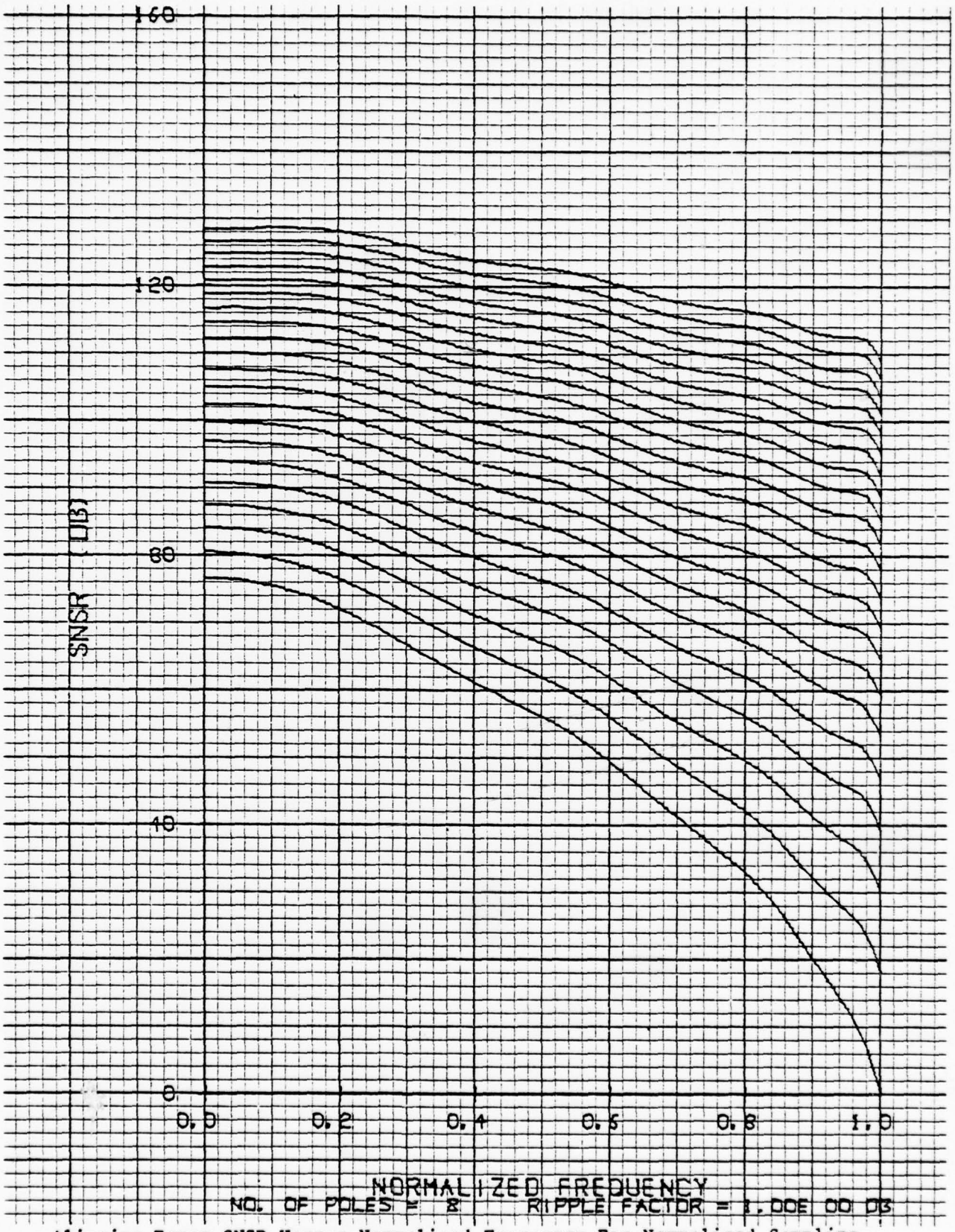

Aliasing Error SNSR Versus Normalized Frequency For Normalized Sampling Rates of 2.0, 2.1, ... 3.9, 4.0.

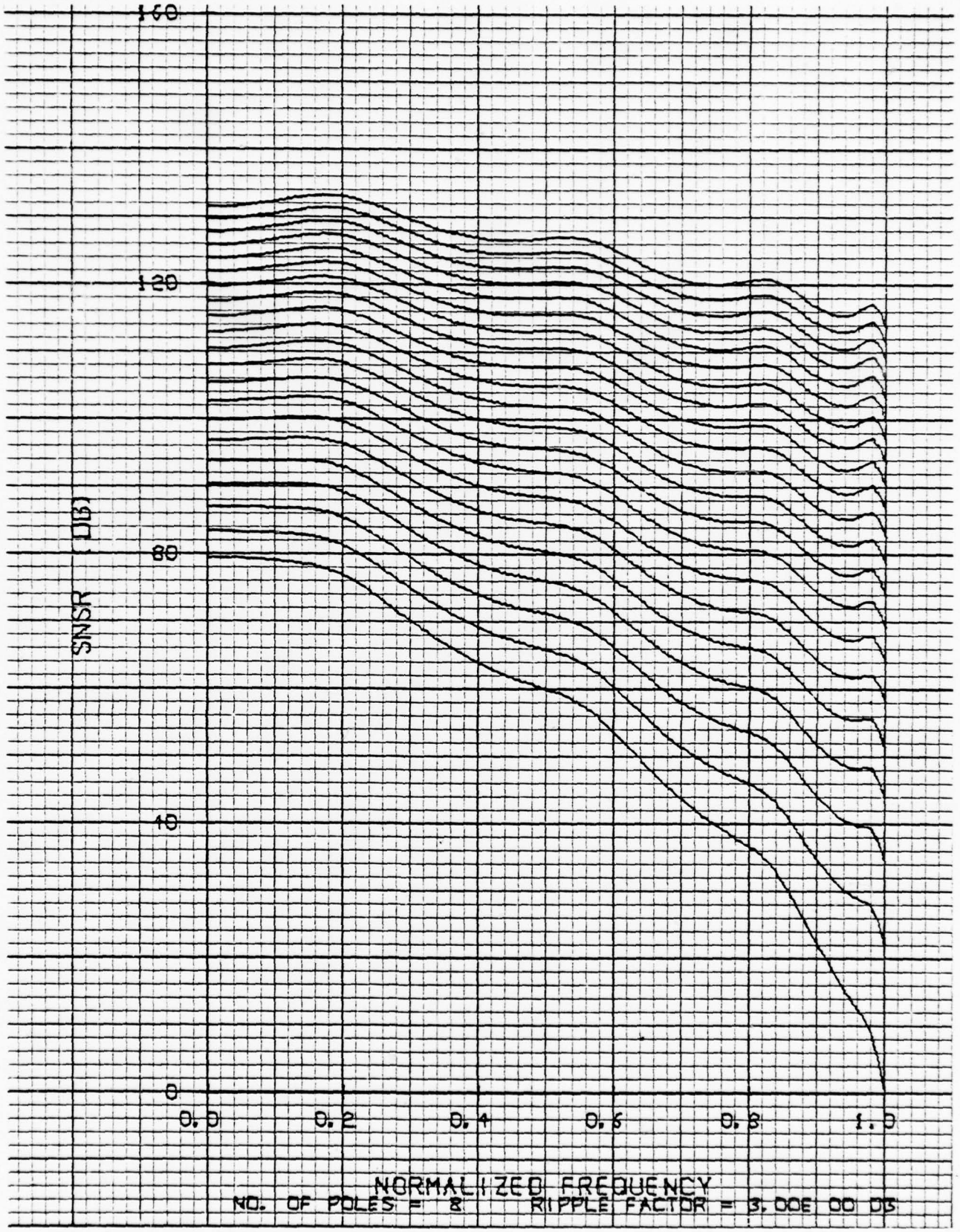

Aliasing Error SNSR Versus Normalized Frequency For Normalized Sampling Rates of 2.0, 2.1, ... 3.9, 4.0.

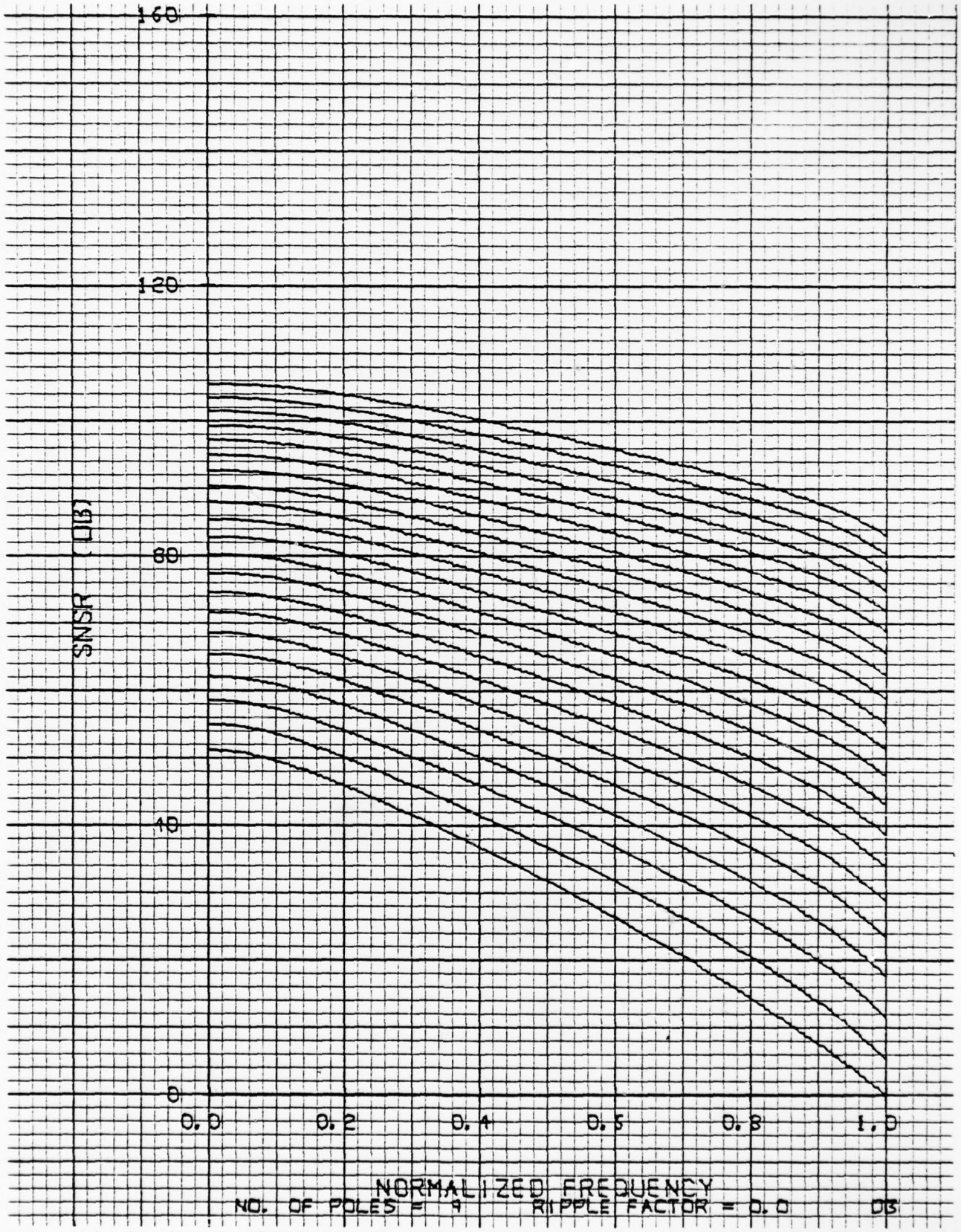

Aliasing Error SNSR Versus Normalized Frequency For Normalized Sampling Rates of 2.0, 2.1, ... 3.9, 4.0.

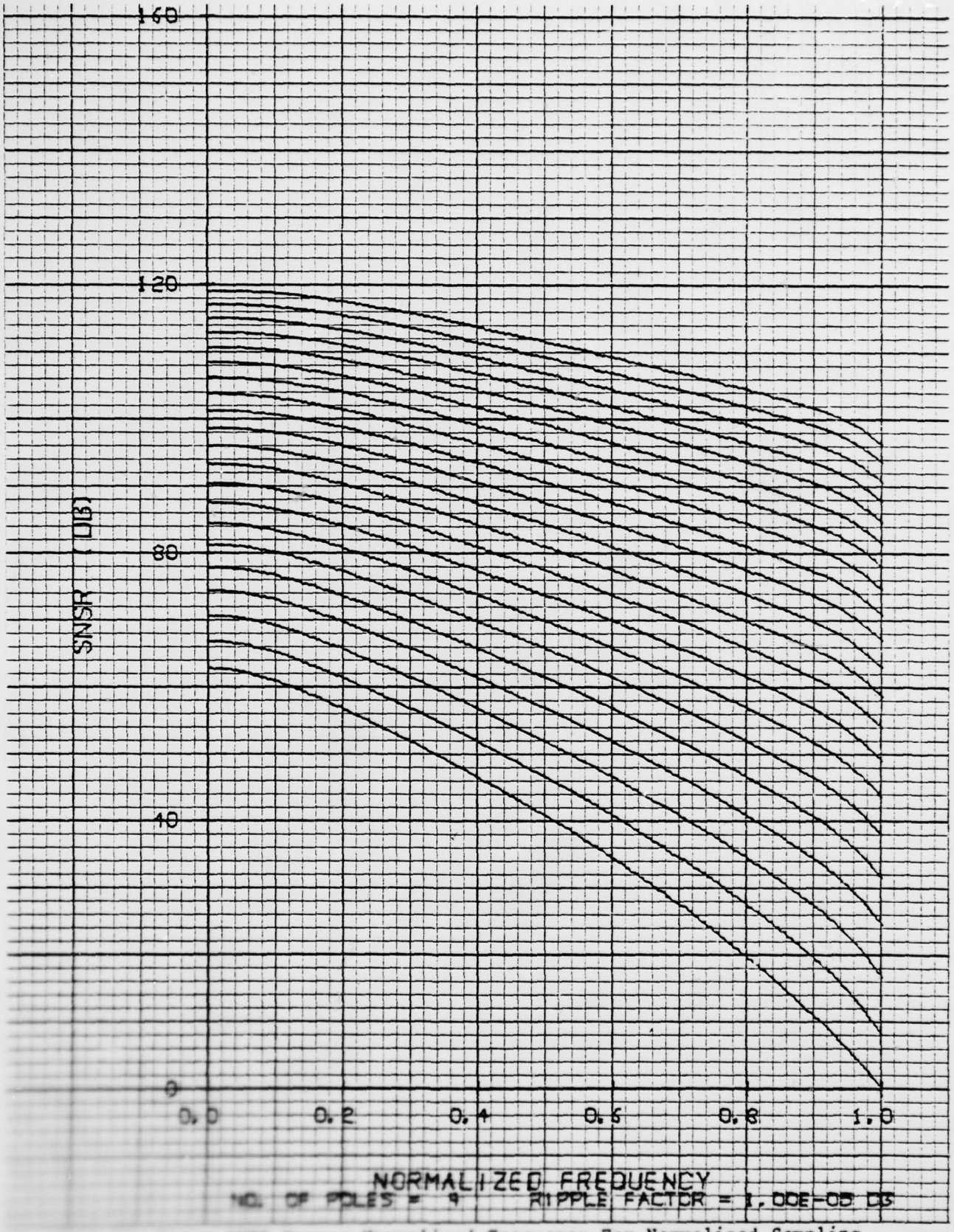

Aliasing Error SNSR Versus Normalized Frequency For Normalized Sampling Rates of 2.0, 2.1, ... 3.9, 4.0.

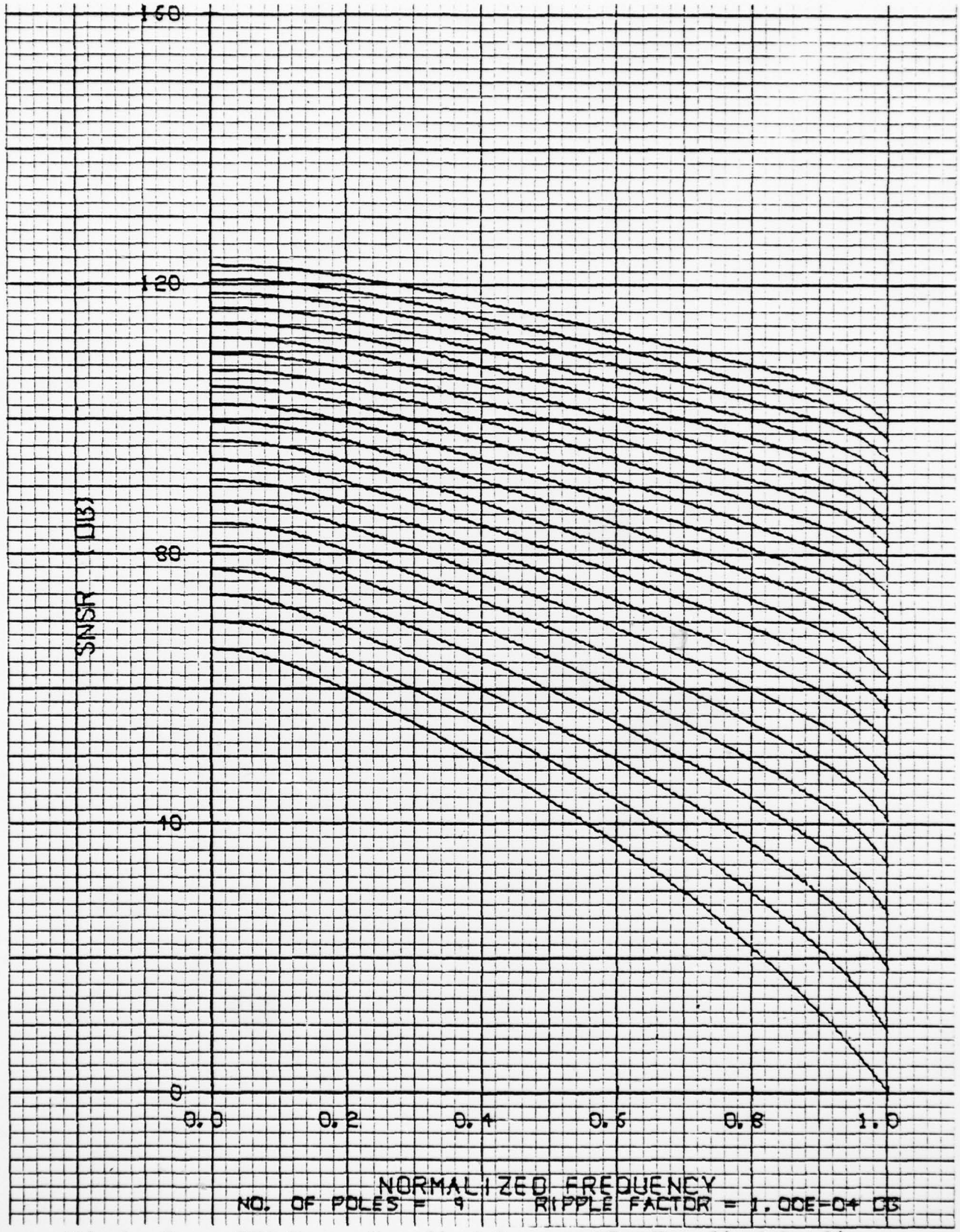

Aliasing Error SNSR Versus Normalized Frequency For Normalized Sampling Rates of 2.0, 2.1, ... 3.9, 4.0.

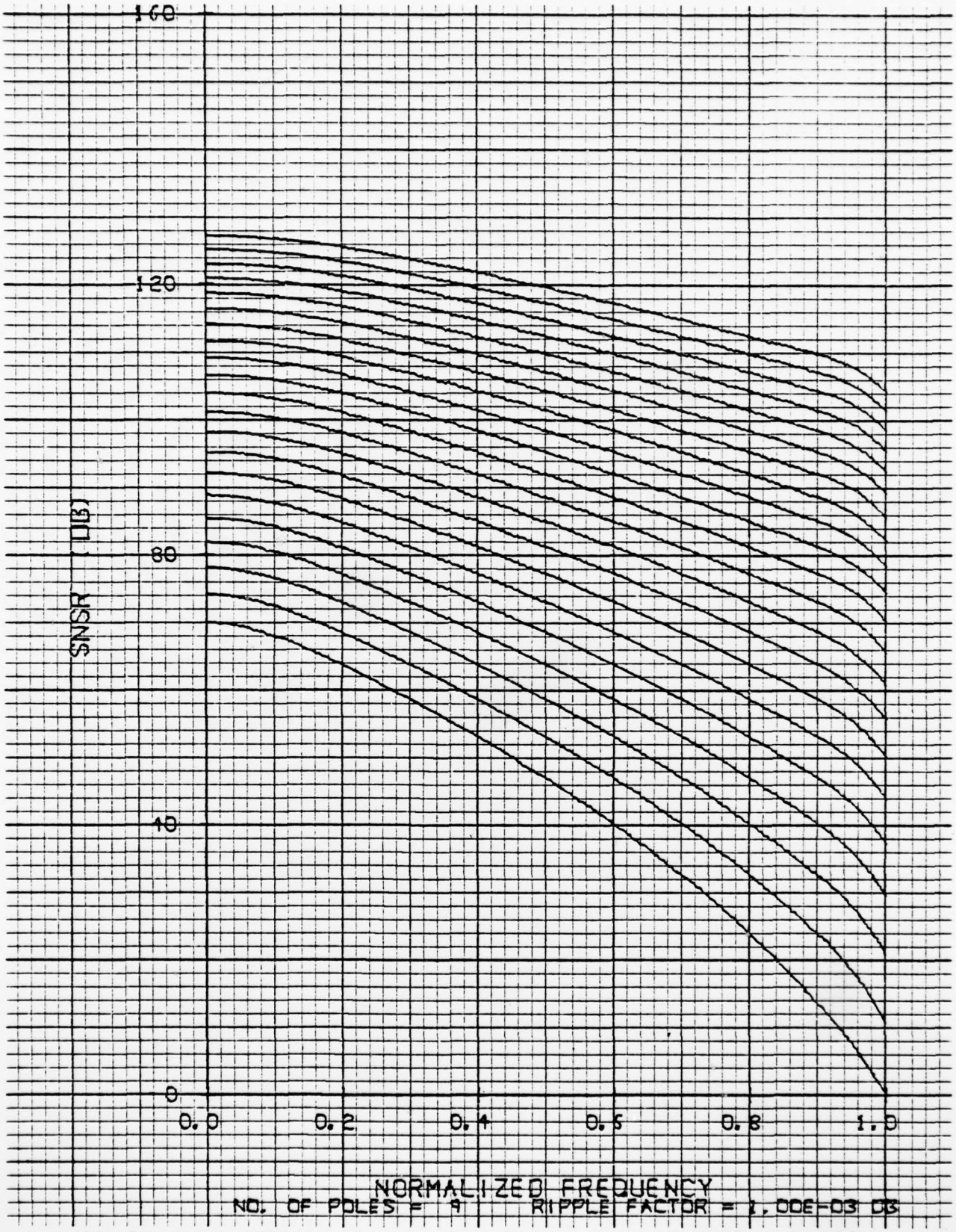

Aliasing Error SNSR Versus Normalized Frequency For Normalized Sampling Rates of 2.0, 2.1, ... 3.9, 4.0.

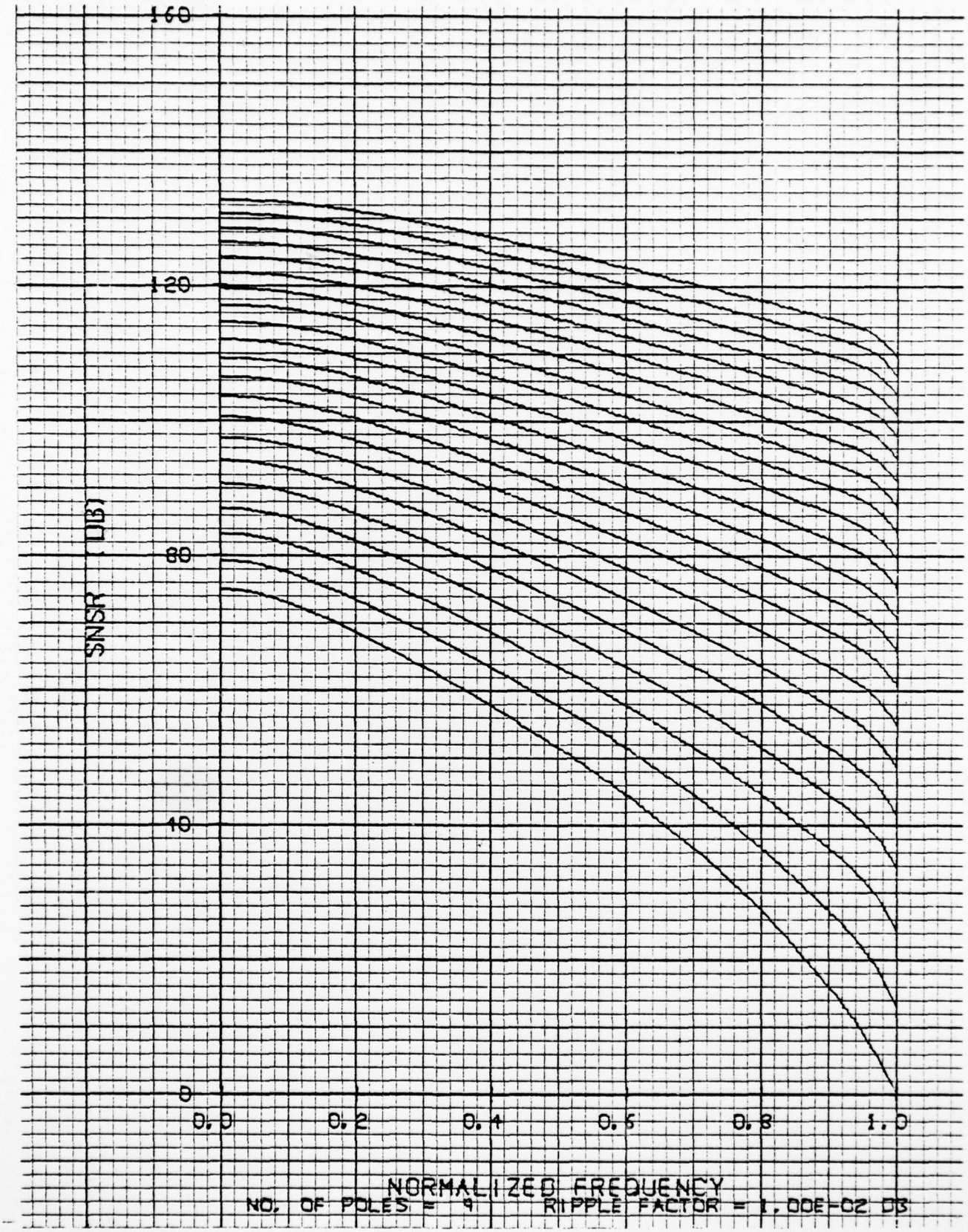

Aliasing Error SNSR Versus Normalized Frequency For Normalized Sampling Rates of 2.0, 2.1, ... 3.9, 4.0.

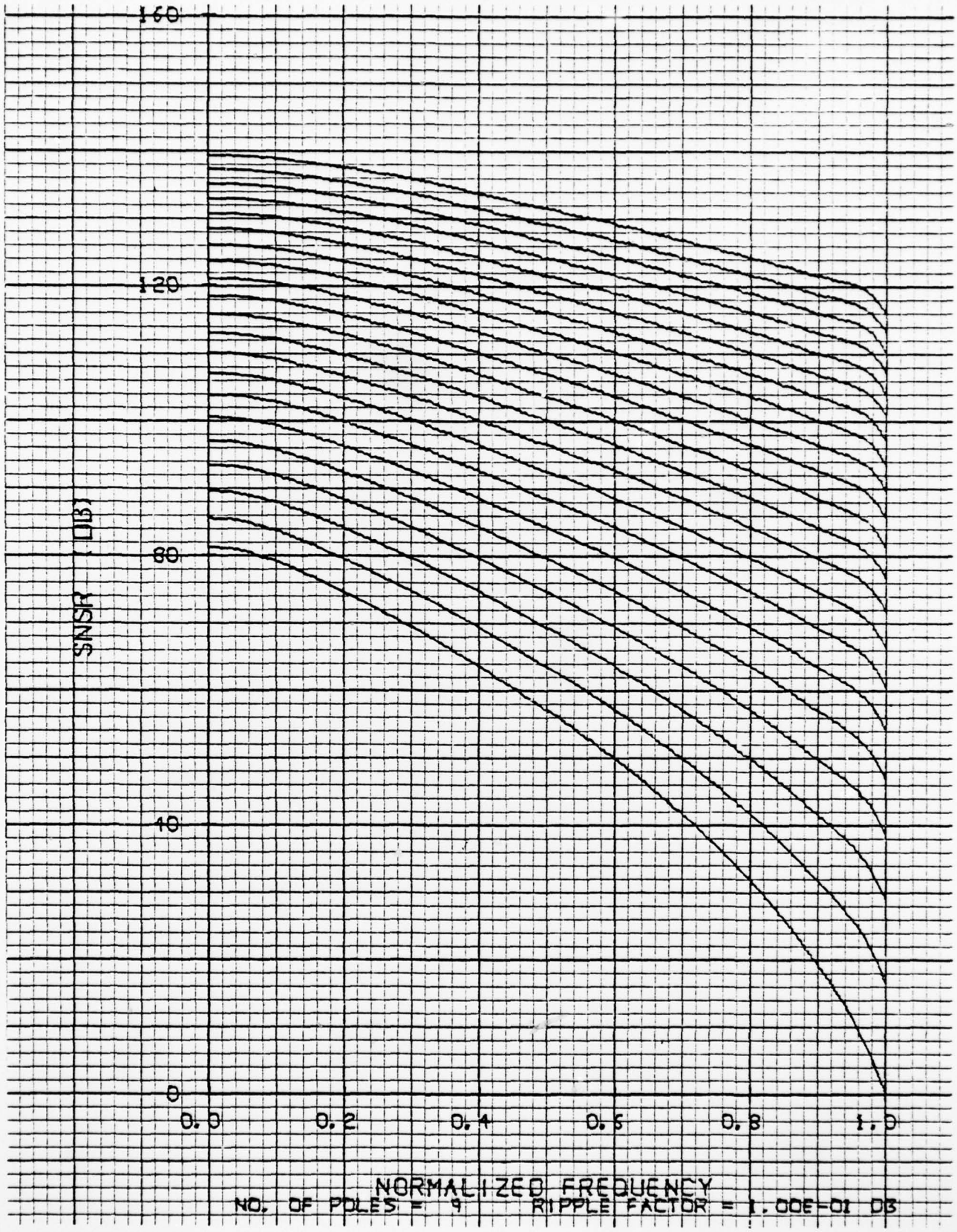

Aliasing Error SNSR Versus Normalized Frequency For Normalized Sampling Rates of 2.0, 2.1, ... 3.9, 4.0.

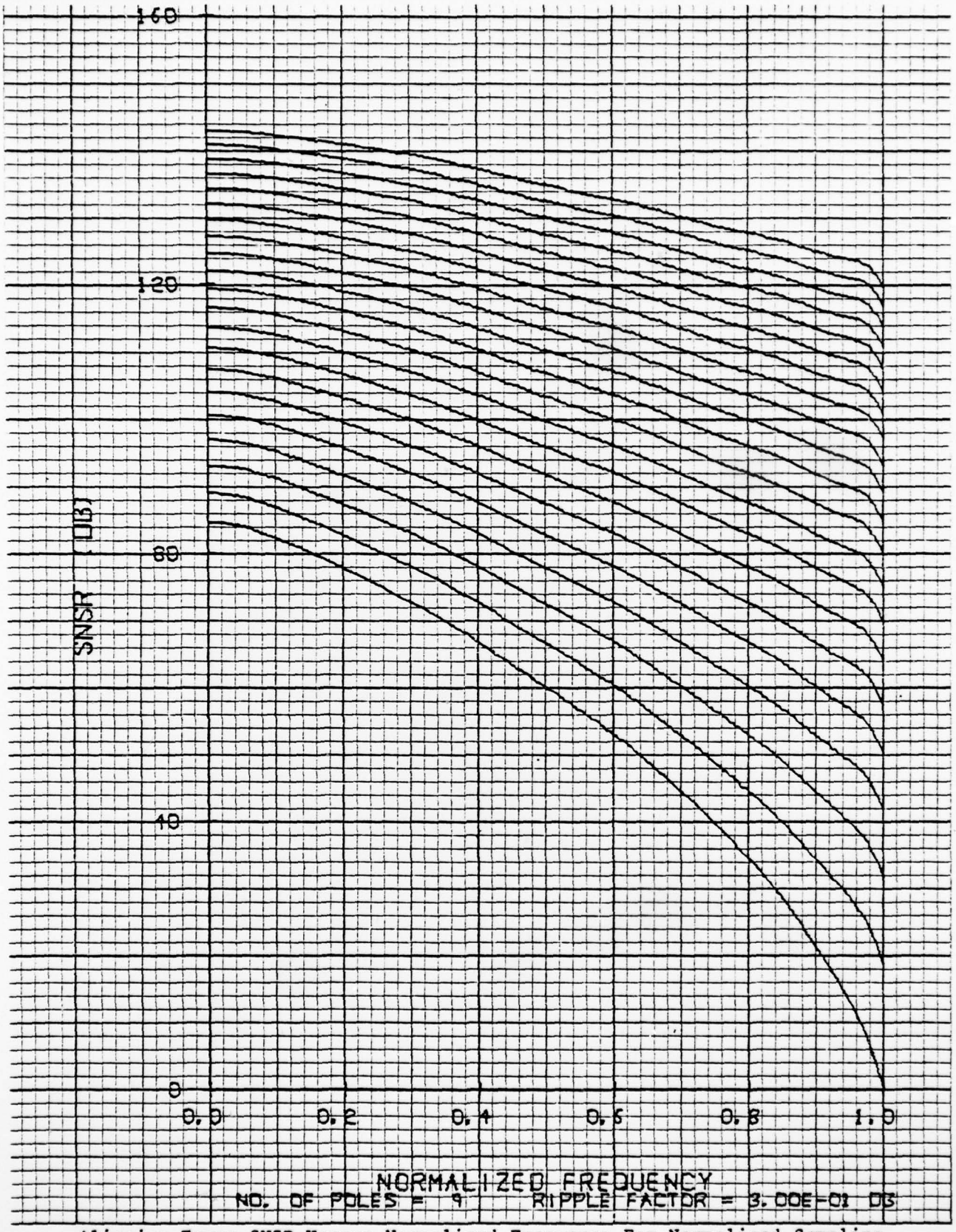

Aliasing Error SNSR Versus Normalized Frequency For Normalized Sampling Rates of 2.0, 2.1, ... 3.9, 4.0.

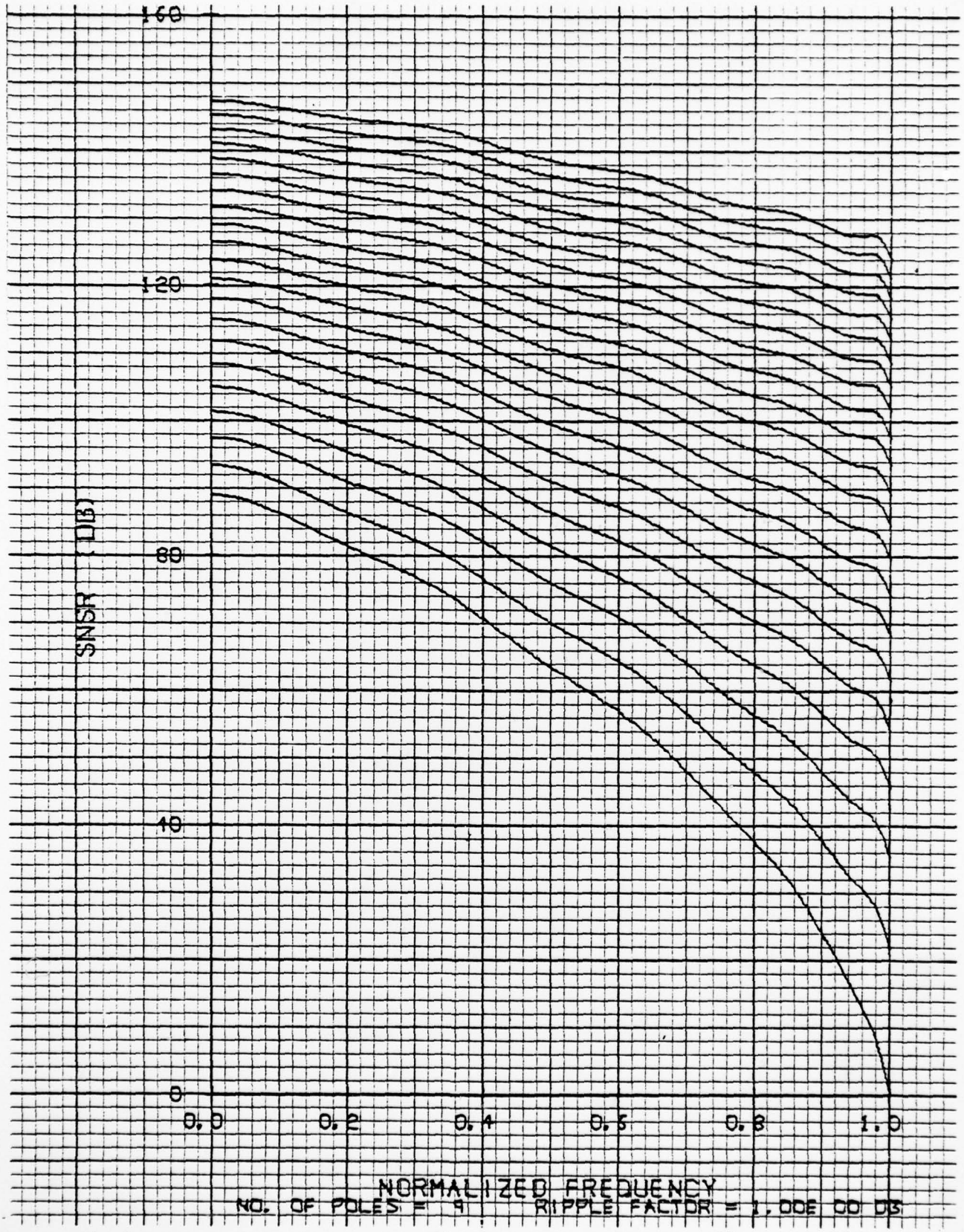

Aliasing Error SNSR Versus Normalized Frequency For Normalized Sampling Rates of 2.0, 2.1, ... 3.9, 4.0.

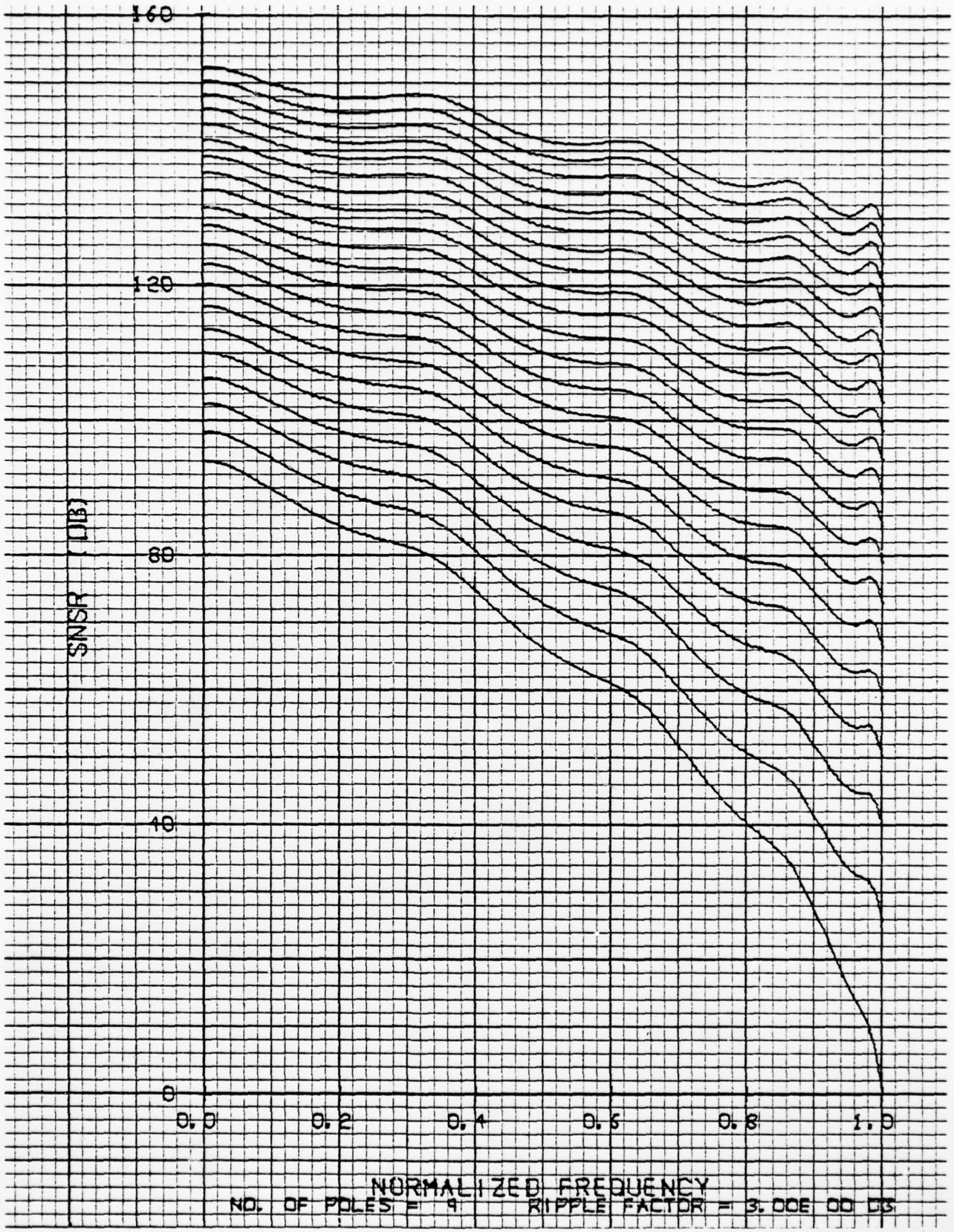

Aliasing Error SNSR Versus Normalized Frequency For Normalized Sampling Rates of 2.0, 2.1, ... 3.9, 4.0.

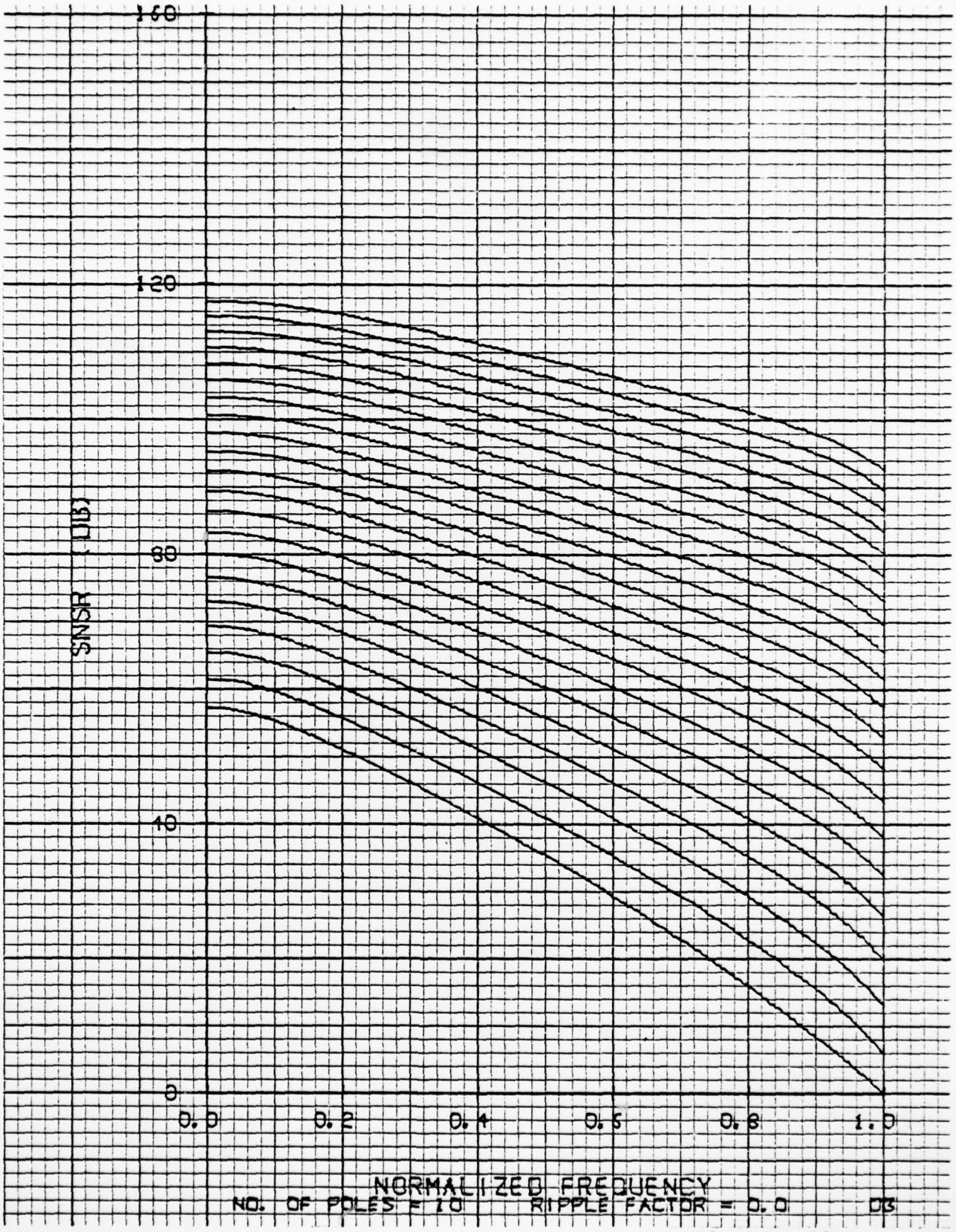

Aliasing Error SNSR Versus Normalized Frequency For Normalized Sampling Rates of 2.0, 2.1, ... 3.9, 4.0.

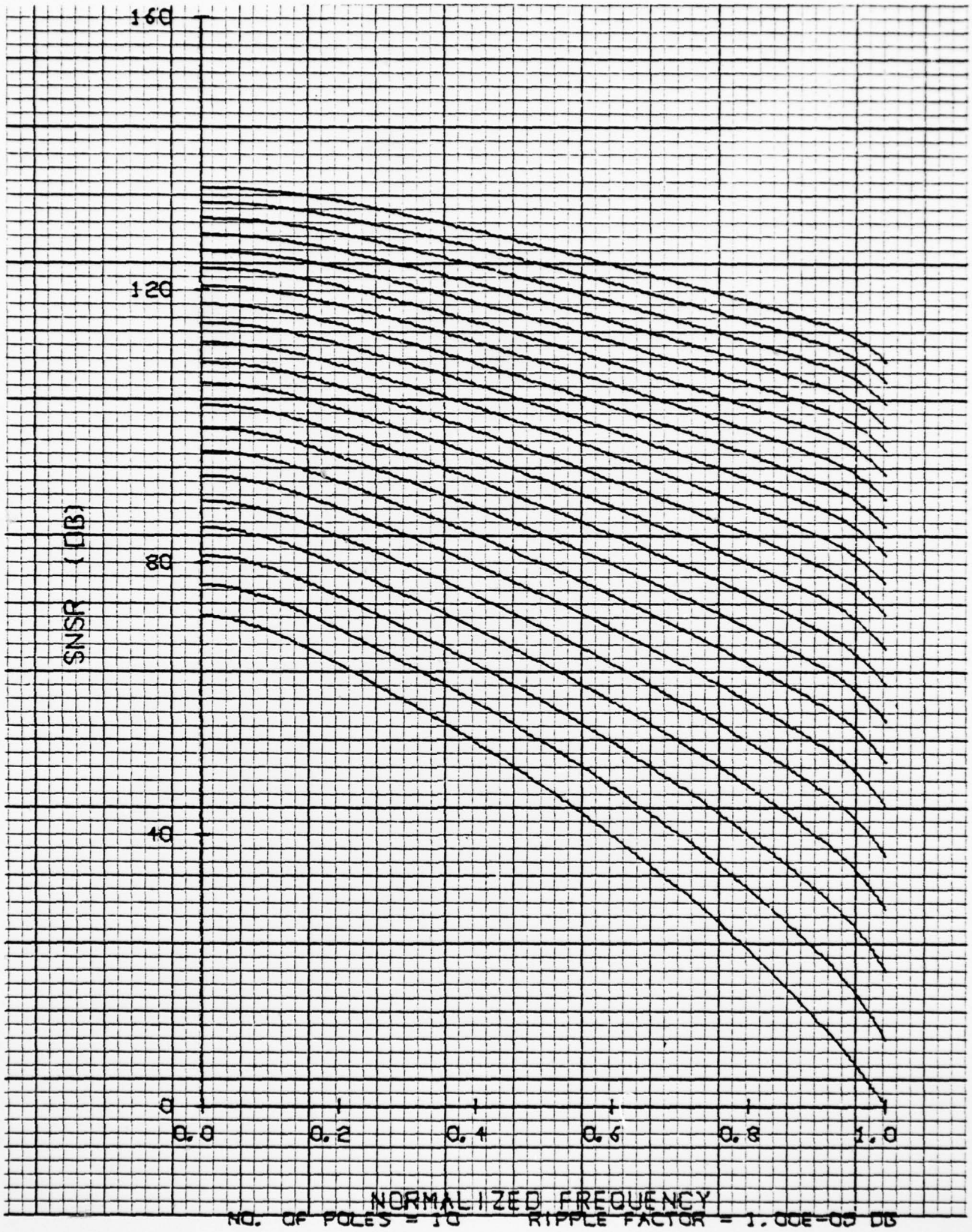

Aliasing Error SNSR Versus Normalized Frequency For Normalized Sampling Rates of 2.0, 2.1, ... 3.9, 4.0.

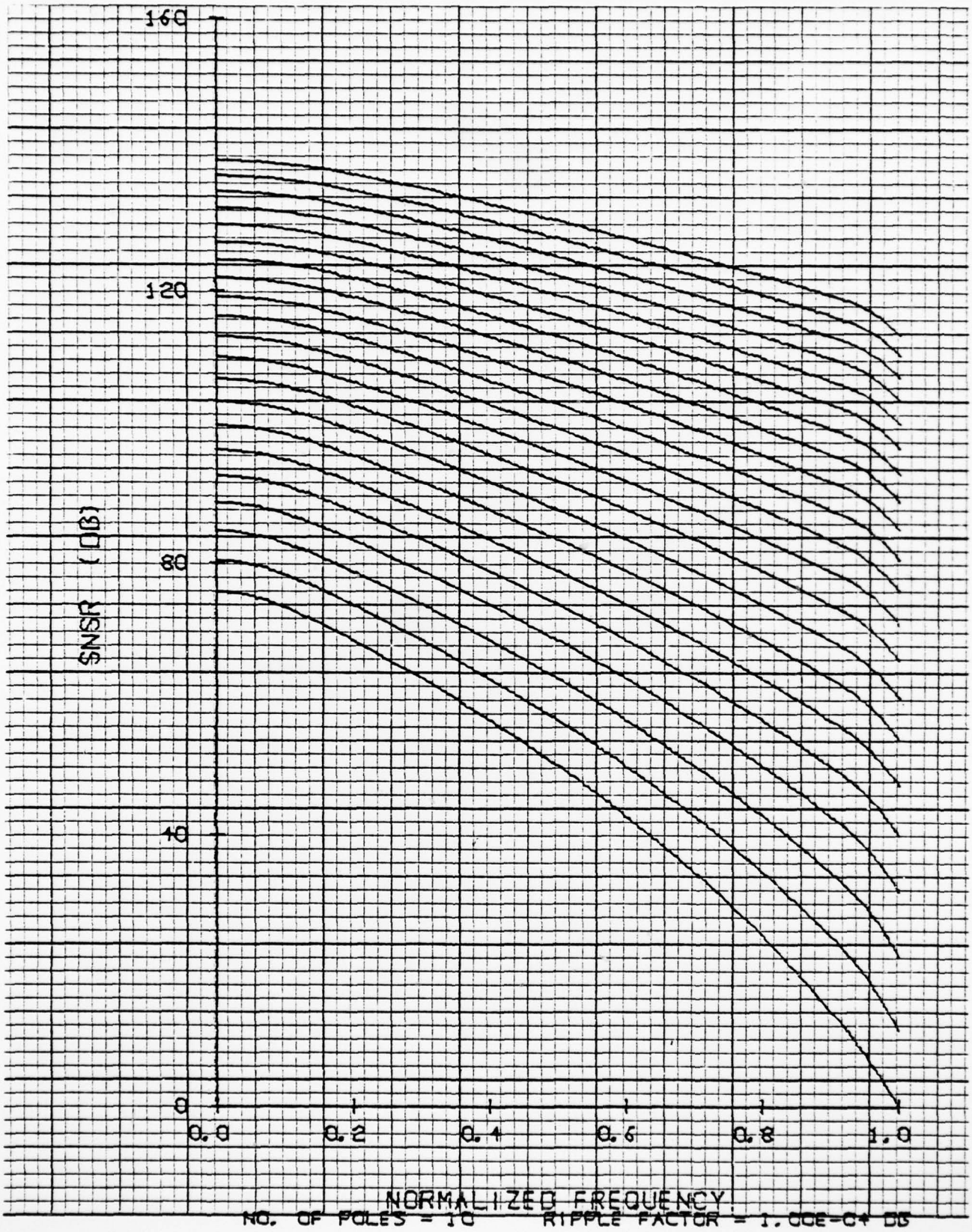

Aliasing Error SNSR Versus Normalized Frequency For Normalized Sampling Rates of 2.0, 2.1, ... 3.9, 4.0.

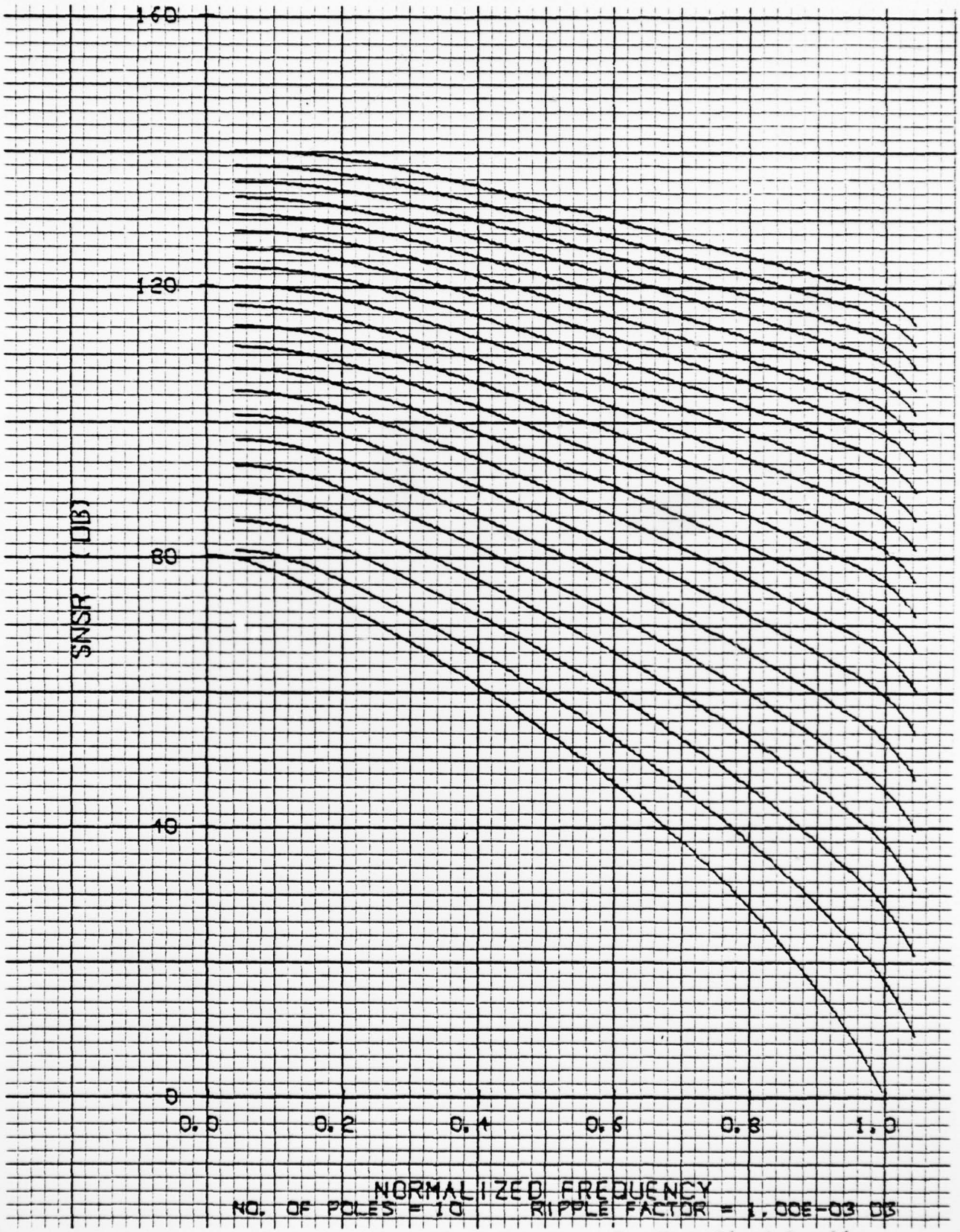

Aliasing Error SNSR Versus Normalized Frequency For Normalized Sampling Rates of 2.0, 2.1, ... 3.9, 4.0.

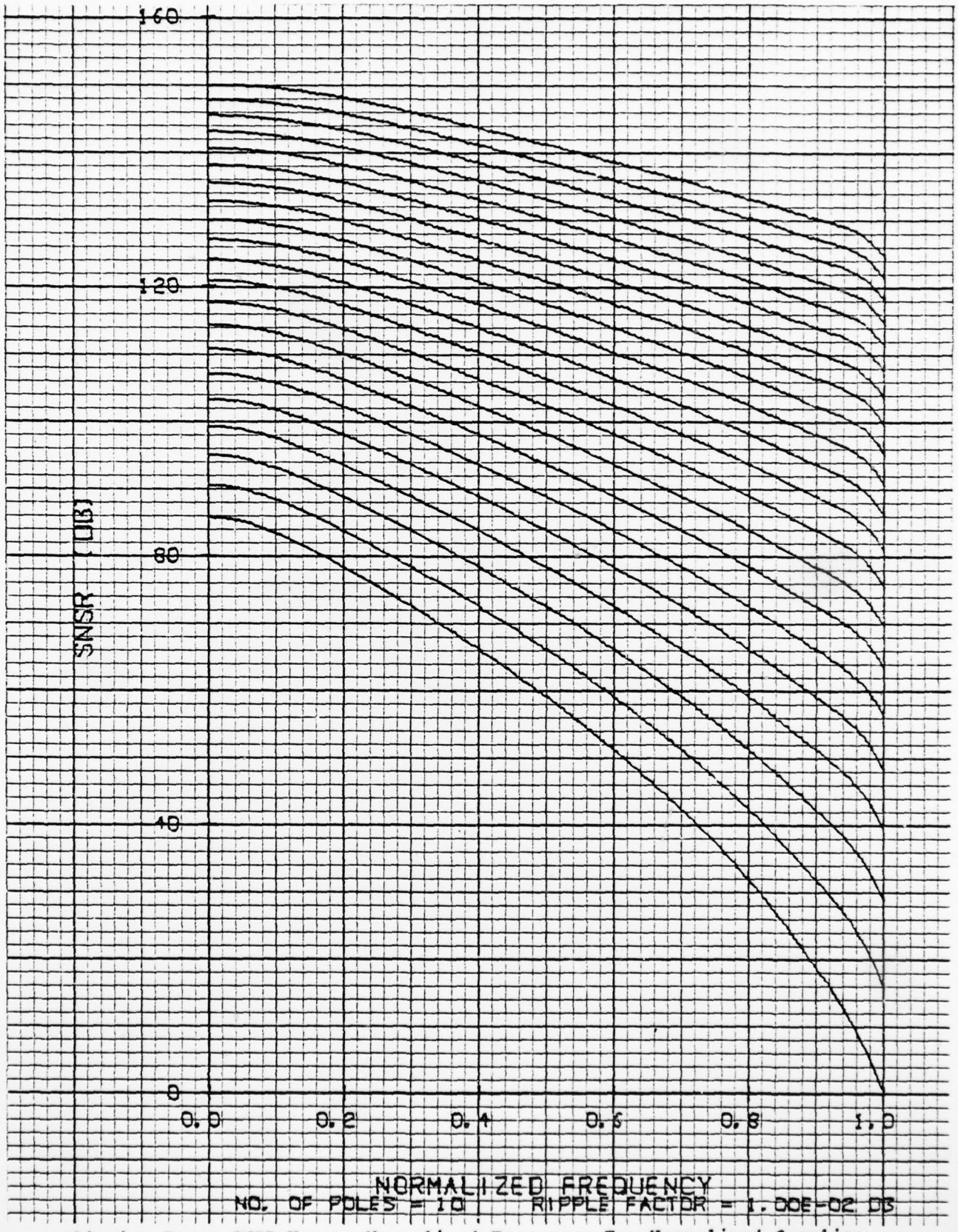

Aliasing Error SNSR Versus Normalized Frequency For Normalized Sampling Rates of 2.0, 2.1, ... 3.9, 4.0.

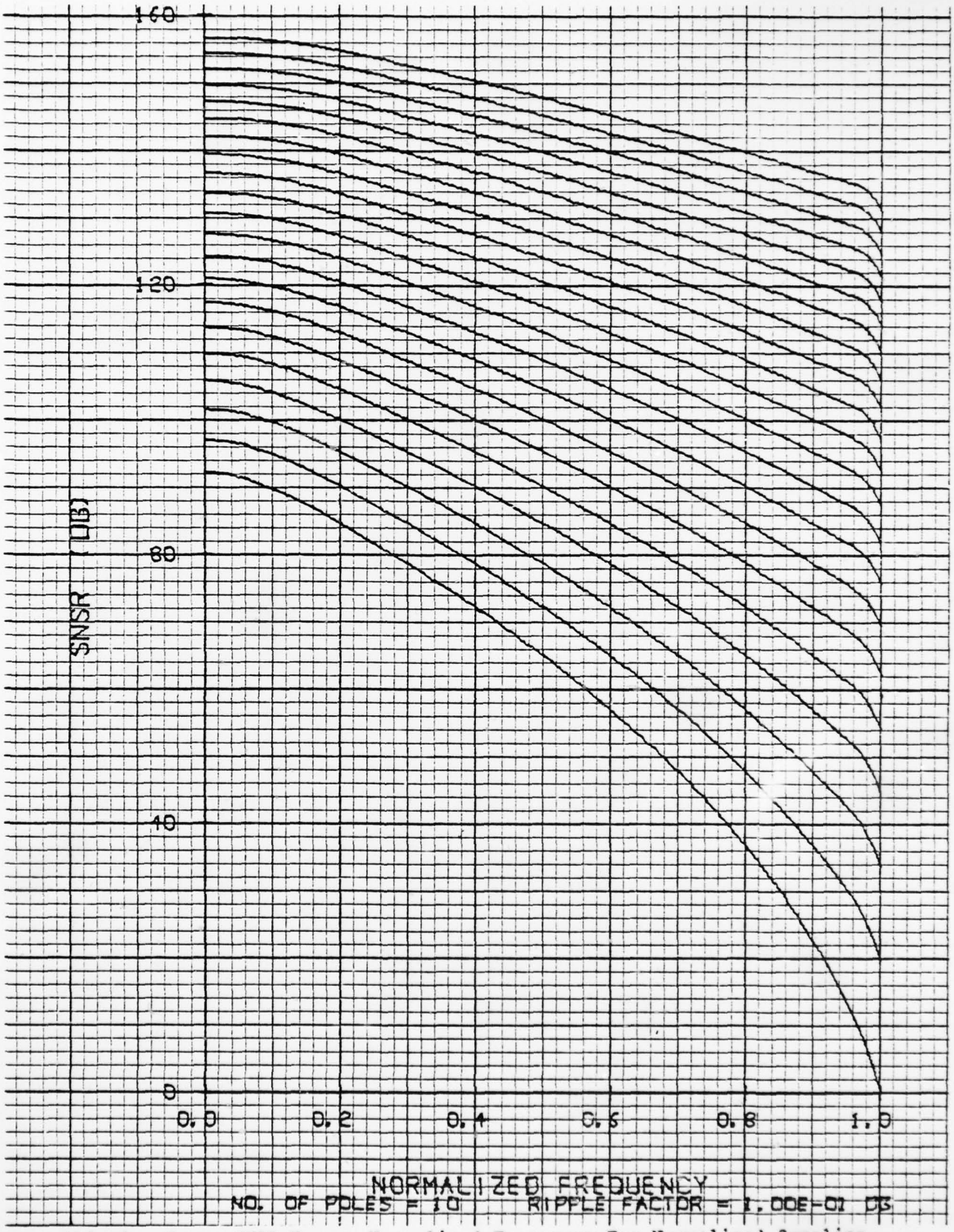

Aliasing Error SNSR Versus Normalized Frequency For Normalized Sampling Rates of 2.0, 2.1, ... 3.9, 4.0.

AD-A060 430 SPERRY SYSTEMS MANAGEMENT RESTON VA F/G 9/5

A STATISTICAL DESIGN MANUAL FOR HIGH SPEED ANALOG-DIGITAL-ANALO--ETC(U)

1974 J F HOLLAND N00039-77-C-0124

UNCLASSIFIED NL

3 OF 3

AD
A060430

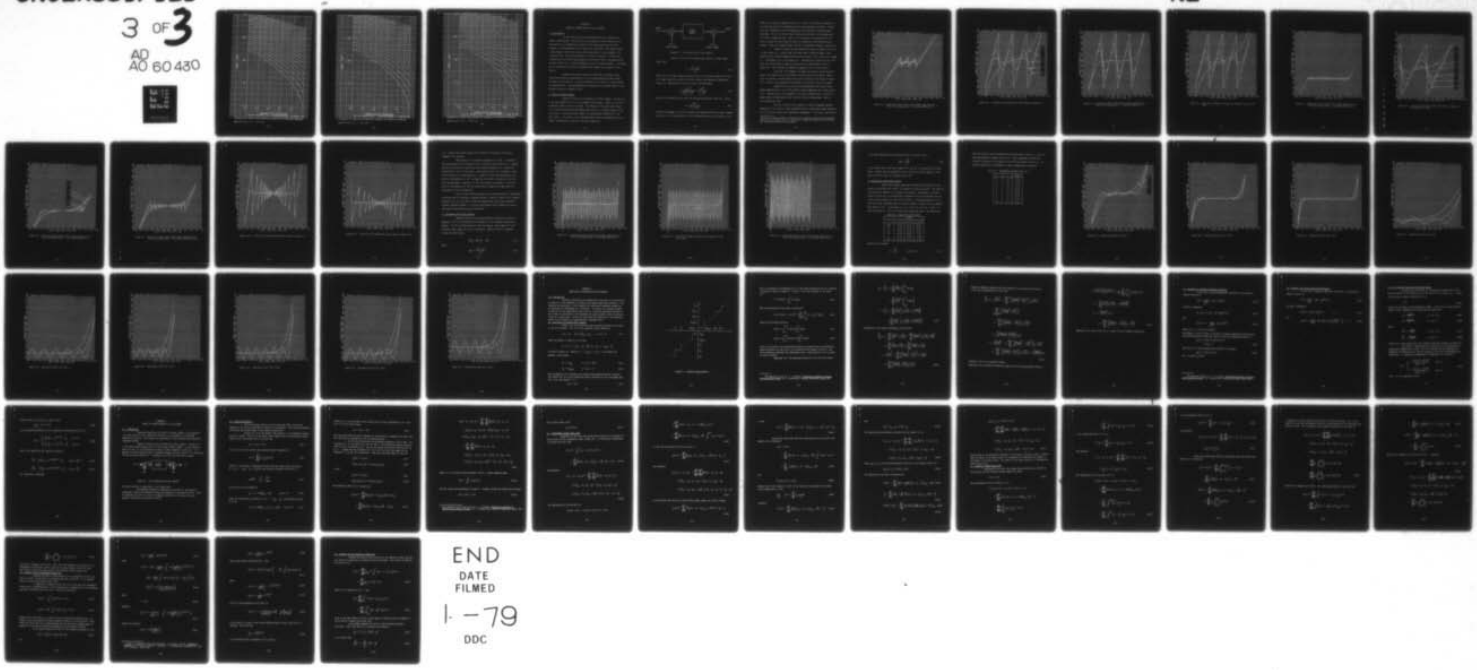

END
DATE
FILMED
1-79
DDC

SIFIED

3 OF 3

AD
AO 60 430

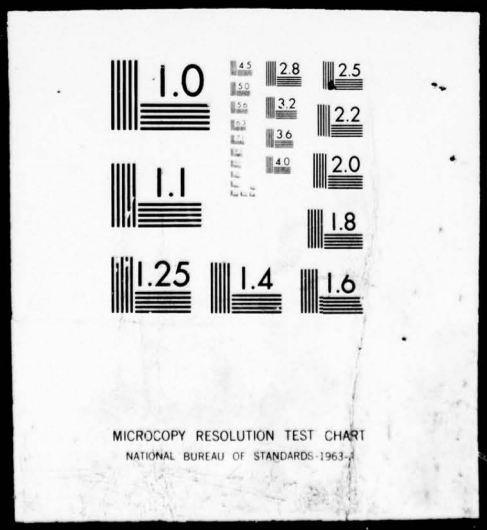

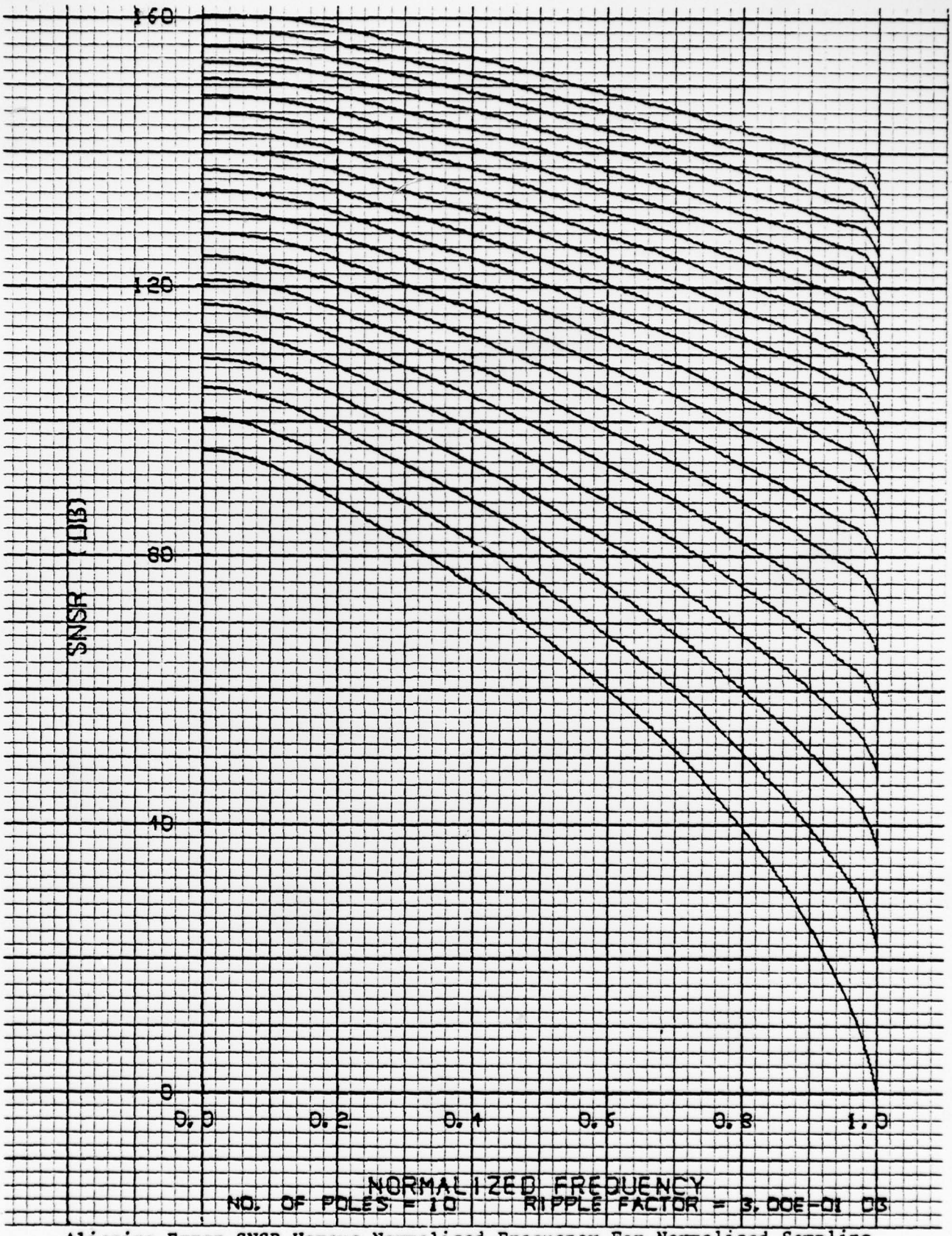

Aliasing Error SNSR Versus Normalized Frequency For Normalized Sampling Rates of 2.0, 2.1, ... 3.9, 4.0.

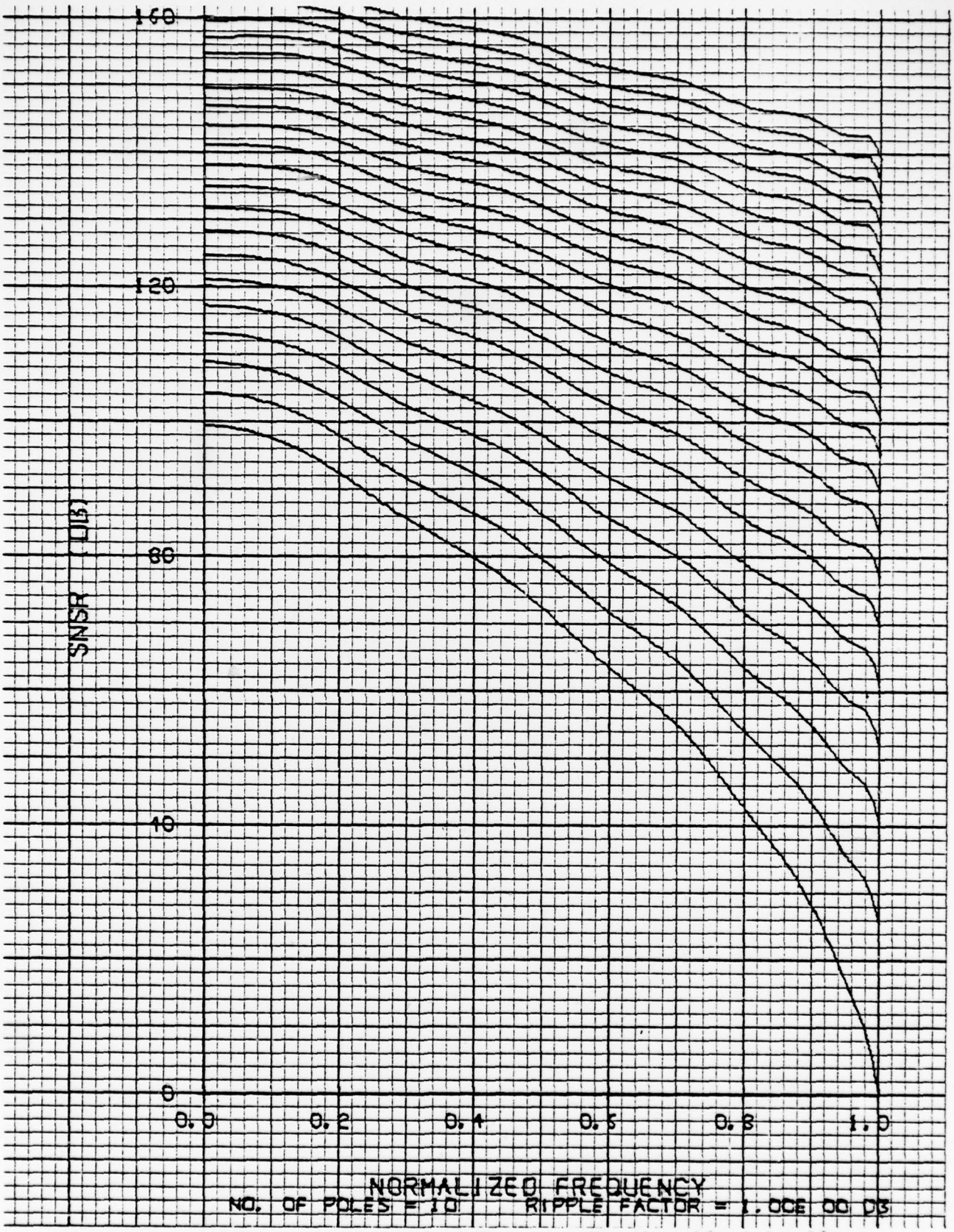

Aliasing Error SNSR Versus Normalized Frequency For Normalized Sampling Rates of 2.0, 2.1, ... 3.9, 4.0.

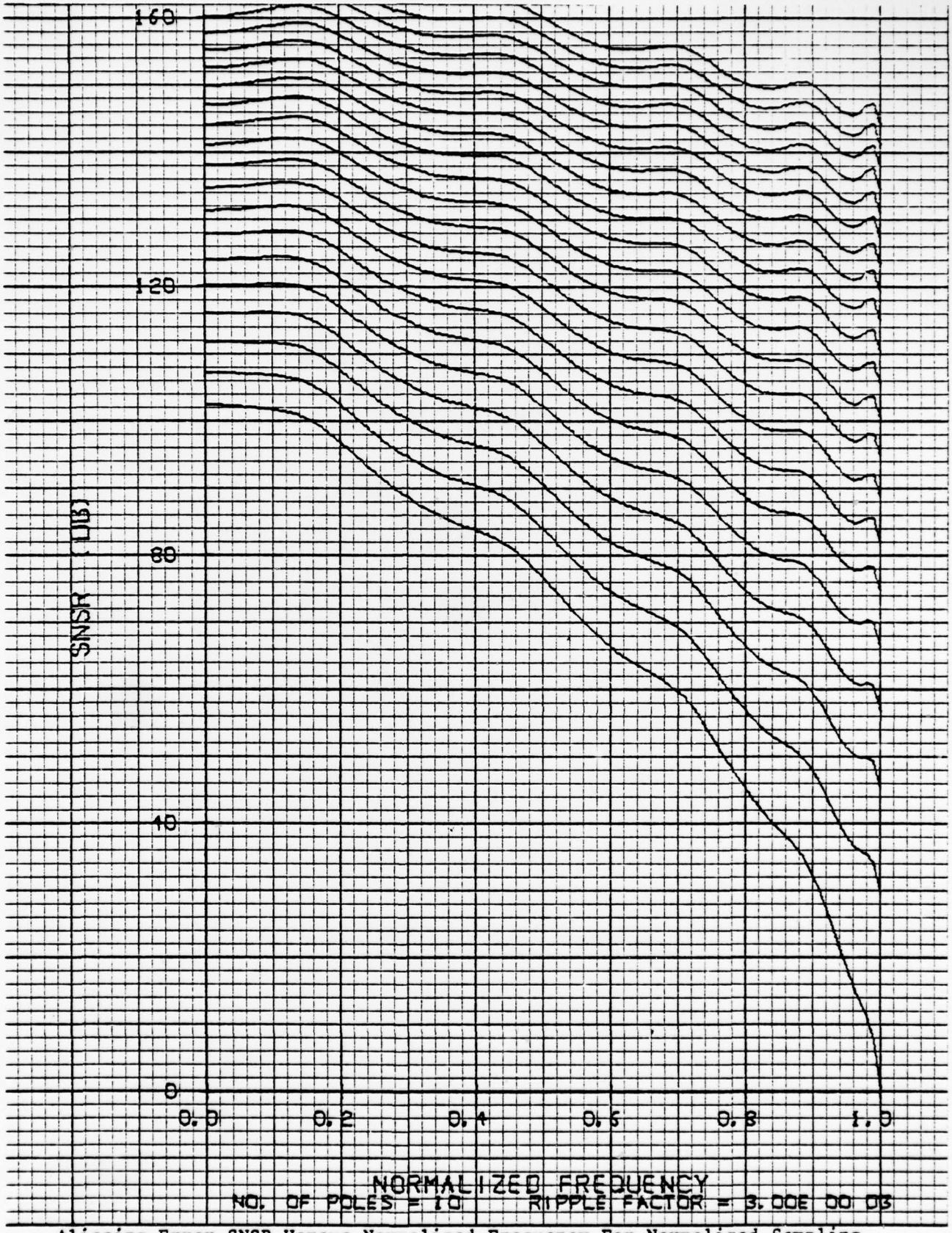

Aliasing Error SNSR Versus Normalized Frequency For Normalized Sampling Rates of 2.0, 2.1, ... 3.9, 4.0.

SECTION VI

EFFECT OF DITHER SIGNALS IN A-D-A SYSTEMS

1. Introduction

In the previous sections, performance has been considered in terms of SNSR and SNR. The fact that the instantaneous error associated with quantization is a deterministic function of the input signal has not been examined. This deterministic error results in contouring. With image signals, a ramp change in grey scale results after quantization in step changes in the intensity level. This staircase effect is called contouring. Pictures with contouring are often more objectionable than pictures without contouring having the same output SNR. A similar phenomenon occurs with speech signals. Contouring may be eliminated by the use of wideband dither signals as discussed in this section.

Equations and design curves for predicting the dynamic range limitations imposed by quantization in A-D-A systems employing dither signals are given in this section. A general discussion on the effect of dither signals is presented first. Then performance and optimization are examined based on the equations derived in Appendix A and B.

2. Effect Of Dither Signals

Figure 6-1 shows an A-D-A system with dither signals. Process $y(t)$ is the input signal and $r(t)$ is the wideband dither signal. Delay T is the total propagation delay of the A-D-A system. The purpose of the input dither signal is to introduce random zero mean quantization errors in a fashion similar to A/D level errors. The output dither signal then synchronously subtracts out the input dither. The result is that the quantization error is randomized and is no longer a deterministic function of the input signal $y(t)$.

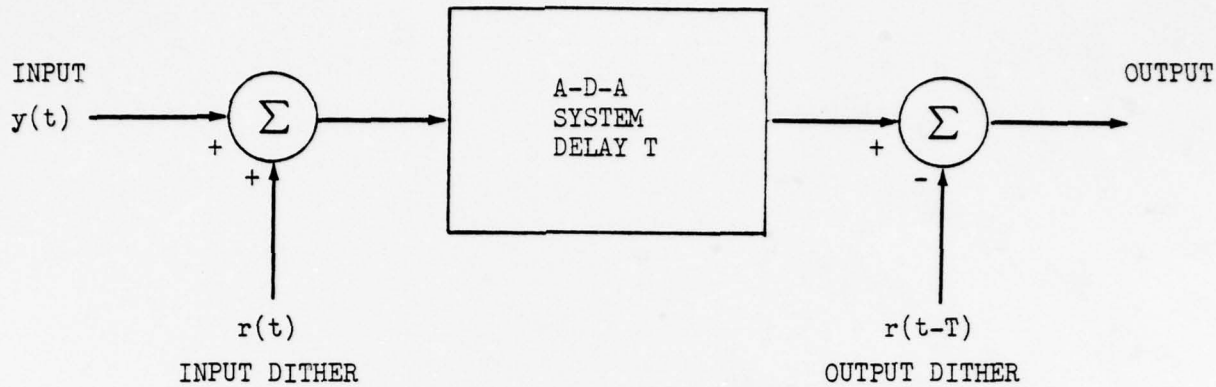

Figure 6-1. A-D-A System With Dither Signals

Define B to be the A-D-A system input signal to dither signal power ratio

$$B = \frac{\sigma_s^2 + \sigma_r^2}{\sigma_r^2} \tag{6-1}$$

where σ_s^2 is the input signal y(t) power and σ_r^2 is the dither signal r(t) power. Let η again denote crest factor (CF) and μ denote the logarithmic compression factor (u). Equations (3-5) and (6-1) give the relationship

$$\eta = \frac{E\ 2^{q-1}}{\sqrt{\sigma_s^2 + \sigma_r^2}} = \frac{E\ 2^{q-1}}{\sigma_r \sqrt{B}} \tag{6-2}$$

where q is the number of bits and E is the uniform quantizer step size. Hence,

$$B = \frac{4^{q-1}}{\eta^2\ (\sigma_r/E)^2} \tag{6-3}$$

Consider for example a 2 bit A-D-A system with Gaussian dither and linear companding (μ=0). For a crest factor of 2 the instantaneous error as a function of the

input y(t) is given in Figures 6-2 and 6-3.* The B = 60 dB case corresponds to no dither and shows the deterministic error which produces contouring. Observe that this deterministic error diminishes as the dither power increases and B decreases. The B = 10 dB case still contains oscillation so the optimum value of B must be something less. The B = 1.0 dB case has no oscillation but the error is large for most values of input y(t) because too much dither noise is present. Hence, the optimum value of B must lie somewhere between 1.0 and 10 dB.

Figure 6-4 shows the same quantization error as Figure 6-3 but for a crest factor of 4. Observe that the curves have a different shape. From equation (6-3) B varies quadratically with crest factor η and a factor of 2 change in η corresponds to a 6.0 dB change in B. Decreasing the values of B by 6.0 dB gives the curves shown in Figure 6-5 which have the same shape as those in Figure 6-3. This verifies the quadratic dependence of B on crest factor η.

From this 2 bit example, the shape of the error curves should be clear. Too large a value of B results in an oscillatory error and too small a value of B gives a nonoscillatory error which is large for most values of input y(t). This is true regardless of the number of bits used in the A-D-A system.

Figures 6-6, 6-7, and 6-8 show quantization error versus input signal amplitude for a 5 bit A-D-A system, linear companding, and a crest factor of 3. Observe that B = 20 dB appears to be nearly optimum since it results in small values of quantization error over the entire encoding range. Thus, no contouring would occur.

The use of dither is not limited to linearly companded systems. Figures 6-9, 6-10, and 6-11 show quantization error versus input signal amplitude for a 5 bit A-D-A system with logarithmic companding, μ = 100, and a crest factor

*Because of a finite number of points and the computer interpolation algorithms, plots of the no dither case (B = 60 dB) have transitions which are not vertical and extreme values which are irregular.

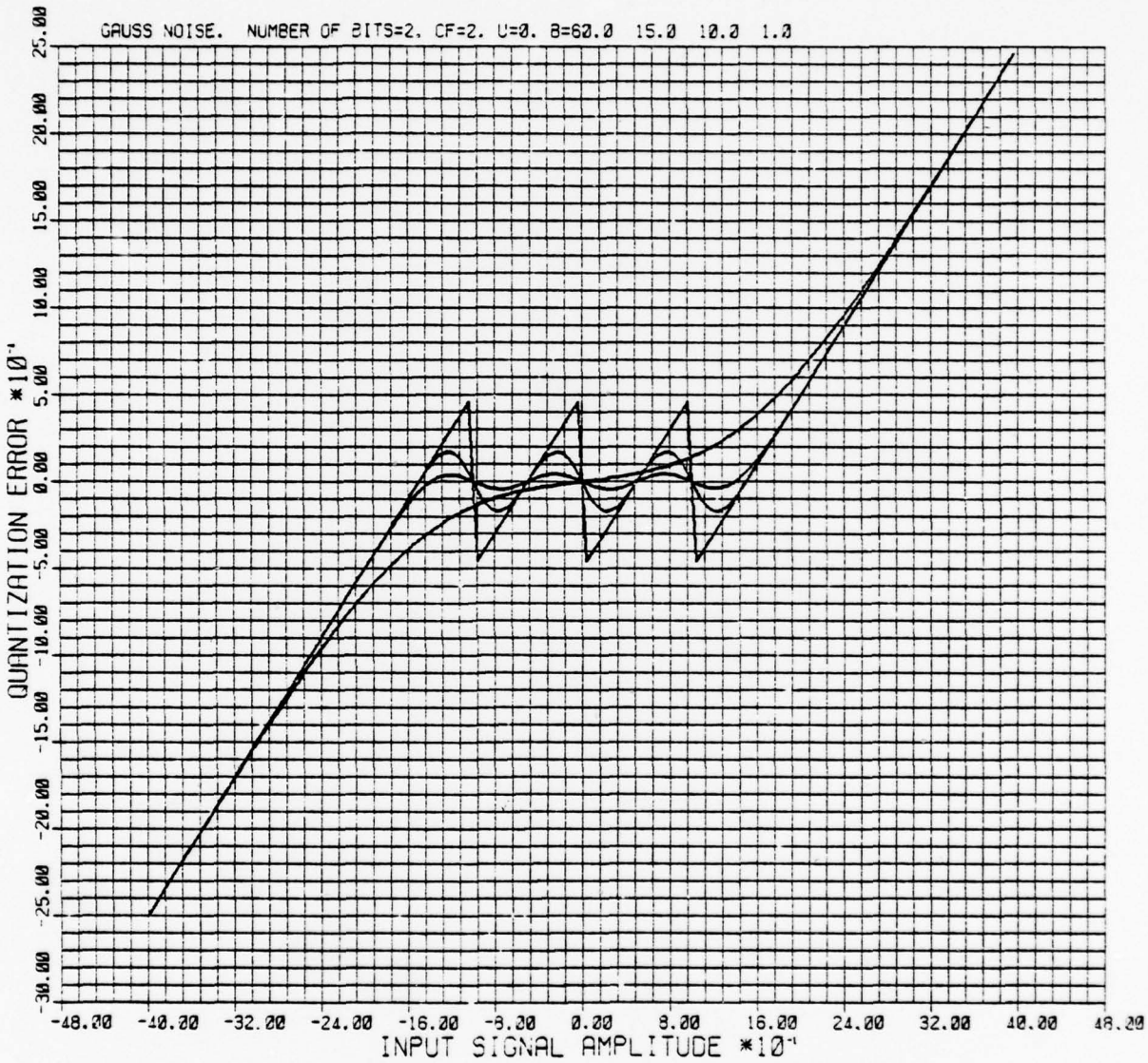

Figure 6-2. Quantization Error Versus Input Signal Amplitude For A 2 Bit A-D-A System With $\mu = 0$ And Crest Factor Of 2.

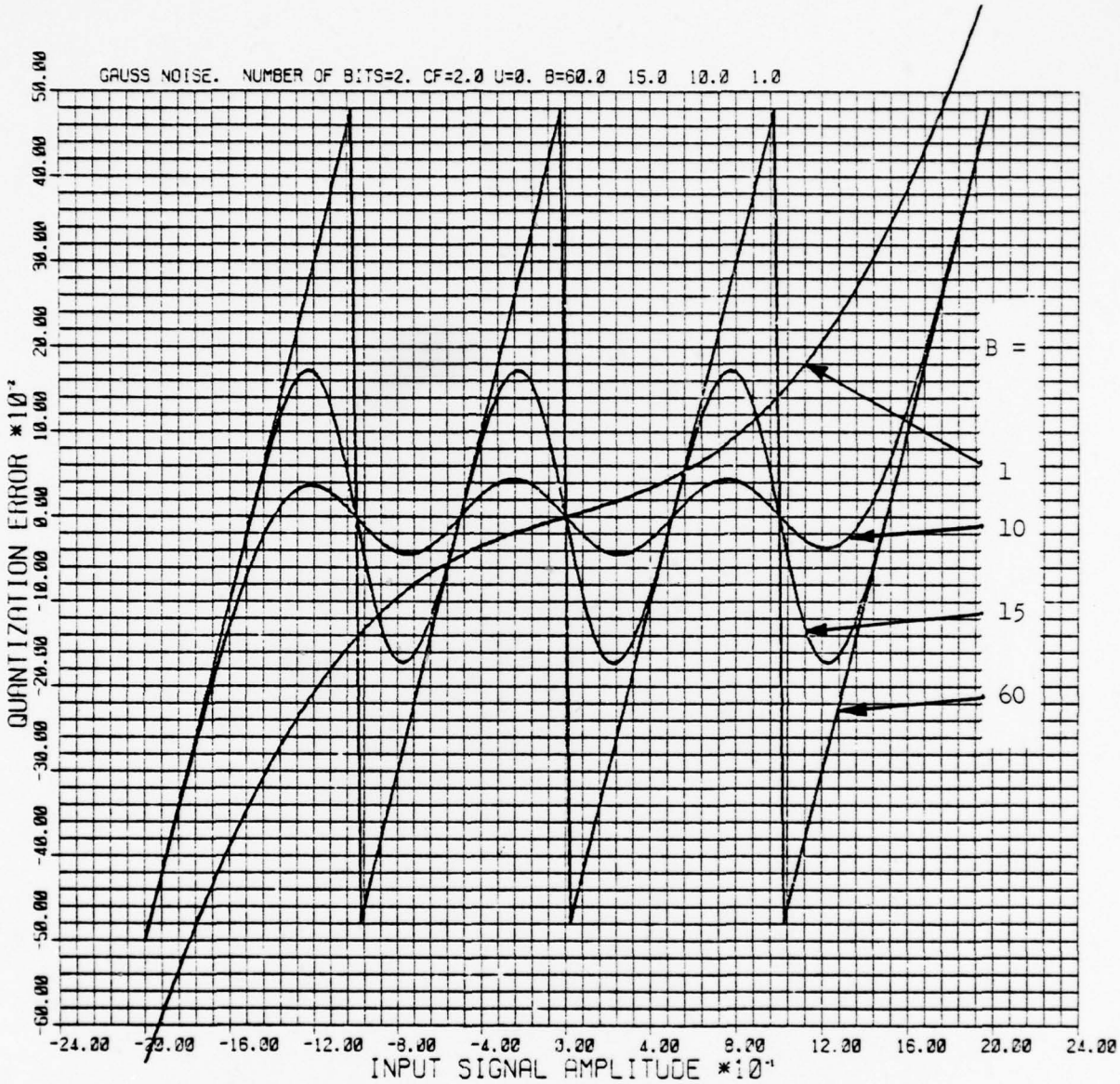

Figure 6-3. A Blow-up Of The Quantization Error Shown In Figure 6-2.

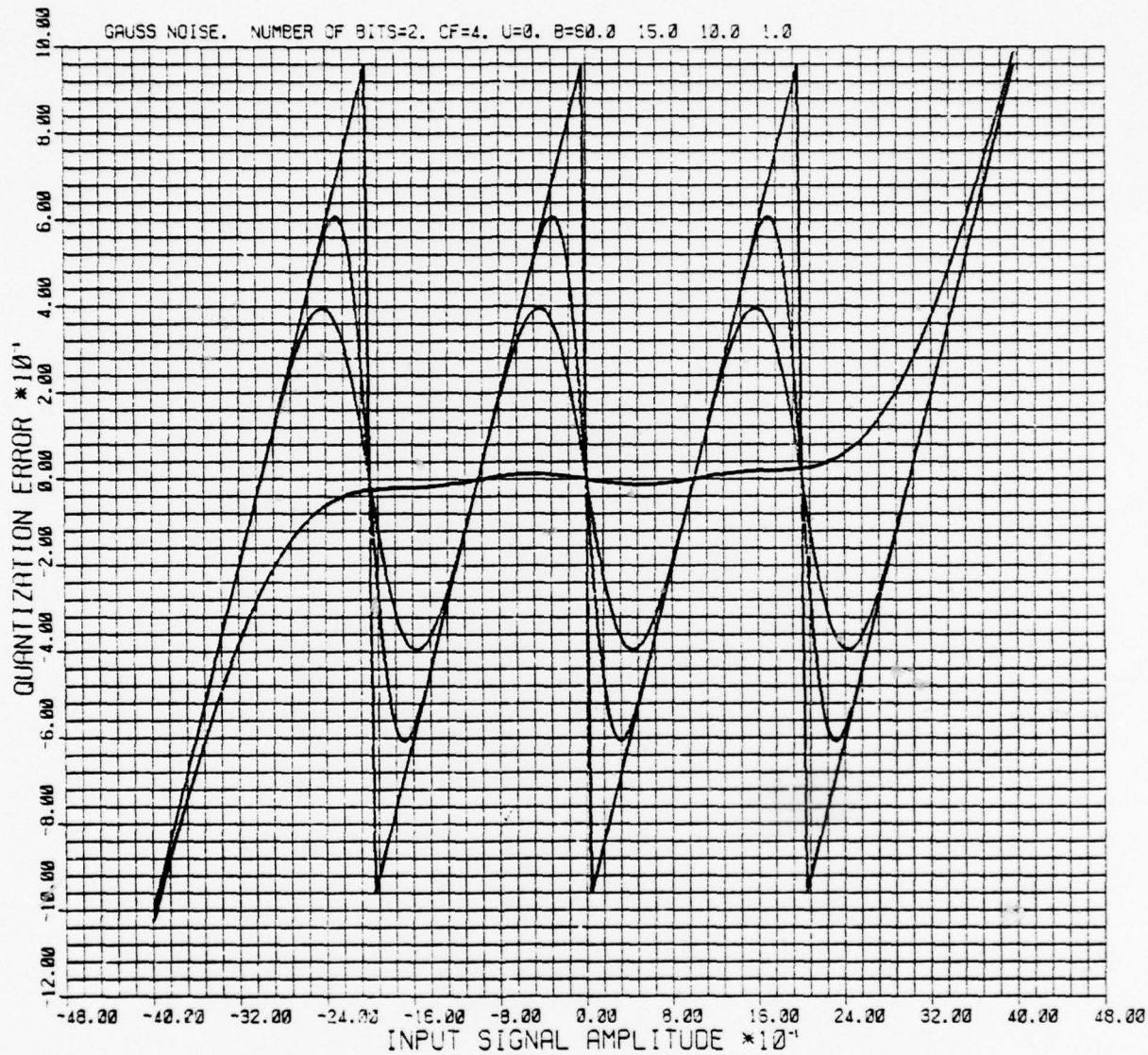

Figure 6-4. Quantization Error Versus Input Signal Amplitude For A 2 Bit A-D-A System With $\mu' = 0$ And Crest Factor Of 4.

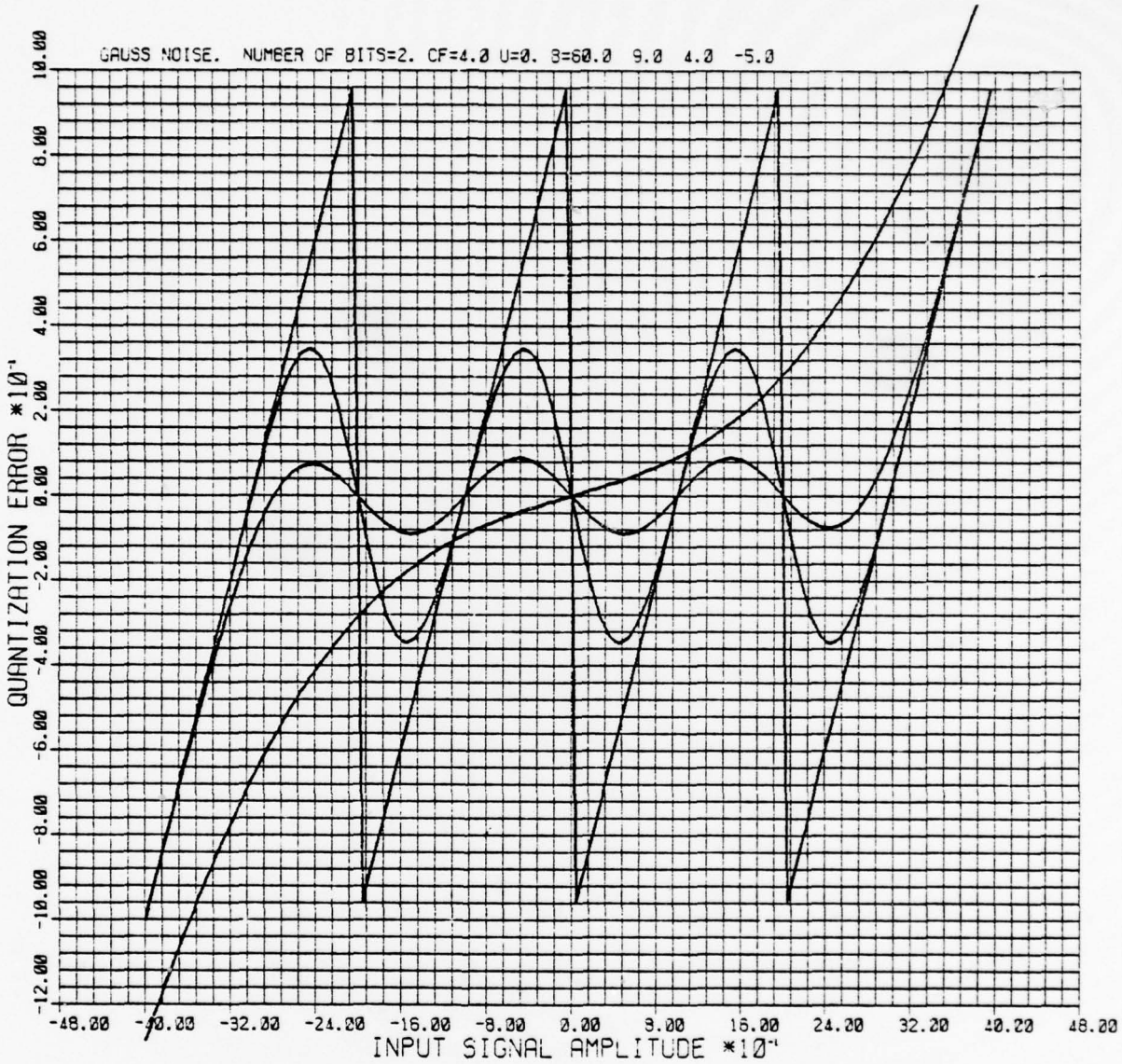

Figure 6-5. Same Case As Figure 6-4 Except The Values Of B Are 6.0 dB Less.

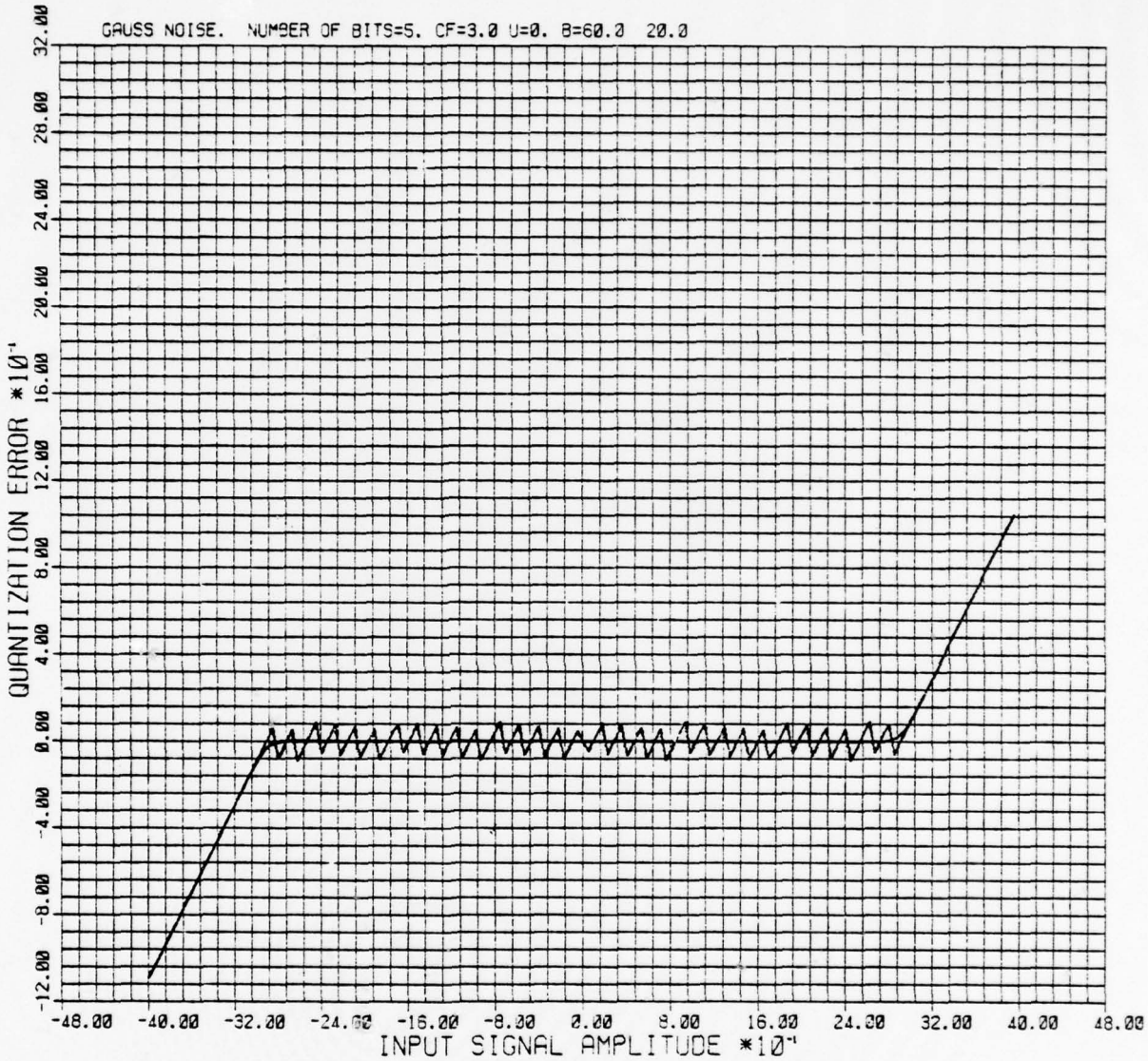

Figure 6-6. Quantization Error Versus Input Signal Amplitude For A 5 Bit A-D-A System With $\mu = 0$ And Crest Factor Of 3.

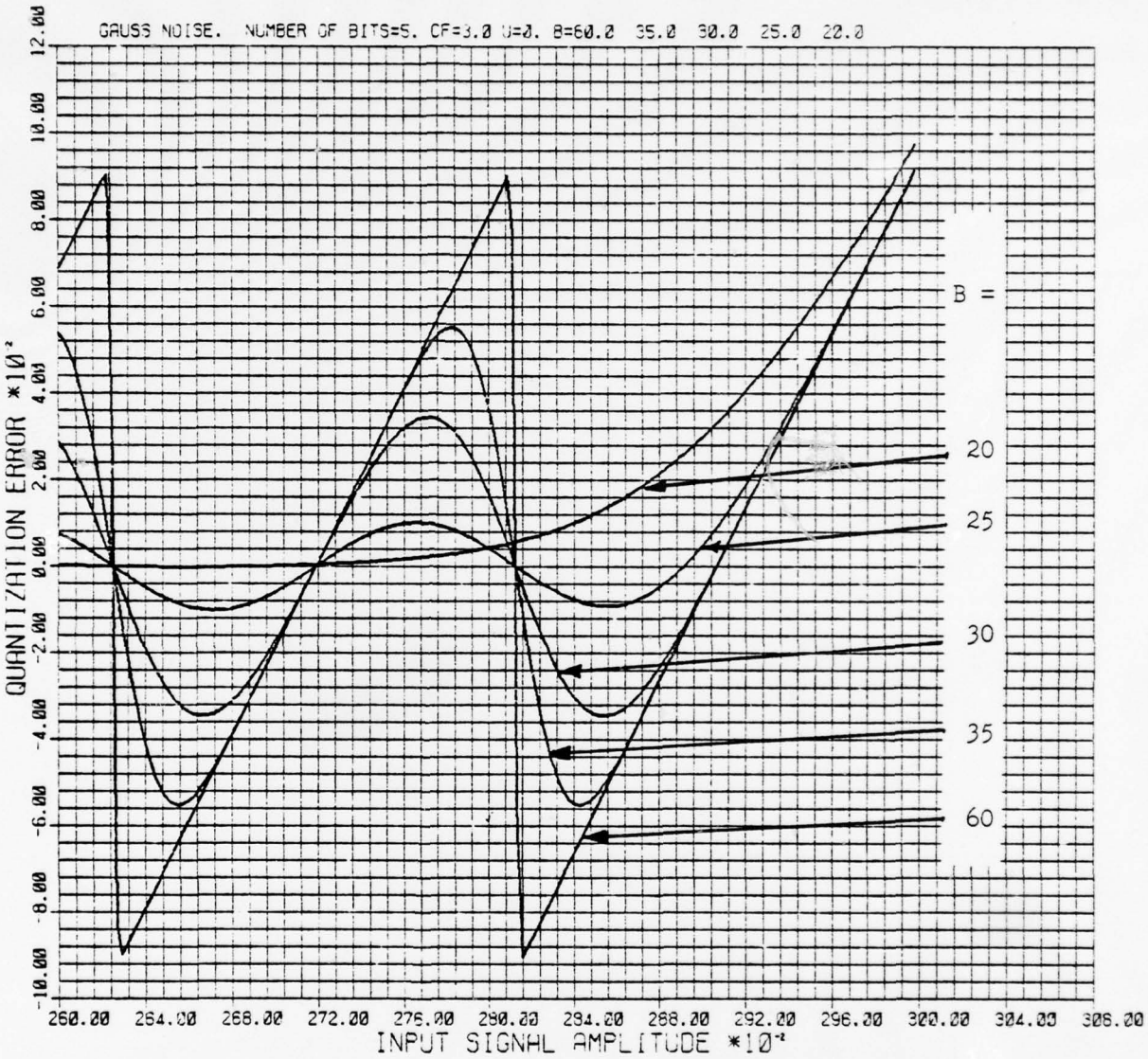

Figure 6-7. A Blow-up Of The Quantization Error Shown In Figure 6-6 Plus Additional Cases.

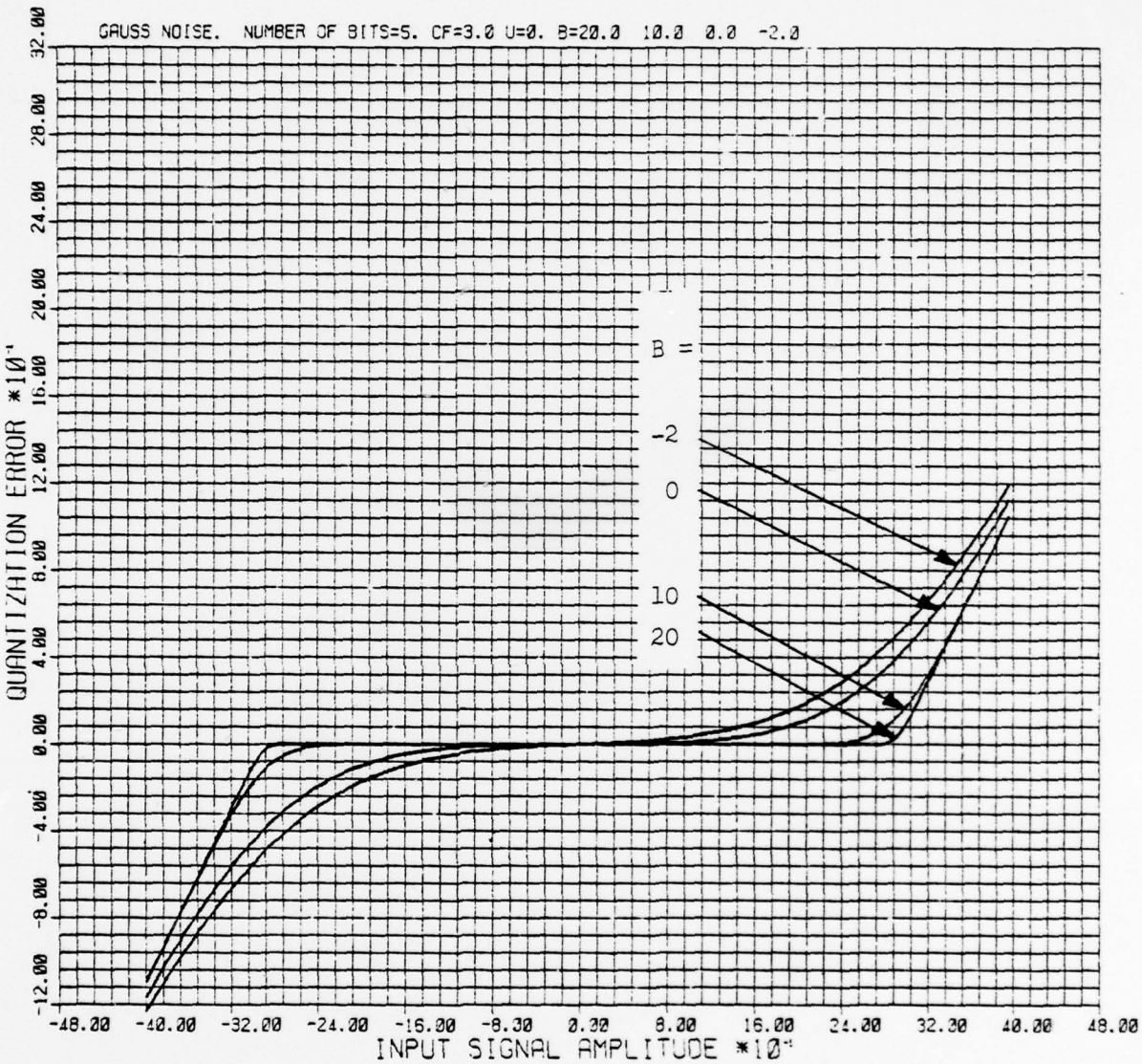

Figure 6-8. Quantization Error Versus Input Signal Amplitude For A 5 Bit A-D-A System With $\mu = 0$ And Crest Factor Of 3.

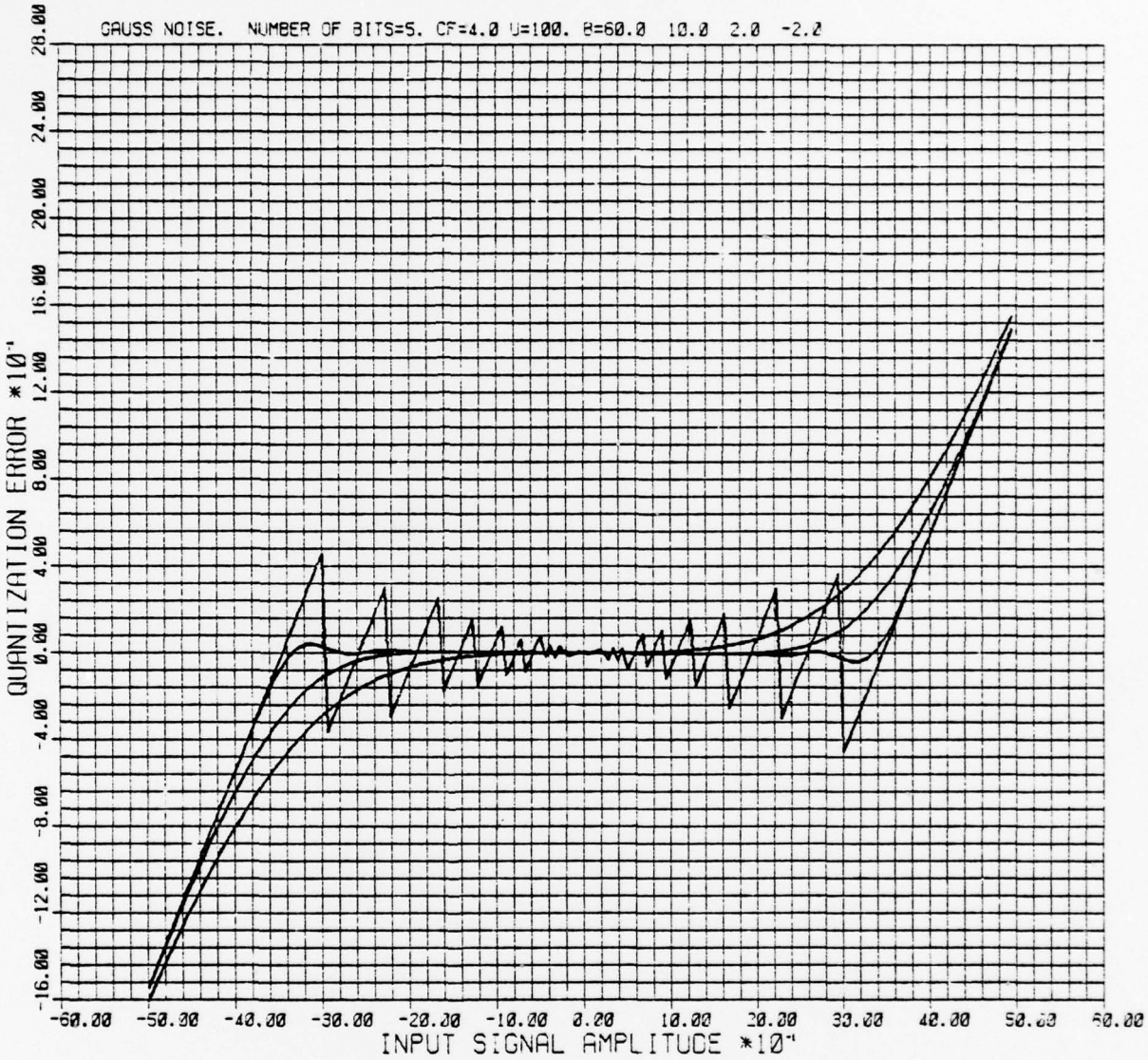

Figure 6-9. Quantization Error Versus Input Signal Amplitude For A 5 Bit A-D-A System With μ = 100 And A Crest Factor Of 4.

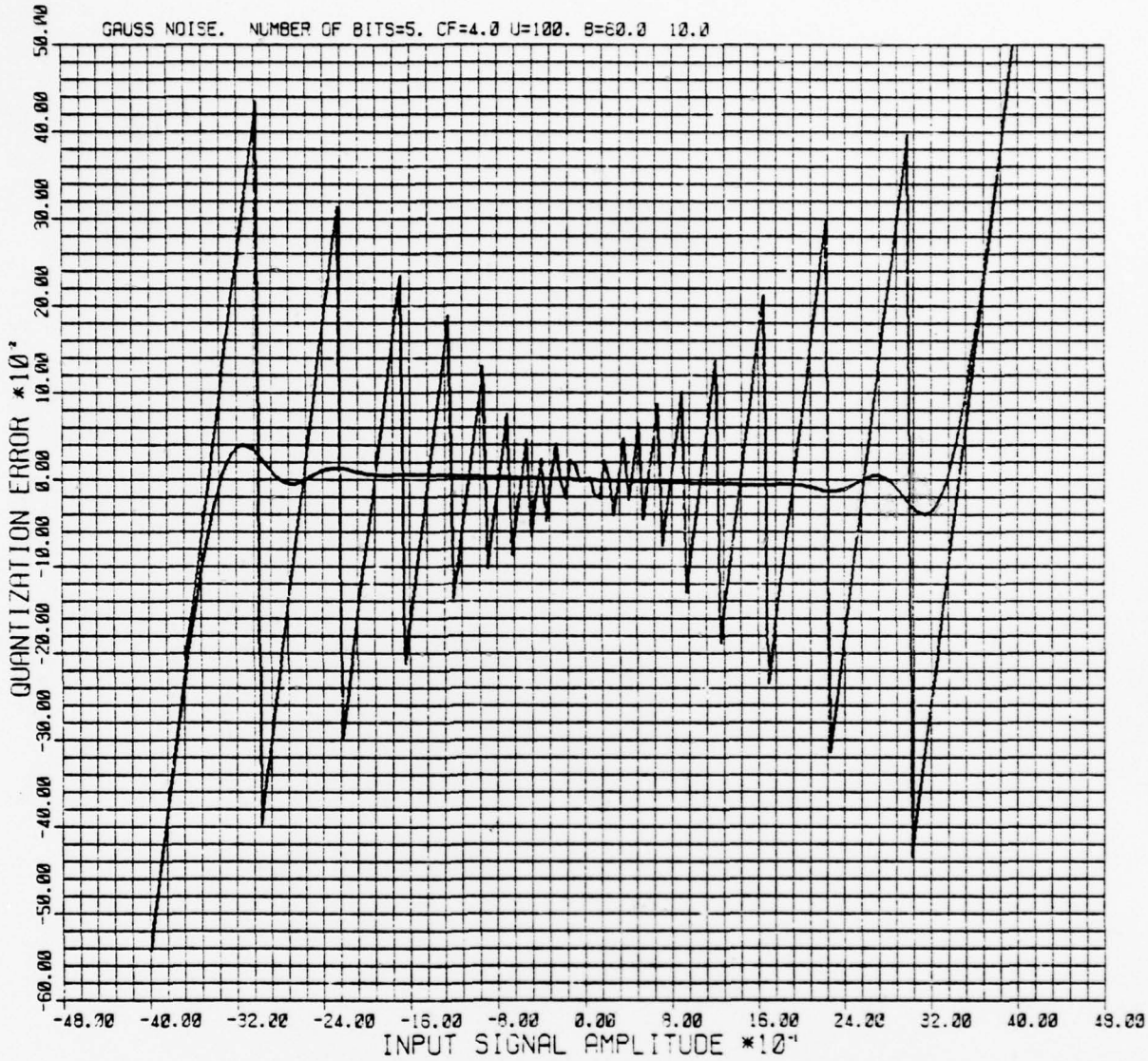

Figure 6-10. A Blow-up Of The Quantization Error Shown In Figure 6-9.

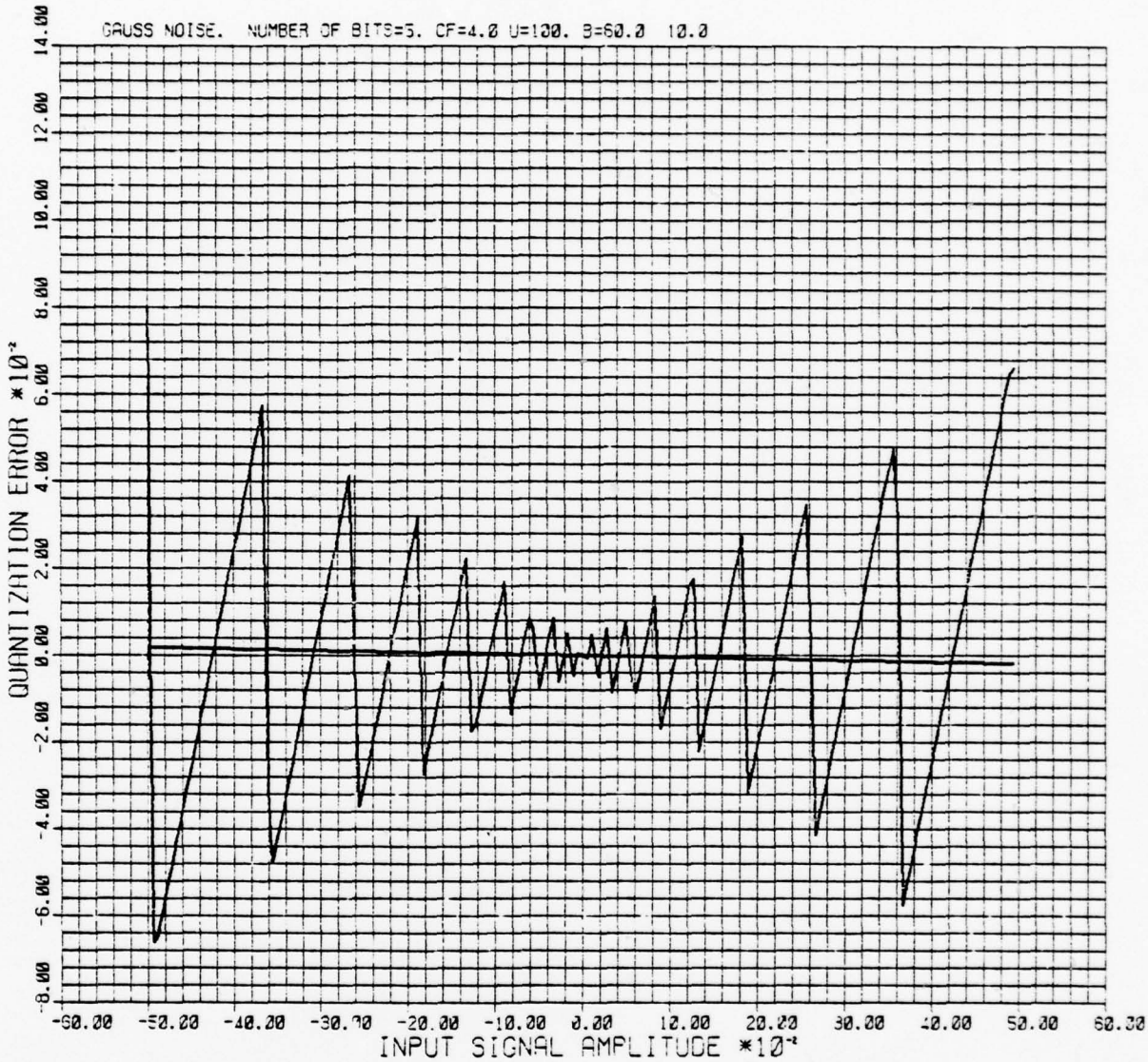

Figure 6-11. A Blow-up Of The Quantization Error Shown In Figure 6-10.

of 4. Observe that dither signals even eliminate contouring in nonlinearly companded A-D-A systems.

Return again to the linearly companded 5 bit case. In Figure 6-6 the quantization error is plotted for B = 20 dB and a crest factor of 3. Increasing the crest factor to 4 gives the curves shown in Figure 6-12. Observe the oscillation in the B = 20 dB curve. From equation (6-3) a 4/3 increase in crest factor implies a 2.5 dB decrease in B. Figure 6-13 shows the quantization error when B is decreased by 2.5 dB. As expected, the curves in Figures 6-6 and 6-13 have the same shape. Similarly, if the crest factor is increased to 15 and the value of B decreased by 14 dB, the curves shown in Figure 6-14 again have the same shape as those in Figure 6-6.

Thus, the use of dither signals is an effective method of eliminating contouring even in nonlinearly companded systems. However, because of the quadratic dependence of B on crest factor, practical applications are probably limited to linearly companded systems. In practice pseudorandom dither signals are used so that proper synchronization can be maintained.

3. Performance With Dither Signals

General formulas for arbitrary amplitude statistics are given in Appendix A and B for determining the performance of A-D-A systems using dither signals. In the following discussion only the Gaussian input signal y(t) with Gaussian dither signal r(t) case is considered. Equation (B-65) of Appendix B gives the relationship

$$SNR_y = SNR_T \left[1 - 1/B\right] \tag{6-4}$$

where

$$SNR_T = \frac{\sigma_s^2 + \sigma_r^2}{\sigma_q^2} \tag{6-5}$$

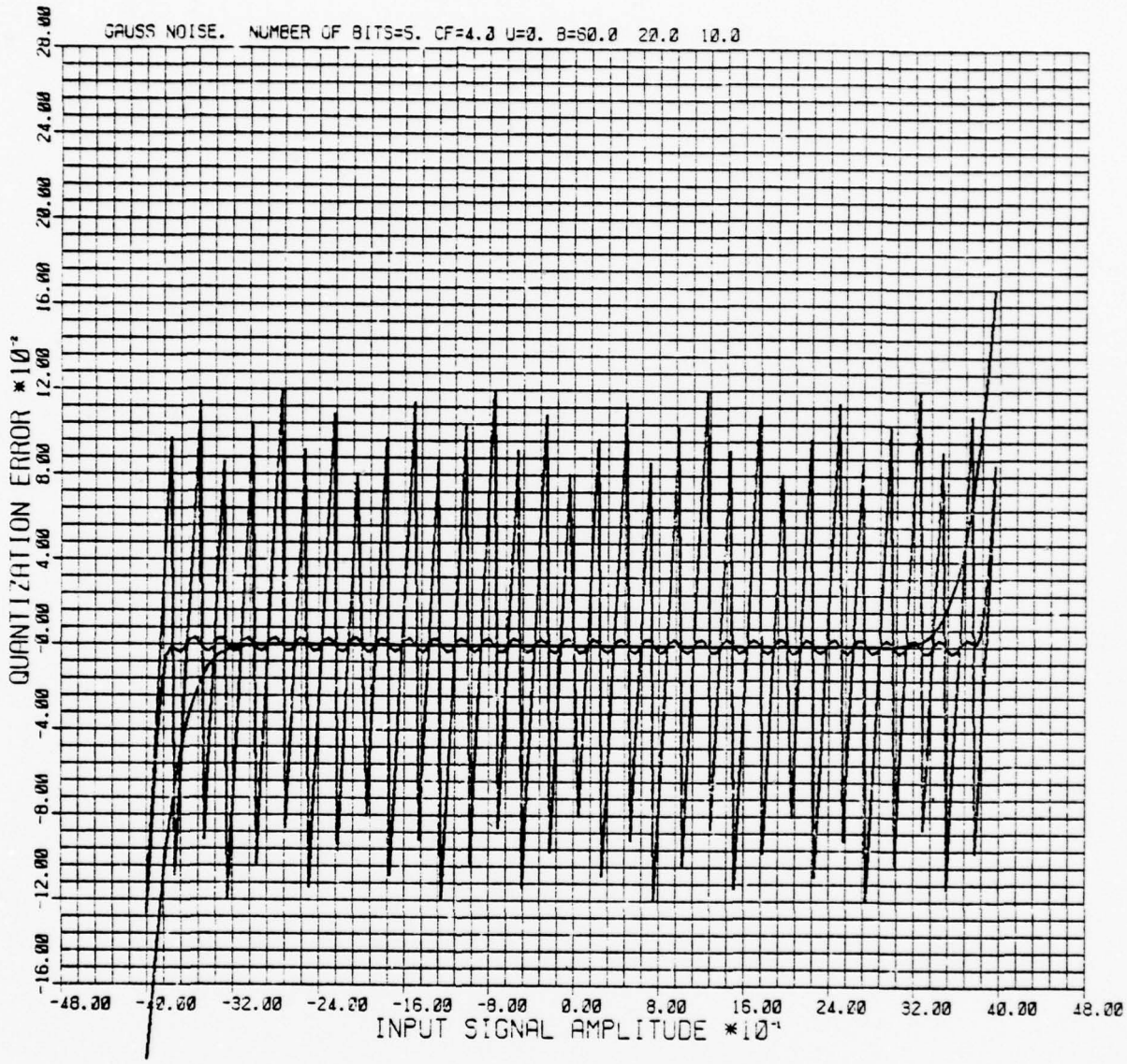

Figure 6-12. Quantization Error Versus Input Signal Amplitude For A 5 Bit A-D-A System With $\mu = 0$ And Crest Factor Of 4.

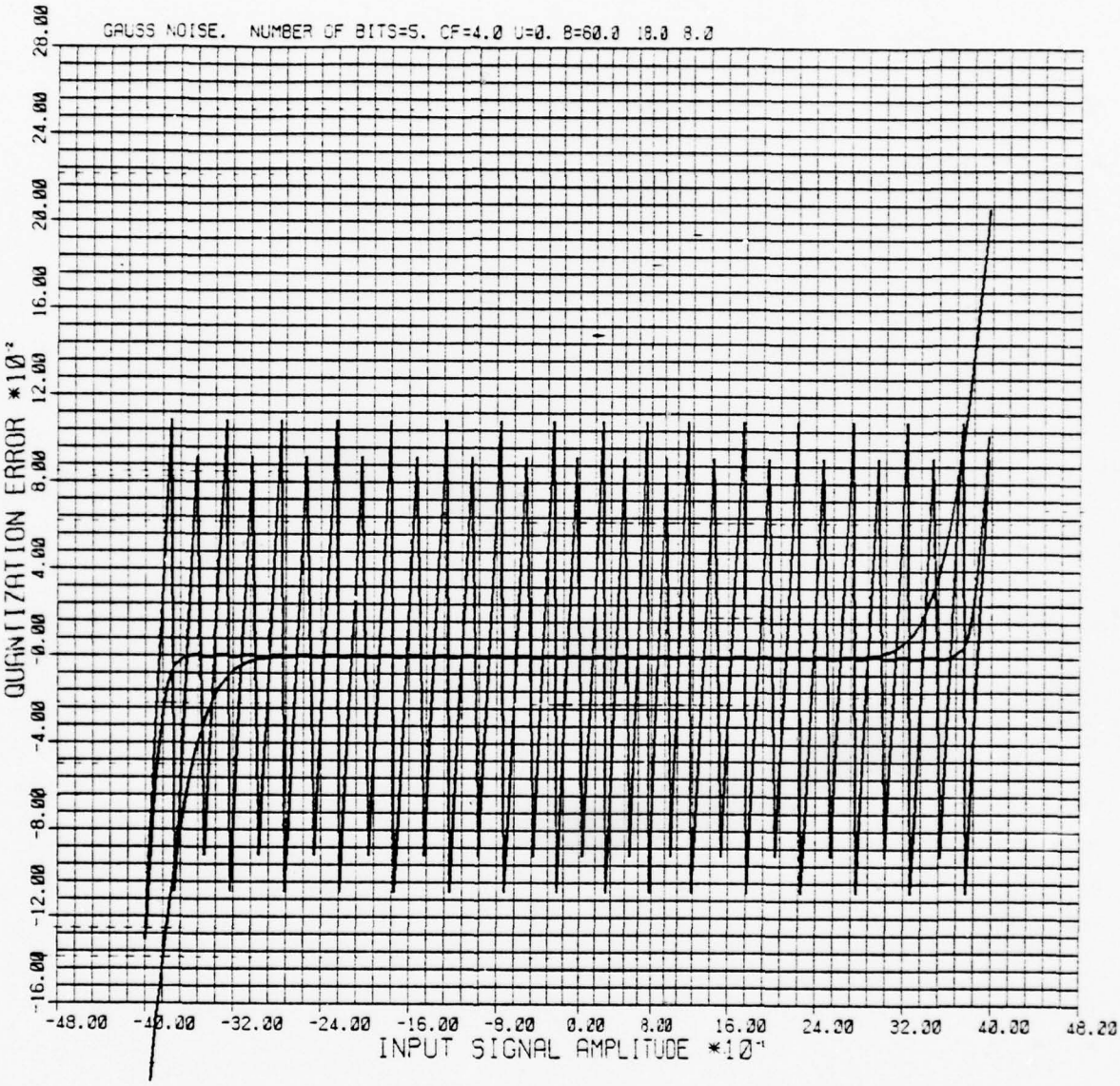

Figure 6-13. Same Case As Figure 6-12 Except The Values Of B Are 2.5 dB Less.

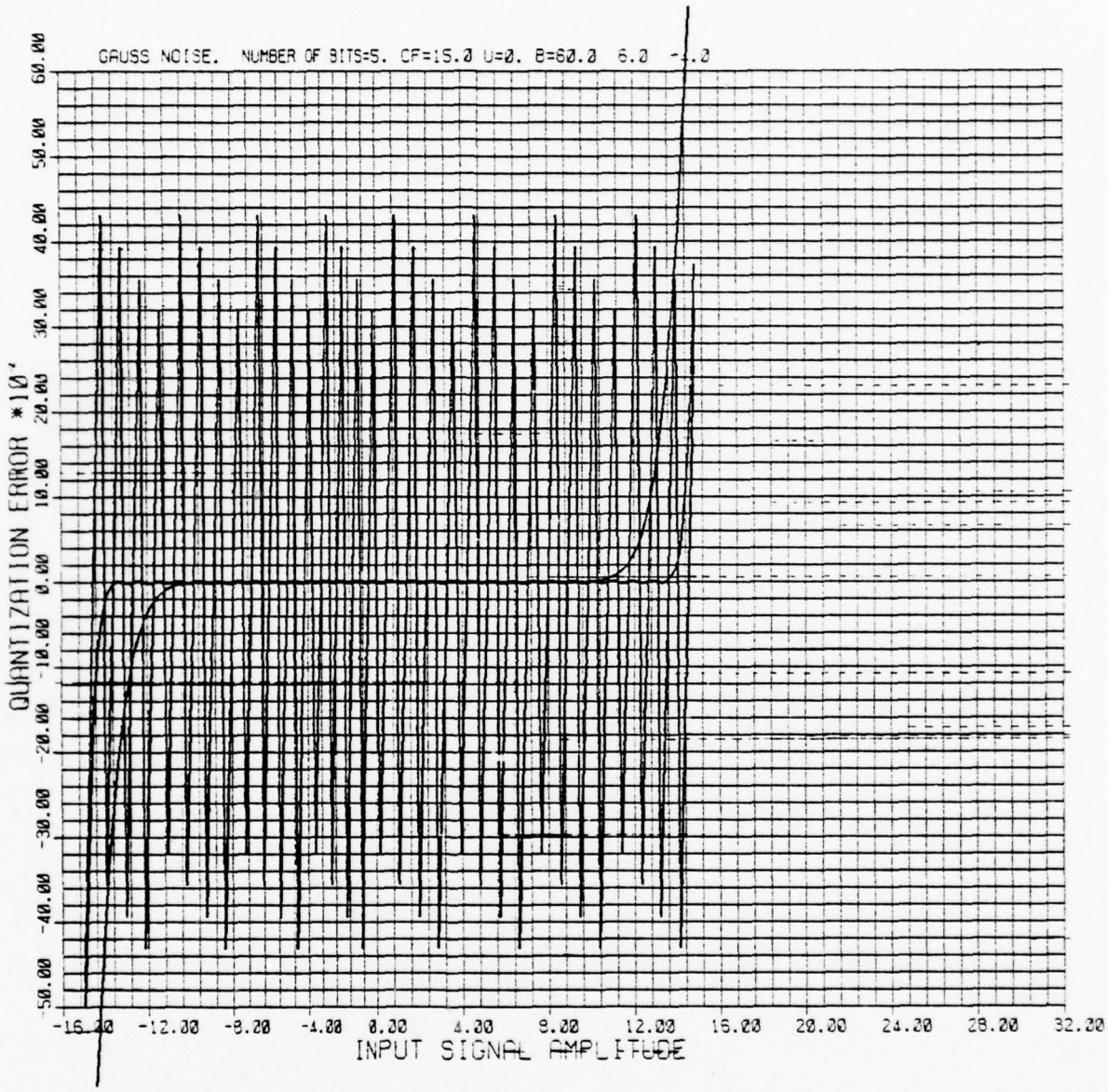

Figure 6-14. Quantization Error Versus Input Signal Amplitude For A 5 Bit A-D-A System With $\mu = 0$ And Crest Factor Of 15.

is the SNR determined from the design curves in Sections 3 and 4,

$$SNR_y = \frac{\sigma_s^2}{\sigma_q^2} \tag{6-6}$$

is the output SNR for the input signal y(t), and σ_q^2 is the quantization noise power. Observe that the degradation due to the use of dither signals is less than 0.5 dB for values of B greater than 10 dB.

4. Optimization With Dither Signals

Rather than adopting some rigid mathematical procedure for optimizing A-D-A systems with dither, our approach is purely practical. The objective in using dither signals is to eliminate contouring. Consequently, we choose a value of B such that the instantaneous quantization error is minimized over the values of input signal y(t) that are of interest. Considering again the 5 bit case with linear companding Table 6-1 gives a number of values for B as computed from equation (6-3). From Figures 6-6, 6-7, 6-8, 6-13, and 6-14, $(\sigma_r/E) = 0.5$ gives good results. This is an intuitively satisfying value. For this value

Table 6-1. Value For B With 5 Bits

(σ_r/E)	B(dB)		
	$\eta = 3$	$\eta = 4$	$\eta = 15$
1/16	38.62	36.12	24.64
1/8	32.60	30.10	18.62
1/4	26.58	24.08	12.60
1/2	20.56	18.06	6.58
1	14.54	12.04	0.56
3/2	11.02	8.52	- 2.96

equation (6-3) becomes

$$B = \frac{4^q}{\eta^2} \qquad (\sigma_r/E) = 0.5 \tag{6-7}$$

From this equation and the optimum crest factors given in Section 3, Table 6-2 gives approximately optimum values for B. These approximate optimums are verified in Figures 6-15 through 6-23 for the cases listed in Table 6-2. In specific applications, refinements in these optimums may be desirable.

Table 6-2. Approximate Optimum Values Of B

q	η	B(dB)
2	2.0	6.02
3	2.4	10.46
4	2.7	15.46
5	3.0	20.56
6	3.4	25.49
7	3.7	30.78
8	4.0	36.12
9	4.3	41.52
10	4.5	47.14

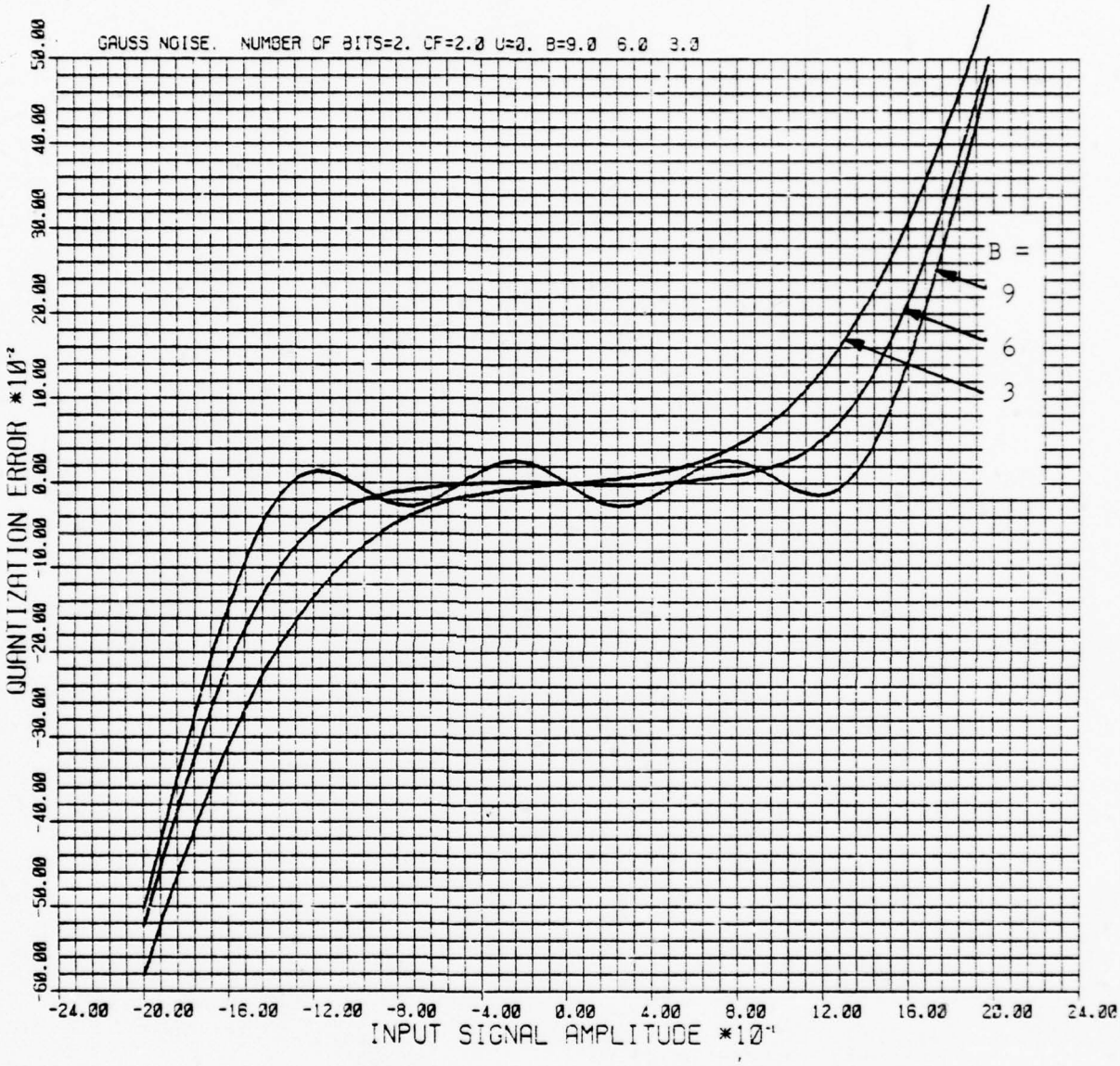

Figure 6-15. Quantization Error For 2 Bits.

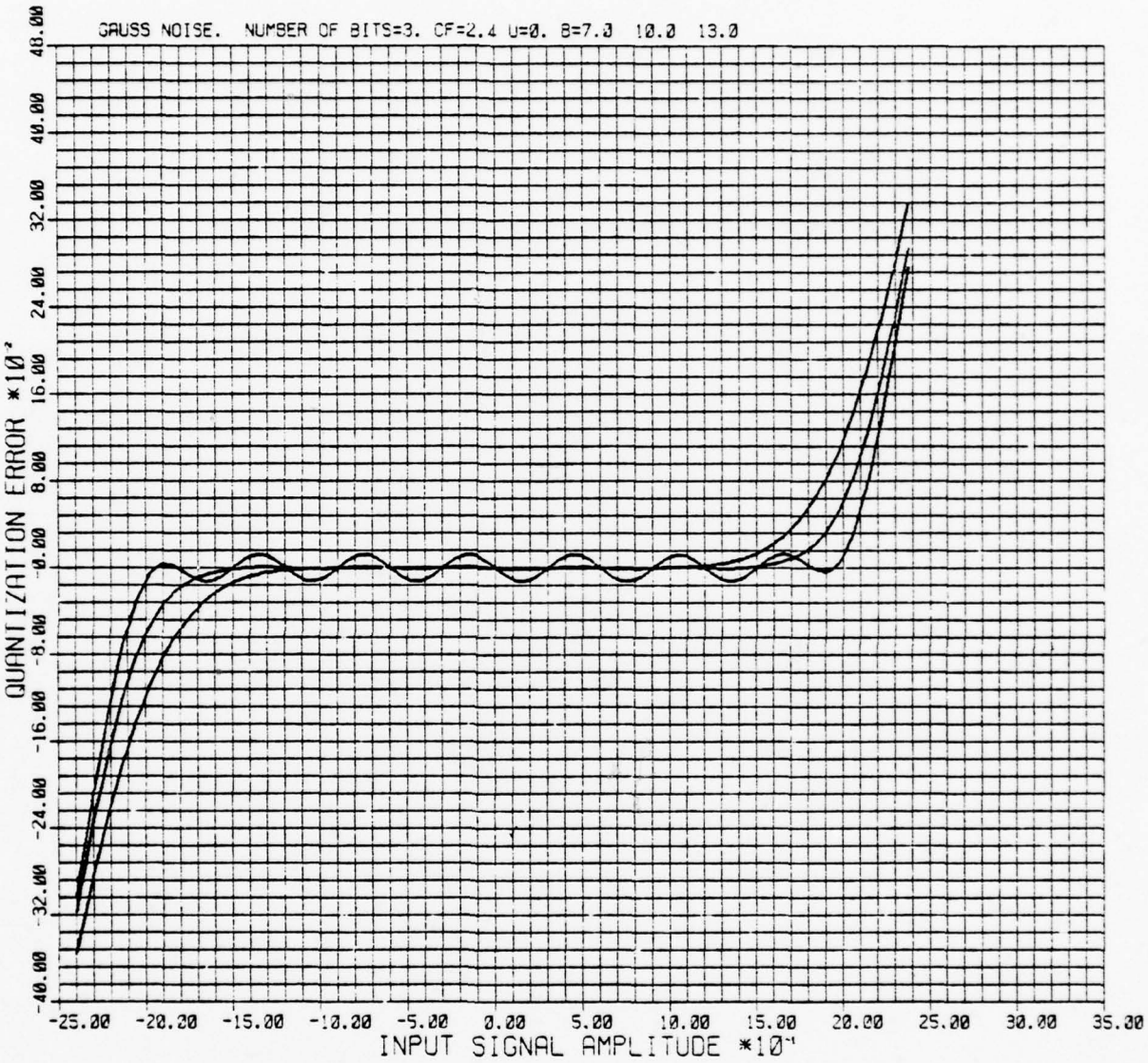

Figure 6-16. Quantization Error For 3 Bits.

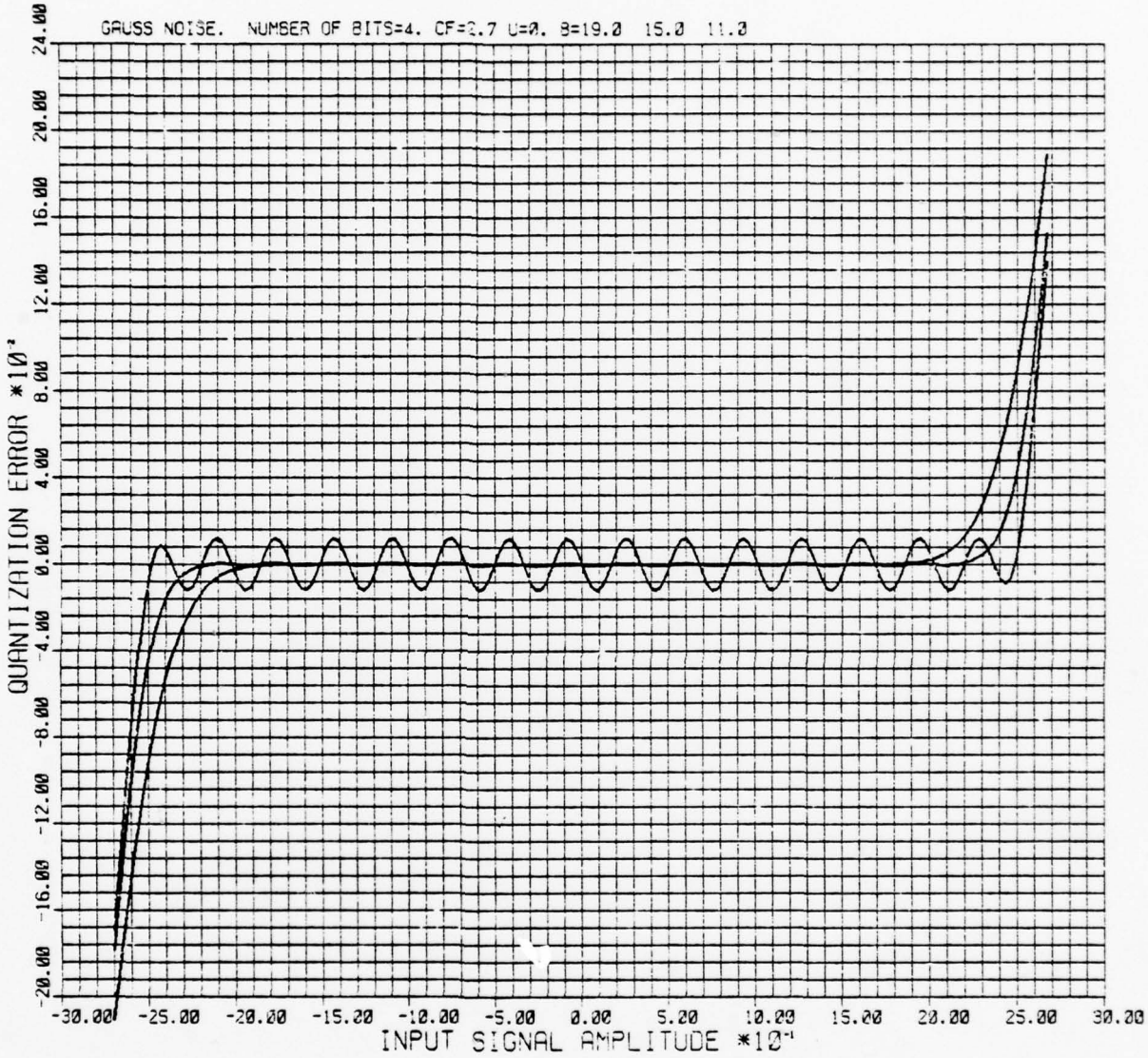

Figure 6-17. Quantization Error For 4 Bits.

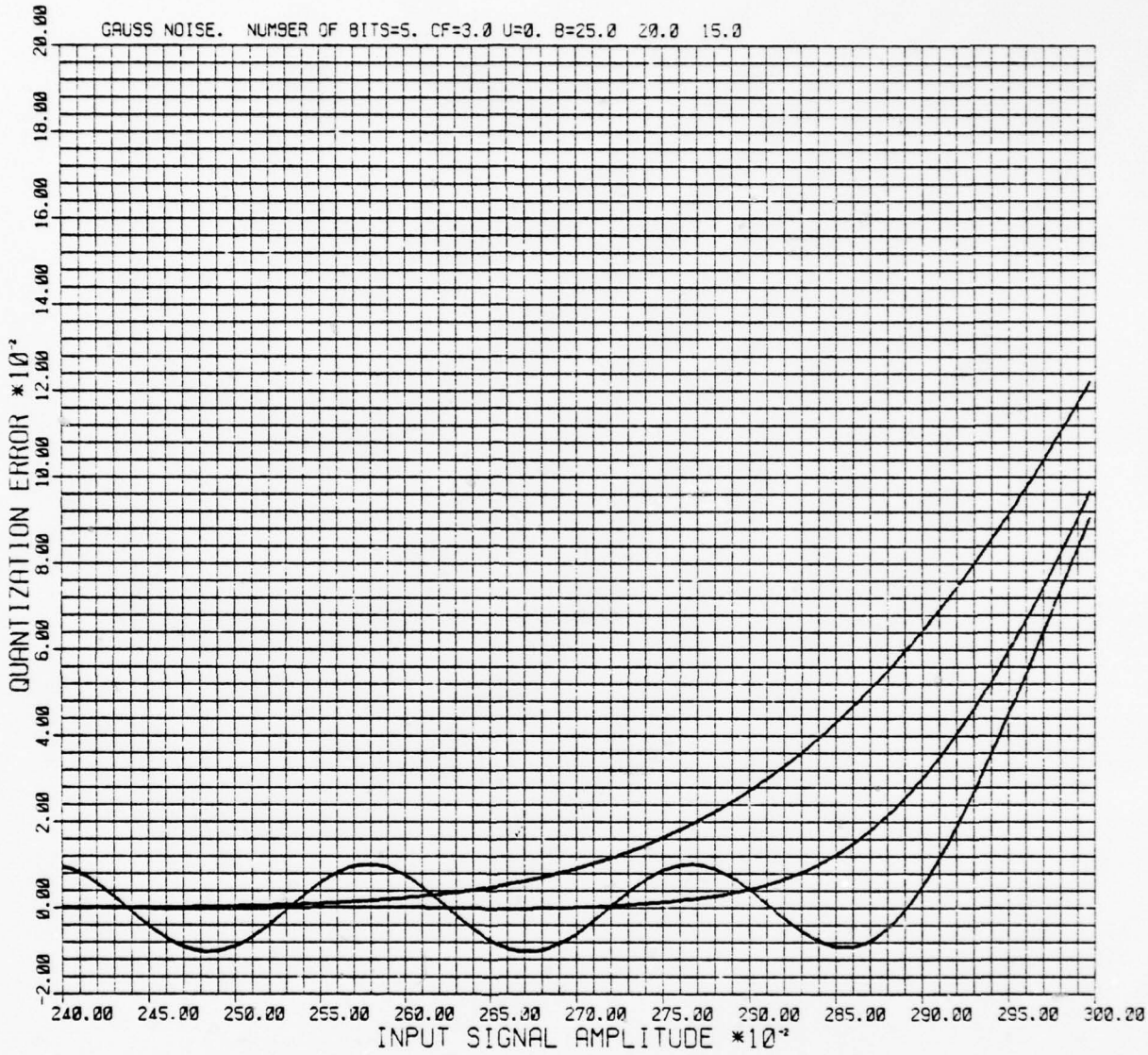

Figure 6-18. Quantization Error For 5 Bits.

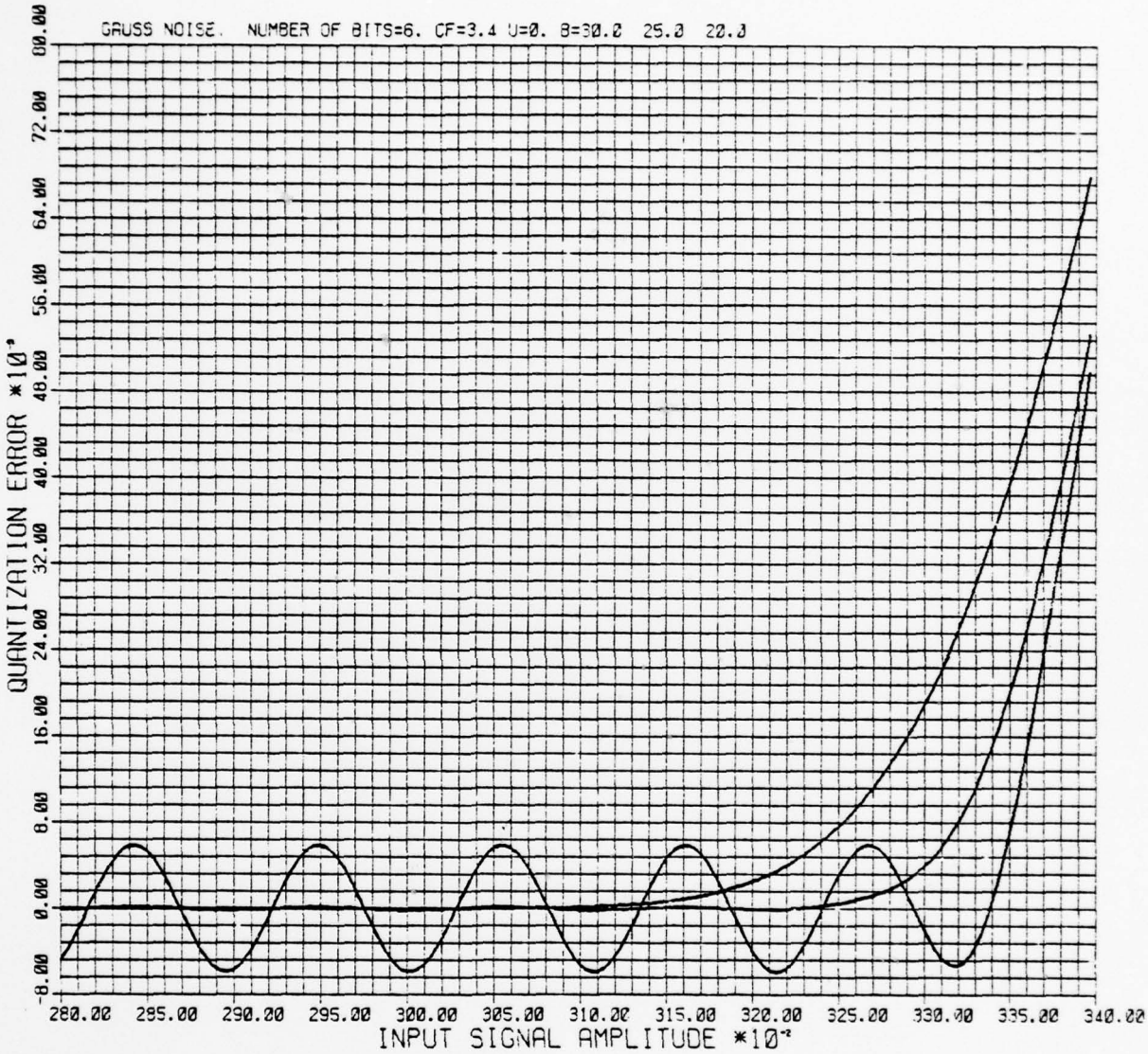

Figure 6-19. Quantization Error For 6 Bits.

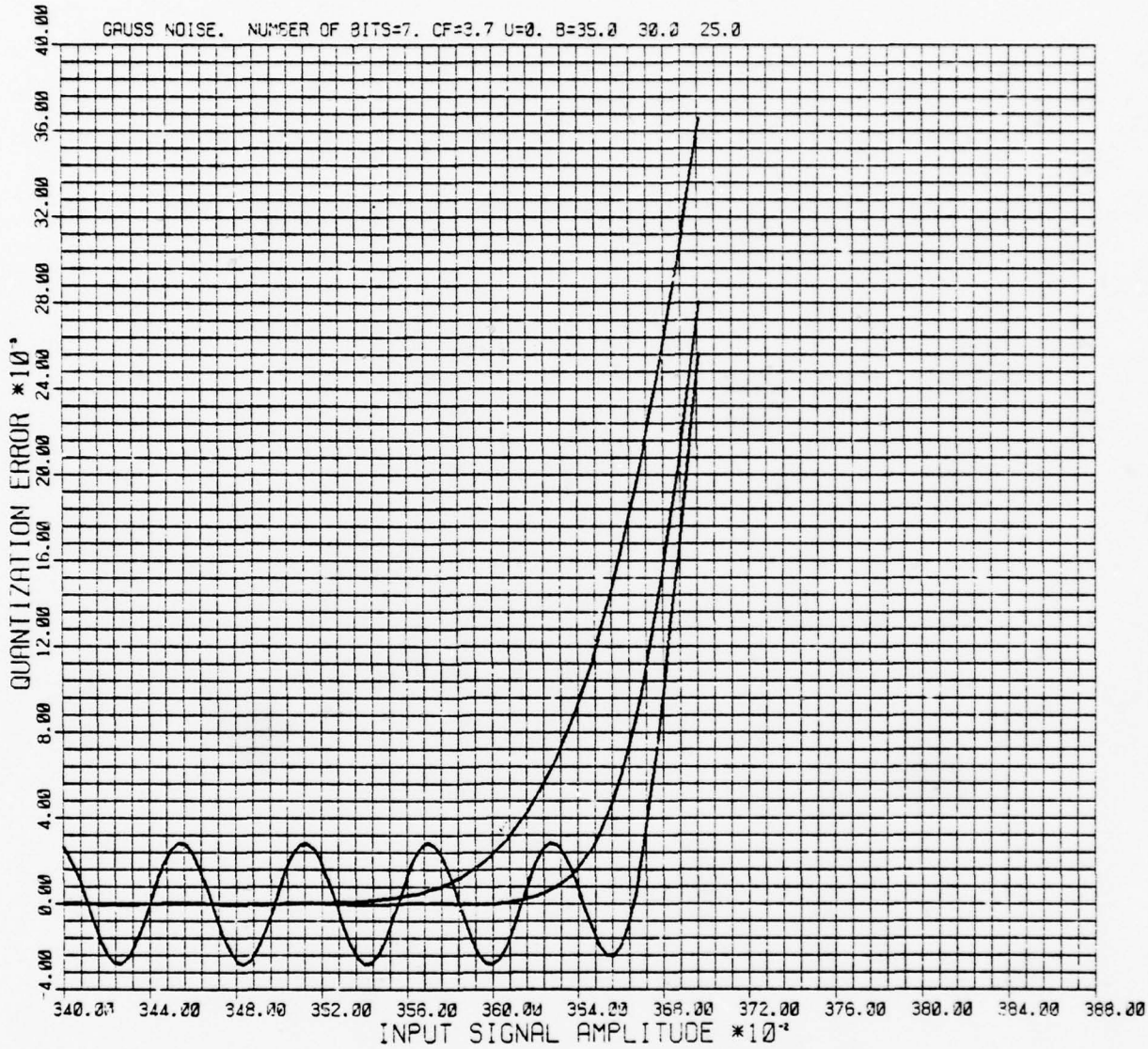

Figure 6-20. Quantization Error For 7 Bits.

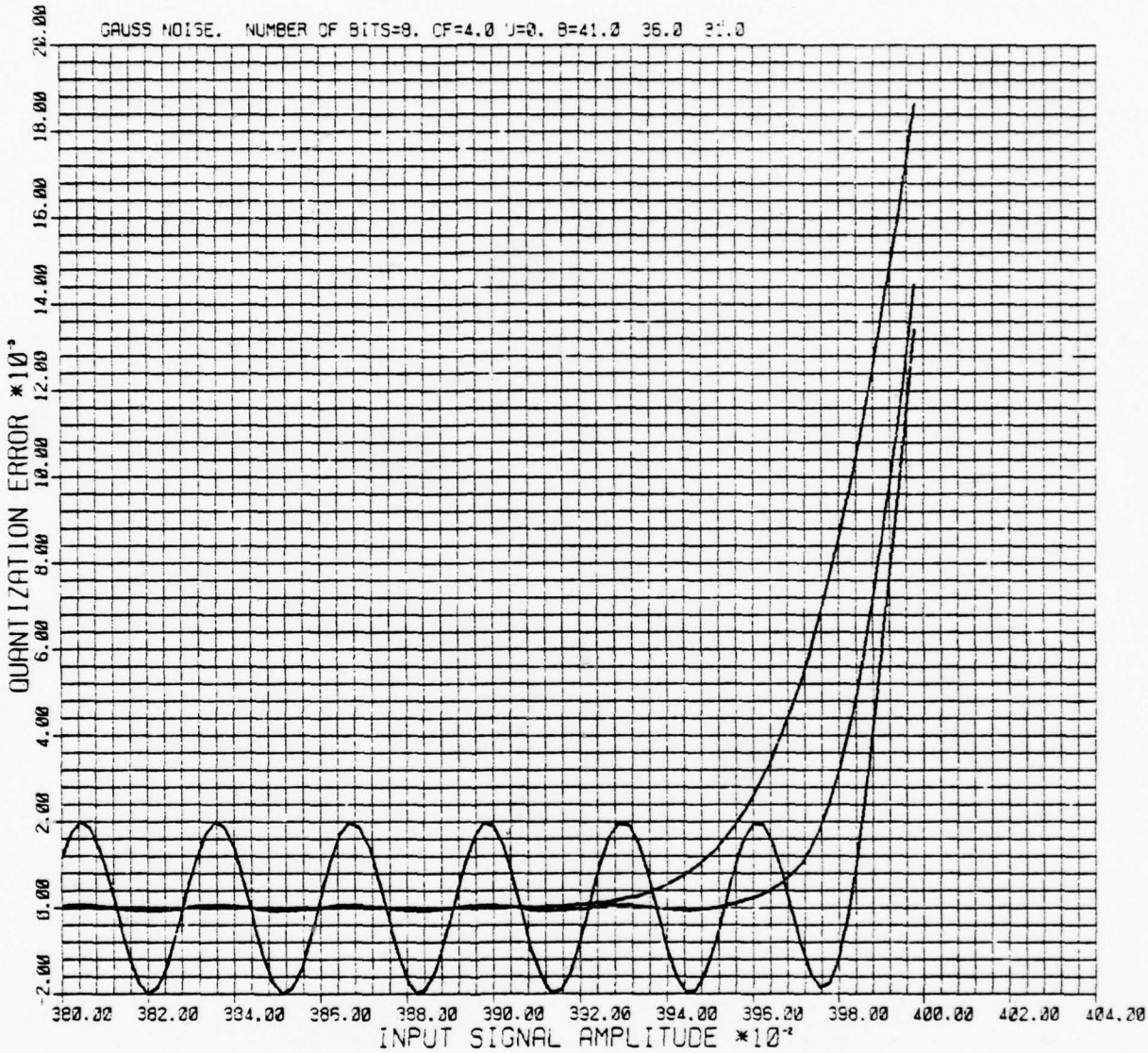

Figure 6-21. Quantization Error For 8 Bits.

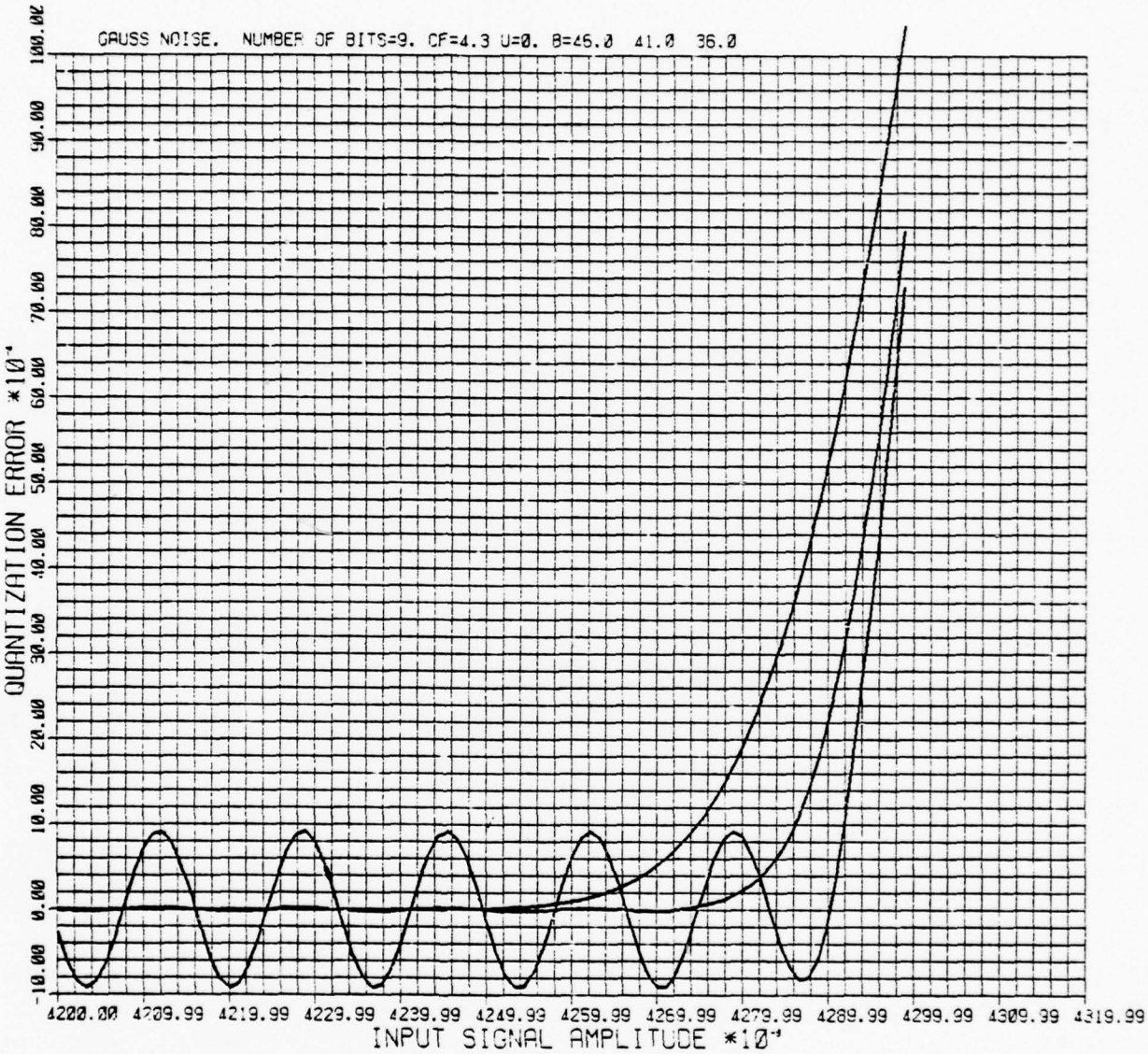

Figure 6-22. Quantization Error For 9 Bits.

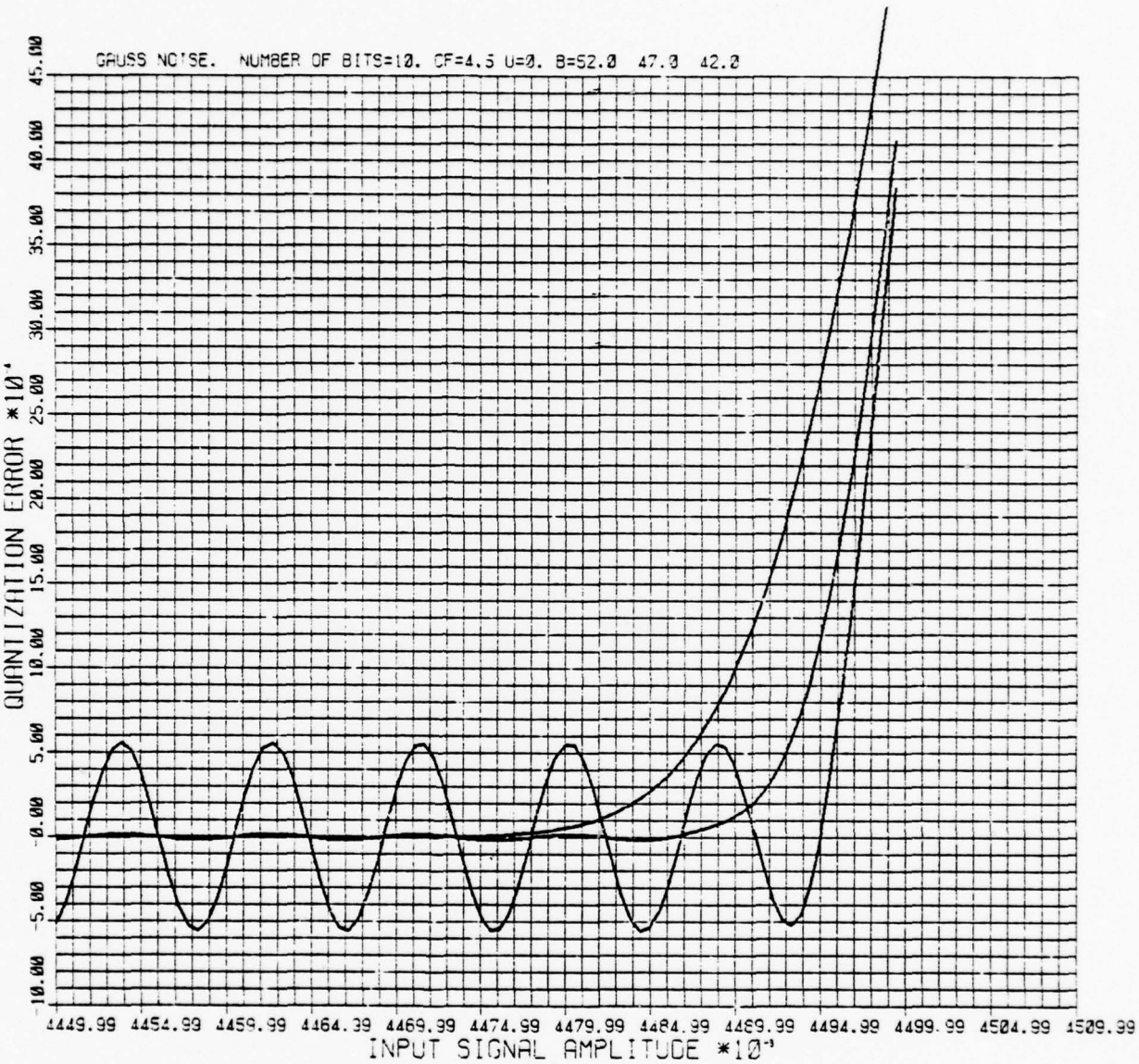

Figure 6-23. Quantization Error For 10 Bits.

APPENDIX A

DERIVATION OF QUANTIZATION NOISE FORMULAS

A1. Introduction

Equations describing the quantization noise power in A-D-A systems are derived in this appendix for Gaussian and Laplace amplitude statistics. The formulas are applicable to both linearly and nonlinearly companded systems and are suitable for programming on a calculator. In Section A2 a general equation is derived for the quantization noise power for arbitrary amplitude statistics. This result is specialized to the Gaussian and Laplace special cases in Sections A3 and A4, respectively. Section A5 then gives the equations for the quantizer steps for the linearly and logarithmically companded cases.

A2. Derivation of General Noise Formula

Define $y(t)$ to be the wide sense stationary process at the input to the A/D converter. Let $z(t)$ be the quantizer output defined by

$$z(t) = Z_n \qquad y(t) \in \left[Y_{n-1}, Y_n\right] \qquad n = 1,2,\cdots N \tag{A-1}$$

where the number of levels $N \geq 4$ is even,

$$Y_0 < Y_1 < \cdots < Y_{N-1} < Y_N, \quad \text{and} \quad Z_1 < Z_2 < \cdots < Z_{N-1} < Z_N$$

as shown in Figure A1. Define $Y_0 = -\infty$, $Y_{N/2} = 0$, $Y_N = \infty$, and assume the symmetry relationships

$$Y_n = -Y_{N-n} \qquad n = 1,2,\cdots \frac{N}{2} - 1 \tag{A-2}$$

$$Z_n = -Z_{N-n+1} \qquad n = 1,2,\cdots N \tag{A-3}$$

These assumptions are consistent with nearly every manufactured A/D converter. Also define $f(y)$ to be the probability density function for $y(t)$ and assume that $f(y)$ is an even function, i.e.,

$$f(-y) = f(y) \tag{A-4}$$

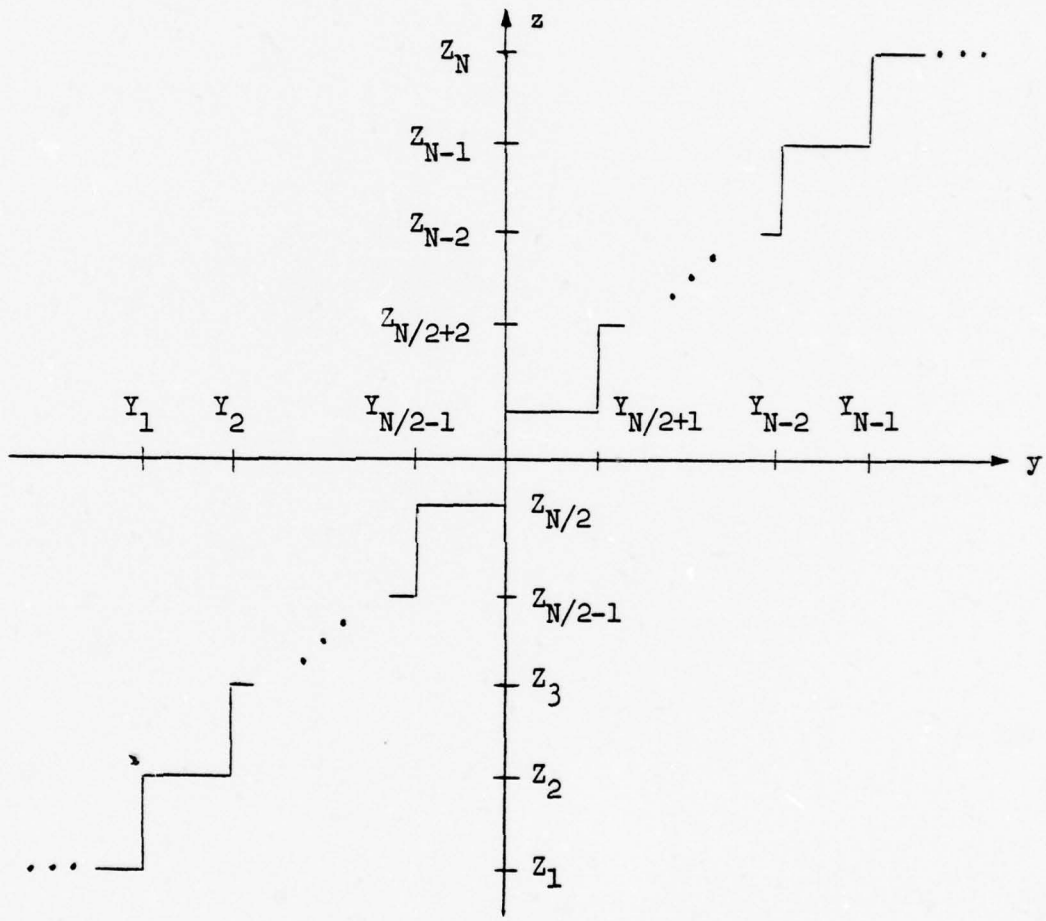

FIGURE A1. QUANTIZER CHARACTERISTIC

This is consistent with assuming y(t) is a zero mean process and the A/D converter is bipolar as shown in Figure A1. Define σ^2 to be the variance of the input y(t).

$$\sigma^2 = E\{y^2(t)\} = \int_{-\infty}^{\infty} y^2 f(y)dy \tag{A-5}$$

Then the quantization noise power is given by*

$$\sigma_q^2 = E\{[y(t) - z(t)]^2\} = \sum_{n=1}^{N} \int_{Y_{n-1}}^{Y_n} [y - Z_n]^2 f(y)dy \tag{A-6}$$

Define the following functions

$$F_0(y/\sigma) = \int_{-\infty}^{y/\sigma} \sigma f(\sigma x)dx = \int_{-\infty}^{y} f(x)dx \tag{A-7}$$

$$F_1(y/\sigma) = \int_{-\infty}^{y/\sigma} \sigma x f(\sigma x)dx = \frac{1}{\sigma}\int_{-\infty}^{y} x f(x)dx \tag{A-8}$$

$F_0(y/\sigma)$ is related to the distribution function associated with the probability density function f(y) and $F_1(y/\sigma)$ is the partial first moment of $y(t)/\sigma$. The below derivation expresses the quantization noise power given by (A-6) in terms of these functions.

Expanding (A-6) and applying definitions (A-7) and (A-8) yields

---

*See equation (2-73) of: J. F. Holland, Statistical Analysis of Analog-Digital-Analog Systems, Ph.D. dissertation, Stanford University, March 1974.

$$\sigma_q^2 = \sigma^2 \left\{ 1 - 2 \sum_{n=1}^{N} \left(\frac{Z_n}{\sigma}\right) \frac{1}{\sigma} \int_{Y_{n-1}}^{Y_n} y f(y) dy \right.$$

$$\left. + \sum_{n=1}^{N} \left(\frac{Z_n}{\sigma}\right)^2 \int_{Y_{n-1}}^{Y_n} f(y) dx \right\}$$

$$= \sigma^2 \left\{ 1 - 2 \sum_{n=1}^{N} \left(\frac{Z_n}{\sigma}\right) \left[F_1\left(\frac{Y_n}{\sigma}\right) - F_1\left(\frac{Y_{n-1}}{\sigma}\right) \right] \right.$$

$$\left. + \sum_{n=1}^{N} \left(\frac{Z_n}{\sigma}\right)^2 \left[F_0\left(\frac{Y_n}{\sigma}\right) - F_0\left(\frac{Y_{n-1}}{\sigma}\right) \right] \right\} \qquad \text{(A-9)}$$

Elimination of the terms containing Y_0 and Y_N gives

$$\frac{\sigma_q^2}{\sigma^2} = 1 + \sum_{n=1}^{N-1} \left(\frac{Z_n}{\sigma}\right)^2 F_0\left(\frac{Y_n}{\sigma}\right) - \sum_{n=1}^{N-1} \left(\frac{Z_{n+1}}{\sigma}\right)^2 F_0\left(\frac{Y_n}{\sigma}\right) + \left(\frac{Z_N}{\sigma}\right)^2$$

$$-2 \sum_{n=1}^{N-1} \left(\frac{Z_n}{\sigma}\right) F_1\left(\frac{Y_n}{\sigma}\right) + 2 \sum_{n=1}^{N-1} \left(\frac{Z_{n+1}}{\sigma}\right) F_1\left(\frac{Y_n}{\sigma}\right)$$

$$= 1 + \left(\frac{Z_n}{\sigma}\right)^2 - \sum_{n=1}^{N-1} \left[\left(\frac{Z_{n+1}}{\sigma}\right)^2 - \left(\frac{Z_n}{\sigma}\right)^2 \right] F_0\left(\frac{Y_n}{\sigma}\right)$$

$$+2 \sum_{n=1}^{N-1} \left[\left(\frac{Z_{n+1}}{\sigma}\right) - \left(\frac{Z_n}{\sigma}\right) \right] F_1\left(\frac{Y_n}{\sigma}\right) \qquad \text{(A-10)}$$

Using the symmetry conditions and the properties of even and odd functions, (A-10) may be manipulated into the form

$$\frac{\sigma_q^2}{\sigma^2} = 1 + \left(\frac{Z_N}{\sigma}\right)^2 - 2 \sum_{n=1}^{N/2-1} \left[\left(\frac{Z_{n+1}}{\sigma}\right)^2 - \left(\frac{Z_n}{\sigma}\right)^2\right] F_0\left(\frac{Y_n}{\sigma}\right)$$

$$- \sum_{n=N/2+1}^{N-1} \left[\left(\frac{Z_{n+1}}{\sigma}\right)^2 - \left(\frac{Z_n}{\sigma}\right)^2\right]$$

$$+ 4 \sum_{n=1}^{N/2-1} \left[\left(\frac{Z_{n+1}}{\sigma}\right) - \left(\frac{Z_n}{\sigma}\right)\right] F_1\left(\frac{Y_n}{\sigma}\right)$$

$$+ 2 \left[\left(\frac{Z_{N/2+1}}{\sigma}\right) - \left(\frac{Z_{N/2}}{\sigma}\right)\right] F_1(0)$$

$$= 1 + \left(\frac{Z_{N/2}}{\sigma}\right)^2 - 2 \sum_{n=1}^{N/2-1} \left[\left(\frac{Z_{n+1}}{\sigma}\right)^2 - \left(\frac{Z_n}{\sigma}\right)^2\right] F_0\left(\frac{Y_n}{\sigma}\right)$$

$$+ 4 \sum_{n=1}^{N/2-1} \left[\left(\frac{Z_{n+1}}{\sigma}\right) - \left(\frac{Z_n}{\sigma}\right)\right] F_1\left(\frac{Y_n}{\sigma}\right) - 4 \left(\frac{Z_{N/2}}{\sigma}\right) F_1(0) \tag{A-11}$$

Equation (A-11) is the desired formula.

Similarly, the correlation between the input y(t) and the quantization noise is

$$\xi = \frac{E\{y(t)\left[y(t)-z(t)\right]\}}{\sigma^2} = \frac{1}{\sigma^2} \sum_{n=1}^{N} \int_{Y_{n-1}}^{Y_n} y\left[y-Z_n\right] f(y)dy$$

$$= 1 - \sum_{n=1}^{N} \left(\frac{Z_n}{\sigma}\right)\left[F_1\left(\frac{Y_n}{\sigma}\right) - F_1\left(\frac{Y_{n-1}}{\sigma}\right)\right]$$

$$= 1 - 2\left(\frac{Z_{N/2}}{\sigma}\right) F_1(0)$$

$$+ 2 \sum_{n=1}^{N/2-1} \left[\left(\frac{Z_{n+1}}{\sigma}\right) - \left(\frac{Z_n}{\sigma}\right)\right] F_1\left(\frac{Y_n}{\sigma}\right) \qquad \text{(A-12)}$$

Equations (A-11) and (A-12) are in a useful form for computer evaluation.

A3. Formulas for Gaussian Amplitude Statistics

In the case of Gaussian amplitude statistics, the probability density function is

$$f(y) = \frac{1}{\sqrt{2\pi}\,\sigma} \exp\left(-y^2/2\sigma^2\right) \tag{A-13}$$

By direct integration

$$F_0\,(y/\sigma) = \tfrac{1}{2}\left[1 + \operatorname{erf}\left(y/\sqrt{2}\,\sigma\right)\right] \tag{A-14}$$

and

$$F_1\,(y/\sigma) = -\frac{1}{\sqrt{2\pi}} \exp\left(-y^2/2\sigma^2\right) \tag{A-15}$$

where erf ( ) is the error function.

Furthermore, it can be shown in the case of Gaussian amplitude statistics that the crosscorrelation between the input y(t) and the quantization noise is*

$$\begin{aligned} R_{yq}(\tau) &= E\{y(t+\tau)\left[y(t)-z(t)\right]\} \\ &= \xi\, R_{yy}\,(\tau) \end{aligned} \tag{A-16}$$

where $R_{yy}\,(\tau)$ is the autocorrelation function of the input

$$R_{yy}(\tau) = E\{y(t+\tau)\; y(t)\} \tag{A-17}$$

and ξ is given by (A-12).

---

*See equation (2-168) of: J. F. Holland, Statistical Analysis of Analog-Digital-Analog Systems, Ph.D. dissertation, Stanford University, March 1974.

A4. Formulas for Laplace Amplitude Statistics

In the case of Laplacian amplitude statistics, the probability density function is

$$f(y) = \frac{1}{\sqrt{2}\,\sigma} \exp\left(-\sqrt{2}\,|y|/\sigma\right) \tag{A-18}$$

By direct integration

$$F_0(y/\sigma) = \tfrac{1}{2} \exp\left(\sqrt{2}\,y/\sigma\right) \qquad y < 0 \tag{A-19}$$

and

$$F_1(y/\sigma) = \frac{1}{2\sqrt{2}} \exp\left(\sqrt{2}\,y/\sigma\right)\left[\sqrt{2}\left(\frac{y}{\sigma}\right) - 1\right] \qquad y < 0 \tag{A-20}$$

A5. A/D Converter Transition and Output Values

The final set of formulas for evaluating the quantization noise power are those for the transitions $\langle Y_n \rangle$ and those for the outputs $\langle Z_n \rangle$. Define the crest factor (peak to RMS ratio) to be

$$\eta = \frac{V}{\sigma} \tag{A-21}$$

where 2V is the peak to peak quantization range. In the case of uniform quantization (linear companding) the transitions and outputs are

$$Y_n = \frac{(2n-N)}{N} V \qquad n = 1,2,\cdots N-1 \tag{A-22}$$

$$Z_n = \frac{(2n-1-N)}{N} V \qquad n = 1,2,\cdots N \tag{A-23}$$

Hence,

$$\frac{Y_n}{\sigma} = \eta \frac{(2n-N)}{N} \qquad n = 1,2,\cdots N-1 \tag{A-24}$$

$$\frac{Z_n}{\sigma} = \eta \frac{(2n-1-N)}{N} \qquad n = 1,2,\cdots N \tag{A-25}$$

Observe that these formulas have the symmetry properties discussed in Section A2.

The effect of compressing the input prior to A/D conversion and subsequently expanding the output of the D/A converter can be represented by expanding the transitions $\langle Y_n \rangle$ and the outputs $\langle Z_n \rangle$ with the corresponding companding law. In logarithmic companding the compression law is given by

$$y(t) = \begin{cases} V \dfrac{\ln\left[1 + \mu\, x(t)/V\right]}{\ln\left[1 + \mu\right]} & x(t) \geq 0 \\[2ex] -V \dfrac{\ln\left[1 - \mu\, x(t)/V\right]}{\ln\left[1 + \mu\right]} & x(t) \leq 0 \end{cases} \tag{A-26}$$

where μ is the compression factor.

Observe that in the limit as μ goes to zero

$$\lim_{\mu \to 0} y(t) = x(t) \tag{A-27}$$

The corresponding expansion law is obtained by solving (A-26) for x(t).

$$x(t) = \begin{cases} \frac{V}{\mu}\left([1+\mu]^{y(t)/V} - 1\right) & y(t) \geq 0 \\ -\frac{V}{\mu}\left([1+\mu]^{-y(t)/V} - 1\right) & y(t) \leq 0 \end{cases} \tag{A-28}$$

Hence, the transitions and outputs are given by

$$\frac{Y_n}{\sigma} = -\frac{n}{\mu}\left([1+\mu]^{-(2n-N)/N} - 1\right) \qquad n=1,2,\cdots\frac{N}{2}-1 \tag{A-29}$$

$$\frac{Z_n}{\sigma} = -\frac{n}{\mu}\left([1+\mu]^{-(2n-1-N)/N} - 1\right) \qquad n=1,2,\cdots\frac{N}{2} \tag{A-30}$$

for logarithmic companding.

APPENDIX B

EFFECT OF DITHER SIGNALS IN A-D-A SYSTEMS

B1. INTRODUCTION

Equations describing the effect of dither signals on the quantization error power in A-D-A systems are derived in this appendix for arbitrary amplitude statistics. The formulas are applicable to both linearly and nonlinearly companded systems.

Figure B1 shows an A-D-A system with dither signals. Process r(t) is the input dither signal and s(t) is the output dither signal. In the classical case r(t) and s(t) are identical and small in power compared to input y(t). In general the dither signals might be unwanted signals received with y(t) or corrupting the A-D-A system output z(t). An example is A/D and D/A level error noises.

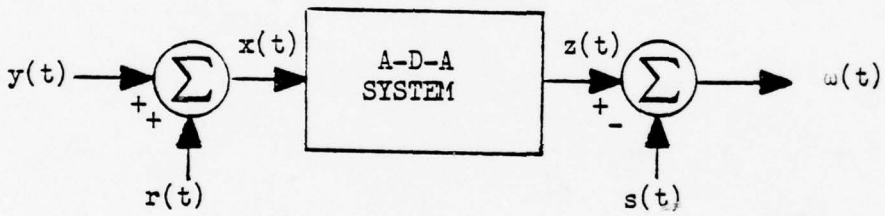

Figure B1. A-D-A System with Dither Signals

The below analysis is applicable to all these cases.

The analysis problem is formulated in Section B2. The cases of independent dithers and identical dithers are examined in Sections B3 and B4. Then the equations are put in a form for computer evaluation in the case of an odd symmetric quantizer in Sections B5 and B6.

B2. PROBLEM FORMULATION

In the following sections a first and second order statistical analysis of the A-D-A system shown in Figure B1 is presented. This section formulates the problem and provides many of the required definitions.

Define $y(t)$ to be the desired input process to be transmitted through the A-D-A system. Let $r(t)$ be the input dither signal which is statistically independent of $y(t)$ and define $x(t)$ to be their sum

$$x(t) = y(t) + r(t) \tag{B-1}$$

Let $z(t)$ be the A-D-A system output defined almost everywhere by

$$z(t) = \sum_{n=1}^{N} Z_n \, I_{S_n}[x(t)] \tag{B-2}$$

where N is the number of quantization levels and the output levels Z_n satisfy $Z_1 < Z_2 < \cdots < Z_{N-1} < Z_N$. $I_S[\cdot]$ is the indicator function for the set S

$$I_S[x] = \begin{cases} 1 & x \in S \\ 0 & x \notin S \end{cases} \tag{B-3}$$

and the sets S_n are defined by

$$S_n = \{x: \; x \in [Y_{n-1}, Y_n]\} \qquad n=1,2,\cdots N \tag{B-4}$$

where the transitions Y_n satisfy $Y_0 < Y_1 < \cdots < Y_{N-1} < Y_N$. Also define the sets E_n to be

$$E_n = \{x: \; x \in [Y_{n-1} - Z_n, Y_n - Z_n]\} \qquad n=1,2,\cdots N \tag{B-5}$$

Define s(t) to be the output dither process statistically independent of y(t) and let $\omega(t)$ be the final output.

$$\omega(t) = z(t) - s(t) \tag{B-6}$$

Both the cases where the dither signals are statistically independent and where they are identical are considered in the following sections.

In the below derivations the following convensions will be used. For a process u(t) let u_n denote $u(t_n)$ for n=1 and 2. The probability density function (PDF) for u(t) is denoted by $f_u(\cdot)$ and the associated distribution function (DF) by $F_u(\cdot)$. Assume that the processes y(t), r(t), and s(t) have zero means and the variances σ^2, σ_r^2, and σ_s^2, respectively. Then the conditional PDFs for x(t) are

$$f_x(x|y) = f_r(x-y) \tag{B-7}$$

$$f_x(x_1, x_2|y_1,y_2) = f_r(x_1-y_1,x_2-y_2) \tag{B-8}$$

so that

$$F_x(x|y) = F_r(x-y) \tag{B-9}$$

$$F_x(x_1,x_2|y_1,y_2) = F_r(x_1-y_1,x_2-y_2) \tag{B-10}$$

The conditional PDF for z(t) is given by

$$f_z(z|y) = \sum_{n=1}^{N} \left[F_x(Y_n|y) - F_x(Y_{n-1}|y)\right] \quad \delta(z-Z_n)$$

$$= \sum_{n=1}^{N} \left[F_r(Y_n-y) - F_r(Y_{n-1}-y)\right] \quad \delta(z-Z_n) \tag{B-11}$$

$$f_z(z_1, z_2 \mid y_1, y_2) = \sum_{n=1}^{N} \sum_{m=1}^{N} \Big[F_x(Y_n, Y_m \mid y_1, y_2)$$

$$- F_x(Y_{n-1}, Y_m \mid y_1, y_2) - F_x(Y_n, Y_{m-1} \mid y_1, y_2)$$

$$+ F_x(Y_{n-1}, Y_{m-1} \mid y_1, y_2)\Big] \quad \delta(z_1 - Z_n)\ \delta(z_2 - Z_m)$$

$$= \sum_{n=1}^{N} \sum_{m=1}^{N} \Big[F_r(Y_n - y_1, Y_m - y_2)$$

$$- F_r(Y_{n-1} - y_1, Y_m - y_2) - F_r(Y_n - y_1, Y_{m-1} - y_2)$$

$$+ F_r(Y_{n-1} - y_1, Y_{m-1} - y_2)\Big] \quad \delta(z_1 - Z_n)\ \ \delta(z_2 - Z_m) \tag{B-12}$$

where $\delta(\cdot)$ is the Dirac delta function.* Let $E\{\cdot\}$ denote expected value

$$E\{x\} = \int_{-\infty}^{\infty} x\, f_x(x)\, dx \tag{B-13}$$

and $P\{a\}$ denote the probability of event a. Finally, define the output error process

$$e(t) = y(t) - \omega(t) \tag{B-14}$$

---

* See equations (2-43) and (2-44) of: J. F. Holland, Statistical Analysis of Analog-Digital-Analog Systems, Ph. D. dissertation, Stanford University, March 1974.

and its mean square value

$$\sigma_q^2 = E\{e^2(t)\} \tag{B-15}$$

B3. INDEPENDENT DITHER SIGNAL CASE

Equations for the first and second order statistics are derived in this section for the independent dither signal case. By statistical independence it follows from (B-6) that

$$f_\omega(\omega|y) = \int_{-\infty}^{\infty} f_z(\omega - z|y)\, f_s(-z)\, dz$$

$$= \sum_{n=1}^{N} \left[F_r(Y_n - y) - F_r(Y_{n-1} - y)\right] \; f_s(-\omega + Z_n) \tag{B-16}$$

and similarly

$$f_\omega(\omega_1, \omega_2 \mid y_1, y_2) = \sum_{n-1}^{N} \sum_{m=1}^{N} \left[F_r(Y_n - y_1, Y_m - y_2)\right.$$

$$- F_r(Y_{n-1} - y_1, Y_m - y_2) - F_r(Y_n - y_1, Y_{m-1} - y_2)$$

$$\left. + F_r(Y_{n-1} - y_1, Y_{m-1} - y_2)\right] \; f_s(-\omega_1 + Z_n, -\omega_2 + Z_m)$$

(B-17)

The conditional DF for the error is

$$F_e(e|y) = P\{y - \omega \leq e|y\} = P\{s \leq e + z - y|z\}$$

$$= \sum_{n=1}^{N} P\{s \leq e + Z_n - y,\ r + y \in [Y_{n-1}, Y_n) | y\}$$

$$= \sum_{n=1}^{N} [F_r(Y_n - y) - F_r(Y_{n-1} - y)] \int_{-\infty}^{e-y} f_s(s + Z_n)\, ds \tag{B-18}$$

so that the conditional PDF for the error is

$$f_e(e|y) = \sum_{n=1}^{N} [F_r(Y_n - y) - F_r(Y_{n-1} - y)]\ f_s(e + Z_n - y) \tag{B-19}$$

and similarly

$$f_e(e_1, e_2 \mid y_1, y_2) = \sum_{n=1}^{N} \sum_{m=1}^{N} [F_r(Y_n - y_1, Y_m - y_2)$$

$$- F_r(Y_{n-1} - y_1, Y_m - y_2) - F_r(Y_n - y_1, Y_{m-1} - y_2)$$

$$+ F_r(Y_{n-1} - y_1, Y_{m-1} - y_2)]\ f_s(e_1 + Z_n - y_1, e_2 + Z_m - y_2) \tag{B-20}$$

In the special case where the output dither signal equals zero (B-19) becomes

$$f_e(e|y) = \sum_{n=1}^{N} [F_r(Y_n - y) - F_r(Y_{n-1} - y)]\ \delta(e + Z_n - y) \tag{B-21}$$

so that

$$f_e(e) = \sum_{n=1}^{N} \left[F_r(Y_n - e - Z_n) - F_r(Y_{n-1} - e - Z_n)\right] \; f_y(e + Z_n) \; . \tag{B-22}$$

Using these conditional PDFs the conditional first and second order moments can be evaluated.

$$\mu_\omega(y) = E\{\omega|y\}$$

$$= \sum_{n=1}^{N} \left[F_r(Y_n - y) - F_r(Y_{n-1} - y)\right] \int_{-\infty}^{\infty} \omega f_s(-\omega + Z_n) \, d\omega$$

$$= \sum_{n=1}^{N} Z_n \left[F_r(Y_n - y) - F_r(Y_{n-1} - y)\right] \tag{B-23}$$

and

$$E\{\omega_1|y_1, y_2\} = \mu_\omega(y_1) \tag{B-24}$$

Observe that (B-23) reduces to (B-2) in the limit as the variance of the input dither signal goes to zero.

$$\lim_{\sigma_r \to 0} \mu_\omega(y) = \sum_{n=1}^{N} Z_n \, I_{S_n}[y] \tag{B-25}$$

Similarly

$$E\{\omega^2|y\} = \sum_{n=1}^{N} Z_n^2 \left[F_r(Y_n - y) - F_r(Y_{n-1} - y)\right] + \sigma_s^2 \tag{B-26}$$

and

$$E\{\omega_1^2 \mid y_1, y_2\} = E\{\omega_1^2 \mid y_1\} \tag{B-27}$$

The conditional autocorrelation function for the output $\omega(t)$ is

$$E\{\omega_1, \omega_2 \mid y_1, y_2\} = \sum_{n=1}^{N} \sum_{m=1}^{N} Z_n Z_m \Big[F_r(Y_n - y_1, Y_m - y_2)$$

$$- F_r(Y_{n-1} - y_1, Y_m - y_2) - F_r(Y_n - y_1, Y_{m-1} - y_2)$$

$$+ F_r(Y_{n-1} - y_1, Y_{m-1} - y_2)\Big] + K_{ss}(t_1, t_2) \tag{B-28}$$

where $K_{ss}(t_1, t_2)$ is the autocorrelation function for the dither process $s(t)$.

$$K_{ss}(t_1, t_2) = E\{s(t_1)\ s(t_2)\} \tag{B-29}$$

The equations for the error statistics are

$$E\{e(t)\} = \sum_{n=1}^{N} E\{\big[y - Z_n\big]\ \big[F_r(Y_n - y) - F_r(Y_{n-1} - y)\big]\} \tag{B-30}$$

$$\sigma_q^2 = \sum_{n=1}^{N} E\{\big[y - Z_n\big]^2\ \big[F_r(Y_n - y) - F_r(Y_{n-1} - y)\big]\} + \sigma_s^2 \tag{B-31}$$

$$E\{y(t_1)\ e(t_2)\} = \sum_{n=1}^{N} E\{y_1\ \big[y_2 - Z_n\big]\big[F_r(Y_n - y_2) - F_r(Y_{n-1} - y_2)\big]\} \tag{B-32}$$

$$K_{ee}(t_1, t_2) = E\{e(t_1)\ e(t_2)\}$$

$$= \sum_{n=1}^{N} \sum_{m=1}^{N} E\{[y_1 - Z_n][y_2 - Z_m][F_r(Y_n - y_1, Y_m - y_2)$$

$$- F_r(Y_{n-1} - y_1, Y_m - y_2) - F_r(Y_n - y_1, Y_{m-1} - y_2)$$

$$+ F_r(Y_{n-1} - y_1, Y_{m-1} - y_2)]\} + K_{ss}(t_1, t_2) \qquad \text{(B-33)}$$

which reduce to the appropriate equations in the limit as σ_r^2 goes to zero. Observe that the effect of the input dither is to randomize the transitions Y_n similar to the effect of A/D level errors. The effect of the output dither is to increase the output noise by σ_s^2.

B4. IDENTICAL DITHER SIGNAL CASE

Equations for the first and second order statistics are derived in this section for the identical dither signal case where

$$s(t) = r(t) \qquad \text{(B-34)}$$

The conditional DF for the output $\omega(t)$ is

$$F_\omega(\omega|y) = P\{z - r \leq \omega|y\} = P\{r \geq z - \omega|y\}$$

$$= \sum_{n=1}^{N} P\{r \geq Z_n - \omega,\ r + y \in [Y_{n-1}, Y_n) \mid y\}$$

$$= \sum_{n=1}^{N} \int_{Z_n - \omega}^{\infty} f_r(r)\ I_{S_n}(r + y)\ dr$$

$$= \sum_{n=1}^{N} \int_{-\omega}^{\infty} f_r(r + Z_n)\, I_{E_n}(r + y)\, dr \tag{B-35}$$

so the conditional PDF for $\omega(t)$ is

$$f_\omega(\omega|y) = \sum_{n=1}^{N} f_r(-\omega + Z_n)\, I_{E_n}(-\omega + y) \tag{B-36}$$

and similarly

$$f_\omega(\omega_1, \omega_2 \mid y_1, t_2) = \sum_{n=1}^{N} \sum_{m=1}^{N} f_r(-\omega_1 + Z_n, -\omega_2 + Z_m)$$

$$\bullet\ I_{E_n}(-\omega_1 + y_1)\, I_{E_m}(-\omega_2 + y_2) \tag{B-37}$$

The conditional DF for the error $e(t)$ is

$$F_e(e|y) = P\{y - \omega \leq e|y\} = P\{r \leq e + z - y|y\}$$

$$= \sum_{n=1}^{N} P\{r \leq e + Z_n - y,\ r + y \in [Y_{n-1}, Y_n)|y\}$$

$$= \sum_{n=1}^{N} \int_{-\infty}^{e+Z_n-y} f_r(r)\, I_{S_n}(r + y)\, dr$$

$$= \sum_{n=1}^{N} \int_{-\infty}^{e-y} f_r(r + Z_n)\, I_{E_n}(r + y)\, dr \tag{B-39}$$

so the conditional PDF for e(t) is

$$f_e(e|y) = \sum_{n=1}^{N} f_r(e - y + Z_n)\, I_{E_n}(e) \tag{B-39}$$

and similarly

$$f_e(e_1, e_2 \mid y_1, y_2) = \sum_{n=1}^{N} \sum_{m=1}^{N} f_r(e_1 - y_1 + Z_n, e_2 - y_2 + Z_m)$$

$$\times\, I_{E_n}(e_1)\, I_{E_m}(e_2) \tag{B-40}$$

Using these conditional PDFs the conditional first and second order moments can be evaluated.

$$\mu_\omega(y) = E\{\omega|y\} = \sum_{n=1}^{N} \int_{Z_n - Y_n + y}^{Z_n - Y_{n-1} + y} \omega\, f_r(-\omega + Z_n)\, d\omega$$

$$= \sum_{n=1}^{N} Z_n \left[F_r(Y_n - y) - F_r(Y_{n-1} - y)\right] \tag{B-41}$$

$$E\{\omega^2|y\} = \sum_{n=1}^{N} Z_n^2 \left[F_r(Y_n - y) - F_r(Y_{n-1} - y)\right] + \sigma_r^2$$

$$- 2 \sum_{n=1}^{N} Z_n \int_{Y_{n-1} - y}^{Y_n - y} x\, f_r(x)\, dx \tag{B-42}$$

A comparison of these equations with (B-23) and (B-26) shows that $\mu_\omega(y)$ is the same but in the case of identical dither the second moment has the additional term given in (B-42). The conditional autocorrelation function for the output is

$$E\{\omega_1\ \omega_2 \mid y_1, y_2\} = \sum_{n=1}^{N}\sum_{m=1}^{N} Z_n\ Z_m \left[F_r(Y_n - y_1, Y_m - y_2)\right.$$

$$- F_r(Y_{n-1} - y_1, Y_m - y_2) - F_r(Y_n - y_1, Y_{m-1} - y_2)$$

$$\left. + F_r(Y_{n-1} - y_1, Y_{m-1} - y_2)\right] + K_{rr}(t_1, t_2)$$

$$- \sum_{n=1}^{N} Z_n \int_{Y_{n-1}-y_1}^{Y_n-y_1} E\{x_2 \mid x_1\}\ f_r(x_1)\ dx_1$$

$$- \sum_{m-1}^{N} Z_m \int_{Y_{m-1}-y_2}^{Y_m-y_2} E\{x_1 \mid x_2\}\ f_r(x_2)\ dx_2 \qquad \text{(B-43)}$$

which may be compared with (B-28). The conditional mements of the error are

$$E\{e|y\} = \sum_{n=1}^{N} \int_{-\infty}^{\infty} e\ f_r(e - y + Z_n)\ I_{E_n}(e)\ de$$

$$= \sum_{n=1}^{N} \int_{-\infty}^{\infty} \left[x + y - Z_n\right]\ f_r(x)\ I_{S_n}(x + y)\ dx$$

$$= \sum_{n=1}^{N} [y - Z_n] \left[F_r(Y_n - y) - F_r(Y_{n-1} - y)\right] \qquad \text{(B-44)}$$

$$E\{e^2|y\} = \sum_{n=1}^{N} [y - Z_n]^2 \left[F_r(Y_n - y) - F_r(Y_{n-1} - y)\right] + \sigma_r^2$$

$$- 2 \sum_{n=1}^{N} Z_n \int_{Y_{n-1}-y}^{Y_n-y} x\, f_r(x)\, dx \qquad \text{(B-45)}$$

which may be compared with (B-30) and (B-31). Similarly,

$$E\{y(t_1)\, e(t_2)\} = \sum_{n=1}^{N} E\{y_1 \left[y_2 - Z_n\right] \left[F_r(Y_n - y_2) - F_r(Y_{n-1} - y_2)\right]\}$$

(B-46)

$$E\{e_1\, e_2 \mid y_1, y_2\} = \sum_{n=1}^{N}\sum_{m=1}^{N} [y_1 - Z_n][y_2 - Z_m][F_r(Y_n - y_1, Y_m - y_2)$$

$$- F_r(Y_{n-1} - y_1, Y_m - y_2) - F_r(Y_n - y_1, Y_{m-1} - y_2)$$

$$+ F_r(Y_{n-1} - y_1, Y_{m-1} - y_2)] + K_{rr}(t_1, t_2)$$

$$- \sum_{n=1}^{N} Z_n \int_{Y_{n-1}-y_1}^{Y_n-y_1} E\{x_2 \mid x_1\}\, f_r(x_1)\, dx_1$$

$$- \sum_{m=1}^{N} Z_m \int_{Y_{m-1}-y_2}^{Y_m-y_2} E\{x_1 \mid x_2\} f_r(x_2)\, x_2 \tag{B-47}$$

which may be compared with (B-33). Thus, the first moments are the same for the independent and identical dither cases but the second moments differ by terms which tend to reduce the noise power in the identical dither signal case.

B5. FORMULAS FOR THE INDEPENDENT DITHER CASE

Formulas are given in this section for the independent dither case. They are worked out explicitly for Gaussian amplitude statistics. It is assumed that the output dither signal equals zero.

A comparison of equation (B-26) and (A-6) shows that the independent dither case is a generalization of the formulas given in Appendix A for odd symmetric quantizers satisfying (A-2) and (A-3). Define the functions:

$$F_0(y/\sigma) = \int_{-\infty}^{\infty} f_y(x)\, F_r(y - x)\, dx \tag{B-48}$$

$$F_1(y/\sigma) = \frac{1}{\sigma} \int_{-\infty}^{\infty} x\, f_y(x)\, F_r(y - x)\, dx \tag{B-49}$$

Observe that in the limit as σ_r goes to zero the distribution function $F_r(y - x)$ becomes a unit step function and these equations reduce to (A-7) and (A-8). Thus, (B-48) and (B-49) are just a generalization and the same basic formulas given in Appendix A can be used to evaluate performance in the presence of dither.

As an example suppose $y(t)$ and $r(t)$ are Gaussian processes so that

$$F_r(x) = \frac{1}{2} \left[1 + \mathrm{erf}(x/\sqrt{2}\,\sigma_r)\right] \tag{B-50}$$

and

$$f_y(x) = \frac{1}{\sqrt{2\pi}\,\sigma} \exp(-x^2/2\sigma^2) \tag{B-51}$$

Then*

$$F_0(y/\sigma) = \frac{1}{2} + \frac{1}{2\sqrt{2\pi}\,\sigma} \int_{-\infty}^{\infty} \operatorname{erf}\left(\frac{y-x}{\sqrt{2}\,\sigma_r}\right) e^{-x^2/2\sigma^2}\, dx$$

$$= \frac{1}{2} + \frac{\beta}{2\sqrt{\pi}} \int_{-\infty}^{\infty} \operatorname{erf}(x) \exp\left\{-\left[\beta x - \frac{y}{2\,\sigma}\right]^2\right\} dx$$

$$= \frac{1}{2}\left[1 + \operatorname{erf}\left(\frac{y}{\sqrt{2}\,\sigma\sqrt{\beta^2+1}}\right)\right] \tag{B-52}$$

where

$$\beta = \sigma_r/\sigma \tag{B-53}$$

Similarly

$$F_1(y/\sigma) = \frac{1}{2\sqrt{2\pi}\,\sigma^2} \int_{-\infty}^{\infty} x \operatorname{erf}\left(\frac{y-x}{\sqrt{2}\,\sigma_r}\right) e^{-x^2/2\sigma^2}\, dx \tag{B-54}$$

Define the functions

$$g_1(x) = \operatorname{erf}\left(\frac{y-x}{\sqrt{2}\,\sigma_r}\right) \tag{B-55}$$

---

* "A Table Of Integrals Of The Error Function," E. Ng and M. Geller, Journal Of Research of the National Bureau of Standards - B. Mathematical Sciences, Vol. 73B, No. 1, January - March 1969.

$$g_2'(x) = \frac{x}{\sqrt{2\pi}\ \sigma^2}\ e^{-x^2/2\sigma^2} \tag{B-56}$$

where prime denotes differentiation. Then

$$F_1(y/\sigma) = \frac{1}{2}\ g_1(x)\ g_2(x)\Big|_{-\infty}^{\infty} - \frac{1}{2}\int_{-\infty}^{\infty} g_1'(x)\ g_2(x)\ dx \tag{B-57}$$

where

$$g_1'(x) = -\frac{2}{\sqrt{2\pi}\ \sigma_r}\ e^{-(x-y)^2/2\sigma_r^2} \tag{B-58}$$

$$g_2(x) = -\frac{1}{\sqrt{2\pi}}\ e^{-x^2/2\sigma^2} \tag{B-59}$$

and after some manipulation the result is

$$F_1(y/\sigma) = -\frac{1}{\sqrt{2\pi}\sqrt{\beta^2+1}}\ \exp\left(-\frac{y^2}{2\sigma^2\ [\beta^2+1]}\right) \tag{B-60}$$

In the limit as σ_r goes to zero these formulas reduce to (A-14) and (A-15) as expected. Also note that

$$\frac{V}{\sigma} = \eta\sqrt{\beta^2 + 1} \tag{B-61}$$

in the formulas given in Appendix A for Y_n and Z_n.

B6. FORMULAS FOR THE IDENTICAL DITHER CASE

Formulas are given in this section for the identical dither case and are worked out explicitly for Gaussian inputs and dithers. From (B-39) the PDF for the error e(t) is

$$f_e(e) = \sum_{n=1}^{N} I_{E_n}(e) \int_{-\infty}^{\infty} f_r(e - y + Z_n)\, f_y(y)\, dy$$

$$= \sum_{n=1}^{N} I_{E_n}(e)\, f_x(e + Z_n) \qquad \text{(B-62)}$$

where x(t) is defined by (B-1). Then

$$\sigma_q^2 = \sum_{n=1}^{N} \int_{-\infty}^{\infty} e^2\, f_x(e + Z_n)\, I_{E_n}(e)\, de$$

$$= \sum_{n=1}^{N} \int_{Y_{n-1}}^{Y_n} \left[x - Z_n\right]^2 f_x(x)\, dx \qquad \text{(B-63)}$$

which is the same formula as (A-6) so that again the formulas given in Appendix A can be used to evaluate the dither case.

As an example suppose y(t) and r(t) have Gaussian amplitude statistics. Then their sum x(t) is Gaussian with variance

$$\sigma_x^2 = \sigma^2 + \sigma_r^2 = \sigma^2 \left[\beta^2 + 1\right] \qquad \text{(B-64)}$$

so it follows that

$$\frac{\sigma_q^2}{\sigma^2} = \frac{\sigma_q^2}{\sigma_x^2} \left[\beta^2 + 1\right] \qquad \text{(B-65)}$$